VALIDATION OF THE BIOLOGICAL RESPONSES OF REFERENCE DRUGS IN THE ZEBRAFISH EMBRYO BY ELECTROCARDIOGRAPHIC ANALYSIS AND BY NOVEL PHENOTYPING TOOLS

by

SUNDEEP SINGH DHILLON

A thesis submitted to

The University of Birmingham

for the degree of

DOCTOR OF PHILOSOPHY

Department of Medical and Molecular Genetics

School of Clinical and Experimental Medicine

College of Medical and Dental Sciences

The University of Birmingham

October 2014

Abstract

Drug toxicities represent a major problem in drug discovery and development; therefore there is a push to develop new technologies to detect these early on. In this thesis I investigated the utility of zebrafish embryos and larvae in evaluating the biological activity of novel compounds and developed new methods for assaying the potential toxic effects of drugs *in vivo*. An electrocardiogram (ECG) recording set-up for zebrafish embryos and larvae was developed to assay drug-induced cardiotoxicity. The set-up was validated by testing drugs known to induce cardiotoxicity in humans in zebrafish larvae. The results obtained were in agreement with those documented in humans demonstrating the utility of the zebrafish larva in detecting drug-induced cardiotoxicity. The zebrafish embryo was also found to be a useful model for probing the biological activity of novel and marketed compounds providing an insight into the relationship between chemical properties and biological effects. Additionally, the assessment of the anti-inflammatory activity of a set of reference drugs revealed that the zebrafish larva also presents a promising model for therapeutic drug screens. Overall, the results described in this thesis show that the zebrafish presents an effective, reliable and rapid model for assessing the biological activity of drugs *in vivo*.

Acknowledgements

I would firstly like thank my supervisor Professor Ferenc Müller for his continued support, enthusiasm, advice, encouragement and guidance during my PhD. Secondly; I would like to thank my co-supervisor Professor Attila Sik for his continued support and for his help particularly with the zebrafish electrocardiogram (ECG) work. I would also like to thank my supervisor at KIT (Karlsruhe Institute of Technology, Germany) Dr. Urban Liebel for his advice, guidance and encouragement during my time in Germany.

I would like to thank all past and present colleagues at the University of Birmingham, especially Harmeet Gill, Rhiannon Hurst, Sahar Avazzadeh, Irene Miguel, Jennifer Roberts and Nan Li for creating such a great working environment. I would like to thank all my colleagues at KIT, especially Yu Liang, Ravindra Peravali and Jochen Gehrig. I would also like to thank all my former colleagues at Biotecont Ltd., especially Eva Doro for introducing me to zebrafish ECGs. I would like to thank our collaborators at AcureOmics AB, especially Professor Torbjörn Lundstedt and Associate Professor Katrin Lundstedt-Enkel for all their help and support and for introducing me to multivariate analysis. I would also like to thank our collaborators at the School of Chemistry Dr. John S. Fossey, Antonio Feula and Mariwan M. Salih for creating such a fruitful collaboration. I would like to thank Marie Curie Actions for funding my PhD and everyone from the 'Biology of Liver and Pancreatic Development and Disease' (BOLD) Initial Training Network for all the great discussions and meetings. Finally, I would like to thank both my parents, as without their continued support I would not be where I am now. I would also like to thank my brother for his invaluable support and help and for taking an interest in my research.

List of abbreviations

ECG	electrocardiogram
NSAID	non-steroidal anti-inflammatory drug
COX	cyclooxygenase
CYP	cytochrome P450
ADR	adverse drug reaction
dpf	days post fertilisation
hpf	hours post fertilisation
GI	gastrointestinal
DMSO	dimethyl sulphoxide
GC-MS	gas chromatography-mass spectrometry
LC-MS	liquid chromatography-mass spectrometry
GFP	green fluorescent protein
SAR	structure activity relationship
QSAR	quantitative structure activity relationship
ADME	absorption, distribution, metabolism and excretion
ABC	adenosine triphosphate binding-cassette
ATP	adenosine triphosphate
DNA	deoxyribonucleic acid
RNA	ribonucleic acid
MDR1	multi-drug resistance protein 1
DMT1	divalent metal transporter
OP	organophosphate
TILLING	targeted induced local lesions in genome
NAPQI	n-acetyl-p-benzoquinone-imine
ROS	reactive oxygen species
UTP	uridine triphosphate
UDP	uridine diphosphate
REACH	registration, evaluation, authorisation and restriction of chemicals
OECD	organisation for economic co-operation and development
ICH	international conference on harmonisation
ZFET	zebrafish embryo toxicity test
LC50	lethal concentration 50
EC50	effective concentration 50
NOEC	no observed effect concentration
LOEC	lowest observed effect concentration
PCA	principal component analysis
PLS	partial least squares

OPLS	orthogonal partial least squares
OPLS-DA	orthogonal partial least squares discriminant analysis
PTU	phenylthiourea
MS222	ehtyl-3-aminobenzoate methane sulphonic acid
PFA	paraformaldehyde
PBS	phosphate buffered saline
PBST	phosphate buffered saline tween
Cx40	connexin-40
TdP	torsades de pointes
C-LTCC	l-type voltage dependent calcium channel
AV	atrioventricular
hERG	human ether-à-go-go-related gene
zERG	zebrafish ether-à-go-go-related gene
bpm	beats per minute
ms	milliseconds
nm	nanometres
mV	millivolts
Hz	hertz
cAMP	cyclic adenosine monophosphate
BDM	2,3-butanedione-monoxime
PAS	per-arnt-sim
*f*H	heart rate
PVC	premature ventricular contractions
DILI	drug-induced liver injury
IVH	intraventricular hemorrhage
VBH	ventricular brain hemorrhage
BDA	cis-2-butene-1,4-dial
MW	molecular weight
logP	partition coefficient
clogP	computed logP
logD	distribution constant
V	molecular volume
S	molecular surface area
O	ovality
ELUMO	energy of lowest unoccupied molecular orbital
EHOMO	energy of highest occupied molecular orbital
H	hardness
DM	dipole moment
NPSA	non-polar surface area
PSA	polar surface area

HBA	number of hydrogen bond acceptors
HBD	number of hydrogen bond donors
HB	sum of hydrogen bond acceptors and donors
pKa	acid dissociation constant
ICM	intermediate cell mass
zMPO	zebrafish myeloperoxidase
NK	natural killer
NADPH	nicotinamide dinucleotide monophosphate
Duox	dual oxidase
ChIn	chemically induced inflammation assay
ORO	oil red o
nAChR	nicotinic acetylcholine receptor
TR	toxic ratio
TI	teratogenic index

Table of Contents

List of figures

List of tables

Chapter One: GENERAL INTRODUCTION

1.1 Drug development

Traditionally, the discovery of new drugs came about through chance, such as in the case of penicillin. However, advances in science and increased understanding of compound chemistry led to the systematic screening and isolation of novel compounds from plants and microbes (Patel and Gordon, 1996). The extraction of such compounds was found to be time consuming, hence with the introduction of combinatorial chemistry there was suddenly a huge rise in the creation of synthetic drugs. Almost all drugs marketed today are synthetic drugs. Synthetic drugs are created based on Lipinski's rule of five where a compound is considered to be drug-like if it has <10 hydrogen bond acceptors, <5 hydrogen bond donors, a molecular weight <500 g/mol and a logP value <5 (Andrews et al., 2000). Compounds that do not meet these criteria are less orally bioavailable, are more likely to bind to plasma proteins and cause non-specific effects including toxicity (Andrews et al., 2000).

Current drug screening approaches are based on *in vitro* methods where large libraries consisting of natural and synthetic compounds are screened against specific cellular or molecular targets (Mayr and Bojanic, 2009). These approaches are cheap and extremely rapid but are biased towards a specific target and are not representative of the *in vivo* scenario. For example, a drug may be able to bind to its target to induce therapeutic effects but may also lead to unwanted side effects due to metabolism into a reactive intermediate in the body (**Figure 1.1**). This is seen with the non-steroidal anti-inflammatory drug (NSAID) diclofenac. The therapeutic properties of diclofenac are attributed to its inhibition of the

cyclooxygenase (COX) 2 enzyme, which attenuates the inflammatory response (Bort et al., 1999). However, liver toxicity has been reported in some patients as an unwanted side effect of diclofenac treatment (Bort et al., 1999). Liver toxicity is a result of the metabolism of diclofenac by cytochrome P450 (CYP) enzymes into a 5-hydroxydiclofenac metabolite which impairs the function of mitochondria (Bort et al., 1999).

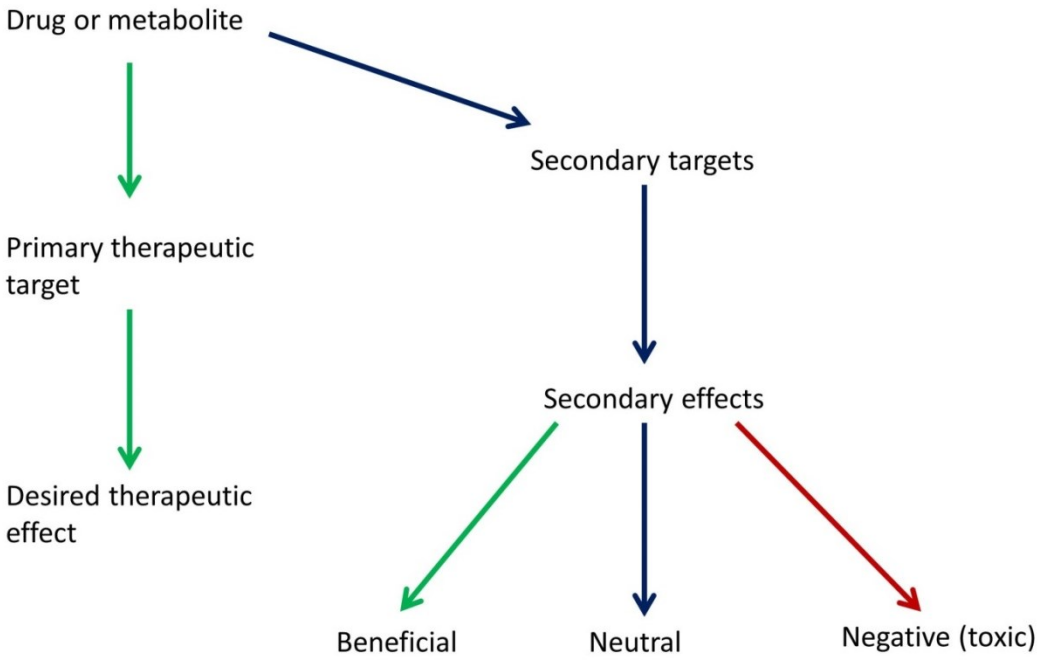

Figure 1.1 – Beneficial and undesired properties of drug candidates.
Drugs are designed to have an effect on a specific target in order to induce a therapeutic effect. However, parent drugs themselves or metabolites can bind to secondary targets either leading to a beneficial therapeutic effect, a neutral effect or a negative toxic effect.

The drug candidates that are identified from initial *in vitro* screening approaches are optimised for potency and selectivity by making changes to their chemical structures based on structure activity relationships (SARs). These optimised compounds then undergo *in vitro* toxicity tests where cytotoxicity is recorded at several concentrations (Li, 2001). Those drugs presenting with little or no toxicity at therapeutic concentrations (high therapeutic index) are then taken forward so that absorption, distribution, metabolism and excretion (ADME) studies can be performed (Li, 2001). These studies involve using Caco-2 cell lines and

hepatocyte co-cultures expressing various CYP enzymes to enable intestinal permeability and metabolic stability of these compounds to be determined (Li, 2001). Following on from this *in vitro* cellular or functional activity assays are performed. Those drugs showing good cellular or functional activity are then selected for testing *in vivo*. A drug candidate which shows high efficacy (specific binding to target), low toxicity (few or no side effects) and very good bioavailability (excellent absorption into the bloodstream) is then selected for testing in humans in phase 1-3 clinical trials. In human clinical trials, the dose of the lead compound and the formulation is optimised. In addition to this, human pharmacokinetic/pharmacodynamic assessments are performed as well as further evaluations on the safety of the compound. If the lead compound displays serious toxic side effects, the drug development process will be halted and the whole process has to be initiated from scratch. However, if the compound is successful in human clinical trials and presents a significant benefit over existing drugs for the therapeutic indication it is being targeted for it can be prepared for marketing. Once marketing authorisation is received the lead compound can be marketed as a drug. Post-marketing surveillance of the drug is performed for at least a year to further evaluate the safety of the drug and to collect data on possible side effects. If the side effects reported are severe and life-threatening the drug can be taken off the market. The whole drug development process is outlined in **Figure 1.2**.

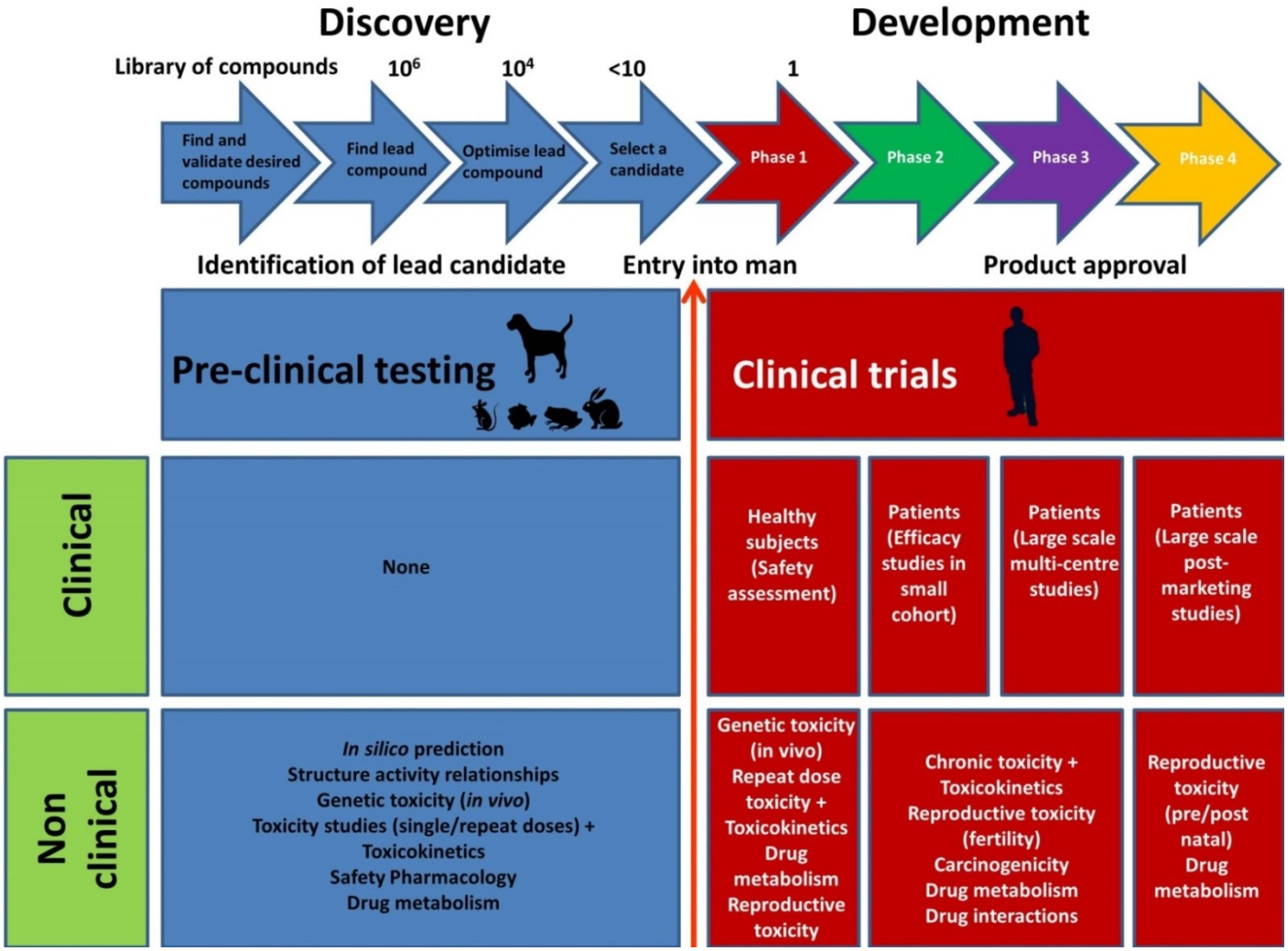

Figure 1.2 – Overview of the drug development process. *To bring one drug on the market it can take up to 15 years and cost between 500 million and 1 billion US dollars.*

1.1.1 Adverse drug reactions (ADRs)

Following the release of a new compound, post-marketing surveillance is carried out to identify any adverse drug reactions (ADRs) that could develop which may have not been picked up in pre-clinical studies or in human clinical trials (Edwards and Aronson, 2000). ADRs represent a major problem with a relative incidence rate of 1 in 10,000 individuals, accounting for around 100,000 deaths per year (Edwards and Aronson, 2000). ADRs can be broadly classified into five different categories (shown below in **Table 1.1**).

Table 1.1 – Different types of ADRs.
Source: Table adapted from Edwards and Aronson (2007)

Type of ADR	Description	Incidence
A (Predictable)	Dose-dependent, predictable from primary, secondary and safety pharmacology	Main cause of ADRs (around 75%), high morbidity, low mortality (e.g. hemorrhage with anti-coagulants)
B (Idiosyncratic)	No dose-dependency, not predictable, idiosyncratic response	Responsible for only 25% ADRs, but the majority of these are life-threatening (e.g. acute porphyria)
C (Chronic effects)	Long term adaptive changes, can be anticipated	Occurs commonly with some drug classes (e.g. benzodiazepines)
D (Delayed effects)	Effects that occur later on, e.g. teratogenicity and carcinogenicity	Low number of cases
E (End of treatment effects)	Rebound effects following discontinuation of therapy	Occurs commonly with some drug classes (e.g. benzodiazepines)

ADRs are mainly manifested in the form of cardiotoxicity and hepatotoxicity and present a real problem to pharmaceutical industries and health authorities. Particularly, idiosyncratic toxicity which is not predictable and occurs rarely is difficult to detect early on during the drug development process. For example, in 1993 the nucleoside analogue fialuridine went

into human clinical trials after prior animal tests in mice, rats, dogs and primates showed no adverse effects (Xu et al., 2014). However, once clinical trials were initiated trial subjects developed liver toxicity (Xu et al., 2014). Out of the 15 trial subjects tested, two needed liver transplants and five died (Xu et al., 2014). This demonstrates the importance of being able to detect and exclude compounds with the potential to cause idiosyncratic responses early on in the drug development process, as failure to do so can have fatal consequences.

1.2 The zebrafish embryo as a model for drug screening

1.2.1 Zebrafish background

The zebrafish (*Danio rerio*) is a freshwater fish (cyprinoid teleost) originating from south Asia (Briggs, 2002). An adult zebrafish can grow up to 6 cm in length and can live for two to three years (Briggs, 2002). The adult zebrafish reaches sexual maturity within 3-5 months of age and one mating pair is able to produce around 100 eggs (Briggs, 2002). Zebrafish can be maintained in artificial aquaria and have become a popular model organism for scientific experimentation around the world.

1.2.2 Zebrafish embryo development and anatomy

Zebrafish development can be split up into several stages. The first stage of zebrafish development is the zygote stage (1-cell stage) which occurs from 0 to 0.75 hours post fertilisation (hpf) followed by the cleavage stage (0.75-2.25 hpf) where the cell starts to divide (Kimmel et al., 1995). Following on from this is the blastula stage (2.25-5.25 hpf) where epiboly (cell movement) begins (Kimmel et al., 1995). During the gastrula stage (5.25-

10.33 hpf) epiboly continues and the tail bud is formed. This is followed by the segmentation stage (10.33-24 hpf) where the somites and pronephros form. The pharyngula period (24-48 hpf) marks initiation of the heartbeat and the beginning of pigment development in the zebrafish embryo (Kimmel et al., 1995). The hatching period (48-72 hpf) which is characterised by the formation of pectoral fins and fin blades is followed by the larval period (72 hpf-29 dpf) where continued growth of the zebrafish and the completion of organ development occurs (Kimmel et al., 1995). From 48/72 hpf until 120 hpf zebrafish are regarded as post-hatched embryos (Strähle et al., 2012). The juvenile period lasts from 30 until 89 dpf and is characterised by the formation of adult fins and pigments (Kimmel et al., 1995). From 90 dpf onwards the zebrafish is regarded as an adult.

Zebrafish embryos do not require an outside nutrient source whilst they are developing as the yolk sac contains lipids necessary for growth of the embryo (Langheinrich, 2003). Only after five days when most of the yolk sac has been consumed is there a requirement for an external food source (Langheinrich, 2003). Adult zebrafish like other fish species can obtain oxygen through their gills, however zebrafish at embryonic stages obtain oxygen by transdermal diffusion, as oxygen supply is not dependent on cardiovascular function (Jacob et al., 2002)(Rombough, 2002). In terms of general anatomy zebrafish embryos show differences to humans in that they do not have a prostate gland, long bones, limbs or lungs and in place of a stomach have an intestinal bulb (Lieschke and Currie, 2007). Despite these anatomical differences zebrafish do possess many organs such as a liver and pancreas which are very similar to their human counterparts and have a conserved function in both species. The main features of a 2 dpf zebrafish embryo are outlined in **Figure 1.3**.

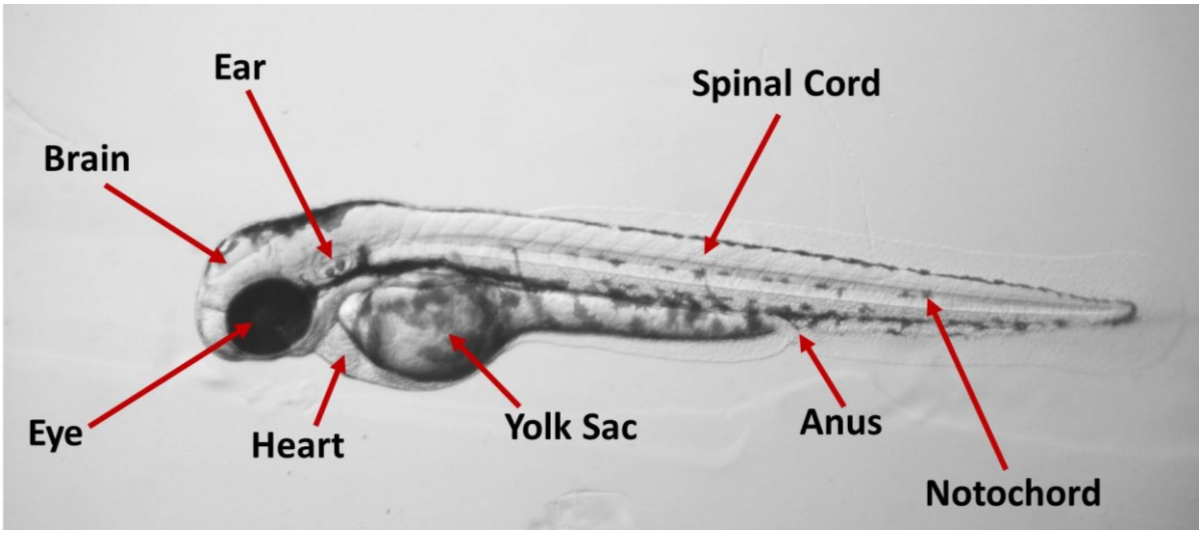

Figure 1.3 – Anatomy of the 2 day old zebrafish embryo.

1.2.3 The zebrafish embryo as a drug screening tool

As previously described, *in vivo* models are essential in order to evaluate drug candidates for efficacy, metabolism and toxicity during the drug development process. Using i*n vivo* models, such as rodents requires large amounts of compound and long treatment regimes. Zebrafish embryos on the other hand have several advantages which make them suitable for drug screening (see section **1.2.3.1** for further details). The zebrafish embryo is particularly useful for the identification of new drug targets, modelling specific diseases and determining the toxicity mechanisms of novel compounds (Zon and Peterson, 2005)(Hill et al., 2005).

1.2.3.1 Advantages and disadvantages of the zebrafish embryo as a model for drug screening

Zebrafish embryos have many advantages over other animal models in regards to their use for scientific research and also specifically for drug screening. General features of zebrafish embryos that make them advantageous to use for scientific research include: 1) low

maintenance costs, 2) small size, 3) optical transparency, 4) external fertilization, 5) fast development, 6) survival without external feeding up to 5 days post fertilization (dpf) and 7) similarities in toxic responses to humans and other mammals (Langheinrich, 2003). Additionally, the use of zebrafish embryos contributes to the 3Rs (reduction, refinement and replacement) of animals in research, as zebrafish embryos are not protected and do not require a licence until after 5 dpf.

For drug screening purposes rodents are widely used as the *in vivo* model of choice due to their close ancestral relation to humans, as many developmental and physiological processes are conserved between the two species. Additionally, the same drug administration routes as those planned for human use can be employed when using rodents. Despite rodents being a mainstay for drug screening and particularly toxicological testing, compared to zebrafish, rodent development is slow and occurs *in utero* (Wheeler and Brändli, 2009). Additionally, maintenance costs are more expensive when using rodents, rodent studies have more stringent regulatory restrictions surrounding their use and large amounts of compound are required for dosing regimens (Hill et al., 2005).

Early development in all vertebrate species is highly conserved with similarities evident in the genes, receptors and molecular pathways utilized (Hill et al., 2005). Therefore, using simple vertebrates such as zebrafish may be representative of what happens in more complex animals, such as humans despite the evolutionary distance (Hill et al., 2005).

Features which make zebrafish embryos particularly suited for drug screening include: 1) the ability to absorb chemicals (especially low molecular weight compounds) transdermally, 2) the ability to survive in very small volumes of liquid as low as 50 µL in 96 well or 384 well plates, 3) the possibility to test large numbers at one time, 4) the possibility to perform automated drug screens and 5) the possibility to fluorescently label tissues or organs of interest (Goldsmith, 2004). Additionally, after 3 dpf (4-5 dpf) zebrafish can ingest compounds orally, as they have a fully functional gastrointestinal (GI) tract which can aid diffusion of drugs that cannot be absorbed by transdermal diffusion (Goldsmith, 2004)(Belanger et al., 2010). Dimethyl sulphoxide (DMSO) is often used as a solvent to solubilise compounds that are not readily soluble in water. Zebrafish embryos are DMSO tolerant up to 1.5%, which means that they can also be used to test poorly water soluble compounds.

Zebrafish also show high similarity to humans in terms of pharmacology, physiology and genetics (Crawford et al., 2011), as well as presenting with similar toxic and teratogenic effects to humans after drug exposure (Parng et al., 2002). The zebrafish genome has two more chromosome pairs than humans and has many duplicated genes (Hill et al., 2005). However, many of these duplicated genes have a new function and may be expressed in different tissues compared to their ancestors (Hill et al., 2005). This has its benefit as knockdown of a specific gene in zebrafish embryos may not be embryo lethal compared to the mammalian counterpart (Hill et al., 2005). Additionally, the high fecundity of zebrafish also has its advantages when establishing a new transgenic line, as it is much quicker and cheaper than establishing one in rodents (Murphey et al., 2006).

The disadvantages of using zebrafish embryos for scientific research include their evolutionary distance to humans, meaning that some processes cannot be modelled in zebrafish (e.g. lung development) due to differences in anatomy. Additionally, the same drug administration routes intended for human use cannot be employed in zebrafish embryos, which therefore make rodents a more suitable model for this purpose. Studies on the ADME properties of a compound are more difficult to perform when using zebrafish embryos, as studies addressing this have only begun to be developed (Diekmann and Hill, 2013). Furthermore, drug metabolism pathways have not been as extensively characterised in zebrafish compared to rodents and other mammals.

1.2.3.2 Advantages and disadvantages of the zebrafish embryo as a model for drug screening compared to other fish models

The closest fish model to zebrafish is the medaka (*Oryzia latipes*), which compared to zebrafish can generally only survive in the laboratory for 1 year and it produces very few embryos which are difficult to remove, clean and collect (Hill et al., 2005). Apart from medaka, the carp (*Cyprinus carpio*) is particularly useful for toxicological studies and the puffer fish for genetic studies, as it lacks junk deoxyribonucleic acid (DNA) (Hill et al., 2005). However, the zebrafish is still the preferred option over these aforementioned fish species for scientific research, as it has been extensively studied, so far greater resources and published literature are available compared to other fish species. For example, information is readily available on the physiology, genetics and biochemistry of zebrafish at all stages of

development (Hill et al., 2005). Additionally, the technology and techniques available for zebrafish are far more than for any other fish species (Kari et al., 2007).

1.2.3.3 Advantages of the zebrafish embryo *in vivo* model over *in vitro* models for use in drug screening

In comparison to cell culture models, the zebrafish embryo *in vivo* model enables the interaction between different cells and tissues to be investigated in a complex multicellular organism with the opportunity to study cell-cell and cell-matrix interactions, as well as the uptake, metabolism and excretion of a compound (Scholz et al., 2008). Despite the popularity of *in vitro* approaches and particularly the growing interest in toxicogenomics which enables gene expression changes upon exposure to a compound to be monitored at high throughput with miniscule compound consumption; these *in vitro* approaches do have their drawbacks (Pettit et al., 2010). For example, *in vitro* approaches do not replicate what happens in the whole organism as cell or organ cultures are used (Pettit et al., 2010). Additionally, large datasets are generated which take time to process and the results that are obtained are often further complicated by normal variations in gene expression (Pettit et al., 2010). Additionally, cell culture serum required for maintaining cell cultures can pose a barrier to drug penetration, as serum proteins can interact and bind to drugs preventing them from reaching their targets or being activated (Wheeler and Brändli, 2009).

Induced pluripotent stem (iPS) cells are also becoming increasingly popular in scientific research. These cells are derived directly from humans and have the capability to differentiate into various cell types including endodermal, mesodermal and ectodermal cells

(Yamanaka, 2009). These cells offer advantages over *in vivo* and other *in vitro* methods in that they are directly derived from the patient and therefore contain the same genetic information (Yamanaka, 2009). This is particularly useful for performing drugs screens in diseased cells, especially diseases where the genotype can influence the severity of the disease (e.g. long QT syndrome) (Yamanaka, 2009). Due to iPS cells being a relatively new technology there are some obstacles that still need to be overcome, such as the possibility of the cells forming teratomas (germ cell tumours) and there being no way to confirm whether nuclear programming has been completed (Yamanaka, 2009). Additionally, as mentioned above using iPS cells does not replicate the *in vivo* scenario, highlighting the same limitation of other *in vitro* methods.

Zebrafish offer the advantage in conjunction with rodent models that initial ADME assessments can be performed. *In vitro* ADME assessments can also be performed but they only allow certain parts of the ADME response to be modelled at one time (Wheeler and Brändli, 2009). For example, Caco-2 cells can only be used to determine intestinal stability, whereas hepatocyte co-cultures can only be used to determine metabolism, so the whole ADME response cannot be modelled all at once (Li, 2001). In addition to ADME, zebrafish embryos can also be used to determine toxicity of compounds *in vivo*, which takes into account several factors including ADME. Therefore, more screens are shifting from cell-based to whole animal *in vivo* screens, particularly zebrafish screens due to the above mentioned advantages (Choi and Tontonoz, 2013).

1.2.3.4 The zebrafish embryos as a complementary model to existing *in vitro* models

In drug development, the goal would be to introduce the zebrafish embryo test as a complementary method to existing *in vitro* and *in vivo* tests already in place. Specifically, the zebrafish embryo model could be utilised as a pre-screen after selection of candidate drugs from the initial *in vitro* screening approaches. This would therefore help to exclude any toxic compounds before they are tested in rodents.

A cell cycle inhibitor screen was performed by Murphey and colleagues using three different methods to compare *in vitro* and *in vivo* drug screening approaches (Murphey et al., 2006). The screening methods employed included: 1) a mammalian cell line method, 2) a zebrafish cell line method and 3) a zebrafish embryo screening method (Murphey et al., 2006). When using the zebrafish embryo screening method 14 novel compounds were found, which were previously not identified using the mammalian cell line approach (Murphey et al., 2006). Six of them were found to have an effect in the mammalian cell line, suggesting that their effects were conserved among vertebrates (Murphey et al., 2006). Three compounds were found to be inactivated by serum in cell line culture and therefore not effective in the mammalian or zebrafish cell lines and three compounds were found to only be active in zebrafish embryos (Murphey et al., 2006). Interestingly, one compound was found to be effective only in the zebrafish cell line and zebrafish embryos, suggesting the effect of this compound was species specific (Murphey et al., 2006). The lessons learnt from this study are that the way forward in drug development would not be to replace the existing *in vitro*

screening methods with the zebrafish embryo test, but to actually combine them together as complementary methods, as no one single test can address all the questions being asked.

1.2.4 Zebrafish embryo drug screens

As mentioned previously, the many advantages of zebrafish embryos make them particularly attractive as models for drug screening applications. The first chemical screen utilising zebrafish embryos was carried out by Peterson and colleagues where compound-treated zebrafish embryos were visually assessed during development to identify any abnormal morphological features that developed after compound exposure (Peterson et al., 2000). Some of the phenotypes that were observed after compound exposure included hyperpigmentation and abnormal ear development (Peterson et al., 2000). Since then, many compound screens have been performed, specifically looking at vasculature (Tran et al., 2007), dorsoventral patterning (Bowman and Zon, 2010), pigmentation (Peal et al., 2010) and erythropoiesis (Wheeler and Brändli, 2009).

When searching for compounds that could have a therapeutic effect, targeted screening is generally employed where compounds that inhibit or suppress a particular phenotype are screened for (Hong and Brewster, 2006). To create an abnormal phenotype of interest (e.g. skin cancer) a particular compound could be administered or a genetic technique (e.g. zinc-finger nucleases/morpholino knockdown/TILLING [targeted induced local lesions in genomes]) could be employed to knockdown a specific gene that leads to the mutant phenotype. Recovery of the normal state or reduced severity of the phenotype would then be used as an endpoint for such assays.

A zebrafish embryo screen performed by Peterson and colleagues involved using a targeted gene knockdown approach where a zebrafish gridlock mutant was generated (Peterson et al., 2004). In this mutant aortic blood flow was affected (a similar condition occurs in humans) meaning that the trunk and tail regions of the fish did not receive any blood (Peterson et al., 2004). After screening a library of compounds to find suppressors of this mutation, two novel compounds were identified that could rescue this phenotype, presenting potential therapies for humans suffering from this condition (Peterson et al., 2004).

Additionally, in a zebrafish embryo screen performed by Jung and colleagues the compound PPA was used to induce a hyperpigmentation phenotype in zebrafish embryos (Jung et al., 2005). Initial biochemical studies revealed that PPA affected the ATPase synthase pathway (Jung et al., 2005). Therefore, a zebrafish embryo screen was performed to identify inhibitors of this pathway (Jung et al., 2005). Novel inhibitors were identified from this screen which could attenuate this phenotype, representing potential therapies for sufferers of hyperpigmentation disorders (Ni-Komatsu and Orlow, 2007).

The advent of high throughput screening techniques has meant that drug screens can now be automated at every stage of the process by using embryo sorting robots, liquid handling robots and automated imaging/analysis tools.

The first high throughput screen utilising zebrafish embryos was an organ-specific screen developed by Burns and colleagues where the myocardium was labelled with the green

fluorescent protein (GFP) (Burns et al., 2005). Using automated video monitoring and custom-written video analysis scripts, the heartbeats of the zebrafish embryos in each well could be automatically determined (Burns et al., 2005). Hence, small molecules could then be screened in 96 well plates to see how they modulated the heart rate (Burns et al., 2005).

With the latest technological developments and the growing understanding of the zebrafish embryo the number of high throughput screens has increased (Gerlai, 2010)(Pardo-Martin et al., 2010)(George et al., 2011)(Ishaq et al., 2013)(Veneman et al., 2013)(Lin et al., 2013). This number will keep on increasing and in the future many screens may only require minimal manual input.

1.3 Solubility and penetration of compounds into zebrafish embryos

To determine whether a compound will diffuse readily into a zebrafish embryo and distribute to its target, the logP (logarithm of the partition ratio between octanol and water) can be calculated based on the chemical structure of the compound or by empirical measurement (Taylor et al., 2010).

At early developmental stages the chorion can be a barrier to diffusion of large molecules, as the chorion has pores of a certain size and so very large and bulky molecules may not be able to penetrate into the zebrafish embryo (Milan et al., 2003). These compounds tend to have logP values <1 and are most commonly either weak acids or bases (Milan et al., 2003). However, the problem of penetration can be overcome by: 1) injecting compounds directly into the zebrafish embryos immediately after fertilization, 2) by injecting the compounds

directly into the blood circulation of zebrafish embryos at later stages of development or 3) by dechorionating the zebrafish embryos either manually or with an enzyme before performing drug treatments (Milan et al., 2003). Generally, for drug screening zebrafish embryos in their chorions are used, as microinjection and dechorionation techniques are more time consuming and therefore not feasible when screening thousands of compounds. Additionally, for poorly water soluble highly hydrophobic compounds DMSO can be used as a solubilisation aid (Milan et al., 2003).

In studies carried out by Milan and colleagues and Sachidanandan and colleagues compounds with logP values >1 were found to be absorbed readily in zebrafish embryos (Milan et al., 2003)(Sachidanandan et al., 2008). Additionally, bioanalysis studies have confirmed that compounds with logP values >1 have better uptake into zebrafish embryos, as they are more lipophilic in nature (Alderton et al., 2010).

In humans even after a compound has entered the circulation, the compound may bind to plasma proteins affecting the amount of free compound still available (Wood, 1986). Generally, compounds that are weak bases will bind α1-glycoprotein and compounds that are weak acids will bind albumin (Wood, 1986). Furthermore, in zebrafish there may be the possibility that some compounds bind to yolk sac proteins, therefore limiting the amount of free drug available. Additionally, pKa is also an important factor that needs to be taken into consideration regarding drug penetration, as the pH can influence the amount of free drug available. In the gastrointestinal tract the pH gradients can have a strong impact on the

uptake of compounds and therefore lead to differences in uptake between humans/mammals and zebrafish.

The only method to determine accurately the amount of free drug is to carry out bioanalysis of samples and measure the parent drug and metabolite levels both inside and outside the zebrafish (Alderton et al., 2010). Such approaches are currently being explored and implemented into zebrafish screens, as they enable pharmacokinetic aspects to be investigated (Alderton et al., 2010) (Diekmann and Hill, 2013).

Pharmacokinetics differ greatly between zebrafish embryos and mammals due to the different exposure routes employed. Zebrafish embryos undergo constant water-borne drug exposure and receive drugs mainly by dermal diffusion, whereas mammals are exposed to drug as a single dose either orally, dermally or via inhalation, thereby relying on intestinal absorption or intravascular delivery. In zebrafish embryos the liver is by-passed and the drug directly enters the systemic circulation. As in mammals drugs are most commonly administered orally there is potential for extensive drug metabolism to occur in the liver (first-pass metabolism) before it reaches the systemic circulation (Julkunen et al., 1985). This is because after oral administration the drug needs to pass through the digestive tract into the hepatic portal system where the drug is then transported to the liver (Julkunen et al., 1985). With certain drug types first pass effects can lead to either increased risk of toxicity or reduced risk of toxicity.

An additional effect that can also occur is enterohepatic circulation where the drug passes through the liver into the intestine, is absorbed by enterocytes and then travels back to the liver again (Roberts et al., 2002). This can occur with certain types of drugs and can lead to an increase in the drug half-life which can be potentially dangerous (Roberts et al., 2002).

The differences in exposure routes make it difficult to extrapolate drug effects from zebrafish embryos to mammals. To determine whether the different exposure routes lead to differences in internal drug concentrations it would be particularly useful to determine pharmacokinetic parameters. These include the area under the curve (AUC) which reflects the exposure of the body to the drug, the C_{max} which represents the peak plasma concentration and the elimination rate constant k_e which represents the time taken for the drug to be cleared from the body. Determining such parameters in zebrafish embryos could aid extrapolation.

1.4 Zebrafish embryo drug metabolism

Drug metabolism involves two phases, namely phase 1 and phase 2 reactions (**Figure 1.4**). In phase 1 reactions, compounds are either inactivated/activated by CYP enzymes (haem-containing mono-oxygenases) or by non-CYP enzymes, e.g. alcohol/aldehyde dehydrogenases, peroxidases, xanthine oxidase, mono/diamine oxidases, aromatases and flavin mono-oxygenases (Roberts, 2005). In phase 2 reactions, these intermediary metabolites are then conjugated to glutathione (glutathione S-transferase) or glucuronic acid (uridine diphosphate [UDP] glucuronosyl transferases), acetylated (N-acetyl transferases), sulphated (sulphotransferases) or methylated (methyltransferases) so that

they can then be excreted more easily (Roberts, 2005). Occasionally, a phase 3 reaction may also occur where phase 2 metabolites are further metabolised (e.g. conversion of glutathione conjugates to acetyl cysteine conjugates) (Goldstone et al., 2010).

Additionally, in humans polymorphic variants of CYP enzymes (e.g. CYP2D6) and also phase 2 enzymes (e.g. N-acetyl transferases) exist, meaning that in some individuals drug metabolism may be faster and in others it may be slower. It is therefore important to take this into consideration when creating new drugs in order to prevent toxicity and the development of ADRs (Dorne et al., 2003).

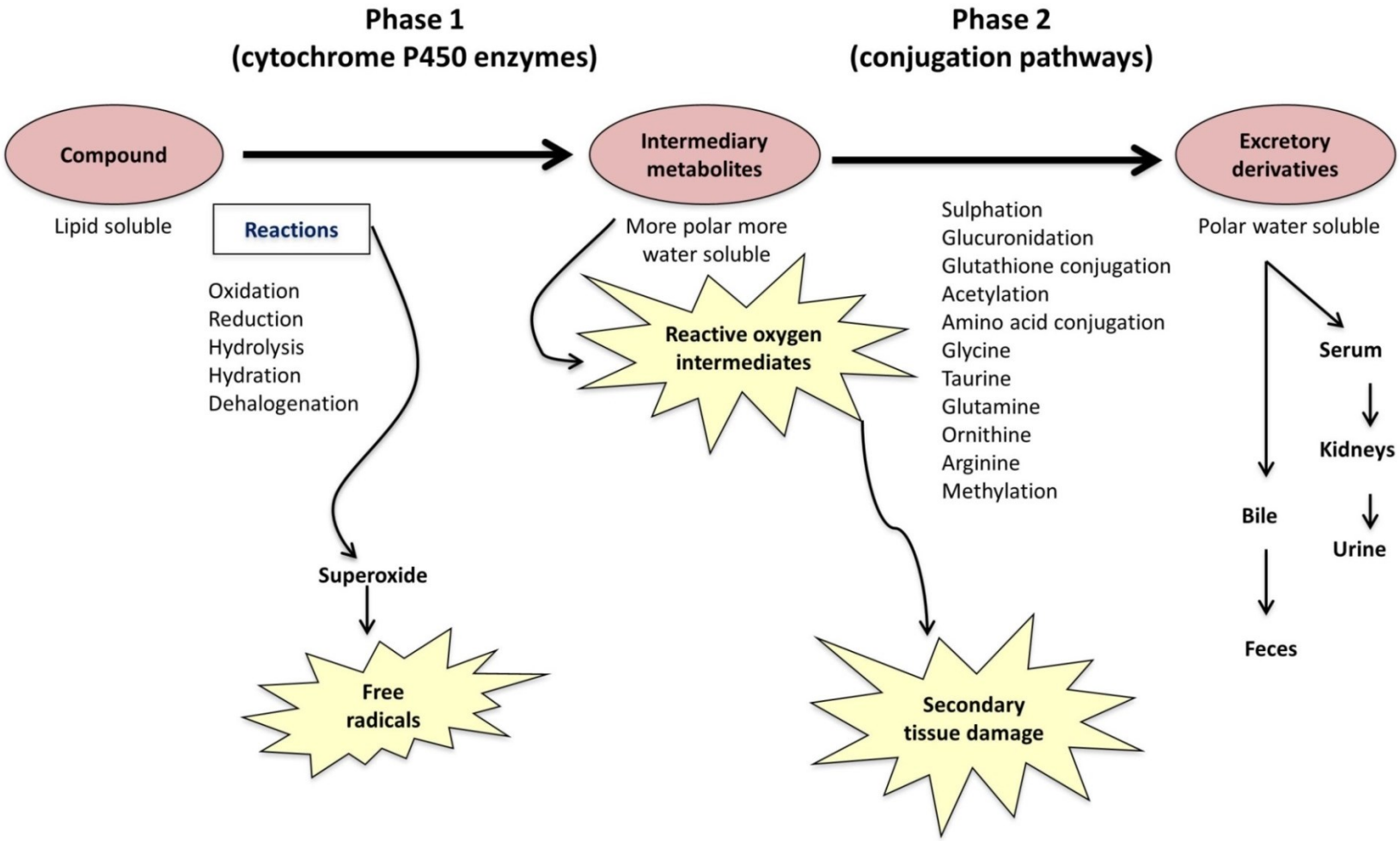

Figure 1.4 – Summary of phase 1 and phase 2 reactions that occur in humans. *Compounds undergoing phase 1 and phase 2 metabolism can form metabolites that are unreactive which can be safely excreted from the body or they can form toxic metabolites, such as reactive oxygen intermediates or free radicals which can cause cell or tissue damage.*

Zebrafish embryos and larvae have been shown to be able to perform both phase 1 and phase 2 reactions (Alderton et al., 2010). Non-CYP phase 1 enzymes, such as monoamine oxidase and alcohol/aldehyde dehydrogenase have also been identified in zebrafish embryos (Alderton et al., 2010).

Compared to rodents, zebrafish metabolism has not been as extensively characterised. There is more data for phase 1 reactions compared to phase 2 reactions. It has been found that in total zebrafish have 94 CYP enzymes (Goldstone et al., 2010). CYP families 5 to 51 have mainly endogenous functions (steroidogenic and hydroxylase enzymes), however these CYPs share the most sequence similarity to humans and account for a third of the total CYPs found in zebrafish (Goldstone et al., 2010). CYP families 1 to 3 are much more complex; however these include the main enzymes involved in drug metabolism (Goldstone et al., 2010). There are fewer orthologues of human CYPs in the zebrafish CYP families 1 to 3 and particularly CYP family 2 has many more genes compared to humans, as well as a few clusters unique to zebrafish (e.g. CYP2J1) (Goldstone et al., 2010)(Alderton et al., 2010). Additionally, it has been found that expression of CYP genes in the zebrafish embryo is highly dependent on developmental stage with different CYP genes beginning expression at different developmental time points (Goldstone et al., 2010). CYP1A1 has been most extensively studied in zebrafish and it has been found to be induced in both embryonic and adult stages (Spitsbergen and Kent, 2003). The similarity in CYP enzymes between zebrafish and humans means that the zebrafish represents a good model to study CYP-mediated drug metabolism. For example, the classic metabolic conversion of phenacetin to paracetamol by CYP1A2 in humans is also replicated in zebrafish embryos (Alderton et al., 2010).

Additionally, classical drug-drug interactions such as those seen between cimetidine and terfenadine also occur in zebrafish with cimetidine potentiating the effects of terfenadine by inhibiting CYP3A4 (Milan et al., 2003). CYP3A4 accepts a variety of substrates and is responsible for the metabolism of around 50% of marketed drugs (Dorne et al., 2003).

In terms of phase 2 reactions, the zebrafish is able to carry out sulphation via cytosolic sulphotransferase and has also been found to carry out glucuronidation and glutathione conjugation (Goldsmith, 2004)(Alderton et al., 2010). However, phase 2 metabolism does show some differences to humans, as fish have lower glucuronosyl activity (Alderton et al., 2010). For example, cisapride metabolism in zebrafish yields a main metabolite that is found only in minor quantities in dogs and there is no evidence of zebrafish producing glucuronide metabolites commonly seen in humans following cisapride exposure (Alderton et al., 2010). Therefore, these species specific differences need to be taken into account when extrapolating results to humans.

Additionally, in the zebrafish genome 41 ATP-binding cassette (ABC) transporters have been identified (Dean and Annilo, 2005)(Scholz et al., 2008). ABC transporters are important for getting drugs out of the cell (drug efflux) but require adenosine triphosphate (ATP) for transport, as the energy generated from the hydrolysis of ATP is required to drive the transport process (Brinkmann and Eichelbaum, 2001). Examples of ABC transporters include multi-drug resistance protein 1 (MDR1) which has been extensively studied as its over-expression can hinder drugs getting into a cell to exert an effect (Brinkmann and Eichelbaum, 2001)(Bresolin et al., 2005). Influx transporters, such as the divalent metal transporter 1

(DMT-1), which transports iron into the cell does not require energy and has also been found to be expressed in zebrafish embryos (Donovan et al., 2002). Therefore, it is also possible to study drug entry and exit in the zebrafish embryo.

1.5 Toxicity

The main reason for drug failures during the drug development process is toxicity. Toxicity can be restricted to specific organs or can affect the whole body. Every compound has the potential to be toxic, but it is the dose that defines whether a compound is toxic or not. Toxicity can be caused by parent compounds themselves or chemically reactive intermediates which are formed following metabolism (Gillette et al., 1974). The toxicity of compounds can be divided into eight general groups based on their modes of action (MOA). These eight groups include group 1 (non-polar narcosis), group 2 (polar narcosis), group 3 (uncoupling of oxidative phosphorylation), group 4 (inhibition of the acetylcholinesterase enzyme), group 5 (reactive toxicity), group 6 (glutathione depletion), group 7 (estrogenic activity) and group 8 (drug-induced auto-immunity) (Verhaar et al., 1996)(Nendza and Wenzel, 2006).

Group 1 compounds are non-reactive and have no specific target causing baseline toxicity, which is non-specific toxicity caused by compounds partitioning into biological membranes interfering with membrane structure and function (Nendza and Wenzel, 2006)(Su et al., 2014). Baseline toxicity can be predicted from logP (also known as logKow), which is the octanol-water partition coefficient (Su et al., 2014). A compound with a high logP value is more likely to partition into a biological membrane to cause unspecific effects and

depression of biological activity (narcosis) (Su et al., 2014). An example of a compound that belongs to this group is 1,4-dichlorobenzene (Su et al., 2014).

Group 2 compounds (polar narcotics) like group 1 compounds are not reactive but are slightly more toxic due to hydrogen bond donor acidity (Su et al., 2014)(Ramos et al., 1998). Phenol is an example of a group 2 compound (Nendza and Wenzel, 2006).

Group 3 compounds include compounds which have specific effects on oxidative phosphorylation (process by which ATP is generated) (Nendza and Wenzel, 2006). For example, oligomycin inhibits the ATP synthase enzyme and stops protons flowing through the Fo sub-unit (Terada, 1990).

Group 4 compounds specifically target the acetylcholinesterase enzyme, which has an important function at neuromuscular junctions by terminating synaptic transmissions. The organophosphate (OP) insecticide malathion is a compound that specifically inhibits the acetylcholinesterase enzyme preventing hydrolysis of acetylcholine (Krstić et al., 2008).

Group 5 compounds cause toxicity due to their highly reactive nature. Acrolein is a group 5 compound which is a highly reactive electrophile that binds to and depletes cellular nucleophiles such as glutathione (Kehrer and Biswal, 2000). Acrolein also readily reacts with nucleophilic sites in DNA and with cysteine, lysine and histidine residues of proteins via sulphydryl alkylation (Gillette et al., 1974). Acrolein can also initiate lipid peroxidation, which is a secondary process where lipid radicals are formed that can damage cell membranes

(Kehrer and Biswal, 2000). Nitrobenzaldehyde is another compound that falls into this group (Ramos et al., 1998).

Group 6 compounds cause glutathione depletion. Glutathione, as mentioned previously conjugates reactive intermediates. Glutathione is therefore an important cellular protector and when its levels are reduced, toxic insult can occur (Gillette et al., 1974). Paracetamol metabolism leads to the formation of a reactive intermediate N-acetyl-p-benzoquinone imine (NAPQI) (Gillette et al., 1974). At therapeutic paracetamol doses, this reactive intermediate is removed from the body by conjugation with glutathione (Gillette et al., 1974). Glutathione is a scavenger of free radicals (Gillette et al., 1974). Free radicals include superoxide, nitric oxide, trichloromethyl, thiyl and hydroxyl radicals (Halliwell and Chirico, 1993). These free radicals will act in a chain reaction by removing/adding an electron to biological molecules converting them in the process to radicals as well (Halliwell and Chirico, 1993). Additionally, hydrogen peroxide can also cause direct cellular damage at high levels (Halliwell and Chirico, 1993). To control levels of these reactive species (free radicals and hydrogen peroxide), the cell has several anti-oxidant defence mechanisms which include the enzymes superoxide dismutase (converts superoxide radical to hydrogen peroxide) and catalase/glutathione peroxidase (converts hydrogen peroxide to water) (Halliwell and Chirico, 1993). When levels of these enzymes are low or the generation of reactive oxygen species (ROS) is high, the result will be cellular damage particularly to mitochondria, as free radicals can perturb mitochondrial respiration (Halliwell and Chirico, 1993).

Group 7 compounds are those that affect the estrogen receptor. These compounds are able to mimic natural estrogens, thereby disrupting the endocrine functions of the estrogen receptor leading to malformations of the reproductive tract, as well as reduced fertility (Gould et al., 1998). Bisphenol A is an example of a group 7 compound, as it binds to the α sub-unit of the estrogen receptor resulting in altered estrogenic activity that can lead to sexual dysfunction in humans (Gould et al., 1998).

Compounds from group 8 cause toxicity by binding to proteins in the body and forming a new entity, a hapten (Olsen, 2004). This hapten is recognised as foreign by the immune system eliciting an auto-immune response, such as in the case of minocycline-induced auto-immunity (Olsen, 2004).

1.5.1 Selective toxicity

Metabolism of compounds mainly occurs in the liver. However, some compounds are metabolised only in certain regions of the body where a specific enzyme or target is present. This can in some instances lead to increased toxicity, such as in the case of allylamine, which is converted by amine oxidase to acrolein and hydrogen peroxide in the heart (Nelson and Boor, 1982).

Many compounds that have toxic effects are often metabolised to reactive intermediates, such as in the case of paracetamol, benzo[a]pyrene and benzene (Thakker et al., 1977)(Bolton et al., 2000). However, compounds can also cause toxicity due to them being structurally similar to key endogenous compounds. This is seen with polyporic acid from the

mushroom *Hapalopilus rutilans* that specifically inhibits dihydroorotate dehydrogenase, the enzyme responsible for the production of uridine triphosphate (UTP) (Kraft et al., 1998). Inhibition of UTP synthesis leads to severe clinical effects in humans, as UTP is an important source of energy and an activator of substrates for metabolic reactions (Kraft et al., 1998).

1.5.2 Species specific differences in toxicity

The toxicity of compounds as mentioned previously can differ between species. This is because of differences in toxicokinetics. For example chocolate is particularly toxic to dogs and cats, as it contains the methylxanthine theobromine which can lead to symptoms such as vomiting and tachycardia (Dvorakova and Zapletal, 2001). This is due to the slow rates of CYP metabolism in these two animals compared to humans (Dvorakova and Zapletal, 2001).

For phase 2 reactions the differences between species is most pronounced. For example, the glucuronidation rate in birds is comparable to humans; however in fish and cats glucuronosyl transferase activity is lower (around 10-fold less) (Hayes, 2001). These differences in metabolism are therefore important to consider when evaluating the effects of compounds in animals and extrapolating their effects to humans.

Differences in exposure routes between zebrafish embryos and mammals also contribute to species specific differences. This is because the different exposure routes could lead to differences in internal drug concentrations. It has been shown that if *in vitro* LC50 values are compared to plasma concentrations at the LC50 (LC50plasma), a much better correlation can

be obtained (Ekwall et al., 1998) (Sjöström et al., 2008). Therefore, it may better to determine internal drug concentrations before making comparisons.

1.5.3 The zebrafish embryo as a toxicological model

As mentioned previously, the zebrafish embryo has several advantages over other animal models which makes it particularly suited to drug screening applications, especially for toxicological investigations. The optical transparency of the zebrafish embryo means that simple visual assessments for toxicity can be performed using a light microscope without the need for expensive or complicated equipment. There is also a high similarity in the toxic responses after chemical exposure (e.g. cadmium and methyl mercury chloride) between zebrafish and mammals, particularly on a gene expression level (Yang et al., 2007). This therefore highlights the suitability of the zebrafish embryo as a model for toxicity testing.

There is a high demand to use ethically acceptable alternative testing methods to assess the toxic risk of new chemicals (e.g. pharmaceuticals, waste products and industrial solvents) within the European union (EU) to comply with the 'Registration, Evaluation and Authorisation of Chemicals' (REACH) initiative which aims to reduce testing on vertebrates (Scholz et al., 2013).

The zebrafish embryo acute toxicity test (ZFET) has recently been implemented into the 'Organisation for Economic Co-operation and Development' (OECD) test-guidelines and is now available as OECD test guideline 236 (Busquet et al., 2014). A validation study of this new guideline was performed where 20 chemicals were tested in zebrafish embryos at five

different concentrations in three independent runs and in at least three different laboratories (Busquet et al., 2014). The zebrafish embryos were exposed to the chemicals for 96 hours with 20 zebrafish embryos tested per concentration/control (Busquet et al., 2014). Acute lethality was used as an endpoint with four indicators used to confirm lethality, namely non-detachment of the tail bud from the yolk sac, lack of heartbeat, lack of somite formation and coagulation of the embryo (Busquet et al., 2014). The results obtained showed good reproducibility within and between laboratories (Busquet et al., 2014). However, for more toxic chemicals and those chemicals tested close to their solubility limit the reproducibility was lower (Busquet et al., 2014). Additionally, in a study performed by Berlanger and colleagues the ZFET test was found to have a high predictive power for predicting the acute toxicity of fish to new chemicals (Belanger et al., 2013).

Toxicity can be quantified and compared between species by determining toxicity endpoints. These include LC50 (concentration of compound which is lethal to 50% of the tested population), EC50 (concentration of compound which has an effect in 50% of the tested population), NOEC (no observed effect concentration) and LOEC (lowest observed effect concentration). In a study performed on 60 water-soluble compounds by Ali and colleagues the zebrafish embryo logLC50 values that were calculated were found to show high similarity to rodent logLD50 values (Ali et al., 2011). These findings are quite unexpected considering the differences in exposure routes between zebrafish and rodents. Additionally, the study by Ali and colleagues also showed that compound class significantly influenced toxicity where for example alcohols were found to be less toxic in zebrafish compared to rodents (Ali et al., 2011).

1.6 Multivariate analysis

Multivariate analysis is a useful technique when interpreting and analysing large datasets with many variables, such as toxicity data where there are multiple toxicity endpoints.

1.6.1 Principal component analysis

Principal component analysis (PCA) is a method used to identify patterns in large datasets with multiple variables. PCA reduces the dimensionality of the data (i.e. the number of variables); creating a new coordinate system where principal component 1 points in the direction of the data where there is the highest spread (variance), as shown in **Figure 1.5**. Principal component 2 is plotted orthogonal to principal component 1 and shows the second highest spread in the data. More components can then be added to show further variance within the data.

Once a PCA analysis has been performed two plots are created, the first one is the scores plot and the second one is the loading plot. The scores plot shows the observations (samples) and the loading plot the variables. The scores are representative of the distance of the observations from the origin with scores located in the centre of a scores plot having no influence on the model. Scores that are close to one another show high similarities compared to those that are far apart. Variables that are close together on the loading plot co-vary and show dependency on one another. The score and loading plots are interpreted by superimposing them. This way it is possible to identify relationships/patterns between observations and variables. The closer a score is to a variable the higher a value it has for that variable. When using bimodal plots, the scores and loadings are automatically

superimposed on one plot. For all multivariate analysis models including PCA models the R^2X and Q^2 values determine the dispersion and stability of the data. A model with an R^2X value >0.7 and a Q^2 value >0.4 is deemed to be of good quality.

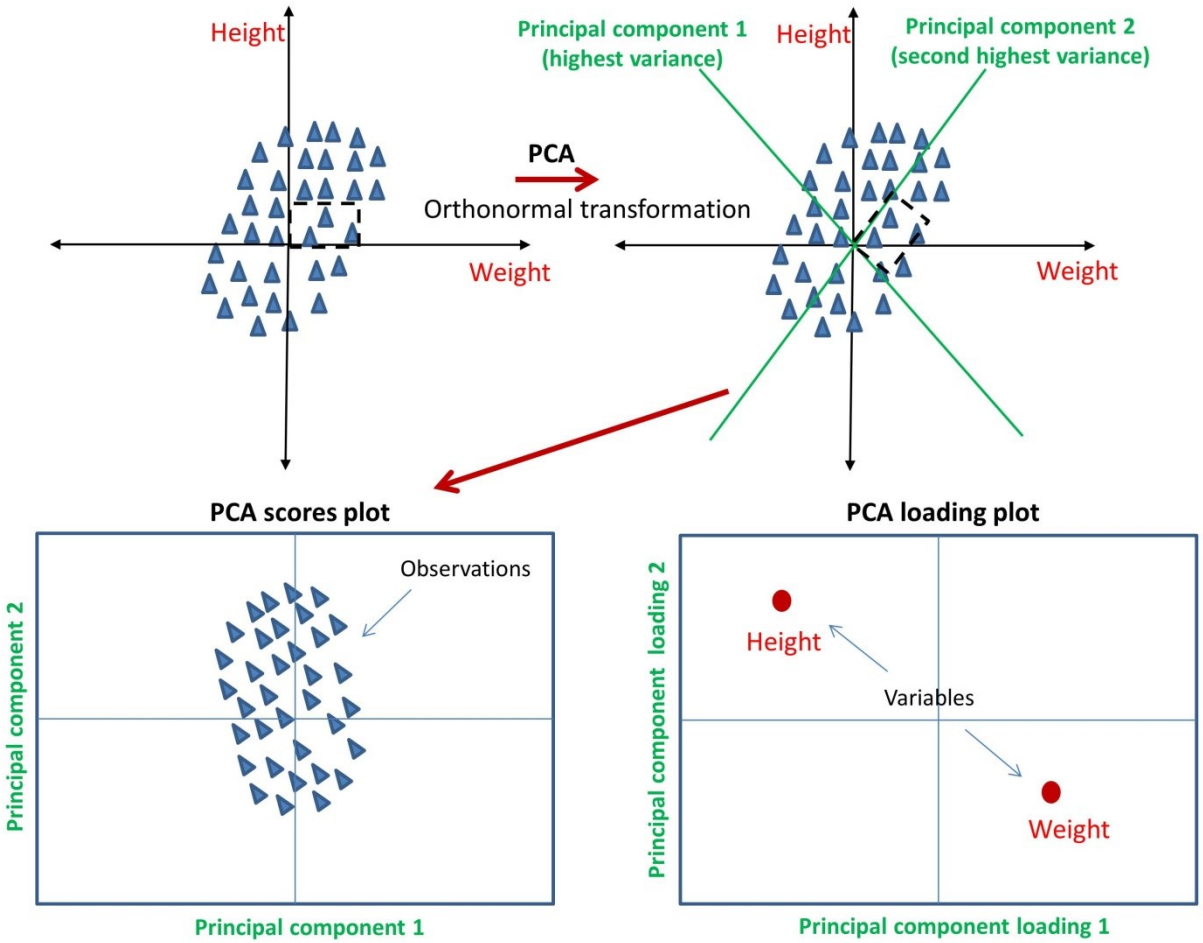

Figure 1.5 – Basis of principal component analysis (PCA). *PCA creates a new coordinate system where the principal components pass through the data where there is the highest variance. Key: blue triangles = observations (obtained data), red circles = variables*

1.6.2 Partial least squares

Partial least squares (PLS) is a method for regression analysis and thus can be used to model the relationship between variables X and Y, as well as predict new values for Y. This makes PLS particularly useful for quantitative structure activity relationship (QSAR) modelling, as for example the X variables (physiochemical descriptors of compounds) can be used to predict

the Y variables (biological effects of compounds). The aim of PLS is to reduce the dimensionality of the data and maximise the covariance between the X-scores designated T and the Y-scores designated U, as shown in **Figure 1.6**. The first PLS component is represented by two lines. The first line is within the X-space and in the direction w1 (X-weight forms the matrix w1). The second line is within the Y-space and in the direction c1 (Y-weight forms the matrix c1). The second PLS component is also represented by two lines and similarly to the first component one line is in the direction w2 and the other in the direction c2. Additional components are added to improve the model as much as possible.

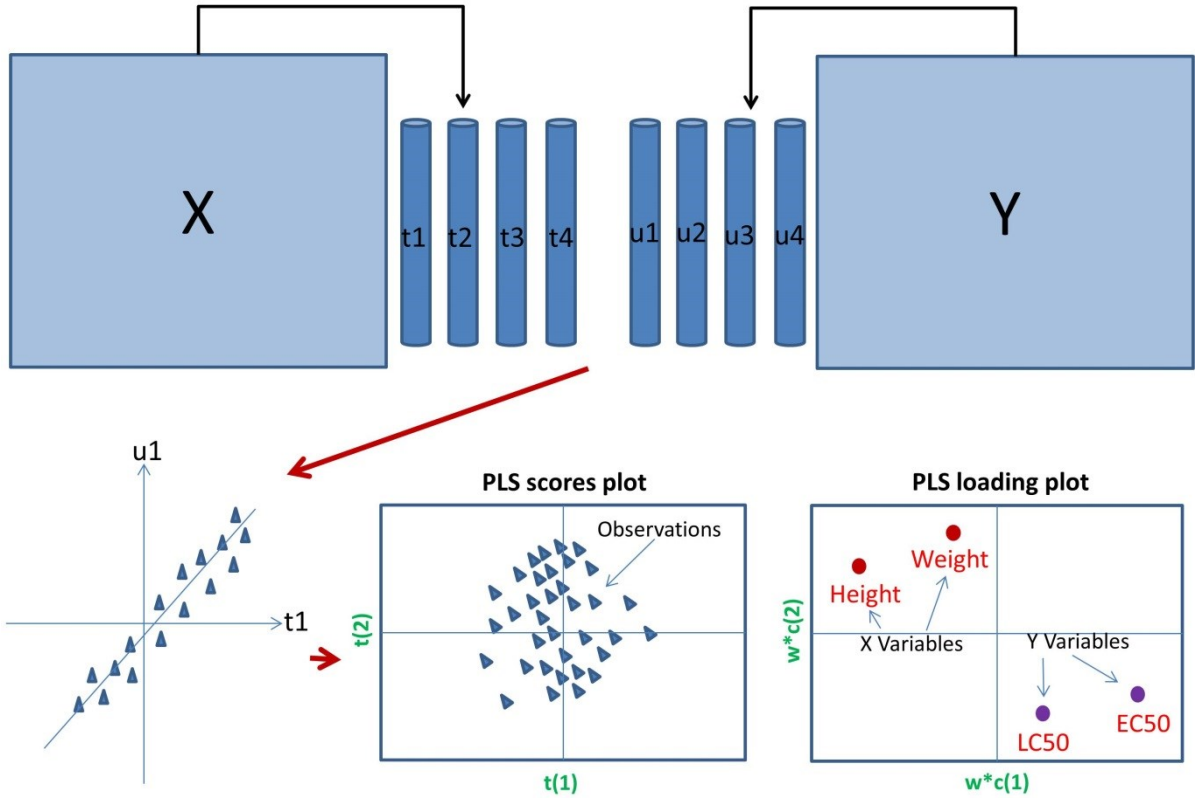

Figure 1.6 - Transformation of data with multiple X and Y variables into a two dimensional representation using partial least squares (PLS). *PLS enables co-variance between X and Y to be investigated when there are multiple X and multiple Y variables. Key: X-scores = T, Y-scores = U, X-weights = w, Y-weights = c, blue triangles = observations, red circles = variables*

Orthogonal partial least squares (PLS) is an extension of PLS where an orthogonal signal correction is applied to remove variation that has no direct relation to the responses observed (Sadeghi-Bazargani et al., 2010).

In a standard PLS the Y vector can be anywhere relative to X. In OPLS modelling however the Y vector is placed in alignment with the first component in the X matrix, as shown in **Figure 1.7**. This separates the correlated and uncorrelated variables. The X and Y loadings are represented by p and q, respectively on an OPLS loading plot.

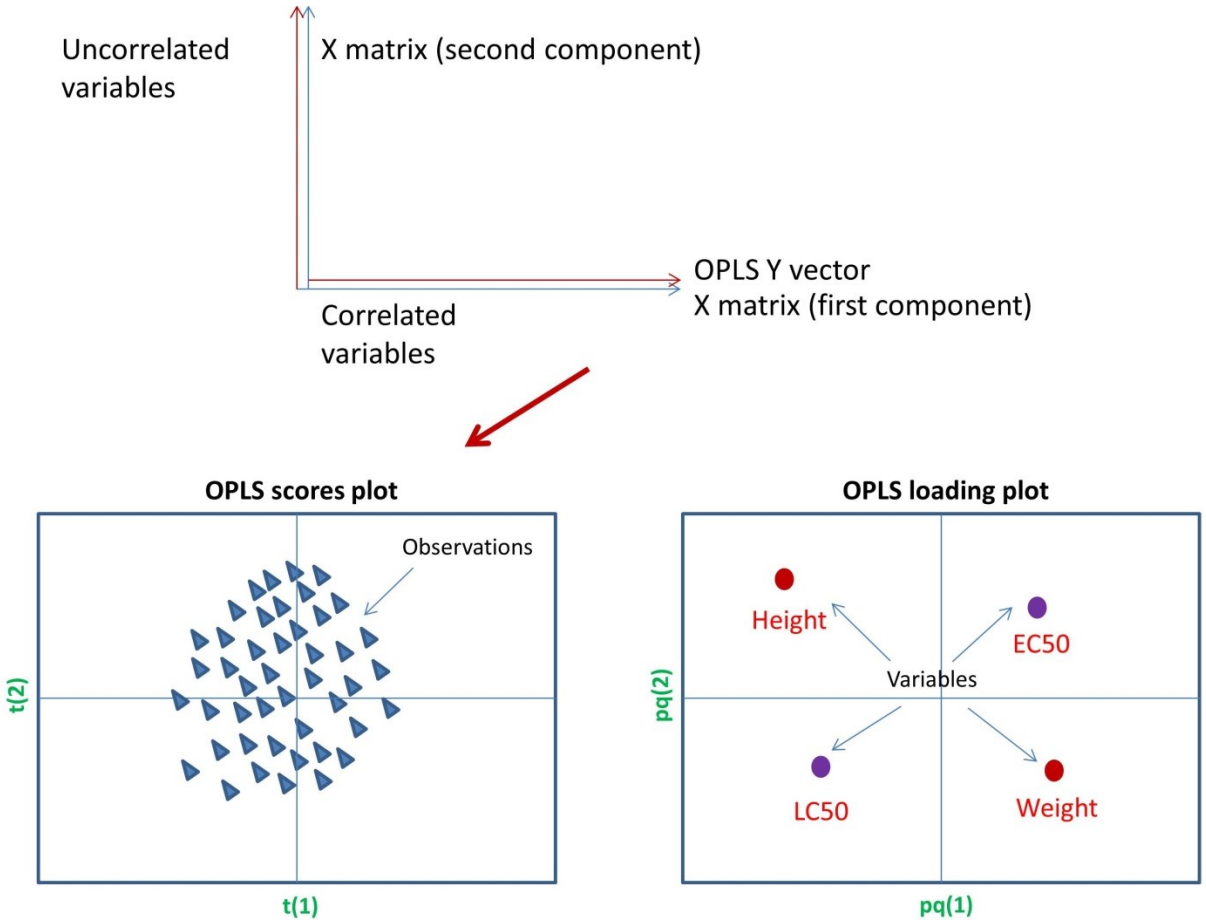

Figure 1.7 – Transformation of data with multiple X and Y variables into a two dimensional representation using orthogonal partial least squares (OPLS). *OPLS enables correlated variables to be distinguished from correlated variables aiding interpretation of the models created. Key: X-scores = T, Y-scores = U, X and Y loadings = pq, blue triangles = responses, purple circles = biological endpoints, red circles = biological variables*

Hierarchical OPLS models are an alternative to conventional OPLS models where the principal components derived from an initial PCA analysis are used as the Y values.

Another variation of OPLS is OPLS-Discriminant Analysis (DA). In OPLS-DA the distinctions between two different groups can be easily made. This is because OPLS-DA is able to separate the variation which is predictive from that which is not (Bylesjö et al., 2006). Discriminant analysis can also be combined with PLS (**Figure 1.8A**), but OPLS-DA models are preferred as they enable much clearer visualisation of differences (**Figure 1.8B**).

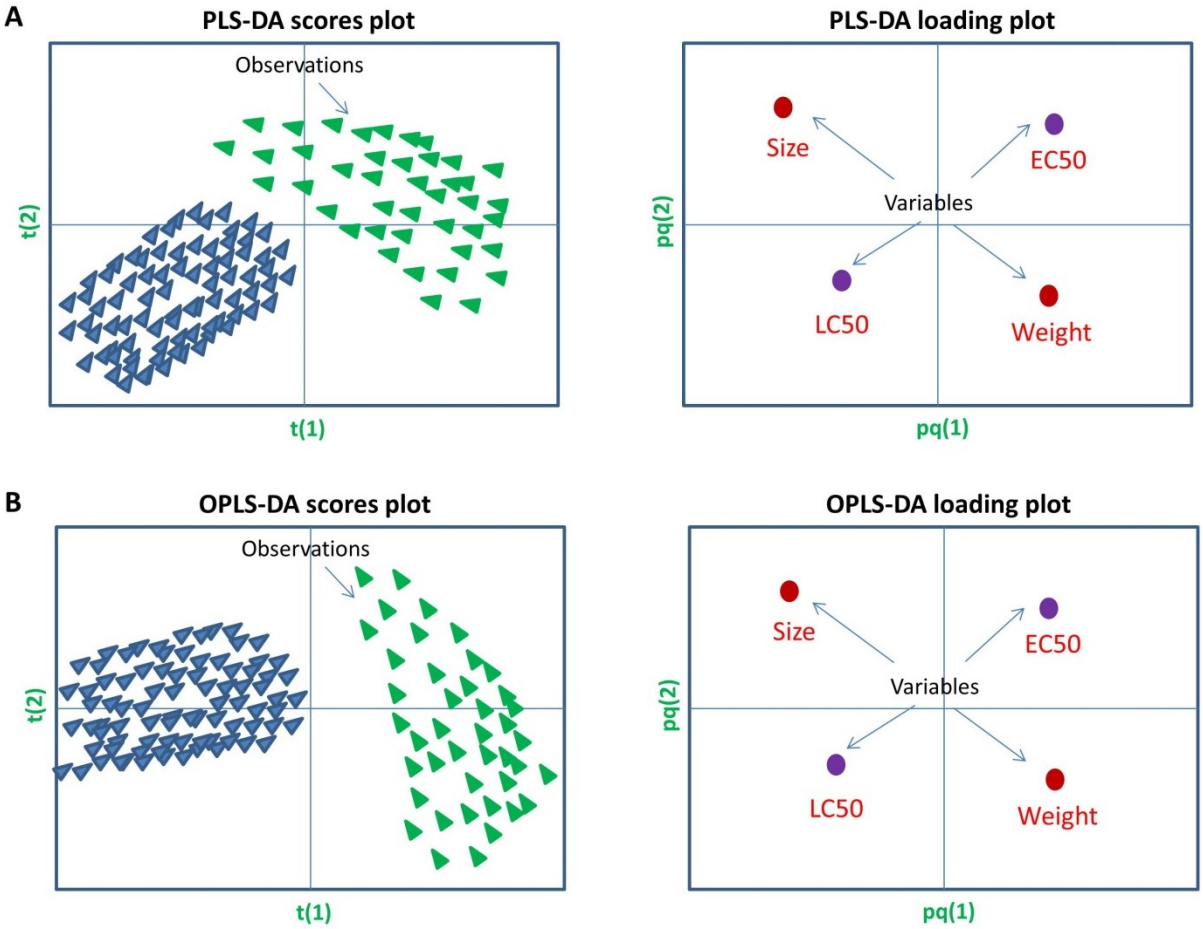

Figure 1.8 – Comparison of PLS-DA and OPLS-DA models. *A) PLS-DA scores and loading plots, B) OPLS-DA scores and loading plots. OPLS-DA enables clear differences between different groups of observations to be observed. Key: X-scores = T, Y-scores = U, X and Y loadings = pq, blue triangles = responses, purple circles = biological endpoints, red circles = biological variables*

1.7 Aims of thesis

In recent years, the pressure on pharmaceutical companies has increased to produce new drugs, which are safe, effective and commercially valuable. However, the drug development process takes a long time and costs a lot of money, thus it is of upmost importance to eliminate drug candidates with the potential to produce toxicity in humans early on in the drug development process. Specifically, organ-specific toxicities which are difficult to detect as they are rare and occur sporadically present a particular problem. Cardiotoxicity presents one of the highest causes of drug failure in drug development. Currently, there is no gold standard model to detect this. Therefore, in this thesis I aimed to develop a cardiotoxicity screening tool using the zebrafish embryo as a model organism. The aim was to develop a screening tool which could also be up-scaled and thus had the capability to be used routinely in pre-clinical testing routines in the future. Another aim of this thesis was to evaluate the zebrafish embryo as a model for assaying biological activity of novel compounds, as well as to develop an innovative predictive tool that could be used to predict the toxicity of novel compounds. The final aim of this thesis was to evaluate the zebrafish embryo as a model for therapeutic drug screening using a high throughput anti-inflammatory screening tool.

Chapter Two: MATERIAL AND METHODS

2.1 Materials

2.1.1 Chemicals

Only chemicals purchased outside of the laboratory are listed (**Table 2.1**). Standard chemicals used in the laboratory, such as solvents (e.g. ethanol) are not listed.

Table 2.1 – Chemicals used for experiments.

Chemical	**Source**
Gentamycin sulphate (BP918-1)	Fisher Scientific, Loughborough, UK
Paraformaldehyde reagent grade (P6148-1KG)	Sigma-Aldrich, Poole, UK & Munich, Germany
Oil red O (O0625-25G)	Sigma-Aldrich, Poole, UK
N-Phenylthiourea (P7629-25G)	Sigma-Aldrich, Poole, UK
Dimethyl sulfoxide (D8418-100ML)	Sigma-Aldrich, Poole, UK & Munich, Germany
Dulbecco's phosphate buffered saline (PBS) (D5662-1L)	Sigma-Aldrich, Munich, Germany & Poole, UK
Tween 20 (P1379-250ML)	Sigma-Aldrich, Poole, UK & Munich, Germany
Ethyl-3-aminobenzoate methane sulfonate (MS222/MESAB) (E10521-10G)	Sigma-Aldrich, Poole, UK
Hydrogen peroxide solution (216763)	Sigma-Aldrich, Munich, Germany
Potassium acetate (98%) (W292001-10KG)	Sigma-Aldrich, Munich, Germany
Sudan black B staining reagent (380B-1KT)	Life technologies, Darmstadt, Germany
Verapamil hydrochloride (0654)	Tocris Bioscience, Bristol, UK
Cromakalim (1377)	Tocris Bioscience, Bristol, UK
Penicillin G sodium salt (P3032)	Sigma-Aldrich, Poole, UK
Haloperidol (H1512-5G)	Sigma-Aldrich, Poole, UK
Pimozide (P1793-500MG)	Sigma-Aldrich, Poole, UK
(-)-Blebbistatin (B0560-1MG)	Sigma-Aldrich, Poole, UK
(+)-Tubocurarine chloride pentahydrate (P3750-250MG)	Sigma-Aldrich, Poole, UK
2,3-Butanedione monoxime (B0753)	Sigma-Aldrich, Poole, UK
Trypan blue solution 0.4% (T8154)	Sigma-Aldrich, Poole, UK
Low melting point agarose (35-20100)	PEQLAB Biotechnologie, Erlangen, Germany
TWEEN® 20 (P5927)	Sigma-Aldrich, Munich, Germany
Potassium hydroxide (03564 Fluka)	Sigma-Aldrich, Munich, Germany
Methylene blue solution (03978)	Sigma-Aldrich, Munich, Germany & Poole, UK

Unscented paraffin wax (327204)	Sigma-Aldrich, Poole, UK
Propylene Glycol (134368)	Sigma Aldrich, Poole, UK
Sodium acetate (S7899-100ML)	Sigma Aldrich, Poole, UK
Acridine Orange (A6014-10G)	Sigma Aldrich, Poole, UK
SYTOX® blue nucleic acid stain (S11348)	Sigma-Aldrich, Munich, Germany
Copper II sulphate pentahydrate (1027871000)	Merck Millipore, Darmstadt, Germany

2.1.1.1 28 Reference compounds

The 28 marketed reference drugs used in this thesis are listed in **Table 2.2**.

Table 2.2 – List of 28 reference compounds used.

Compound name	Supplier	Order code	CAS no.	LogP	pKa
Amantadine hydrochloride	Sigma-Aldrich	A1260-5G	768-94-5	2.5	10.7
Amiloride hydrochloride	Axxora Llc	LKT-A5133-M500	2609-46-3	-0.3	8.7
Bendroflumethiazide	Fluka Sigma-Aldrich	B5775-1G	73-48-3	1.9	8.5
Captopril	Calbiochem®	211875-1GM	62571-86-2	0.3	4.0
Carbamazepine	Sigma-Aldrich	C4024-1G	298-46-4	2.5	16.0
Chlorprothixene hydrochloride	Sigma-Aldrich	C1671-1G	6469-93-8	5.2	9.8
Chlorzoxazone	Sigma-Aldrich	C4397-25G	95-25-0	1.6	9.4
Erythromycin	Sigma-Aldrich	E5389-1G	114-07-8	3.1	8.9
Fenofibrate	Sigma-Aldrich	F6020-5G	49562-28-9	5.3	-4.9
Flupenthixol dihydrochloride	Tocris Bioscience	4057	2413-38-9	4.5	15.6
Folic acid	Sigma-Aldrich	F8798-5G	59-30-3	-2.5	3.4
Glipizide	Sigma-Aldrich	G117-500MG	29094-61-9	1.9	5.9
Hydrochlorothiazide	Sigma-Aldrich	H2910-5G	58-93-5	-0.1	7.9
3,4-Dihydroxy-L-phenylalanine	Sigma-Aldrich	D9628-5G	59-92-7	-2.4	2.3
L-thyroxine	Sigma-Aldrich	T2376-500MG	51-48-9	4.0	0.3
Meclizine dihydrochloride	Molekula	89967039	1104-22-9	5.8	8.1
Metoclopramide hydrochloride	Sigma-Aldrich	M0763-10G	7232-21-5	2.6	9.3
Prednisone	Sigma-Aldrich	P6254-1G	53-03-2	1.5	12.6
Sulindac	Sigma-Aldrich	S4429-5G	38194-50-2	3.4	4.7
Terfenadine	Sigma-Aldrich	T9652-5G	50679-08-8	7.1	13.2
Tetracycline	Sigma-Aldrich	T3258-5G	60-54-8	-1.3	3.3

2-Mercapto-1-methylimidazole	Sigma-Aldrich	301507-5G	60-56-0	-0.3	10.4
Enalapril maleate salt	Sigma Aldrich	E6888-250MG	76095-16-4	0.1	3.0
3,3′,5-Triiodo-L-thyronine	Sigma Aldrich	T2877-250MG	6893-02-3	2.9	0.3
Malathion	Sigma Aldrich	36143-100MG	121-75-5	2.4	-6.8
D-penicillamine	Sigma Aldrich	P4875-1G	52-67-5	-1.8	1.8
Metformin hydrochloride	Tocris Bioscience	2864	1115-70-4	-0.5	12.4
Tioguanine	Sigma Aldrich	A4882-500MG	154-42-7	-0.1	10.5

2.1.1.2 Six Validation drugs

The six validation drugs used to validate the quantitative structure activity (QSAR) model are listed in **Table 2.3**.

Table 2.3 – List of six validation drugs used.

Compound name	**Supplier**	**Order code**	**CAS no.**	**LogP**	**pKa**
Diclofenac sodium	Calbiochem-Novabiochem GmbH	287840-1GM	15307-79-6	4.51	4.15
(+-)-Ibuprofen	Calbiochem-Novabiochem GmbH	401003-1GM	15687-27-1	3.97	4.91
Hydroxycarbamide	Sigma-Aldrich	H8627-1G	127-07-1	-1.80	10.14
Riboflavin	Sigma-Aldrich	R4500-5G	83-88-5	-1.46	10.20
Doxorubicin	Sigma-Aldrich	44853-1MG	25316-40-9	1.27	9.53
Glutamic acid	Sigma-Aldrich	G1251-100G	56-86-0	-3.69	2.23

2.1.1.3 Azetidines

The selection of azetidines probed for biological activity in this thesis is listed in **Table 2.4**.

Table 2.4 – List of selected azetidines used. *Compounds kindly provided by Antonio Feula (UoB)*

Compound name	Full compound name	Molecular weight (g/mol)	LogP
2a	1-(((cis)-1-Benzyl-4-phenylazetidin-2-yl)methyl)piperidine	321.23	3.6
2b	N-(((cis)-1-Benzyl-4-phenylazetidin-2-yl)methyl)propan-2-amine	295.22	2.9
2c	1-((cis)-1-Benzyl-4-phenylazetidin-2-yl)-N-(pyridin-2-ylmethyl)methanamine	344.21	-1.6
2d	N-Benzyl-1-((cis)-1-benzyl-4-(furan-3-yl)azetidin-2-yl)methanamine	333.20	2.6
2e	N-Benzyl-1-((cis)-1-benzyl-4-(2-bromophenyl)azetidin-2-yl)methanamine	421.13	5.3
2f	2-((((cis)-1-Benzyl-4-(pyridin-3-yl)azetidin-2yl)methyl)amino)ethanol	320.17	0.66

2.1.1.4 Y-lactams

The selection of Y-lactams probed for biological activity in this thesis is shown in **Table 2.5**.

Table 2.5 – List of Y-lactams used. *Compounds kindly provided by Mariwan H. Salih (UoB)*

Compound name	Full compound name	Molecular weight (g/mol)	LogP
3a	*N*-benzyl-3-hydroxy-3-methyl-5-phenylpyrrolidin-2-one	281.14	2.81
3b	*N*-benzyl-5-(3,4-dimethoxyphenyl)-3-hydroxy-3-methylpyrrolidin-2-one	341.40	2.48
3c	*N*-benzyl-3-hydroxy-3-methyl-5-(naphthalen-1-yl)pyrrolidin-2-one	331.41	4.53
3d	*N*-(4-chlorobenzyl)-3-hydroxy-3-methyl-5-phenylpyrrolidin-2-one	315.79	3.52
3e	*N*-(4-methoxybenzyl)-3-hydroxy-3-methyl-5-phenylpyrrolidin-2-one	311.37	2.73
3f	*N*-benzyl-5-(furan-3-yl)-3-hydroxy-3-methylpyrrolidin-2-one	271.31	1.98
3g	*N*-benzyl-3-hydroxy-3-methyl-5-(thiophen-2-yl) pyrrolidin-2-one	287.38	2.45
3h	*N*-benzyl-5-(2-bromophenyl)-3-hydroxy-3-methylpyrrolidin-2-one	326.35	1.05
3i	*N*-benzyl-3-hydroxy-3-methyl-5-(4-nitrophenyl) pyrrolidin-2-one	360.25	3.67

2.1.2 Enzymes

Streptomyces griseus type XIV pronase (Sigma-Aldrich, Poole, UK & Munich, Germany).

2.1.3 Equipment

Items used regularly in the lab such as plastic Pasteur pipettes, Petri dishes and water baths are not included on the list but everything else that was used is (**Table 2.6**).

Table 2.6 – Equipment and software used.

Equipment	**Source**
Disposable scalpel (No 10)	Sigma-Aldrich, Munich, Germany
Digital microscope camera DFC300 FX	Nikon, Kingston, UK
Fluorescence stereo microscope (MZ10F)	Leica, Bensheim, Germany
Camera software for fluorescence microscope (Irfanview)	www.irfanview.net
Incubator for fish embryos	Heraeus, Hanau, Germany
Scan^R high content screening station	Olympus Biosystems, Munich, Germany
Image J (version 4.2)	http://rsbweb.nih.gov/ij/
Stereomicroscope (SMZ800) with camera (DMX1200)	Nikon, Kingston, UK
Camera software for stereomicroscope (ACT-1 version 2.7)	Nikon, Kingston, UK
Zoom stereomicroscope (SMZ1500) with epi-fluorescence illuminator and camera (DS-Qi1Mc)	Nikon, Kingston, UK
Camera software for zoom stereomicroscope (NIS elements)	Nikon, Kingston, UK
Stereomicroscope (SMZ645) with 2X lens	Nikon, Kingston, UK
Mechanical micromanipulators (MM3)	Nashirige, London, UK
Inchworm step motors	Lumen Dynamics Group
MicroFil (P85)	World Precision Instruments (WPI) UK, Hitchin, England
Borosilicate glass micropipettes (P84)	World Precision Instruments (WPI) UK, Hitchin, England
Differential amplifier	NPI electronics GmbH, Tamm, Germany
PowerLab 4/35 data acquisition unit	ADI Instruments, Oxford, UK
LabChart 7 Pro (version 7.3)	ADI Instruments, Oxford, UK
Puller (PN-31)	Nashirige, London, UK
Black 384 well plate (781900)	Greiner Bio-One GmbH, Frickenhausen,

	Germany
Multipette® plus (4981 000.019)	Eppendorf Vertrieb Deutschland GmbH, Wesseling-Berzdorf, Germany
LabView Vision	National Instruments, Munich, Germany
MATLAB 7.11 R2010b	MathWorks, Ismaning, Germany
PELCO® clear wall glass bottom dishes (35 X 10 mm)	PLANO GmbH, Wetzlar, Germany
High capacity lab table (68-500)	Scientifica, Uckfield, UK
Faraday cage	Scientifica, Uckfield, UK
Temperature controller (Cryocon 24C)	Cryogenic control systems Inc., California, USA
Disposable mini-Petri dishes (S08185)	Fisher Scientific UK Ltd, Loughborough, UK
96 well microtiter plate (655180)	Greiner Bio-One GmbH, Frickenhausen, Germany
Multi-channel Pipette (613-5252)	VWR International GmbH, Darmstadt, Germany
SIMCA (Windows 7 64-bit)	Umetrics AB, Umeå, Sweden
FLIPR Tetra locomotion measurement system	Custom-made by Richter Gedeon Nyrt., Budapest, Hungary
KomiPL software	Custom-made by Pictron Ltd, Budapest, Hungary
Nunc* polystyrene 4 well rectangular dishes (267061)	Thermo Fisher Scientific, Langensbold, Germany

2.1.4 Zebrafish lines

Wild-type zebrafish embryos used for experiments were from the AB* strain with one mating pair found to produce around 1000 fertilized zebrafish embryos. Various transgenic lines were also used, as summarised in **Table 2.7**.

Table 2.7 – Zebrafish transgenic lines used.

Zebrafish transgenic lines	Provided by	Reference
Tg(fli-1:EGFP)	Professor Roy Bicknell, University of Birmingham	(Lawson and Weinstein, 2002)
Tg(fli-1:EGFP)(gata-1:DsRed)	Professor Roy Bicknell, University of Birmingham	(Bill et al, 2008)
Tg(cldnB:GFP)(lyz:DsRed2)nz50	Dr. Clemens Grabher, KIT	(d'Alençon et al, 2010)
Tg(cpa5:GFP)(lyz:DsRed2)nz50	Dr. Clemens Grabher, KIT	(Forrester et al, 2012)
Tg(lyz.HyPer)	Dr. Clemens Grabher, KIT	(Henry et al, 2013)

2.1.5 Solutions

Solutions were made as follows:

-E3 embryo medium stock solution (containing 5 mM sodium chloride, 0.33 mM calcium chloride, 0.33 mM magnesium sulphate and 0.17 mM potassium chloride) was diluted 1 in 60 with deionised water to give a final working dilution which was then stored at 28°C until needed. Gentamycin (0.5 mL) was also added to 1 litre of the final working dilution to prevent bacterial growth.

-Pronase stock solution at 10 mg/mL was prepared by dissolving *Streptomyces griseus* Type XIV powder (Sigma-Aldrich) in E3 medium. Once the stock solution was made it was stored at -20°C. When required, the stock solution was thawed and kept at 37°C. The final working solution of pronase used was 1 mg/mL which was prepared by dissolving the stock solution in E3 embryo medium.

-Paraformaldehyde (PFA) which was required for fixation was prepared by dissolving 8 g of PFA powder in 200 mL of phosphate buffered saline (PBS) solution (2.67 mM potassium chloride, 137.93 mM sodium chloride, 8.06 mM sodium phosphate dibasic heptahydrate and 1.47 mM monopotassium phosphate) to produce a 4% working solution. The 4% working solution was kept in a water bath for 3-4 hours until completely dissolved. Once dissolved

completely the solution was aliquoted into 15 mL falcon tubes and stored at -20°C. When required for use, the aliquots were thawed at room temperature.

-Phenylthiourea (PTU) stock solution (10 mM), was prepared by dissolving 150 mg of PTU powder in 100 mL of E3 embryo medium, heating to 60°C and then stirring until the powder was completely dissolved. The stock solution was then stored at 4°C until ready to use. To make the final working dilution of PTU, a 1 in 50 dilution was performed in E3 embryo medium and the solution was stored at 28°C.

-Ethyl-3-aminobenzoate methane sulphonic acid salt (MS222) stock solution (0.4%) was prepared by dissolving 200 mg of powder in 49 mL of distilled water. To this 1 mL of Tris at pH 9 was added to bring the pH of the solution to 7-7.5. The solution was then vortexed several times and covered in kitchen foil to protect it from light. The solution was stored at 4°C until ready for use. Final working dilutions were made by diluting in E3 embryo medium.

-Drug solutions: Metformin, thiamazole, captopril, amantadine, chlorprothixene, flupenthixol and metoclopramide drug stock solutions were prepared using E3 embryo medium. Copper sulphate stock solution was prepared with distilled water. Fenofibrate stock solution was prepared using acetone with no dilution exceeding 0.01% acetone. All other drug stock solutions were prepared using DMSO with no dilution exceeding 0.1% DMSO. Stock solutions were kept at -20°C until required for use. Working dilutions were prepared fresh on the day of the experiment using E3 embryo medium.

2.2 Stainings

2.2.1 Fixation

Fixation was performed by transferring zebrafish embryos or larvae with as little liquid as possible (maximum of 50 zebrafish) into Falcon tubes containing 5 mL of 4% PFA in PBS at room temperature. The samples were stored overnight at 4°C.

2.2.2 Sudan black staining

Sudan black staining was used to visualise leukocytes. For this fixed zebrafish embryos and larvae were utilised. The fixed samples were first washed twice with PBST (1 mL) before being stained with 60 µL Sudan black reagent (Sigma-Aldrich, Germany) for 20 minutes. After 20 minutes, the stain was washed off thoroughly with 70% ethanol (1 mL) in three washes of 1, 5 and 10 minutes. The samples were then washed twice with PBST (1 mL) and stored at 4°C. Leukocytes were counted at the site of interest using a Leica MZF10 fluorescence stereo microscope (Leica, Germany).

2.3 Statistical analysis

All the graphs presented in this thesis show mean values and standard deviation error bars.

2.3.1 Students T-Test

When comparing only two variables a student's T-test with Welch's correction was performed with the significance level set at $P<0.05$. Microsoft Excel 2010 (Microsoft, UK) was used to perform the analysis.

2.3.2 ANOVA

One-way ANOVA analysis was performed to determine significant differences between the means of three or more independent groups followed by a Holm-Bonferroni post hoc test to protect from family wise error (probability of getting at least one false positive result) with the significance level set at $P<0.05$ and the null hypothesis rejected when $P<\alpha/k$. The equation used was: $\alpha(j) = \alpha(T)/(k - j + 1)$, where j = selected t-test, k = number of t-tests performed in total, $\alpha(T) = 0.05$. GraphPad Prism 5.0 (GraphPad Software Incorporation, USA) and Microsoft Excel 2010 (Microsoft, UK) were used to perform the statistical analyses.

2.3.3 Multivariate analysis

All multivariate analysis including PCA, PLS and OPLS was performed using SIMCA (Umetrics AB, Umeå, Sweden). The significance level was set at $P<0.05$ for all modelling performed. For all models R^2X and Q^2 values were also calculated to determine the dispersion and stability of the data. A model with an R^2X value >0.7 and a Q^2 value >0.4 was deemed to be of good quality.

2.4 Fish husbandry and embryological techniques

2.4.1 Adult zebrafish maintenance

All adult zebrafish were kept in group sizes of around 15 fish in a ZEBTEC™ zebrafish housing system (Tecniplast, Italy). The water quality, water hardness and conductivity were controlled daily and the pH of the water was kept at 7-7.5. The zebrafish were fed twice daily, once with live food (artemia) and once with dry food. The temperature in the fish

room was maintained at 28°C and the light and dark cycle was controlled automatically with 14 hours of light and 10 hours of darkness.

2.4.2 Zebrafish breeding and embryo collection

The day before embryos were required pairs consisting of one adult male and one adult female zebrafish were placed in breeding cages. The breeding cages were equipped with spawning trays to collect the zebrafish embryos and a divider was placed in the breeding cage separating the male from the female. The divider was removed the next morning, zebrafish embryos were collected and then transferred to new Petri dishes containing E3 embryo medium. Zebrafish embryos were kept at 28°C.

2.4.3 Raising of zebrafish embryos

Zebrafish embryos from all lines were bred in house with a constant temperature of 28°C and all procedures were performed in accordance with the Ethics Committee at Karlsruhe Institute of Technology (KIT), the UK Home Office Animals Scientific Procedures Act (1986) and the Hungarian Law for animal experimentation. Zebrafish embryos were raised in E3 medium with the medium replaced daily. When zebrafish embryos were required without pigmentation, zebrafish embryos were first raised in E3 embryo medium for 24 hours before being transferred to 0.002% PTU solution. At the end of experiments, zebrafish embryos and larvae were humanely killed by an overdose of MS222 anaesthetic. For all experiments, no zebrafish larvae were used beyond 5 dpf except in the case of the locomotion studies.

2.4.4 Dechorionation

When there were a small number of zebrafish embryos chorions were removed mechanically by using forceps. With larger numbers of zebrafish embryos the chorions were removed enzymatically using Pronase enzyme (Sigma-Aldrich, UK). For the enzymatic digestion of the chorions zebrafish embryos were first transferred to a new Petri dish with almost all of the liquid removed. A 1 in 10 dilution of the Pronase stock solution (10 mg/mL) was then performed in E3 embryo medium to give a final dilution of 1 mg/mL. This was then added to the Petri dish at a volume of 1 mL. The zebrafish embryos were then swirled for several minutes and constantly observed under the microscope to see when the first few started to emerge out of their chorions. When around a quarter of the zebrafish embryos were out of their chorions they were pipetted into a 500 mL beaker to which 500 mL of E3 embryo medium was added. The zebrafish embryos were then washed three times in 500 mL of E3 embryo medium. After washing, zebrafish embryos were transferred to new Petri dishes containing E3 embryo medium plus gentamycin. After dechorionation zebrafish embryos were found to be morphologically normal, i.e. the same as zebrafish embryos still in their chorions.

For early stage zebrafish embryos which needed to be dechorionated before 1 dpf, dechorionation was performed almost immediately after fertilization. The zebrafish embryos were dechorionated with Pronase using the same procedure outlined above. However, after the final washing step the zebrafish embryos were transferred to agar-coated Petri dishes containing E3 embryo medium.

Chapter Three: DEVELOPMENT OF A ZEBRAFISH EMBRYO AND LARVAL ELECTROCARDIOGRAPHY TOOL FOR THE DETECTION OF CARDIOTOXICITY

Foreword:

All the work presented in this chapter was supervised by Professor Ferenc Müller and Professor Attila Sik. Optimisation of the ECG recording method was performed jointly with Eva Doro (Biotecont Ltd, Hungary). Eva Doro performed invasive ECG recordings and also contributed equally to the immobilization, developmental stage, temperature and electrode positioning data (data was pooled together with mine). All drug treatment experiments performed in regards to exclusion of motion artefact and QTc prolongation were performed solely by me, as well as the experiments addressing ECG signal stability and reproducibility. All of the data analysis and interpretation of results presented in this chapter was performed solely by me.

3.1 Introduction and Overview

3.1.1 The zebrafish embryo as a model for evaluating cardiotoxicity

Cardiotoxicity is one of the leading causes of drug attrition in the pharmaceutical industry with many marketed compounds having been withdrawn from the market and others aborted in late phases of the drug development programme due to risk of cardiotoxicity (Anyukhovsky, 2011).

Cardiotoxicity can manifest itself in various forms and can have a number of different underlying causes. For example QT prolongation (delay in ventricular repolarisation) occurs due to the main potassium ion channel responsible for ventricular repolarisation being blocked by a drug (e.g. terfenadine). QT prolongation can lead to secondary cardiotoxic conditions (e.g. Torsades de Pointes), which can be fatal. QRS prolongation (slowing of ventricular depolarisation) can occur due to the sodium ion channel responsible for ventricular depolarisation becoming blocked by a drug (e.g. flecainide) (Harmer et al., 2011). Paclitaxel (anti-cancer drug) causes heart rhythm disturbances (arrhythmias) by either directly acting on the Purkinje fibres responsible for transmitting an electrical single in the heart or by inducing histamine release stimulating histamine receptors in the myocardium (Brana and Tabernero, 2010)(Schimmel et al., 2004). Doxorubicin is another anti-cancer agent associated with cardiotoxicity. Doxorubicin causes left ventricular dysfunction and heart failure by affecting calcium homeostasis in myocytes and inhibiting the activity of the ATPases in the sarcoplasmic reticulum (Brana and Tabernero, 2010)(Olson and Mushlin, 1990). This leads to cardiomyocyte apoptosis and eventual left ventricular dysfunction, which can ultimately result in heart failure (Olson and Mushlin, 1990).

At the moment there is no gold standard *in vivo* model for evaluating cardiotoxicity, however the zebrafish represents a promising option. As mentioned in **Chapter 1**, zebrafish share many features with mammals in terms of genetics and physiology, which make them good models for drug screening (Zon and Peterson, 2005). In regards to cardiotoxicity testing, despite the zebrafish heart having only two chambers (one atrium and one ventricle), the electrical properties are similar to higher mammals (MacRae, 2013).

3.1.2 Zebrafish heart development

Unlike the human heart which has four chambers (two atria and two ventricles), the zebrafish heart only has one ventricle and one atrium. The heart is one of the first organs to develop during zebrafish embryogenesis (**Figure 3.1**) (Hu et al., 2000). In the zebrafish, heart assembly occurs from mesodermal precursors, which are specific for either the ventricle or atrium (Rottbauer et al., 2001). These come together at the 18-somite stage and then fuse at the 21-somite stage to form a structure known as a 'cone' (Rottbauer et al., 2001). Further fusion then leads to the formation of a tube at 24 hpf, which has two layers, an endocardium and a myocardium (Rottbauer et al., 2001). The heart tube then undergoes a process known as D-looping, where the atrium loops to the right hand side (Stainier et al., 1996). By 48 hpf the basic structure of the heart has formed with the two chambers (ventricle and atrium), valves and a boundary between the atrium and ventricle present (Stainier et al., 1996). Between 72 and 96 hpf, the ventricle continues to grow and thicken developing trabeculae; this aids the development of an immature fast conduction network in the ventricle (Chi et al., 2008). Additionally, during early embryonic development, the L-type voltage dependent calcium channel (C-LTCC) is required for the ventricle to contract (Rottbauer et al., 2001).

This is the main route by which calcium enters myocytes and therefore plays a predominant role in excitation-contraction coupling (Rottbauer et al., 2001).

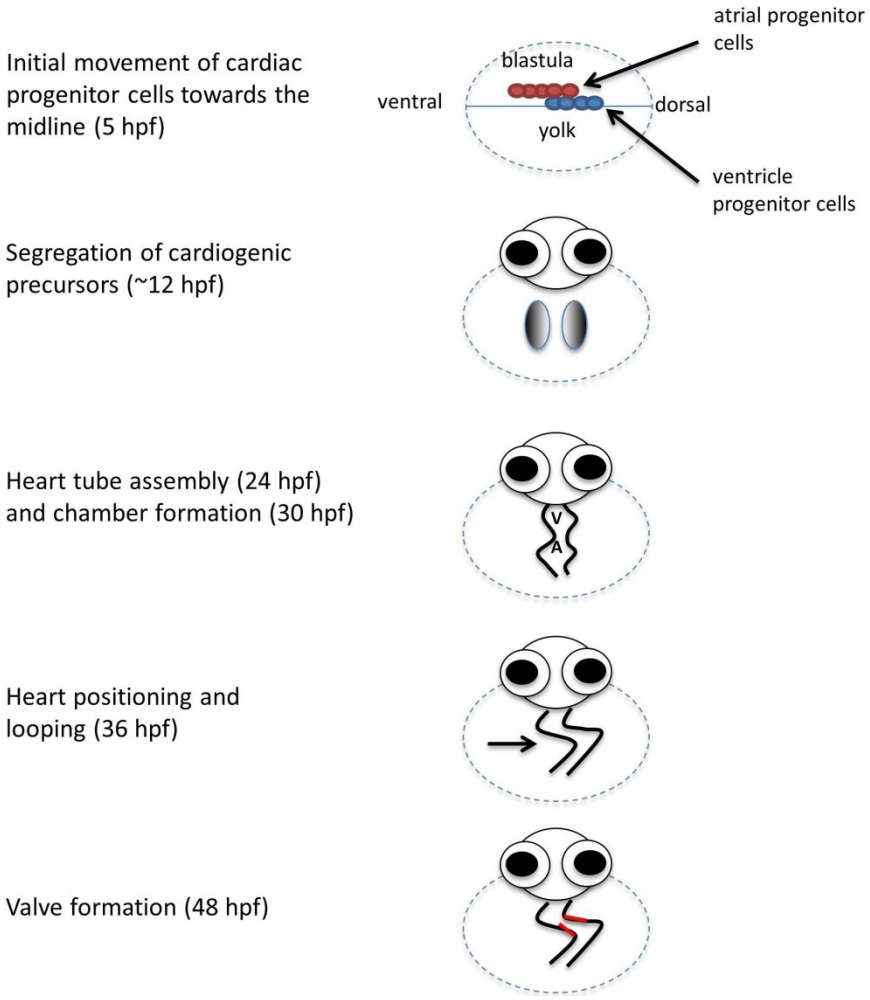

Figure 3.1 – Summary of zebrafish heart development.
Source: Adapted from http://www.bioscience.org/2003/v8/d/1092/fig1.jpg

3.1.3 Electrophysiology of the zebrafish heart

3.1.3.1 Generation of electrical activity in the heart

In humans, pacemaker cells a group of cells that control the heart rate are responsible for initiating electrical activity within the myocardium by generating action potentials (Nerbonne and Kass, 2005). Pacemaker cells are located in the sinoatrial node of the heart and the electrical activity is propagated through the atria into the atrioventricular (AV) node

followed by a short pause (Nerbonne and Kass, 2005). After the short pause the electrical signal travels through to the apex of the heart via Purkinje fibres (specialised fibres responsible for conduction of the electrical signal) into the ventricles (Nerbonne and Kass, 2005). In each region of the heart there are different cell types, for example in the Purkinje fibres, cells specialised for fast conduction are present (Nerbonne and Kass, 2005). Differences in the expression levels of ion channels within these cell types are responsible for the different action potential waveforms observed.

In zebrafish embryos, pacemaker cells have also been identified, which are confined to the sinoatrial junction and marked by expression of the islet-1 gene (Tessadori et al., 2012). However, zebrafish lack Purkinje fibres that are present in humans for fast conduction of the electrical signal to the ventricles. Despite lacking Purkinje fibres, zebrafish have been shown to possess a fast cardiac conduction system (Chi et al., 2008). This is present already at 96 hpf and is characterized by the presence of the Connexin-40 (Cx40) gap junction protein (Chi et al., 2008). The Cx40 gap junction protein is also found in the His-Purkinje conduction system in humans and it is thought to be responsible for ensuring rapid conduction within Purkinje fibres (Chi et al., 2008). Conduction in a unidirectional manner across the myocardium is already observed in zebrafish embryos at around 24 hpf (Chi et al., 2008). Additionally, AV conduction delay is first observed between 36-48 hpf (Chi et al., 2008). The Cx40 gap junction protein is found to be present at low levels in the atrial and ventricular myocytes during this time period, but not in the AV myocardial cells (Chi et al., 2008). It is therefore postulated that the AV myocardial cells, which form a ring structure around the AV canal are responsible for AV delay (Chi et al., 2008). As the ventricle continues to grow and

thicken during zebrafish development a specialised ventricular conduction system responsible for transmitting the electrical signal from the apex to the base of the heart develops (Chi et al., 2008)(Sedmera et al., 2003).

3.1.3.2 Ventricular myocyte action potential cycle

In humans the cardiac ventricular myocyte action potential cycle involves four phases, namely phase 0 (depolarisation), phase 1 (early repolarisation), phase 2 (plateau), phase 3 (repolarisation) and phase 4 (return to resting membrane potential), as shown in **Figure 3.2**.

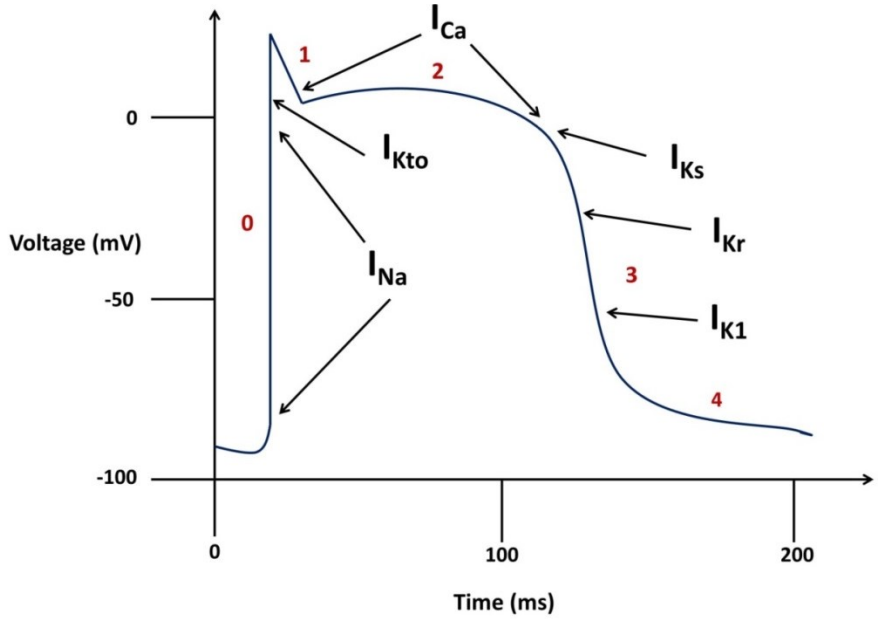

Figure 3.2 – Ventricular myocyte action potential. *Key: 0 = depolarisation, 1 = early repolarisation, 2 = plateau, 3 = repolarisation, 4 = return to resting membrane potential, I_{Na} = rapid inward sodium current, I_{Kto} = transient outward potassium current, I_{Ca} = slow inward calcium current, I_{Ks} = slow delayed rectifier potassium current, I_{Kr} = delayed rectifier potassium current, I_{K1} = Inward rectifier current*

The voltage-gated sodium channel (Nav1.5) through which the current I_{Na} passes can open and close rapidly (Golan et al., 2011). This sodium channel is responsible for the rapid depolarisation during phase 0, where the membrane potential changes from -90 mV to +70 millivolts (mV), as sodium ions rush in, making the inside of the membrane more positive

than the outside (Golan et al., 2011). The channel closes rapidly after 1-2 milliseconds (ms) to prevent further influx of sodium ions (Golan et al., 2011). The time it takes for the sodium channels to recover from their inactivation is known as the refractory period and is a mechanism that protects the heart by ensuring that another action potential is not fired until the first one is completed (Golan et al., 2011). The homotetrameric voltage-gated potassium channel (Kv4.2) through which the transient current I_{to} passes is responsible for early repolarisation in phase 1 by driving out potassium ions (Golan et al., 2011).

The plateau phase (phase 2) is maintained by the voltage-gated calcium channel (Cav1.2), through which the current I_{ca} passes (Golan et al., 2011). There are two types of calcium currents important during the plateau phase, namely the transient current I_{CaT} that passes through T-type calcium channels and the long lasting current I_{CaL} that passes through L-type calcium channels (activate at -30 mV and are susceptible to block by dihydropyridines) (Golan et al., 2011). Both currents are required for influx of calcium ions, which initiates contraction (sliding of thick myosin filaments of the sarcomere past the thin actin filaments) (Golan et al., 2011). During the plateau phase there is a high membrane resistance which helps to insulate the myocyte and therefore allows efficient propagation of the electrical signal (Golan et al., 2011). The voltage-gated slow potassium channels allow potassium to flow out of the cell prolonging the plateau phase.

In phase 3, the voltage-gated potassium channel (Kv11.1) through which the current I_{kr} passes drives the main part of repolarisation (outward flow of potassium ions) (Golan et al., 2011). The Kv11.1 potassium channel is also more commonly known as human ether-à-go-

go-related-gene (hERG) channel. The hERG channel deactivates at -40 mV and is particularly sensitive to block by various classes of compounds (Golan et al., 2011). Additionally, the voltage-gated potassium channel Kv7.1 (KvLQT1) through which the current I_{ks} passes which is active during low heart rates is also able to drive repolarisation and behaves by opening and closing very slowly.

The final phase of the ventricular myocyte action potential cycle involves the inward rectifier heterotetrameric potassium channel (Kir2.X) (Golan et al., 2011). This channel through which the current I_{k1} passes restores the membrane potential to the resting condition of -90 mV (phase 4) (Golan et al., 2011). This occurs by pumping sodium ions out of the cell and potassium ions back into the cell (Golan et al., 2011).

When comparing the ventricular myocyte action potential to the atrial myocyte action potential slight differences are observed (**Figure 3.3**). Due to dissimilarities in ion channel expression, in atrial myocytes the plateau phase (phase 2) is narrower and the repolarization phase (phase 3) more gradual.

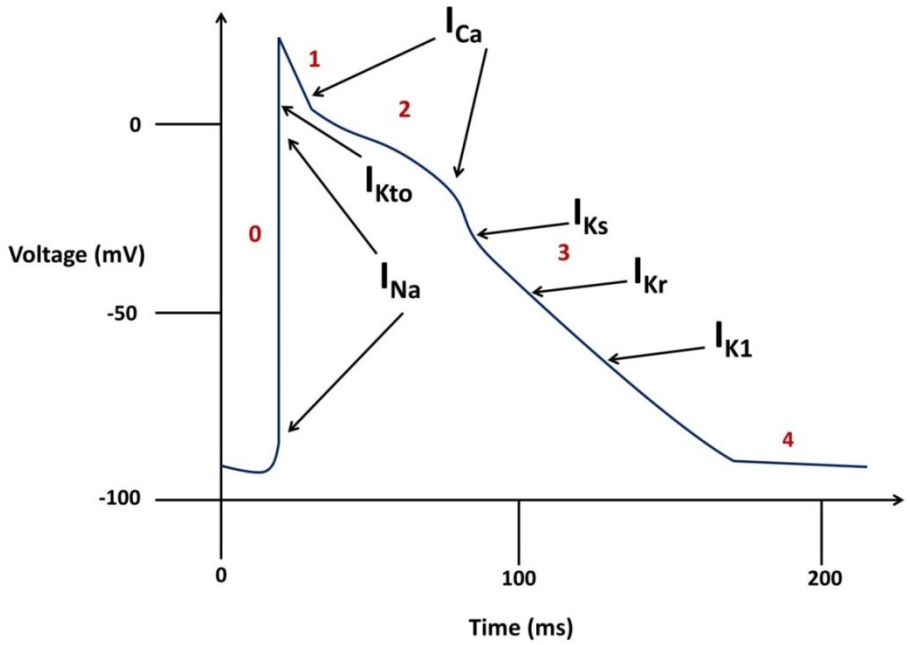

Figure 3.3 – Atrial myocyte action potential. *Key: 0 = depolarisation, 1 = early repolarisation, 2 = plateau, 3 = repolarisation, 4 = return to resting membrane potential, I_{Na} = rapid inward sodium current, I_{Kto} = transient outward potassium current, I_{Ca} = slow inward calcium current, I_{Ks} = slow delayed rectifier potassium current, I_{Kr} = delayed rectifier potassium current, I_{K1} = Inward rectifier current*

Zebrafish embryo atrial and ventricular myocytes are similar in morphology to those of adult zebrafish and humans. Additionally, many counterparts of the human cardiac ion channels are found in zebrafish, such as orthologues of Nav1.5 and hERG (Golan et al., 2011). As in the human and the adult zebrafish heart, the cardiac action potential upstroke (phase 0) is dependent on sodium channels (Alday et al., 2014). However, in zebrafish embryos and adults the T-type calcium channels can also contribute to phase 0, whereas in mammals T-type calcium channels are only present early during development (Alday et al., 2014). In phase 2 of the zebrafish embryo myocyte action potential cycle L-type calcium channels are responsible for action potential generation, just as in humans (Alday et al., 2014). Additionally, phase 3 of the zebrafish embryo cardiac myocyte action potential cycle like in humans is highly dependent on I_{kr} (Alday et al., 2014). However, there is one major

difference between zebrafish embryos and humans in that zebrafish embryos lack the cardiac ion channels Kv7.1 and Kv4.3, which are required for the generation of early repolarisation in phase 1 of the cardiac myocyte action potential cycle in humans (Alday et al., 2014).

3.1.3.3 Adult zebrafish electrocardiogram

An ECG is a recording of the electrical processes involved in the initiation of each heartbeat representing the overall electrical activity of the heart (Golan et al., 2011). The ECG signals that can be obtained from human and adult zebrafish hearts have been shown to be highly similar to one another (Milan et al., 2006)(Chaudhari et al., 2013). The whole cardiac cycle in adult zebrafish is around 480 ms, in humans it is around 1000 ms and in mice it is much shorter around 100 ms (Artman et al., 2008)(Leong et al., 2010). In zebrafish larvae, the cardiac cycle is longer, it becomes shorter as the fish develops (Yu et al., 2010). Additionally, the heartbeat also shows a high similarity between humans and adult zebrafish. In humans the heartbeat is around 60-100 beats per minute (bpm) and in adult zebrafish it is 110-140 bpm (Leong et al., 2010). In mice however the heartbeat is much faster, approximately 500-600 bpm (Leong et al., 2010).

An ECG signal is characterised by three main waves with the first wave (P wave) representing atrial depolarisation, the second wave (QRS wave) representing ventricular depolarisation and the third wave (T wave) representing ventricular repolarization. A typical human ECG waveform is shown in **Figure 3.4**.

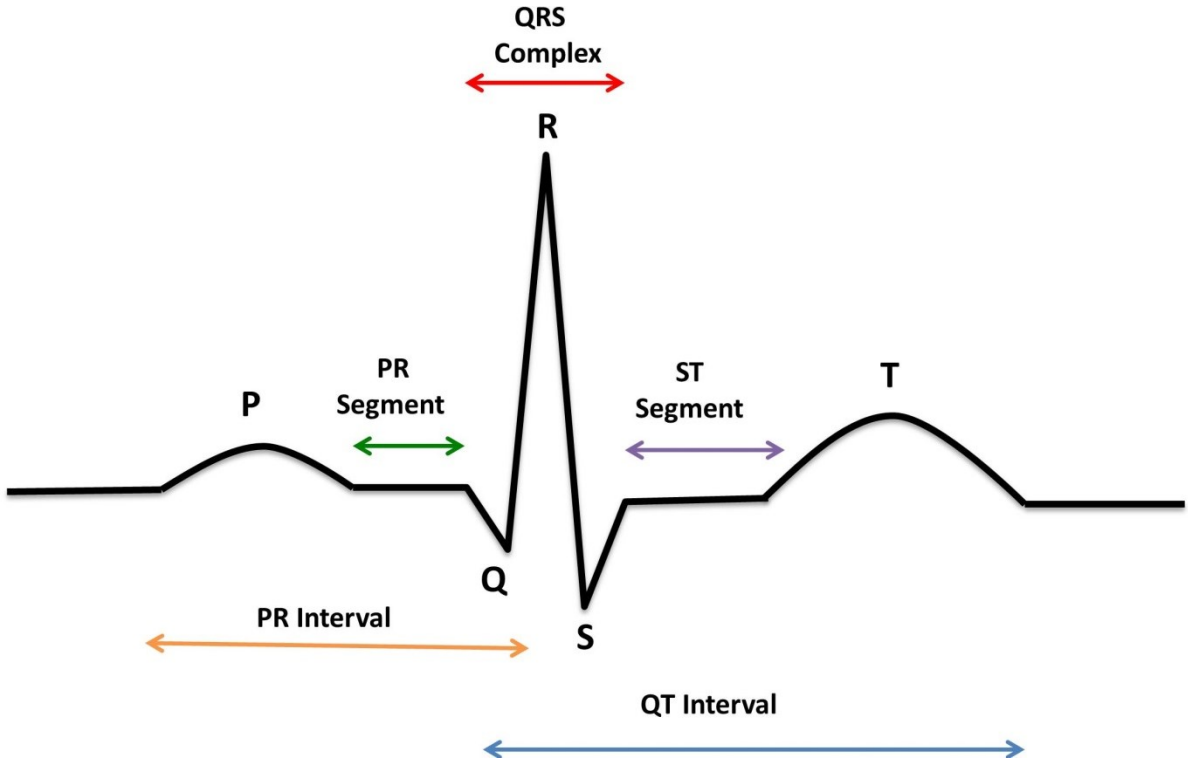

Figure 3.4 – Components of a human ECG recording. *Key: P = atrial depolarization, Q = first part of ventricular depolarisation, R = main part of ventricular depolarisation, S = last part of ventricular depolarisation, QRS = overall ventricular depolarisation, T = ventricular repolarization, PR interval = AV conduction time, PR segment = Flat isoelectric segment between the end of the P wave and the beginning of the Q wave, ST segment = Period from the end of the QRS complex to the beginning of the T wave, QT interval = time duration of ventricular depolarisation and repolarisation*

The P wave which represents the depolarisation of the atria lasts around 80-110 ms in humans. In zebrafish this is shorter, around 50-70 ms (Ahumada, 1987). After the P wave, there is a period known as the PR segment, where the components involved in carrying the electrical impulse are activated (Ahumada, 1987). In humans, the components involved in this process are the bundle branches, His bundles and Purkinje tissue. In zebrafish, the ventricular trabeculae serve as the functional equivalent forming a specialised ventricular conduction system responsible for transmitting the electrical signal from the apex to the base of the heart (Sedmera et al., 2003). The PR segment is followed by the PR interval, which is the period that is measured before the start of the P wave to the beginning of the

QRS complex (Ahumada, 1987). The PR interval in adult zebrafish has been reported to be around 30 ms (Artman et al., 2008) and 66 ms (Milan et al., 2006). This discrepancy in the reported values may be due to differences in the recording methods utilised. However, in general the PR interval is shorter than that seen in humans. This is because in zebrafish electrical transmission from the atrium to the ventricle occurs much faster, as there is less delay between the atrial depolarisation and ventricular depolarisation due to the atrioventricular (AV) node being less well defined (Artman et al., 2008).

The RR interval represents the time duration between the peak of one QRS complex to the next (Ahumada, 1987). In zebrafish the RR interval is around 350-400 ms, which is comparable to that of humans (Artman et al., 2008). The second main wave seen on an ECG recording the QRS complex (tallest peak) represents ventricular depolarisation, usually lasting around 60-100 ms in humans (Ahumada, 1987). In zebrafish this is shorter (around 30 ms) owing to the rapid propagation of the signal (Artman et al., 2008). The P wave and the QRS complex differ in amplitude, because the ventricle is thicker generating a much bigger deflection than the atrium.

The last wave seen on the ECG the T wave represents ventricular repolarisation. This part of the cardiac myocyte action potential cycle enables myocytes to regain a negative charge ready for the next cycle to begin. In zebrafish and humans the T wave is easily observed, but in mice it is not so easily observed as depolarisation and repolarisation occur simultaneously (Leong et al., 2010). Occasionally, in humans the T wave may be followed by a U wave, which is the remaining part of ventricular repolarisation (Wagner, 2008).

The QT interval is a measure of the overall time taken for the ventricular cell action potential to occur (i.e. ventricular depolarisation and repolarisation). In zebrafish the QT interval is around 200-290 ms, comparable to that of humans which is slightly longer at around 300-400 ms; in mice it is notably shorter at around 80 ms (Leong et al., 2010). The QTc interval is a measure of the QT interval independent from the heart rate and is commonly used as a marker for cardiac toxicity (Wagner, 2008). It can be calculated using Bazzet's formula: $QTc=QT/\sqrt{RR}$ (Wagner, 2008). Other formulas however also exist to correct QT for heart rate including the Hodges, Friderica and Framingham formulas (Benatar and Decraene, 2001).

3.1.4 Zebrafish as a model for QT prolongation

The characteristics of the zebrafish cardiac myocyte action potentials closely resemble those of humans. This is because orthologues of the cardiac ion channels found in humans exist in zebrafish, such as orthologues of hERG and Nav1.5 (Nguyen et al., 2008). In humans and zebrafish the main channel involved in ventricular repolarisation is hERG (zERG in zebrafish). Disruption to this ion channel causes a delay in ventricular repolarisation, leading to a prolongation of the QT interval (duration of ventricular depolarisation and repolarisation), which can predispose to arrhythmia (irregular heart rhythm) and Torsades de Pointes (TdP), which is a ventricular tachycardia characterised by twisting of the QRS complex around the isoelectric baseline (Chaudhari et al., 2013). This condition can lead to sudden cardiac deaths, accounting for 50-100 unexpected sudden cardiac deaths for every 100,000 of a population each year in Europe and North America (Niemeijer et al., 2014).

QT prolongation is idiosyncratic in nature and can be acquired (drug-induced) or genetic. Individuals who develop drug-induced QT prolongation generally have an underlying condition such as hepatic impairment, hypokalaemia or structural heart disease (e.g. cardiomyopathy) (Gupta et al., 2007). Additionally, individuals taking QT prolonging drugs or drugs that interfere with their metabolism, as well as individuals with genetic polymorphisms in drug-metabolizing enzymes are at increased risk of developing QT prolongation (Gupta et al., 2007). QT prolongation may also be hereditary as is seen in sufferers of long QT syndrome (LQTS), which has a prevalence of around 1 in 3000 (Goldenberg et al., 2008). LQTS exists in many forms presenting with varying degrees of severity due to mutations in different genes (LQT1-13). The first five LQT genes (LQT1-5) are associated with a prolonged QT interval.

The zebrafish zERG channel protein consists of 1186 amino acids and overall shows 60% sequence identity to human hERG (Hassel et al., 2008). Like in humans, the zERG channel consists of six transmembrane domains with domains S1-S4 involved in sensing the membrane potential and domains S5-S6 making up the potassium selective pore of the channel (**Figure 3.5**) (Hassel et al., 2008). In the S4, S5 and S6 regions amino acid identity is particularly high and can reach up to 100% (Hassel et al., 2008). Additionally, the zebrafish zERG channel also has cyclic adenosine monophosphate (cAMP) binding domains which are found in human hERG, as well as a highly conserved Per-Arnt-Sim (PAS) domain involved in deactivation kinetics (Scholz et al., 2009)(Langheinrich et al., 2003). Additionally, studies with a human specific hERG blocker MK-499 have shown that it is able to inhibit zERG currents *in vitro* (Langheinrich et al., 2003). The zebrafish zERG and the human hERG do show some

minor biophysical differences but overall their functions are highly conserved, indicating that zebrafish are a good model for investigating hERG associated disorders (Scholz et al., 2009).

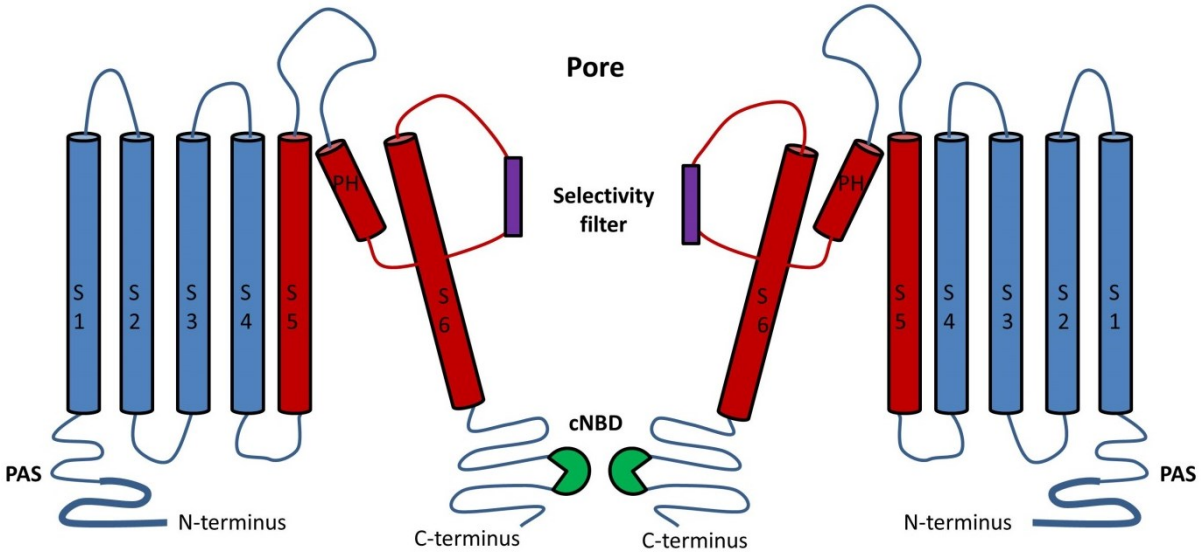

Figure 3.5 – Structure of the zebrafish zERG channel. *Two zERG channel sub-units are shown with S1-S4 forming the voltage sensing domain and S5-S6 the pore domain. Key: PH = pore helix, PAS domain = Per-Arnt-Sim, cNBD domain = cyclic nucleotide binding domain*

Zebrafish mutants with defects in zERG have been shown to be particularly useful to model human hERG disorders. For example, mutations of zERG in the S3 and S5 transmembrane domains have shown that homozygotes are unable to generate spontaneous action potentials and develop arrhythmias (Arnaout et al., 2007). Additionally, a zebrafish model of LQTS presenting with a prolonged QT interval has been established using morpholino knockdown of *kcnh2* (Arnaout et al., 2007). The zebrafish *reggae* mutant presents with a shortened QT interval due to a mutation in the S4 transmembrane domain, which is involved in voltage-sensing (Hassel et al., 2008). These phenotypes, particularly the short and long QT phenotypes mirror what happens in humans who suffer from genetic QT disorders. The zebrafish embryo therefore presents an invaluable model to study such conditions.

3.1.5 Zebrafish as a model for drug-induced QT prolongation

QT prolongation is not only a genetic phenomenon but can also occur due to binding of particular drugs to the drug-binding region of the hERG channel in the S6 transmembrane domain (Langheinrich et al., 2003). The phenylalanine 656 and tyrosine 652 residues of this part of the hERG channel are important for hERG block, as shown in **Figure 3.6** (Zareba, 2007).

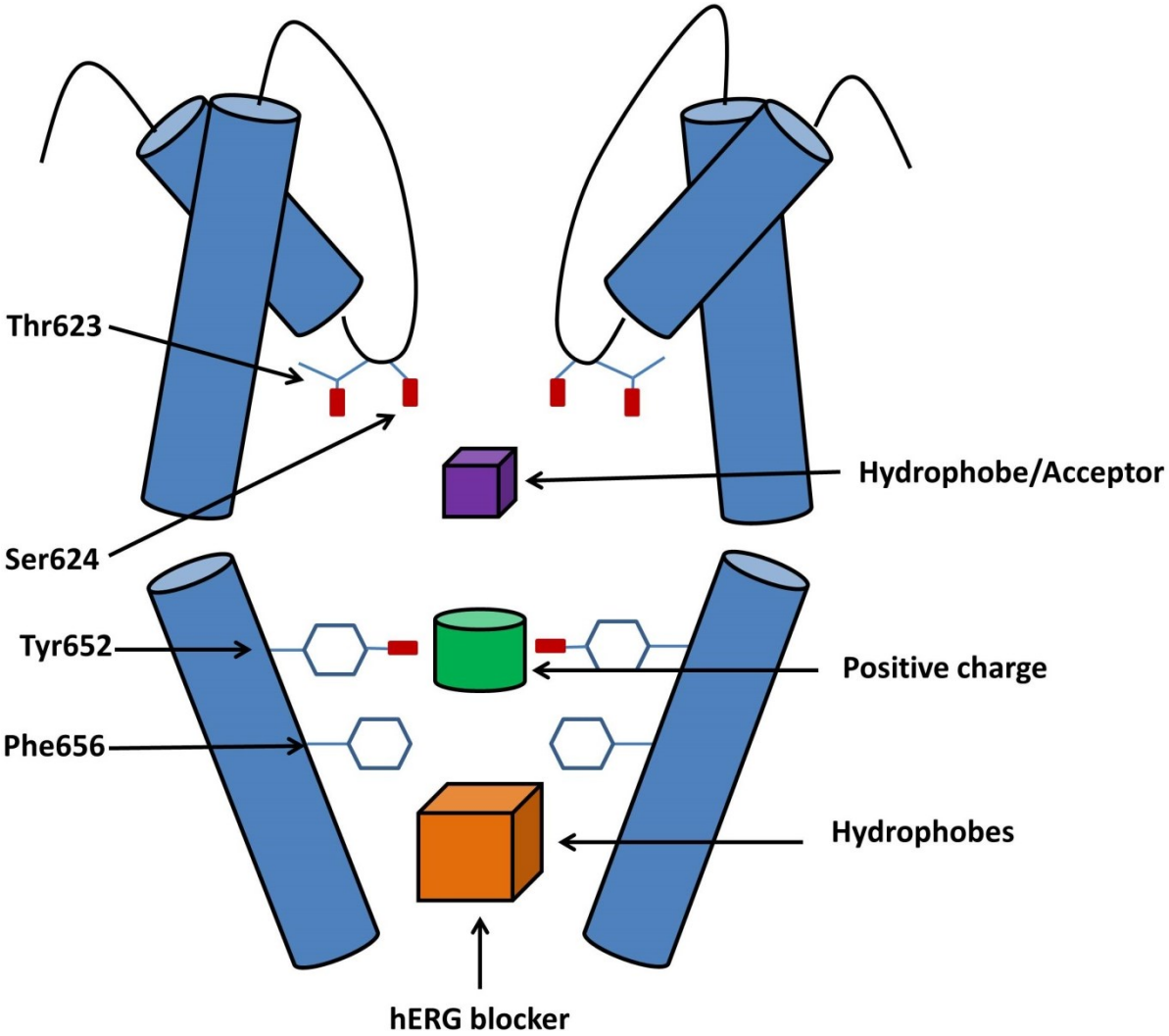

Figure 3.6 – Structural model of the hERG channel pore component.
Source: Figure adapted from (Aronov, 2005)

Between the zERG and hERG channel in the region where the QT-prolonging drugs bind there is a difference of only one amino acid (Langheinrich et al., 2003). Drugs that cause QT prolongation often differ in pharmacological class and function, so it is not so easy to predict which compounds will cause this effect. It has been shown that compounds with molecular weights >250 and computed logP (clogP) values >3.7 are likely to be potent hERG blockers, whereas compounds with clogP values <1 and molecular weights <250 are unlikely to be hERG blockers (Aronov, 2005). This is most likely to do with the large pore size of the hERG channel as well as the highly lipophilic nature of the pore lining (Aronov, 2005). Drug-induced QT prolongation can be caused by blocking of the hERG channel either when it is active/inactive or open/closed (see **Figure 3.7**) (Hecker et al., 2008).

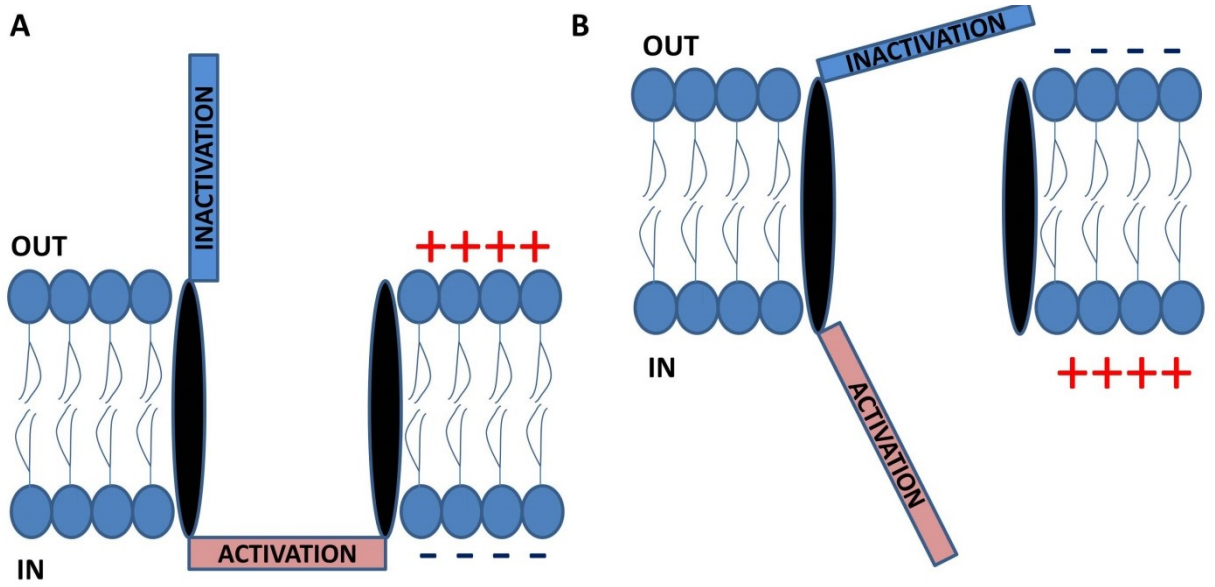

Figure 3.7 – Schematic of hERG channel gating. *A) At negative membrane potentials the activation gate is closed whilst the inactivation gate remains open, B) At positive membrane potentials (e.g. +20mV) during depolarisation the activation gate opens slowly and the inactivation gate closes much of the way so that some current can pass through.*

Drug-induced QT prolongation is responsible for a large number of drug failures in drug development and new tools to screen compounds for QT prolongation could potentially save

money and lives. Detection of QT prolongation during the drug development process is a regulatory requirement, as outlined in the ICH guidelines S7B (ICH Expert Working Group Topic Leaders, 2002). At the moment there is no gold standard model for detecting QT prolongation of drug candidates in the drug development process. Current *in vivo* methods are based on measurement of ECGs in beagle dogs using telemetric devices, as this can be performed without anaesthetisation (Mattera et al., 2012). However, this requires a large number of animals and huge amounts of compound, generates a lot of data, is expensive and time consuming and needs to be performed according to strict regulatory guidelines (Mattera et al., 2012). Currently, the gold standard *in vitro* method used is the hERG cell patch clamp assay, as it is fast and specific (Barros et al., 2008). However, this assay does have its limitations in that it does not take into account plasma protein binding or metabolism (Barros et al., 2008).

The repolarisation of the myocardium is complex with several ion channels and various other components such as cytoskeletal elements and receptors playing an important role (Barros et al., 2008). This has put zebrafish at the helm as a suitable model due to its relative simplicity compared to other mammalian model systems and the ability to investigate repolarisation abnormalities in an *in vivo* scenario (Barros et al., 2008).

Cardiotoxicity screens that have been developed using the zebrafish embryo/larva as a model organism include video recording methods which use changes in heartbeat as a readout (Yoshida et al., 2009)(Fink et al., 2009)(Chan et al., 2009), 3D imaging techniques (Lin et al., 2014), optical mapping techniques (Sabeh et al., n.d.), fluorescence-based

techniques (Wen et al., 2012)(Burns et al., 2005)(Letamendia et al., 2012) and voltage dynamics visualisation techniques (Tsutsui et al., 2010). Recently, a comparative study of 15 compounds was performed using three different methods (Park et al., 2013). The first method involved an *in vivo* zebrafish embryo assay to record changes in heartbeat after compound exposure (Park et al., 2013). The other two methods involved the use of *in vitro* hERG fluorescence polarization and hERG patch clamp assays to evaluate the 15 compounds (Park et al., 2013). A predictive model was generated using the results obtained from all three methods (Park et al., 2013). When validating this model it was found to show very high predictivity for the zebrafish embryo *in vivo* assay (R^2=0.948), i.e. the hERG fluorescence polarization and hERG patch clamp assays could be used to predict with very high accuracy the change in heart rate of the zebrafish embryos after compound exposure (Park et al., 2013).

Despite the many zebrafish embryo/larval cardiotoxicity assays that have been developed so far showing good predictivity and comparability to *in vitro* and other *in vivo* models, they all lack the dynamic and temporal resolution that is needed to analyse components of the cardiac cycle. ECG recordings are able to provide this valuable information. An ECG recording method has been developed to record adult zebrafish ECGs *in vivo* (Sun et al., 2009)(Milan et al., 2006)(Chaudhari et al., 2013), as well as *in vitro* (Tsai et al., 2011). More recently, multi-array electrode systems (Yu et al., 2012) and implantable ECG devices (Zhao et al., 2013)(Cobo et al., 2013) have also been developed for adult zebrafish.

ECG recording methods that can be used for cardiotoxicity testing have been fully established for adult zebrafish (Milan et al., 2006) and late stage larvae (Yu et al., 2010). However, ECG recording methods for early stage larval zebrafish are in their infancy and have not been fully characterised or optimised (Forouhar et al., 2004)(Dong et al., 2012) (Rottbauer et al., 2001). Therefore, a zebrafish embryo/larval ECG recording method that could be used for cardiotoxicity testing is lacking, as well as any direct evidence that QT prolongation occurs in early stage zebrafish larvae.

3.1.6 Zebrafish as a model for arrhythmia and related cardiac disorders

Arrhythmogenesis is complex and involves several components including ion channels, receptors, adaptor proteins and signalling cascades (Zhu et al., 2013). It is one of the most difficult conditions to treat, as the underlying cause can be multifactorial (Milan and MacRae, 2005).

As with QT prolongation at the moment there is no gold standard for detecting the potential of compounds to cause arrhythmia. Many drugs can cause arrhythmias, such as anti-arrhythmics themselves, anti-psychotics, antibiotics, anti-anginals, gastrointestinal stimulants, narcotics and bronchodilators (Barnes and Hollands, 2010). Arrhythmia is also thought to be associated with a genetic component (Milan and MacRae, 2005). Animal models that have been used so far for investigating arrhythmia development include dogs, rabbits and guinea pigs that have a chronic condition of AV block (impaired conduction between atrium and ventricle) (Milan and MacRae, 2005). However, these models are not ideal for investigating arrhythmias as they are firstly expensive to generate and maintain,

they cannot be genetically modified, they show poor reproducibility and they cannot be used for drug screening purposes as they are low throughput (Milan and MacRae, 2005)(Hoffmann and Warner, 2006)(Carlsson et al., 1993)(Chézalviel-Guilbert et al., 1995). The zebrafish on the other hand might provide a solution to this problem, as a wide selection of genetic techniques are available to knockout genes of particular interest that may be related to arrhythmia development with the possibility of also creating stable transgenic lines (Milan and MacRae, 2005). Additionally, zebrafish and humans are very similar on an electrophysiological level and drug studies have already shown that zebrafish can develop various forms of arrhythmias with different degrees of severity (Milan and MacRae, 2005).

The zebrafish embryo has also been shown to be a very good model for drug-induced AV block with zebrafish embryos exposed to known human QT prolonging drugs developing AV block due to zERG block (Langheinrich et al., 2003). AV block occurs due to a disruption in conduction of the electrical signal from the atria to the ventricles (Clarke et al., 1976).

3.2 Aims

Previously, it was shown that ECGs can be recorded from zebrafish larvae as young as 5 dpf and as old as 35 dpf using micropipette-based systems (Forouhar et al., 2004)(Yu et al., 2010). Additionally, it was demonstrated that a known cardiotoxic drug in humans causing QRS prolongation had the same effect on 7 dpf zebrafish larvae (Yu et al., 2010). Furthermore, on adult zebrafish ECGs QT prolongation could be observed following exposure of adult zebrafish to known human QT prolonging drugs (Milan et al., 2006). When 2 and 3 dpf zebrafish embryos/larvae were exposed to these same drugs, QT-related conditions such

as bradycardia and atrioventricular block were observed (Langheinrich et al., 2003)(Milan et al., 2003). The main aim of this work was therefore to develop a zebrafish embryo and larval ECG recording set-up that could be used for investigating cardiac dysfunction.

As it had already been shown that it was possible to record ECGs from zebrafish larvae as young as 5 dpf, the first objective was to reproduce the published data using our own ECG recording set-up. The first experiment therefore involved taking five minute ECG recordings from zebrafish larvae and determining the stability, as well as reproducibility of the ECG signals. The second objective was to then optimise the ECG recording set-up. Various parameters were optimised. The first parameter optimised was the form of immobilization used, as it was important to find an immobilizing agent that would effectively immobilize the zebrafish without having a significant effect on the ECG signal. The second parameter optimised was the recording temperature, as it was important to determine the temperature range at which ECG recordings could be conducted without inducing significant effects on the ECG signal. For this the Q_{10} coefficient (the ratio of the rates of a reaction or process at T+10°C and T°C) was calculated (Hegarty, 1973). The third parameter optimised was the electrode position, as differences in electrode position were previously reported by Forouhar and colleagues to affect ECG signal morphology (Forouhar et al., 2004). The final parameter optimised was the zebrafish developmental stage used for recording purposes, as it was important to identify a developmental stage that was easy to position in the recording plate whilst at the same time producing ECG signals with prominent P, QRS and T waves.

Once the ECG recording set-up had been optimised, the next question addressed was whether it could be utilised as a screening tool to detect cardiotoxic effects of drugs. Drug-induced QT prolongation was of particular interest, as it is a condition caused by blockade of the hERG channel, which is the main cardiac ion channel involved in ventricular repolarisation (Katchman et al., 2006).

Three drugs (terfenadine, haloperidol and pimozide) known to induce QT prolongation in humans were selected and thus tested for their effects on 3 dpf zebrafish larval ECGs. Terfenadine which is an anti-histamine can block several cardiac ion channels including the hERG channel, whereas haloperidol and pimozide (both anti-psychotics) bind to the hERG channel more specifically than to other cardiac ion channels (Testai et al., 2010). In addition to this the anti-arrhythmic agent verapamil was tested, which is known to block hERG *in vitro* but not *in vivo* (Martin et al., 2004). Penicillin was also tested as a negative control as it is known not to block hERG or cause QT prolongation in humans and adult zebrafish (Milan et al., 2006).

3.3 Methods

3.3.1 Preparation of electrocardiogram apparatus

The ECG set-up consisted of several main components including a differential amplifier (NPI electronics GmbH, Germany), mechanical micromanipulator (Nashirige, UK), Inchworm step motor (Lumen Dynamic Group, Canada), PowerLab 4/35 data acquisition unit (ADI Instruments, UK) and a stereomicroscope (Nikon, UK). Everything was housed inside a grounded faraday cage on an air table (Scientifica, UK) to minimise background noise. The

mechanical manipulator was used as an attachment site for the motor and also the connection box for the positive and reference electrodes.

A borosilicate glass micropipette (World Precision Instruments, England) was pulled with a micropipette puller (Nashirige, UK) and the end of the tip was cut with a glass block to give a tip with a 2 µm diameter. This micropipette was then filled using MicroFil (World Precision Instruments, UK) with 3 M potassium acetate solution (Sigma-Aldrich, UK) and coloured with methylene blue solution (Sigma-Aldrich, UK). The micropipette was attached to the end of the motor and locked into place on the motor end via a screw. A chloridised silver wire (recording electrode) which carries the electrical signal to the amplifier was then inserted into the micropipette.

Experiments were performed at room temperature (21°C) unless otherwise stated. The temperature was controlled using a temperature controller (Cryogenic control systems Inc., California, USA) to which a temperature sensor and a homemade heating element were connected.

3.3.2 ECG recording method

For all experiments, except the immobilization optimisation experiments, zebrafish embryos/larvae were anaesthetised in 0.3 mg/mL MS222 (Sigma-Aldrich, UK) for 10 minutes. Once anaesthetised, one zebrafish embryo/larva was then transferred to the ECG recording plate. The recording plate consisted of a Petri dish covered with a 2% layer of agarose into which grooves had been made using a plastic template. To the recording plate 10 mL of fresh

E3 embryo medium without MS222 was added. For ECG recording purposes the zebrafish embryo/larva was always positioned ventrally within a groove in the agarose layer.

The tip of the filled pre-pulled borosilicate glass micropipette was positioned on the skin surface between the ventricle and atrium (no penetration) using the mechanical micromanipulators (Narishige, UK), the Inchworm step motor (Burleigh, UK) and a stereo microscope (Nikon, UK). A second reference electrode was then placed in the surrounding medium in the recording plate. The differential amplifier (NPI electronics, Germany) used for recordings was operated in DC mode with the high pass filter set at 0.1 hertz (Hz). The raw ECG signals were digitised using the PowerLab 4/35 data acquisition unit (ADInstruments, UK) and viewed using LabChart 7 Pro (ADInstruments, UK). When viewing the ECG signal, the digital filter was changed to 15 and the Inchworm step motor (Burleigh, UK) was used to move the micropipette tip forwards and backwards until a stable ECG signal was found (**Figure 3.8**).

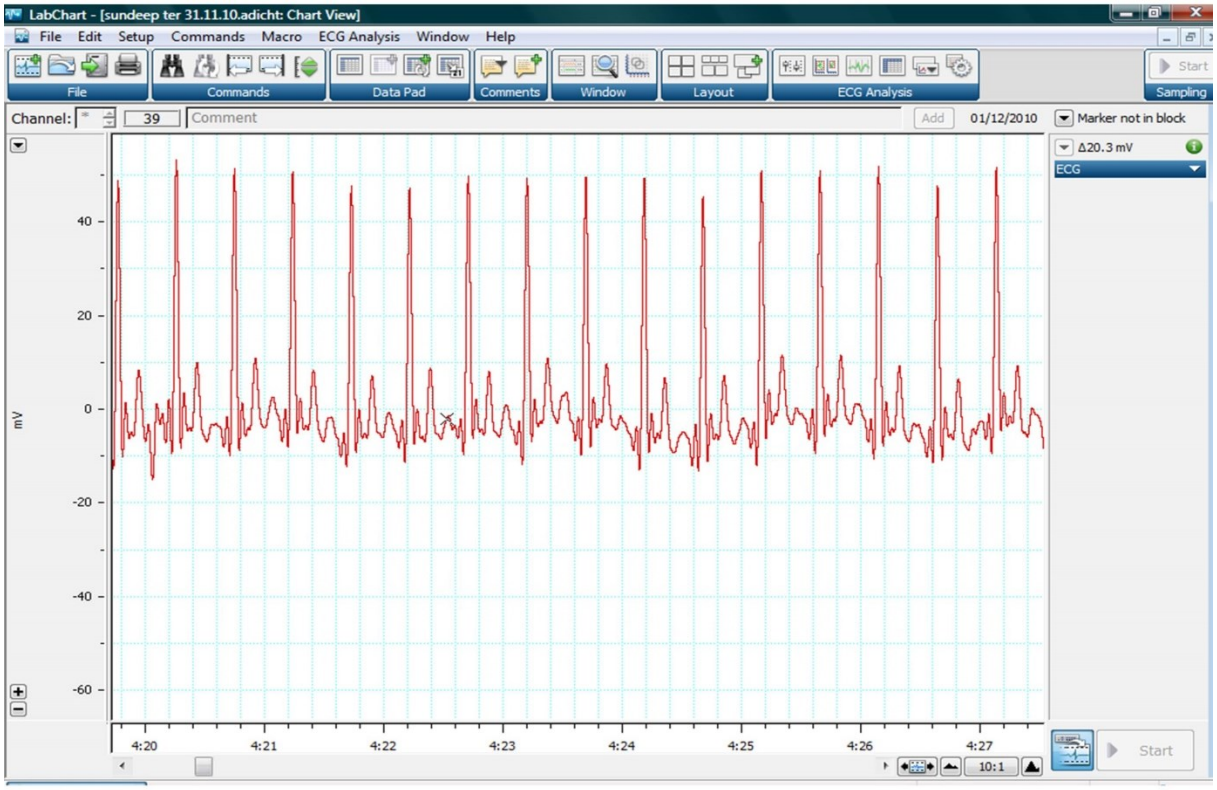

Figure 3.8 – Screenshot of an ECG recording from a 3 dpf zebrafish (digital filter 15). *ECG recordings were taken for 5 minutes immediately after a consistent ECG signal was found that displayed stable P, QRS and T waves.*

3.3.3 ECG temperature experiments

To determine the effect of temperature on ECG recordings, recordings were taken at different temperatures (20, 22, 24 and 28°C). A homemade heating element connected to a temperature controller (Cryogenic control systems Inc., USA) was used to increase the temperature in the recording plate containing 5 mL of E3 embryo medium. This was done by firstly embedding the heating pad of the device in 2% agarose inside a Petri dish. A plastic template was then used to create grooves on the upper surface of the agarose layer; this could then later be used to position the zebrafish larvae during ECG recordings. The temperature was monitored and controlled using a sensor that was placed inside the recording plate. Once the temperature inside the plate had reached the required level, a

zebrafish larva at 3 dpf was transferred to the recording plate and was left to acclimatize for 30 minutes. The zebrafish larva was then transferred for 10 minutes to a 0.3 mg/mL MS222 anaesthetic solution before being transferred back to the recording plate and being positioned within a groove. An ECG recording was then taken for five minutes.

3.3.4 Invasive ECG recordings

For invasive ECG recordings the exact same set-up as for non-invasive ECG recordings was used except that the speed of the step motor was tripled and the distance moved was increased from 5 to 500 µm. Through these changes, the positive electrode could be pushed with enough force directly into the heart by penetrating the skin. For the invasive ECG experiments, initially a non-invasive recording was performed for five minutes first before performing an invasive recording for five minutes.

3.3.5 ECG drug treatments

The compounds used to exclude motion artefact included cromakalim (Tocris Bioscience, UK) which is a K_{ATP} channel opener (Ripoll et al., 1990) along with (-)-blebbistatin (Sigma-Aldrich, UK) & 2,3-butanedione monoxime (BDM) (Sigma-Aldrich, UK) which are excitation-contraction uncouplers (Brines et al., 2012). The compounds used for immobilization of zebrafish embryos/larvae included MS222 (Sigma-Aldrich, UK) which is an anaesthetic that blocks the conductance of sodium and potassium in excitable cells (Rombough, 2007) and (+/-) tubocurarine chloride pentahydrate (Sigma-Aldrich, UK) which is a skeletal muscle relaxing alkaloid (Colquhoun et al., 1979). For the QT prolongation investigation experiments verapamil hydrochloride (Tocris Bioscience, UK) which is an anti-arrhythmic (Somogyi et al.,

1981), haloperidol (Sigma-Aldrich, UK) which is a butyrophenone anti-psychotic (Gerace et al., 2012), terfenadine (Sigma-Aldrich, UK) which a histamine H1 receptor antagonist (Testai et al., 2010), pimozide (Sigma-Aldrich, UK) which is a diphenylbutylpiperidine anti-psychotic (Pa et al., 1968) and penicillin G sodium salt (Sigma-Aldrich, UK) which is an antibiotic (Milan et al., 2006) were tested.

All drug stocks were made using DMSO except MS222 stock which was made with distilled water and verapamil hydrochloride and (+/-) tubocurarine chloride pentahydrate stocks which were both made with E3 embryo medium. All final dilutions made from the initial stock solutions were made up using E3 embryo medium.

The recording plate used for drug treatment experiments consisted of a mini Petri dish (Fisher Scientific UK Ltd, UK) covered with a layer of unscented paraffin wax (Sigma-Aldrich, UK) into which grooves had been made manually. The recording plate was filled with 3 mL of E3 embryo medium. ECG recordings were taken for five minutes before addition of drug. Drug was then added directly to the recording plate (1 mL) to produce the desired drug concentration by undergoing a 1 in 4 dilution. After drug addition, a 15 minute segment where QT prolongation was first apparent by visual observation was selected for analysis. Recording lengths varied depending on the concentration of drug used, e.g. for terfenadine treatments at 0.1, 0.3 and 1 µM recordings were taken for up to 1 hour or more, and for terfenadine treatments at 50 µM recordings were taken for 40 minutes or less.

3.3.6 Agarose-embedded ECG recordings

To obtain ECG recordings from agarose-embedded 3 dpf zebrafish larvae, firstly the zebrafish larvae were individually pipetted into mini-Petri dishes (Fisher Scientific UK Ltd, UK). They were then covered with a 1% solution of molten low melting point agarose (PEQLAB Biotechnologie, Germany) and positioned ventrally within the agarose with the agarose allowed to set for a few minutes before 3 mL of E3 embryo medium was added. Forceps were used to remove the excess agarose from the top portion of the zebrafish larvae exposing the head and the heart. An ECG recording was then taken for five minutes.

3.3.7 ECG data analysis

Analysis of the digitised ECG signal was carried out using LabChart Pro 7 (ADInstruments, UK). After a selection of an ECG recording had been highlighted for analysis the ECG settings function on the LabChart Pro 7 (ADInstruments, UK) programme was used. Using the ECG settings function (shown in **Figure 3.9**) values were automatically calculated for different ECG parameters based on the species tested. If these values did not match up with the ECG recording the correct values could be manually entered. As no set values exist for the recording of fish ECGs on LabChart Pro 7 (ADInstruments, UK), values had to be entered manually each time for each ECG recording analysed. On the ECG settings function, the following were selected: 1) bazett, 2) human, 3) block averaging and 4) rodent T wave. Values were then entered manually for the following parameters: QRS interval width, distance between R waves, pre-P baseline, PR interval, RT interval and ST height. These values were obtained from the ECG recording itself and entered into the appropriate fields in the ECG settings window.

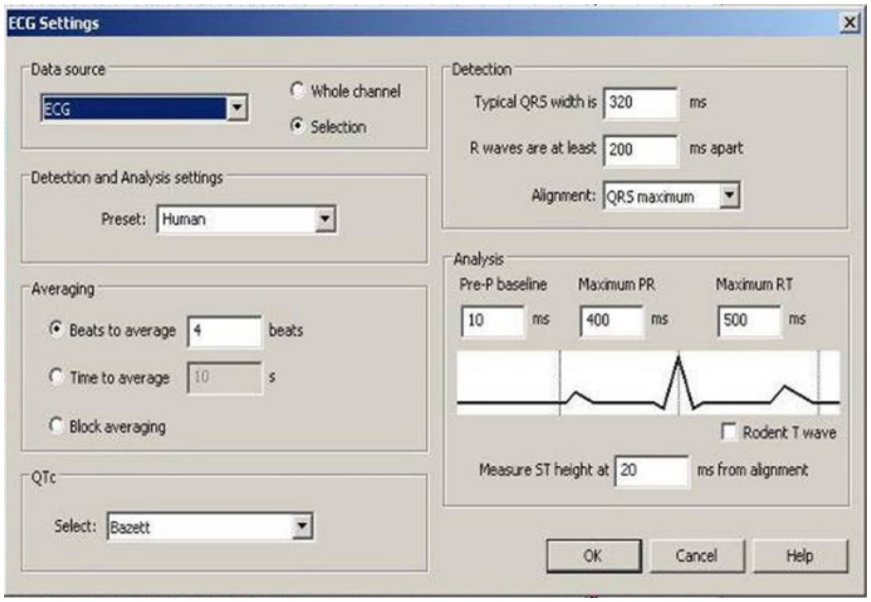

Figure 3.9 – Screenshot of the ECG settings window in LabChart Pro7.

After entering the correct values for the different ECG parameters, the 'analyse' function was selected on the ECG settings window. On the ECG analysis toolbar, 'average view' was selected and a plot was produced showing the average waveform (black) over the selected recording period. Several green waveforms surrounding the average waveform were also generated with each green waveform representing a single cardiac cycle (**Figure 3.10**).

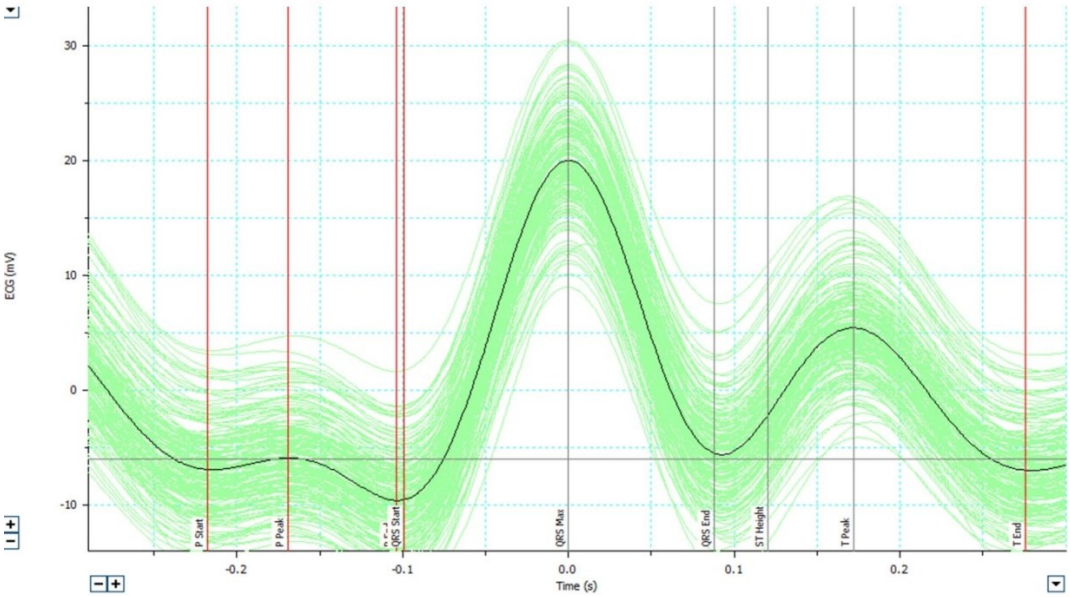

Figure 3.10 – Screenshot of single waveforms (green) and an averaged waveform (black) generated from an analysed ECG recording segment.

Several ECG landmarks (start of P wave, P wave peak, end of P wave, start of QRS, max QRS, end of QRS, T wave peak and T wave end) were then assigned automatically on the plot. Then by selecting the 'tableview' function from the ECG analysis toolbar, a table detailing the time durations of the different ECG parameters, such as the QT interval, RR interval, etc. was generated (**Figure 3.11**).

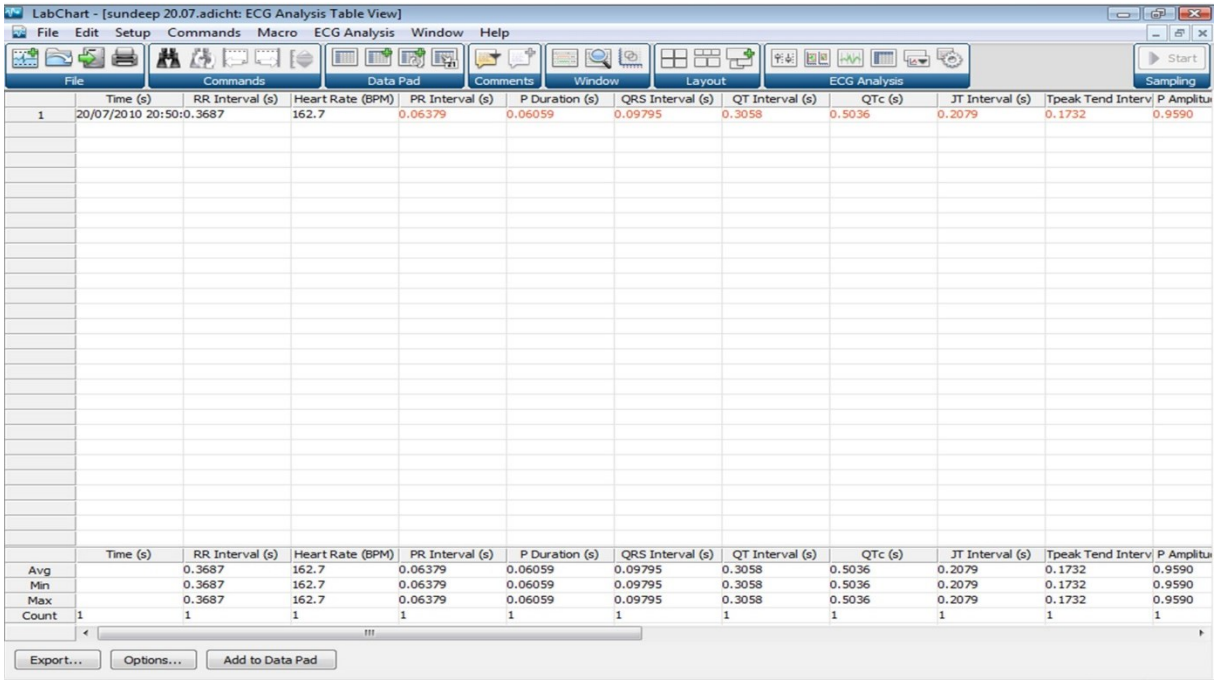

Figure 3.11 – Screenshot of the 'tableview' showing ECG parameters generated from the average waveform.

From the table generated the interval durations for the ECG parameters RR, QRS, QT and QTc were selected for further analysis. These parameters are explained in **Table 3.1** below.

Table 3.1 – ECG parameters measured and their meanings.

ECG parameter	**Meaning**
RR interval	Duration of ventricular cardiac cycle
PR interval	Time interval for the onset of atrial depolarisation to the onset of ventricular depolarisation
QRS interval	Duration of ventricular depolarisation
QT interval	Duration of ventricular depolarisation and repolarisation
QTc interval	QT interval corrected for heart rate

Using these ECG parameter values comparisons could then be made between different ECG recordings or different segments of the same ECG recording. Additionally, for drug treatments the percentage change in the QTc interval duration before and after drug treatment was determined for each tested zebrafish larva. Data obtained from several zebrafish larvae exposed to the same recording conditions were then pooled and averaged and used for graphical representation and statistical analysis.

For the temperature experiments, the temperature coefficient Q_{10} (Reyes et al., 2008) was additionally calculated to quantify the effect of temperature on ECG recordings using the following equation: $Q_{10} = (R2-R1)^{(10/T2-T1)}$ where R1 = heart rate at temperature T1, R2 = heart rate at temperature T2.

3.4 Results

3.4.1 Stability and reproducibility of zebrafish embryo and larval ECG signals

As a glass electrode-based set-up had been previously described for recording ECG signals from zebrafish larvae (Forouhar et al., 2004), the objective of the first experiment was to reproduce this published data by recording ECG signals from 3 dpf zebrafish larvae using our own ECG set-up. The experiment was performed by first anaesthetising 3 dpf zebrafish larvae in 0.3 mg/mL of MS222 anaesthetic for 10 minutes before transferring one zebrafish larva into the recording plate (2% agarose covered plate with grooves) containing 10 mL of E3 embryo medium. Each larva was positioned ventrally within the grooves and the positive electrode was positioned on the surface of the heart at the atrium and ventricle boundary. A

reference electrode was also placed in the recording plate away from the zebrafish larva. Once everything was in place an ECG signal could be recorded (**Figure 3.12**).

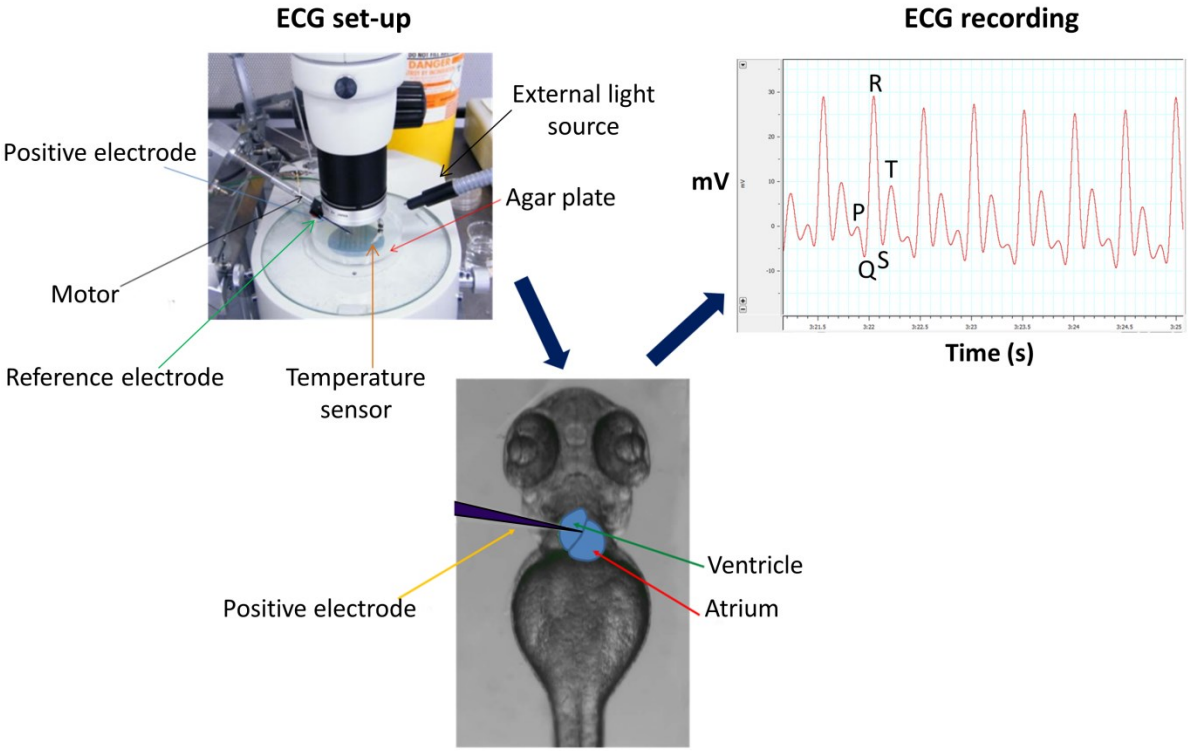

Figure 3.12 – ECG set-up. *For ECG recording purposes all the equipment was housed in a Faraday cage to minimise background noise. A stereomicroscope, external light and forceps were used to position anaesthetised zebrafish embryos/larvae ventrally inside grooves of a 2% agarose-covered Petri dish. A micromanipulator and motor were used to position the positive electrode on the skin surface at the atrium and ventricle boundary. A reference electrode was also placed in the recording plate along with a temperature sensor to monitor the temperature during recordings. The raw ECG signals were digitised and viewed using LabChart 7 Pro (ADInstruments, UK).*

Once all the equipment was in place, the LabChart Pro7 software was used to detect the ECG signal. A representative raw ECG trace from a 3 dpf zebrafish larva is shown in **Figure 3.13A**. In order to make the signal clearer low-pass filtering was introduced to eliminate background noise (**Figure 3.13B**). Using the analysis function on the LabChart Pro7 software a section of the filtered ECG recording was analysed and a mean ECG waveform was generated (black line) (**Figure 3.13C**). The recorded ECG signal was found to be stable (no

change in waveform), as all individual waveforms (grey lines) from the recording period were found to be close to the mean (**Figure 3.13C**). Additionally, the ECG signals recorded were found to have the three distinctive features that make up a typical ECG, including a small P wave representing atrial depolarisation, a large QRS complex representing ventricular depolarisation and a moderate T wave representing ventricular repolarisation (**Figure 3.13D**).

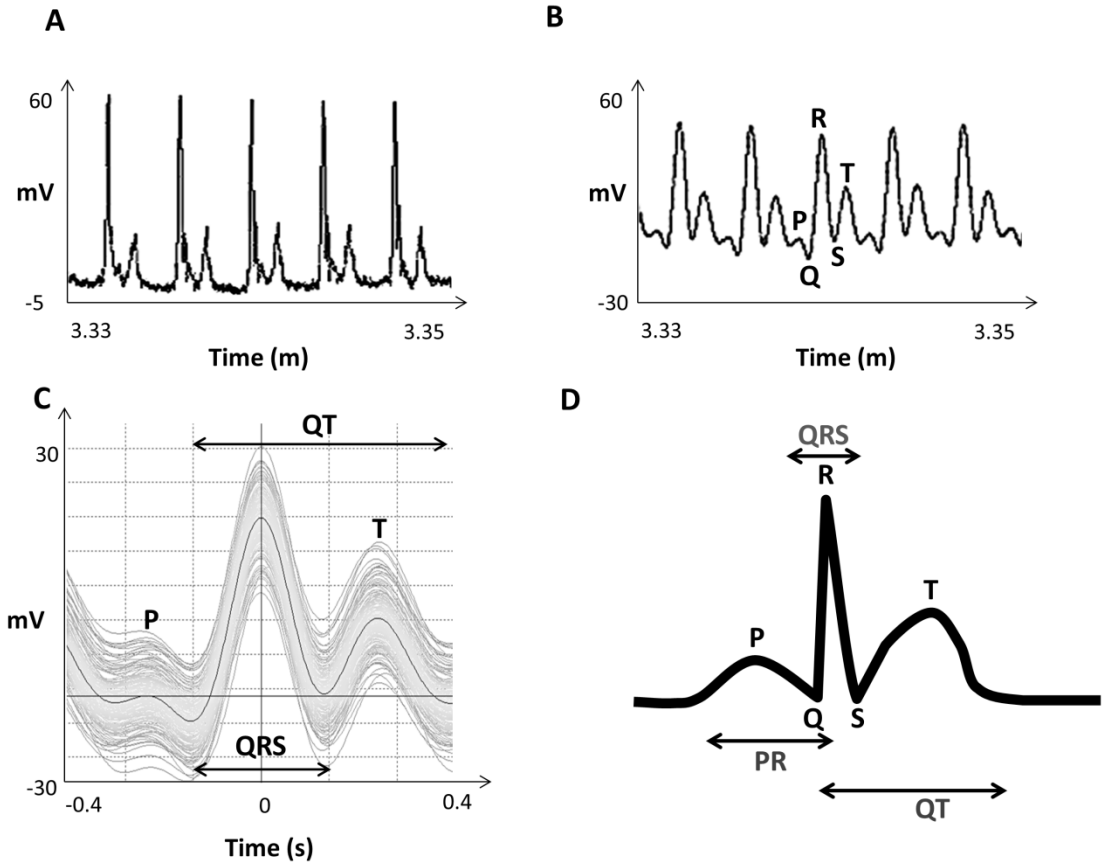

Figure 3.13 – ECG signal filtering and processing. *A) Raw 3 dpf zebrafish ECG signal (two minute segment) before filtering viewed using LabChart 7 Pro, B) Low-pass digitally filtered (digital filter = 15) 3 dpf zebrafish ECG signal (two minute segment) viewed using LabChart 7 Pro, C) Analysed 1 minute segment of a 3 dpf zebrafish ECG recording viewed using LabChart 7 Pro (grey lines = single waveforms, black line = mean), D) Schematic of 3 dpf zebrafish ECG waveform.*

Once the ECG recording set-up was in place the reproducibility of the set-up could be determined. In order to address this issue; surface ECG recordings were taken using the same method described above for 30 zebrafish larvae aged 3 dpf. Mean values were calculated for the RR, QT and QTc time interval durations over a five minute recording period using these 30 zebrafish larvae. All of the results were then collated and averaged (**Figure 3.14A**). The standard deviation (SD) values for RR (0.035), QT (0.028) and QTc (0.032) interval durations were found to be small, thus showing that reproducible ECG signals could be obtained from different 3 dpf zebrafish larvae using this set-up. Additionally, when looking specifically at the QTc interval it was found that with increasing numbers of zebrafish larvae the SD values were found to remain relatively stable in the 0.03 range (**Figure 3.14B**). For example, the SD value for both 15 and 30 zebrafish larvae was found to be 0.032. There was found to be no significant difference between the QTc interval duration values for differing numbers of zebrafish larvae ($P>0.05$), hence this confirmed that the ECG set-up had relatively good reproducibility even when using a small number of zebrafish larvae.

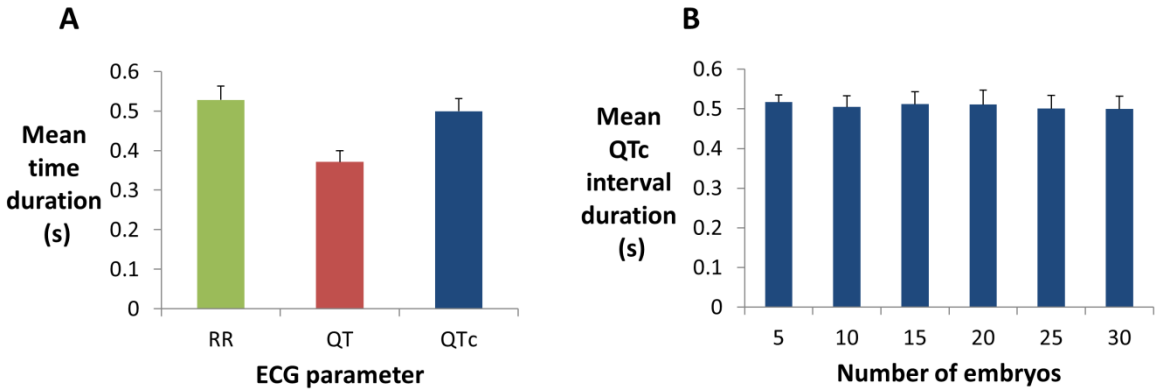

Figure 3.14 – ECG signal reproducibility. *A) Mean time duration values for RR, QT and QTc intervals (n=30 zebrafish larvae aged 3 dpf), B) Mean QTc interval durations for increasing numbers of 3 dpf zebrafish larvae (P>0.05).*

3.4.2 Investigation into methods to exclude motion artefact from zebrafish embryo and larval ECG recordings

The initial experiments performed showed that reproducible recordings could be obtained from zebrafish larvae; however the next question that needed to be addressed was whether motion artefact was responsible for the ECG signals observed. Motion artefact has been extensively documented to contaminate surface ECG recordings (Tong et al., 2001)(Redfern et al., 1993)(Tong et al., 2002). It can occur due to mechanical movements, such as beating of the heart or in the case of mammals additionally due to respiratory motion (Wang et al., 1995)(Tournebize et al., 2006). A number of approaches have been used to counteract this problem including using analogue/digital filters and various mathematical techniques, such as temporal/spatial averaging and independent component analysis which can remove motion artefact from ECG recordings during or after processing (He et al., 2006). However, electro-mechanical uncouplers are commonly used to exclude motion artefact before an ECG recording is taken by preventing the mechanical movement of the heart without perturbing the electrical signal (Brines et al., 2012).

To exclude possible motion artefact due to mechanical movement of the heart in zebrafish larvae two different approaches were used. The first approach was to use a drug, namely cromakalim in order to separate the electrical activity of the heart from the mechanical movement. Cromakalim hyperpolarises potassium channels resulting in relaxation of the cardiac muscle of the heart (Fujii et al., 1990). Seven different concentrations of cromakalim were tested (10, 25, 50, 100, 200, 300 and 400 μM). The reason for using such a wide concentration range was because, it was not known at which concentration this drug would

be active in zebrafish larvae. The experiment was performed by anaesthetising zebrafish larvae in 0.3 mg/mL of MS222 anaesthetic for 10 minutes before transferring one zebrafish larva individually to the recording plate.

The recording plate consisted of a mini Petri dish containing an unscented paraffin wax layer with grooves. After positioning the zebrafish larva in the recording plate a surface ECG recording before drug addition for 5 minutes and then after drug addition for 15 minutes was taken. In addition to this heart contractility was also monitored over the recording period. The percentage change in the mean RR, QT and QTc interval durations was then calculated for each concentration of cromakalim tested (**Figure 3.15**, n=5 zebrafish larvae at 3 dpf per drug concentration). It was found that cromakalim at all of the tested concentrations was found to have no significant effect on the RR interval ($P>0.05$), QT interval ($P>0.05$) or QTc interval ($P>0.05$). Additionally, the contractility of the heart remained unchanged, suggesting that the drug either was not taken up or the concentrations tested were too low.

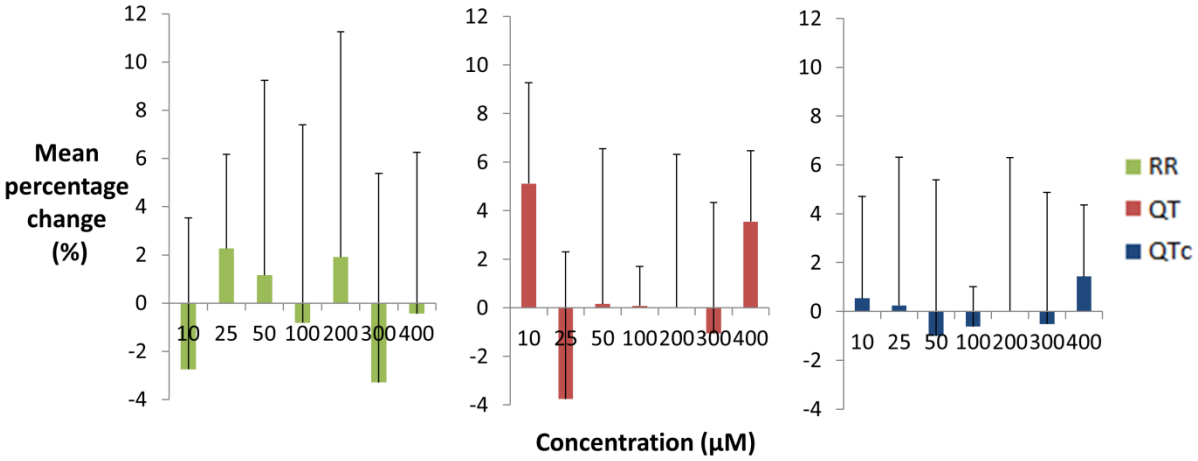

Figure 3.15 – Effect of cromakalim drug treatment on ECG interval durations. *Mean percentage change in RR, QT and QTc interval durations after treatment of zebrafish larvae with different concentrations of cromakalim (n=5 zebrafish larvae at 3 dpf per drug concentration, P>0.05 for RR, QT and QTc).*

As cromakalim was found to have no effect two other drugs were then tested, which included the excitation-contraction uncouplers 2,3-butanedione-monoxime (BDM) and blebbistatin. BDM is a routinely used agent in the field of cardiac electrophysiology and blebbistatin is a synthetic peptide that is a relatively newer agent (Brines et al., 2012).

Zebrafish larvae were first anaesthetised in 0.3 mg/mL of MS222 anaesthetic for 10 minutes before transferring one zebrafish larva individually to the recording plate and then taking a surface ECG recording before drug addition for 5 minutes and then after drug addition for 30 minutes (n=10 zebrafish larvae at 3 dpf per drug concentration). BDM was only tested at 15 mM, whereas blebbistatin was tested at two concentrations; namely 10 and 15 µM. These concentrations were chosen based on those reported in the literature for excised 2 dpf zebrafish embryo hearts (Jou et al., 2010). With both agents there was found to be a complete abolishment of contraction of the zebrafish larval heart. The mean QTc interval durations with both agents were found to be slightly prolonged, however this was found not

to be significant (**Figure 3.16A**,**B**, n=10 zebrafish larvae at 3 dpf per drug concentration, P>0.05). The RR and QT intervals (not shown) were also prolonged but again these changes were found not to be significant (P>0.05). The waveform amplitudes were found to be reduced after treatment with these two drugs. Additionally, both drugs were also found to severely affect the survival of the zebrafish larvae with ECG recordings only obtainable up to 10 minutes in the case of BDM and up to 30 minutes in the case of blebbistatin at 10 and 15 µM. After this time blood accumulation in the heart and necrosis of the extremities (head and tail) was observed.

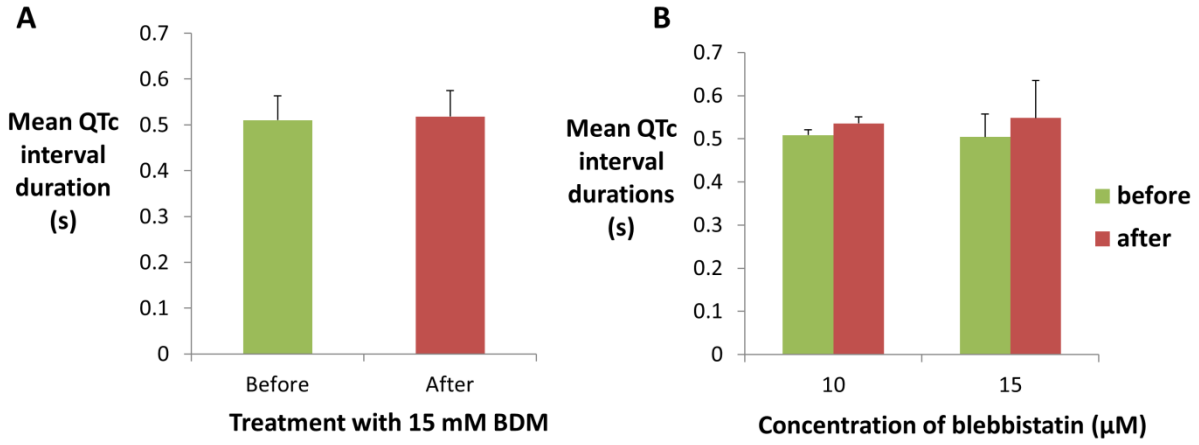

Figure 3.16 - Exclusion of motion artefact through the use of electro-mechanical uncouplers. *A) Mean QTc interval durations before and after 15 mM BDM treatment of 3 dpf zebrafish larvae (n=10 zebrafish larvae at 3 dpf per drug concentration, P>0.05), B) Mean QTc interval durations before and after treatment of 3 dpf zebrafish larvae with 10 & 15 µM blebbistatin (n=10 zebrafish larvae at 3 dpf per drug concentration, P>0.05).*

To overcome the problems observed with the drug treatments (i.e. non-responsiveness and toxicity) a second approach was taken to exclude motion artefact. This involved altering the recording method by puncturing the zebrafish heart and taking an invasive ECG recording.

The invasive ECG recording was performed using the exact same set-up and operating parameters utilised for measuring surface ECGs. The only difference was that the speed of

the step motor was tripled and the distance by which it moved which was increased from 5 to 500 µM. Through these changes, the positive electrode could be pushed with enough force directly into the heart by penetrating the skin. The results obtained from this experiment showed that there were minimal differences between taking an invasive and a non-invasive ECG recording (**Figure 3.17**, n=5 zebrafish larvae at 3 dpf, P>0.05). Taken together these results suggest that the surface ECG recording technique currently being utilized enables true electrical recordings of the heart to be obtained.

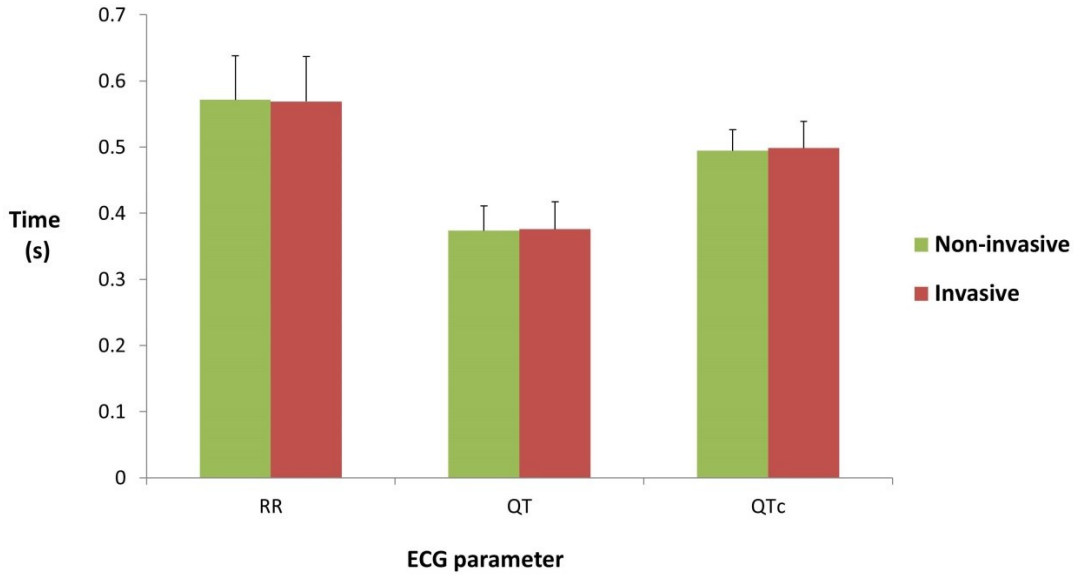

Figure 3.17 – Exclusion of motion artefact by performing an invasive ECG recording. *Changes in ECG parameters for non-invasive and invasive larval zebrafish ECG recordings (n=5 zebrafish larvae at 3 dpf per method, P>0.05 for RR, QT and QTc).*

3.4.3 Investigation into methods to immobilize zebrafish embryos and larvae during ECG recordings

For ECG recording purposes zebrafish embryos and larvae had to immobilized, so that motion artefact from physical movement (e.g. movement of fins) did not interfere with the ECG signals obtained. To address this issue various immobilization methods were explored including the use of low melting point agarose. When using low melting point agarose non-

anaesthetised zebrafish larvae aged 3 dpf were first individually pipetted into mini-Petri dishes and then covered with a 1% solution of molten low melting point agarose. The zebrafish larvae were positioned ventrally within the agarose and the agarose was then allowed to set for a few minutes before 3 mL of E3 embryo medium was added to the plates. Forceps were used to remove the excess agarose from the top portion of the zebrafish larvae exposing the head and the heart (**Figure 3.18A**). Surface ECG recordings were then taken for five minutes (n=10 zebrafish larvae).

Additionally, ECG recordings were also taken from 3 dpf zebrafish larvae which had been anaesthetised with 0.3 mg/mL of MS222 for 10 minutes before being immobilized in the low melting point agarose (n=10 zebrafish larvae). ECG interval durations were determined for the two different methods used and then compared (**Figure 3.18B**). The RR interval was found to differ significantly between unanaesthetised and anaesthetised zebrafish larvae (**Figure 3.18B**, n=10 zebrafish larvae at 3 dpf per condition, $P<0.05$), whereas the QT and QTc interval durations were found to show no significant differences (**Figure 3.18B**, n=10 zebrafish larvae at 3 dpf per condition, $P>0.05$).

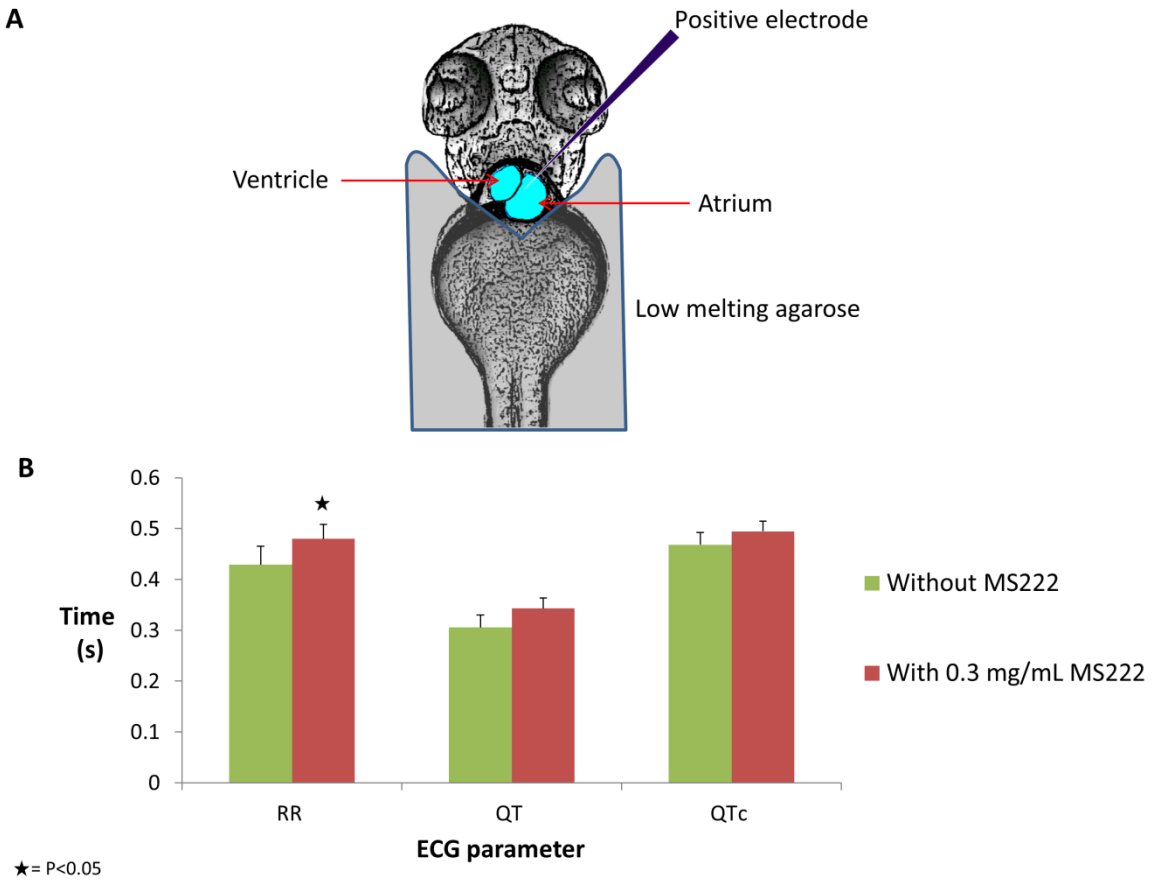

Figure 3.18 – Agarose embedding as a form of immobilization. *A) Schematic of 3 dpf zebrafish larva embedded in low melting point agarose with heart exposed, B) Differences in ECG parameters between non-anaesthetised and 0.3 mg/mL MS222 anaesthetised 3 dpf zebrafish larvae (n=10 zebrafish larvae at 3 dpf per condition, P<0.05 for RR, P>0.05 for QT and QTc).*

As it was time consuming and difficult to position zebrafish larvae in low melting point agarose, the agarose plate method that was initially used for ECG recording purposes was optimised. However, when using the agarose plate method the zebrafish larvae had to be immobilized in some way with a paralysing or anaesthetic agent in order to position them within the agarose grooves and keep them still throughout the recording. The anaesthetic agent MS222 was used for this purpose and was tested at several different concentrations (0.1, 0.3, 0.5 and 1 mg/mL). When using MS222 zebrafish larvae were first anaesthetised for 10 minutes before being individually transferred to the recording plate. ECG recordings were

then taken for 15 minutes. A paralysing agent tubocurarine (Buss et al., 2003) was also tested as an alternative sedating agent at two concentrations (100 and 400 µM). With tubocurarine zebrafish larvae had to be continuously exposed to the agent, hence it was added directly to the recording plate and ECG recordings were then taken for 15 minutes. Both agents were found to produce comparable recordings with little difference observed in the calculated ECG parameters (**Figure 3.19A, B**).

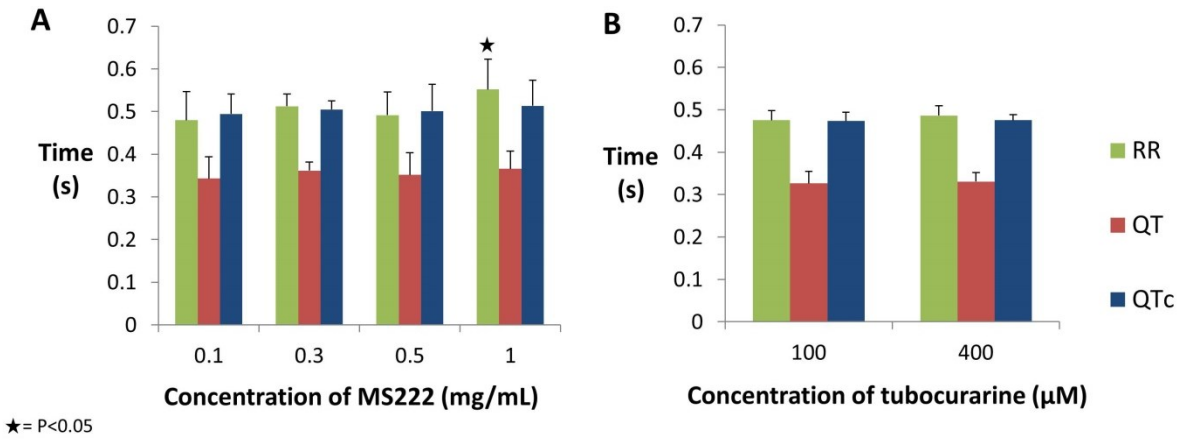

Figure 3.19 – Forms of immobilization. *A) Effect of different concentrations of MS222 on mean ECG interval durations (n=10 zebrafish larvae at 3 dpf per drug concentration, P<0.05 for RR, P>0.05 for QT and QTc), B) Effect of different concentrations of tubocurarine on mean ECG interval durations (n=10 zebrafish larvae at 3 dpf per drug concentration, P>0.05 for RR, QT and QTc).*

For MS222 at the highest tested concentration of 1 mg/mL (n=10 zebrafish larvae at 3 dpf per drug concentration) there was found to be a significant increase in the RR interval ($P<0.05$). The QT interval ($P>0.05$) and the QTc interval ($P>0.05$) on the other hand were found to show no significant differences. When analysing the results obtained for tubocurarine it was found that the RR interval ($P>0.05$), QT interval ($P>0.05$) and QTc interval ($P>0.05$) all showed no significant differences. However, as tubocurarine has been documented to undergo drug-drug interactions, specifically with anti-arrhythmics (Harrah et al., 1970), it was decided not to use it for ECG recording purposes. Therefore, MS222 at 0.3

mg/mL was subsequently used for ECG recordings as at this concentration it was found to have no significant effect on the QTc interval duration or any of the other ECG intervals.

3.4.4 Identification and characterisation of variables of zebrafish embryo and larval ECG recordings

To optimise the ECG recording set-up various factors were addressed that could influence either detection of the ECG signal or heart function itself. One such factor included the ambient temperature at which ECG recordings were taken. As zebrafish are ectothermic animals (organisms where ambient temperature influences body temperature) at lower temperatures the electrical activity of the cardiac myocytes is reduced resulting in a decreased QRS amplitude and heart rate (ƒH) (Seth et al., 2013)(Maricondi-Massari et al., 1998). At higher temperatures the opposite effect is observed where there is an increase in *f*H and the electrical activity of the cardiac myocytes (Maricondi-Massari et al., 1998).

As zebrafish develop normally at 28^{o}C but can also develop at a slower rate at 18^{o}C, four temperatures (20, 22, 24 and 28°C) within this range were subsequently chosen in order to investigate the effects of temperature on ECG recordings. A homemade heating element connected to a temperature controller was used to increase the temperature in the recording plate containing 5 mL of E3 embryo medium. This was done by firstly embedding the heating pad of the device in 2% agarose inside a Petri dish. A plastic template was then used to create grooves on the upper surface of the agarose layer; this could then later be used to position the zebrafish larvae during ECG recordings. The temperature was monitored and controlled using a sensor that was placed inside the recording plate. Once the

temperature inside the plate had reached the required level, a zebrafish larva at 3 dpf was transferred to the recording plate and was left to acclimatize for 30 minutes. The zebrafish larva was then transferred for 10 minutes to 0.3 mg/mL MS222 anaesthetic solution before being transferred back to the recording plate and being positioned within a groove. An ECG recording was then taken for five minutes. This process was repeated several times with ECG recordings taken at each temperature using 10 different 3 dpf zebrafish larvae each time.

After calculating the mean RR, QT and QTc interval durations it could be seen that at higher temperatures the mean RR, QT and QTc interval durations were reduced whereas the opposite effect occurred at lower temperatures (**Figure 3.20A**). The changes observed in the RR ($P<0.05$), QT ($P<0.05$) and QTc ($P<0.05$) interval durations by an increase or decrease in temperature were found to be significant. Additionally, the results also demonstrated that heart function was sensitive to temperature and this was further confirmed by calculating Q_{10} coefficients which were found to be 2.7 over the 10°C range (**Figure 3.20B**).

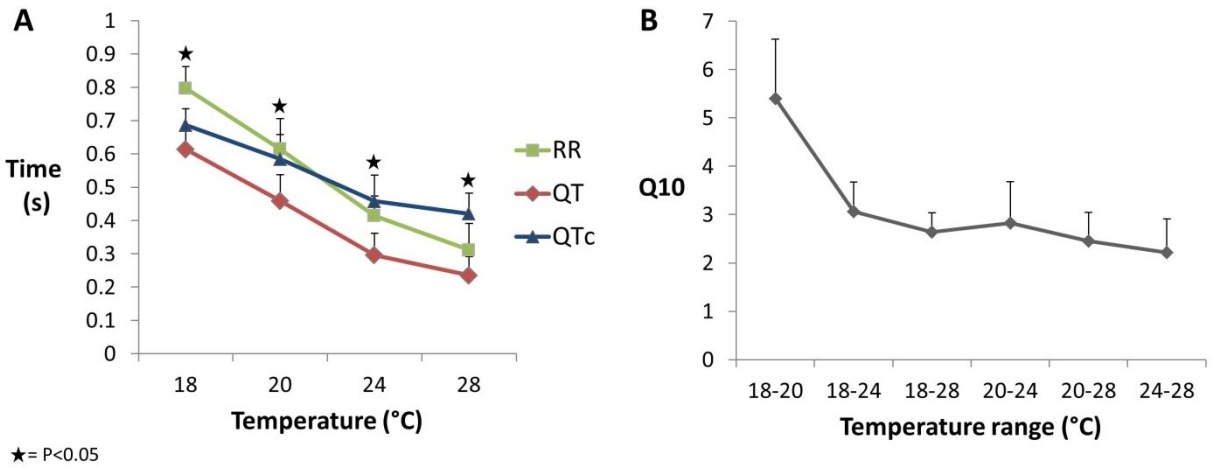

Figure 3.20 – Optimisation of recording temperature. *A) Effect of different recording temperatures on mean ECG interval durations (n=10 zebrafish larvae at 3 dpf, $P<0.05$ for RR, QT and QTc), B) Change in calculated Q_{10} coefficients over a 10°C temperature range.*

The next variable that was addressed was the developmental stage of the zebrafish used for obtaining ECG recordings. At 2 dpf zebrafish have a fully functional ventricle and atrium, however the ventricle continues to mature and thicken during development even after the heart has formed (Glickman and Yelon, 2002)(Rottbauer et al., 2001). This could therefore impact on the ECG signal that is recorded by causing a possible increase in the amplitude of the T wave and a narrowing of the QRS complex (Yu et al., 2010). To determine whether the zebrafish developmental stage had an influence on the morphology of the ECG signal an experiment was performed where ECG recordings were taken from 2, 3, 4 and 5 dpf zebrafish and compared. Eight zebrafish from each developmental stage were tested and ECG recordings were taken for five minutes.

It was found that reproducible ECG recordings could be obtained from all stages tested including at 2 dpf where P, QRS and T waves were clearly visible on the ECG recordings (**Figure 3.21A**). Between 2 dpf zebrafish embryos and 3, 4 and 5 dpf zebrafish larvae there was found to be a significant difference in QT interval durations (**Figure 3.21B**, n=8 zebrafish per developmental stage, $P<0.05$). Additionally, there was found to be a significant difference in QTc intervals between 2 and 5 dpf zebrafish ($P<0.05$). The mean RR interval durations on the other hand did not differ significantly among any of the age groups ($P>0.05$). For subsequent drug treatment experiments 3 dpf zebrafish larvae were used due to ease of manipulation in terms of positioning in the recording plate as with later stages (e.g. 5 dpf) it was more difficult to position the zebrafish properly due to inflated swim bladders.

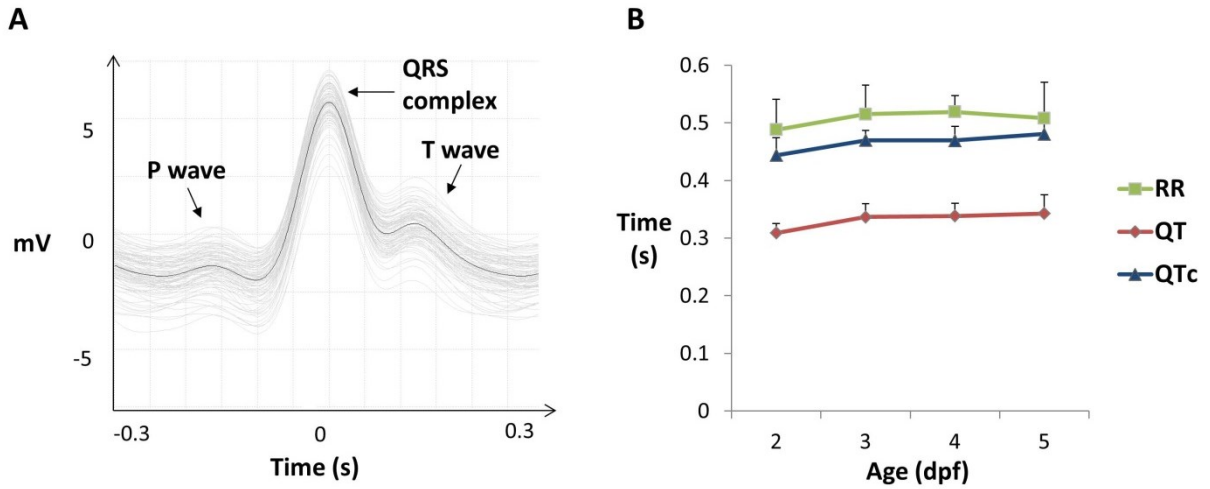

Figure 3.21 – Optimisation of recording stage. *A) Analysed ECG trace from a 2 dpf zebrafish embryo for a one minute recording segment (grey lines = single waveforms, black line = mean), D) Effect of recording age on mean ECG interval durations (n=8 zebrafish per developmental stage, P>0.05).*

Another variable addressed was the electrode position on the heart. In adult zebrafish ECG studies it was noted that differences in electrode position were possibly responsible for the variation in T wave amplitude and morphology (Milan et al., 2006)(Sun et al., 2009). In the experiments described in this chapter, ECG Recordings were performed by placing the electrode on the boundary between the atrium and ventricle (**Figure 3.22A**), the same position used by Forouhar and colleagues, as this position is thought not to disturb the function of cardiac ion channels (Forouhar et al., 2004). To find out whether the electrode position could influence ECG signals, ECG recordings were taken at eight different positions along the heart axis (**Figure 3.22B**). The mean RR, QT and QTc interval durations were then determined for each position (**Figure 3.22C**). The results obtained showed no significant differences in the mean RR ($P>0.05$), QT ($P>0.05$) or QTc ($P>0.05$) interval durations at each of the tested positions.

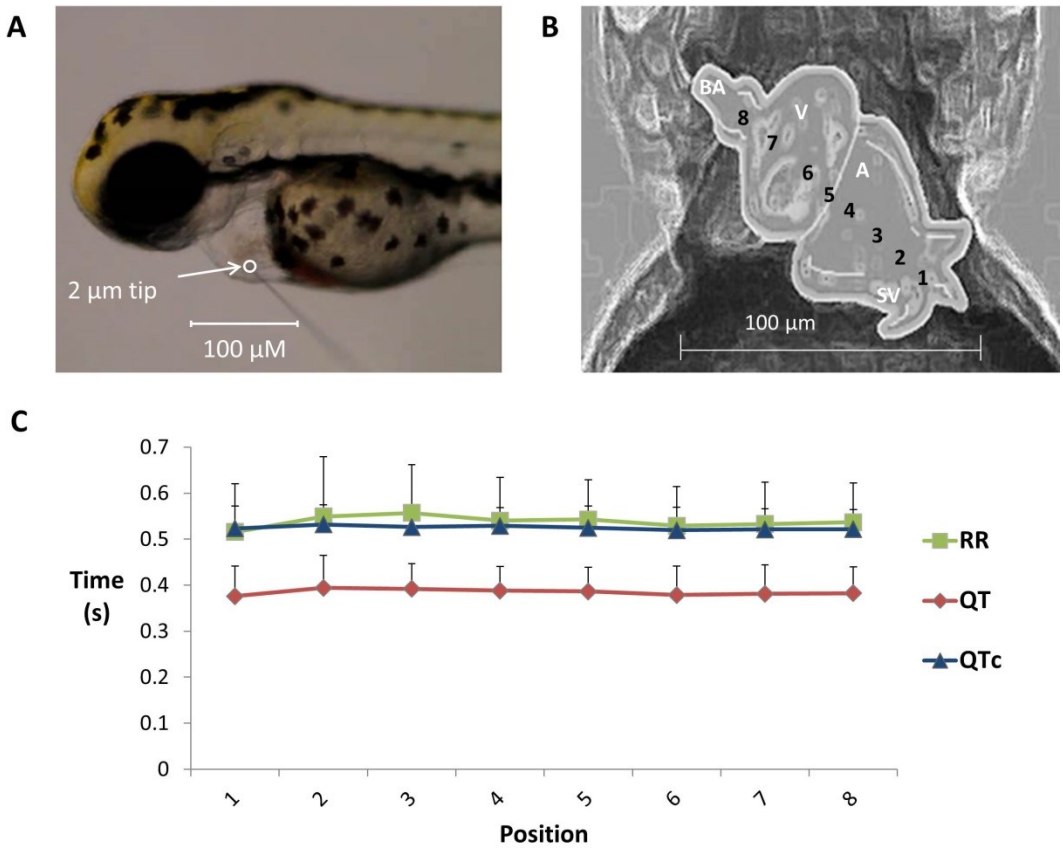

Figure 3.22 – Optimisation of electrode position on zebrafish heart. *A) Picture of a 3 dpf zebrafish larva with the electrode tip positioned between the atrium and ventricle, B) Schematic of a 3 dpf zebrafish larva with different recording positions along the heart axis marked, C) Mean ECG interval durations obtained at different electrode positions on the heart in 3 dpf zebrafish larvae (n=10 zebrafish larvae per position). Key: 1=sinus venosus, 2=between atrium and sinus venosus, 3=base of atrium, 4=apex of atrium, 5=between atrium and ventricle, 6=base of ventricle, 7=apex of ventricle and 8=bulbus arteriosus.*

Furthermore, the distance of the electrode from the surface of the heart was also investigated in order to see if this affected the ECG recordings. There was found to be no statistically significant change in the QTc interval after movement of the electrode longitudinally by 5 and 10 µm towards the surface of the heart ($P>0.05$). The ECG waveform however was found to be influenced with a decrease in the ECG signal amplitude observed (**Figure 3.23A**,**B**, n=3 zebrafish larvae at 5 dpf). Taken together, these findings concluded that electrode positioning was not important when performing ECG recordings.

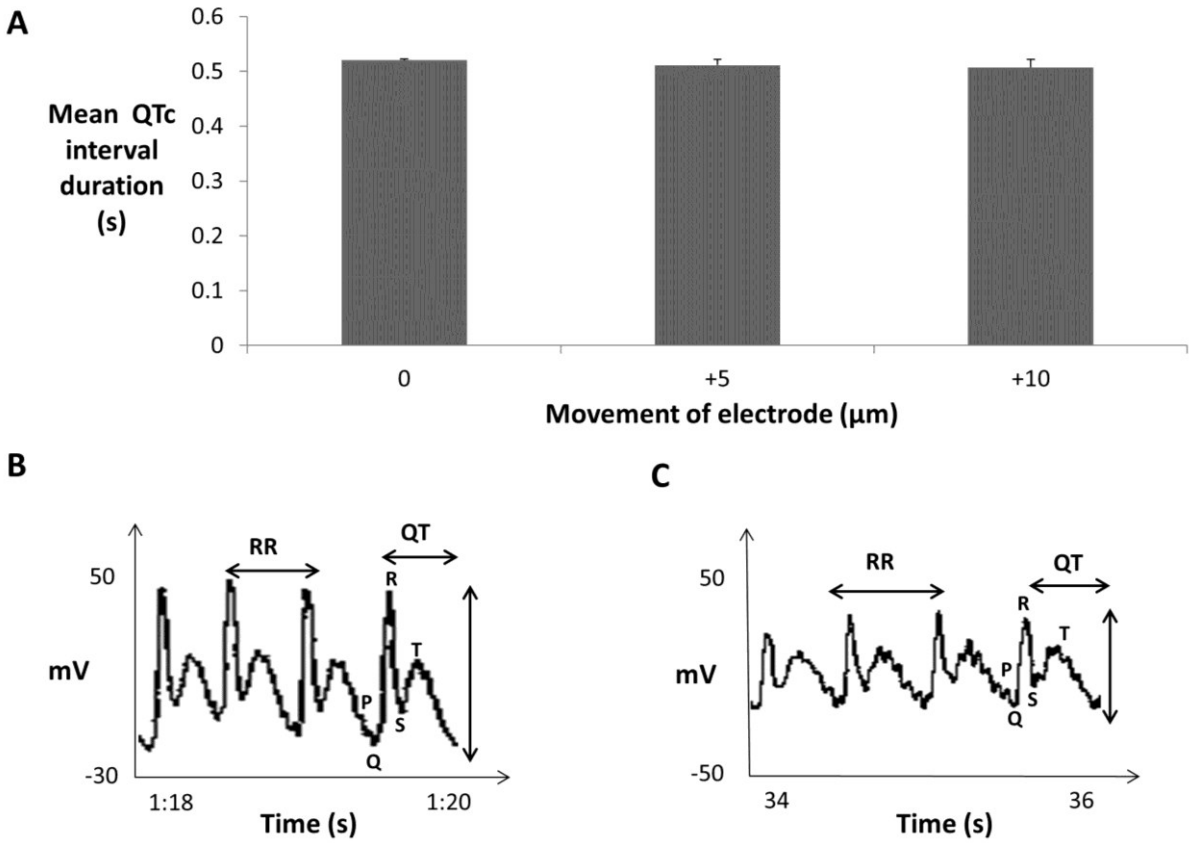

Figure 3.23 – Effect of electrode distance from the zebrafish heart on ECG signal morphology. *A) Mean QTc interval durations obtained from 5 dpf zebrafish larvae at an atrium/ventricle boundary starting position and after movement of the electrode longitudinally by 5 and 10 µm (n=3 zebrafish larvae at 5 dpf), B) 5 dpf zebrafish larval ECG trace (two seconds) after movement of electrode 5 µm longitudinally from initial starting position, C) 5 dpf zebrafish larval ECG trace (two seconds) after movement of electrode longitudinally by 10 µm from initial starting position.*

3.4.5 Zebrafish larval ECG recording set-up as a tool for detecting drug-induced cardiotoxicity

Once the ECG recording set-up had been optimised, the next question addressed was whether this set-up could be utilised as a screening tool to detect cardiotoxic effects of drugs. As mentioned previously drug-induced QT prolongation which is a condition caused by blockade of the hERG channel (the main cardiac ion channel involved in ventricular repolarisation) that can predispose to life threatening conditions such as TdP was of particular interest to study in 3 dpf zebrafish larvae (Katchman et al., 2006). Three drugs

(terfenadine, haloperidol and pimozide) known to induce QT prolongation in humans were selected and thus tested for their effects on 3 dpf zebrafish larval ECG recordings. In addition to this a drug not known in humans to cause QT prolongation (verapamil) (Redfern et al., 2003), as well as a drug not shown in either adult zebrafish or humans to cause QT prolongation (penicillin) were tested (Milan et al., 2006). Drug treatments were performed by first anaesthetising the zebrafish larvae at 3 dpf in 0.3 mg/mL of MS222 anaesthetic for 10 minutes before transferring them to a recording plate with a wax surface. Wax was used instead of agarose, as with agarose there was the possibility that drug would diffuse into it. Once the zebrafish larva was transferred to the recording plate 3 mL of E3 embryo medium was added to the plate. An ECG recording was then taken for five minutes. After five minutes, 1 mL of drug solution was added to the recording plate as carefully as possible, so as not to move the zebrafish larva. Another ECG recording was then taken for a minimum of 15 minutes; however the recording time varied depending on the concentration of drug tested. For example with terfenadine at the lower concentrations of 0.1 and 0.3 µM ECG recordings were taken for more than an hour.

From the ECG recordings the percentage change in the QTc interval after drug treatment compared to before treatment was determined for each drug at each of the tested concentrations. Terfenadine was found to increase the QTc interval in a dose-dependent manner, which was found to be significant for all tested concentrations (**Figure 3.24A**, n=8 zebrafish larvae at 3 dpf per concentration, $P<0.05$). The QTc prolongation observed with terfenadine was characterised by widening of the T wave (**Figure 3.24B**), similar to what has been observed in adult zebrafish ECG recordings following exposure to this drug (Milan et

al., 2006). Additionally, the heart rate was also found to significantly decrease in a dose-dependent manner (**Figure 3.24C**, n=8 zebrafish larvae at 3 dpf per concentration, P<0.05).

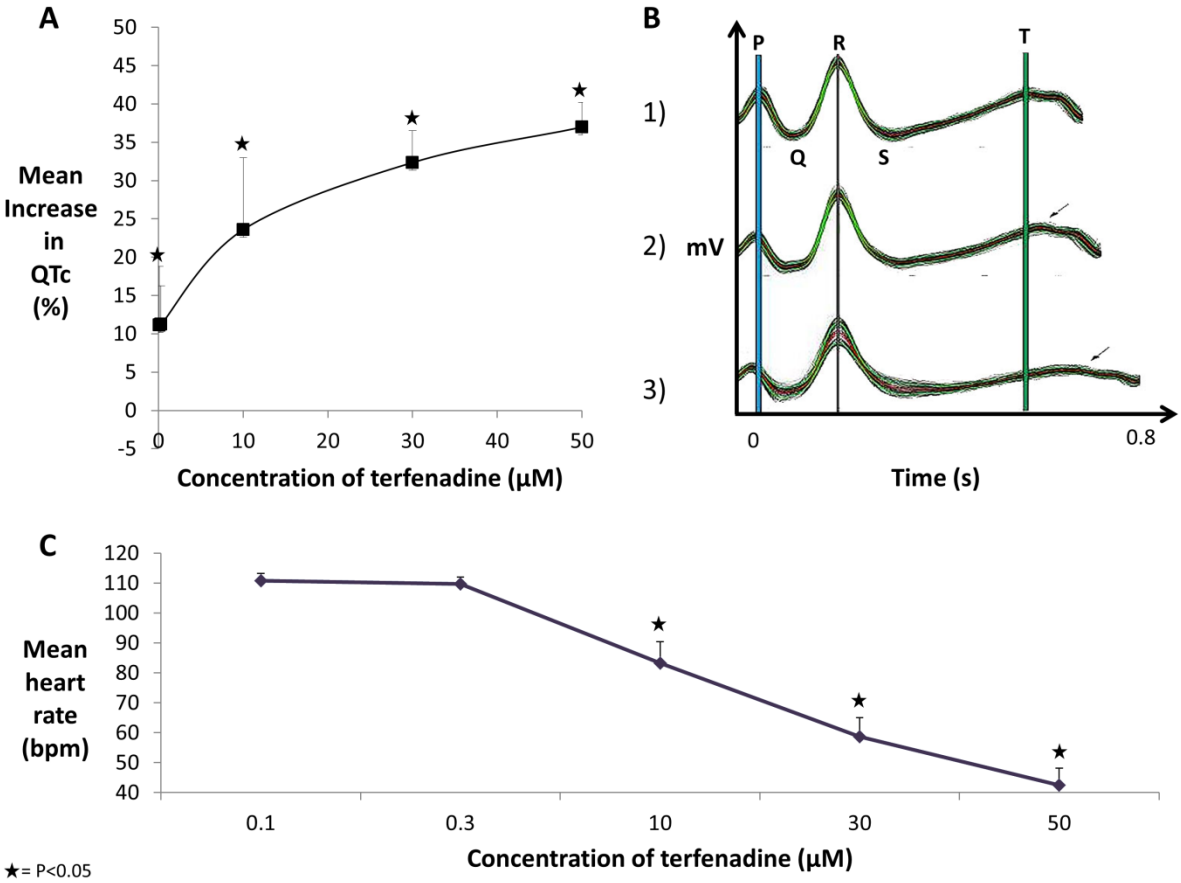

Figure 3.24 – QTc prolongation in zebrafish larvae after treatment with terfenadine. *A) Mean QTc interval percentage change after treatment of 3 dpf zebrafish larvae with different concentrations of terfenadine (n=8 zebrafish larvae at 3 dpf per concentration, P<0.05), B) Schematic of T wave widening after treatment of a 3 dpf zebrafish larvae with 50 µM terfenadine (1 = before, 2 = after 10 minutes, 3 = after 20 minutes), C) Mean heart rate after treatment of 3 dpf zebrafish larvae with different concentrations of terfenadine (n=8 zebrafish larvae at 3 dpf per concentration, P<0.05).*

A similar effect to terfenadine was also seen with the other two QT prolonging drugs, namely haloperidol and pimozide, which were both found to cause a significant increase in the QTc interval duration and a significant decrease in the heart rate (**Figure 3.25**, n=8 zebrafish larvae at 3 dpf per concentration, P<0.05). However, in contrast to terfenadine both pimozide and haloperidol were found not to show concentration-dependence in their

QTc prolonging effects. This could be due to greater specificity of haloperidol and pimozide to bind to the zERG channel, therefore leading to a maximal response at lower concentrations compared to terfenadine (Testai et al., 2010).

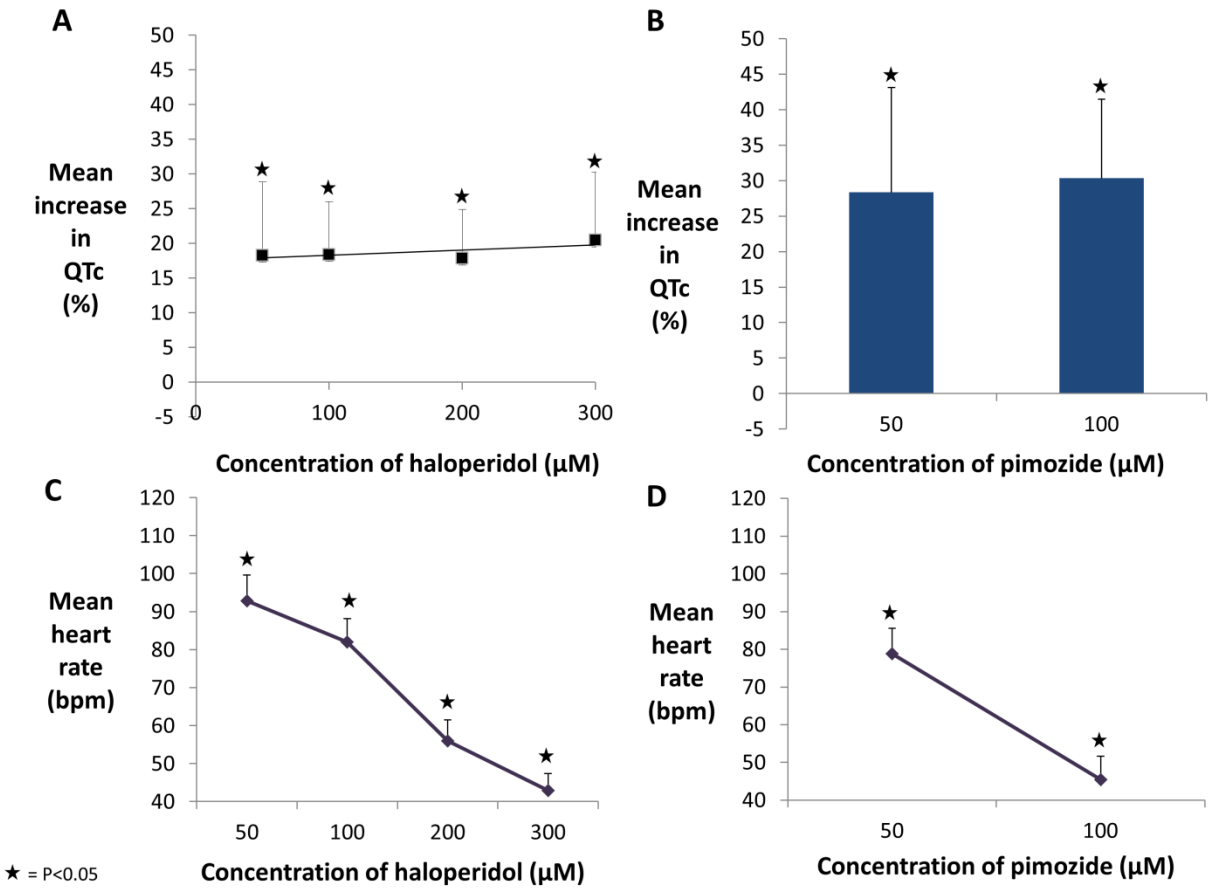

Figure 3.25 – QTc prolongation in zebrafish larvae after treatment with haloperidol and pimozide. *A) Mean QTc interval percentage change after treatment of 3 dpf zebrafish larvae with different concentrations of haloperidol (n=8 zebrafish larvae at 3 dpf per drug concentration, P<0.05), B) Mean QTc interval percentage change after treatment of 3 dpf zebrafish larvae with different concentrations of pimozide (n=8 zebrafish larvae at 3 dpf per drug concentration, P<0.05), C) Mean heart rate after treatment of 3 dpf zebrafish larvae with different concentrations of haloperidol (n=8 zebrafish larvae at 3 dpf per concentration, P<0.05), D) Mean heart rate after treatment of 3 dpf zebrafish larvae with different concentrations of pimozide (n=8 zebrafish larvae at 3 dpf per concentration, P<0.05).*

Penicillin which was used as a negative control as it is a known non-QT prolonging drug in humans and adult zebrafish (Milan et al., 2006) was found to have no significant effect on

the QTc interval duration or heart rate in 3 dpf zebrafish larvae (**Figure 3.26A**,**D**, n=8 zebrafish larvae at 3 dpf per drug concentration, P>0.05). Surprisingly, the anti-arrhythmic agent verapamil which is a known hERG blocker *in vitro* (Martin et al., 2004) but not *in vivo* in humans at therapeutic concentrations (Fossa et al., 2002) was found to cause QTc prolongation in 3 dpf zebrafish larvae but only at the higher concentrations tested (**Figure 3.26B**, n=8 zebrafish larvae at 3 dpf per drug concentration, P<0.05 for 100, 200, 300, 400 and 1000 µM, P>0.05 for 10 and 25 µM). With verapamil at 1 mM widening of the T wave and an increase in its amplitude were clearly evident (**Figure 3.26C**). However, with verapamil no effect on the heart rate was observed (**Figure 3.26E**, n=8 zebrafish larvae at 3 dpf per concentration, P>0.05).

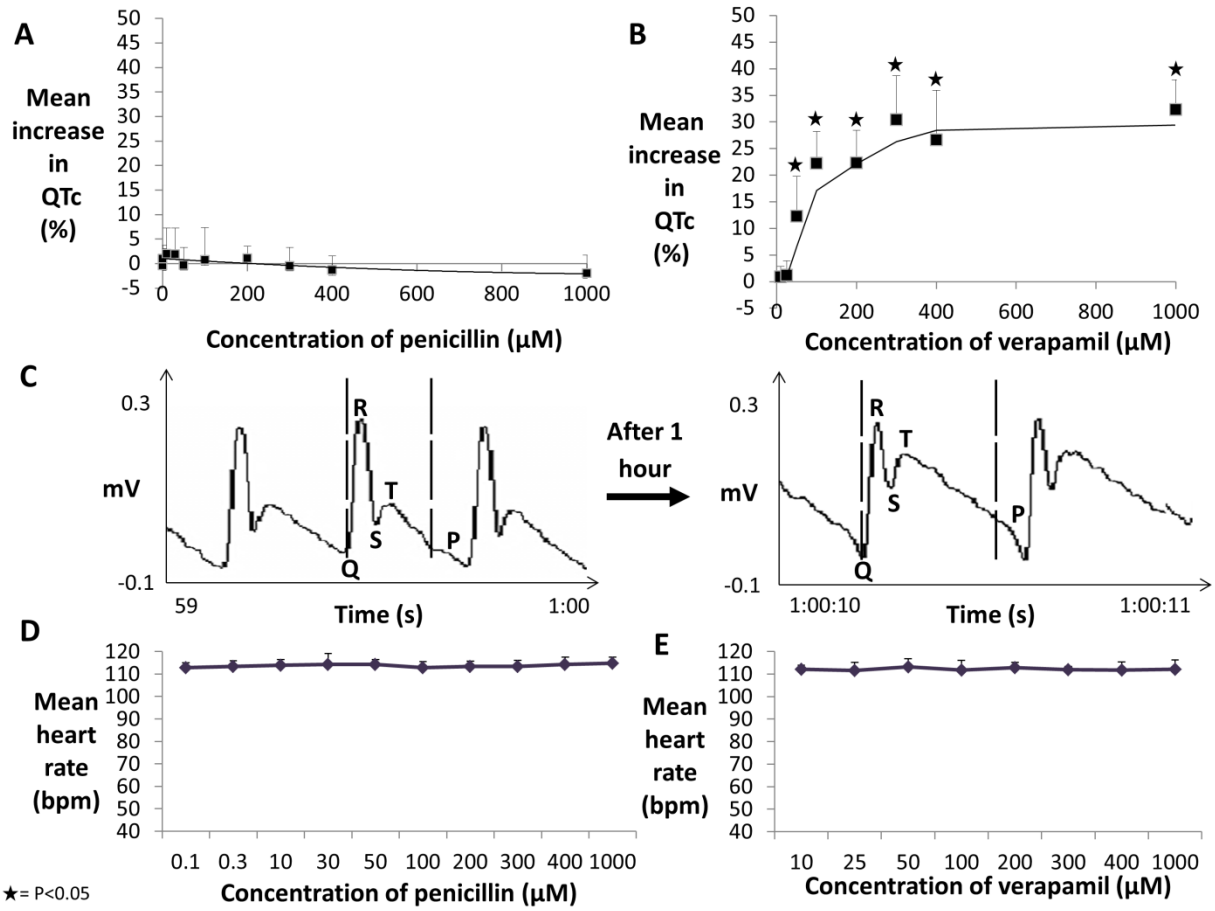

Figure 3.26 – QTc interval changes in zebrafish larvae after exposure to drugs not known to prolong the QT interval in vivo. *A) Mean QTc interval percentage changes after treatment of 3 dpf zebrafish larvae with different concentrations of penicillin (n=8 zebrafish larvae at 3 dpf per drug concentration, P>0.05), B) Mean QTc interval percentage changes after treatment of 3 dpf zebrafish larvae with different concentrations of verapamil (n=8 zebrafish larvae at 3 dpf per drug concentration, P<0.05), C) 3 dpf zebrafish larval ECG traces (one second segments) before and after one hour of treatment with 1 mM verapamil, D) Mean heart rate after treatment of 3 dpf zebrafish larvae with different concentrations of penicillin (n=8 zebrafish larvae at 3 dpf per concentration, P>0.05), D) Mean heart rate after treatment of 3 dpf zebrafish larvae with different concentrations of verapamil (n=8 zebrafish larvae at 3 dpf per concentration, P>0.05).*

With the exception of verapamil the results obtained for the rest of the tested drugs were found to be comparable to those documented in adult zebrafish (Milan et al., 2006), humans (Haverkamp et al., 2000)(Fossa et al., 2002)(Källén et al., 2005) and the commonly used *in vivo* mammalian models, such as the conscious adult dog, guinea pig and rabbit (Haverkamp

et al., 2000). These results confirmed that the set-up was robust enough to detect compounds that had QT prolonging effects.

Apart from QT prolongation, other cardiotoxic conditions such as arrhythmias can also be useful readouts on ECG recordings, particularly when they are difficult to detect and characterise via other means. From the drug treatment ECG recordings various secondary cardiotoxic conditions were observed. These were found to be dose and time dependent. For example, with terfenadine the development of arrhythmias was observed as a secondary effect of QT prolongation at the two highest concentrations tested (25 and 50 μM). The arrhythmias were characterised by premature ventricular contractions (PVC) and ectopic beats and occurred in 50% of cases, generally 20 minutes after initial drug treatment (**Figure 3.27**). The arrhythmias observed were not quantified in terms of severity, only the number of drug-treated zebrafish embryos displaying such an effect was recorded. Arrhythmia is a well-known effect of terfenadine, which has also been found to occur in adult zebrafish (Chaudhari et al., 2013), humans (Salata et al., 1995) and other animal models (Webster et al., 2001)(Usui et al., 1998)(Pinney et al., 1995). With haloperidol and pimozide a similar type of arrhythmia was also observed, but it was less frequent (25%) and also less pronounced than that observed with terfenadine. Haloperidol and pimozide have also been reported to cause arrhythmia in humans (O'Brien et al., 1999)(Hondeghem et al., 2003) and other animal models (Dhein et al., 2008)(Hondeghem et al., 2003).

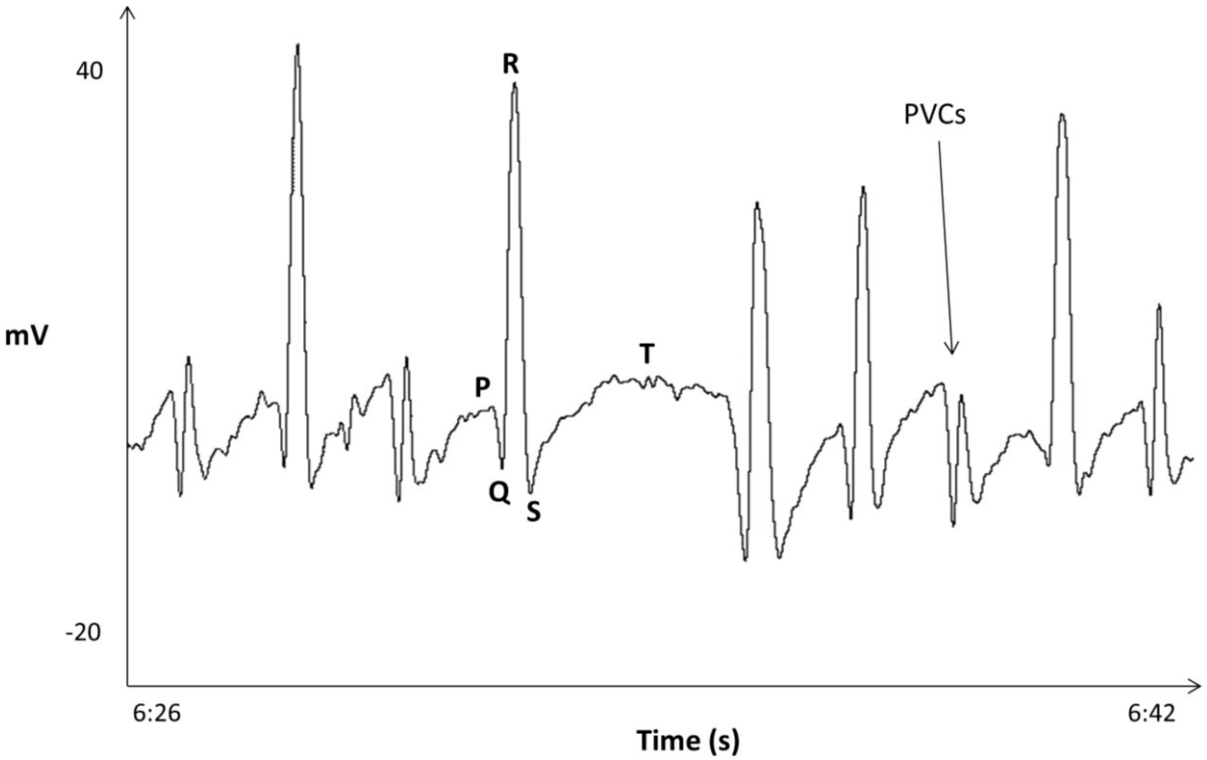

Figure 3.27 – Arrhythmia development in zebrafish larvae after exposure to terfenadine. *ECG trace (16 seconds) showing arrhythmia development in a 3 dpf zebrafish larva after 40 minutes of exposure to 50 µM terfenadine. Key: PVC = premature ventricular contractions*

Another cardiotoxic condition that was observed with terfenadine, haloperidol and pimozide was AV block, which was characterised by widened ECG waveforms and prolonged cardiac cycles (**Figure 3.28**). This condition was found to occur in all of the zebrafish larvae treated with these three drugs, which agrees with what has been documented in the literature (Langheinrich et al., 2003). The AV block was found to occur immediately after the initial QT prolongation. With terfenadine AV block was only observed after treatment at 10, 30 and 50 µM, whereas with pimozide and haloperidol it was observed at all concentrations tested. The AV block observed after 50 µM pimozide treatment presented with a widened QRS interval (**Figure 3.28**) (Zeltser et al., 2004). The AV block was found to worsen with time ultimately leading to complete cardiac arrest.

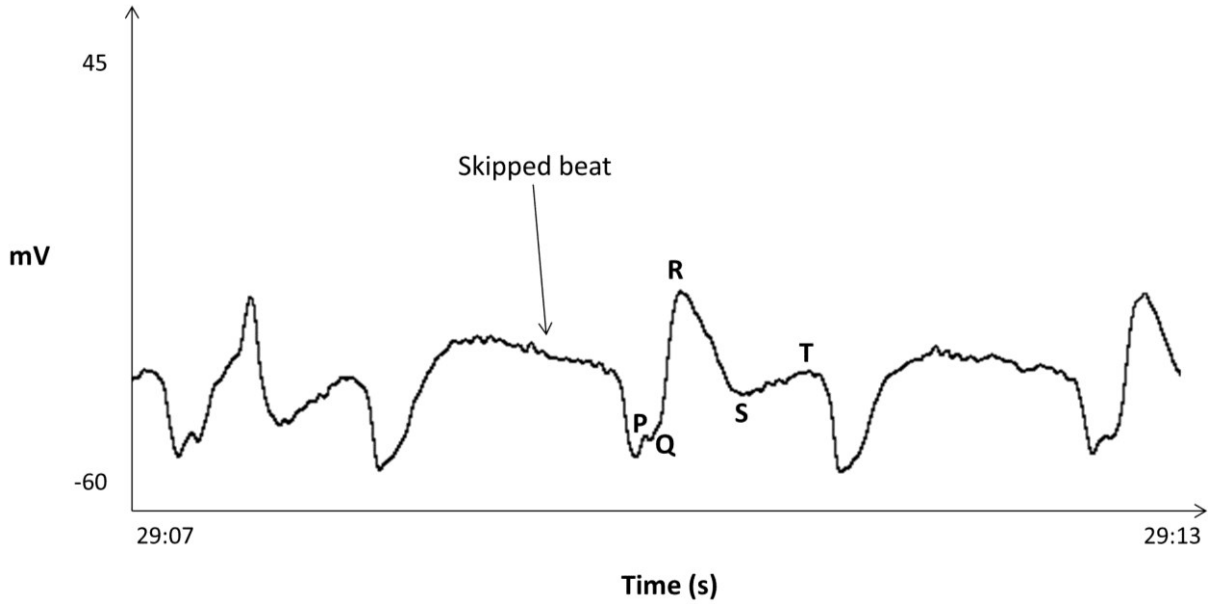

Figure 3.28 – AV block in zebrafish larvae after exposure to the QT prolonging drug pimozide. *ECG trace (six seconds) showing possible AV block in a 3 dpf zebrafish larva after 25 minutes of exposure to 50 µM pimozide.*

With verapamil an AV block was also observed, characterised by severe PR prolongation and a normal QRS interval (**Figure 3.29**) (Zeltser et al., 2004). This effect of verapamil has been reported in humans as well (Epstein and Rosing, 1981). The AV block in zebrafish larvae was only found to occur after a relatively long exposure period (over one hour) following treatment at the highest tested concentration (1 mM) and was not observed at any of the lower concentrations tested due to toxicokinetics.

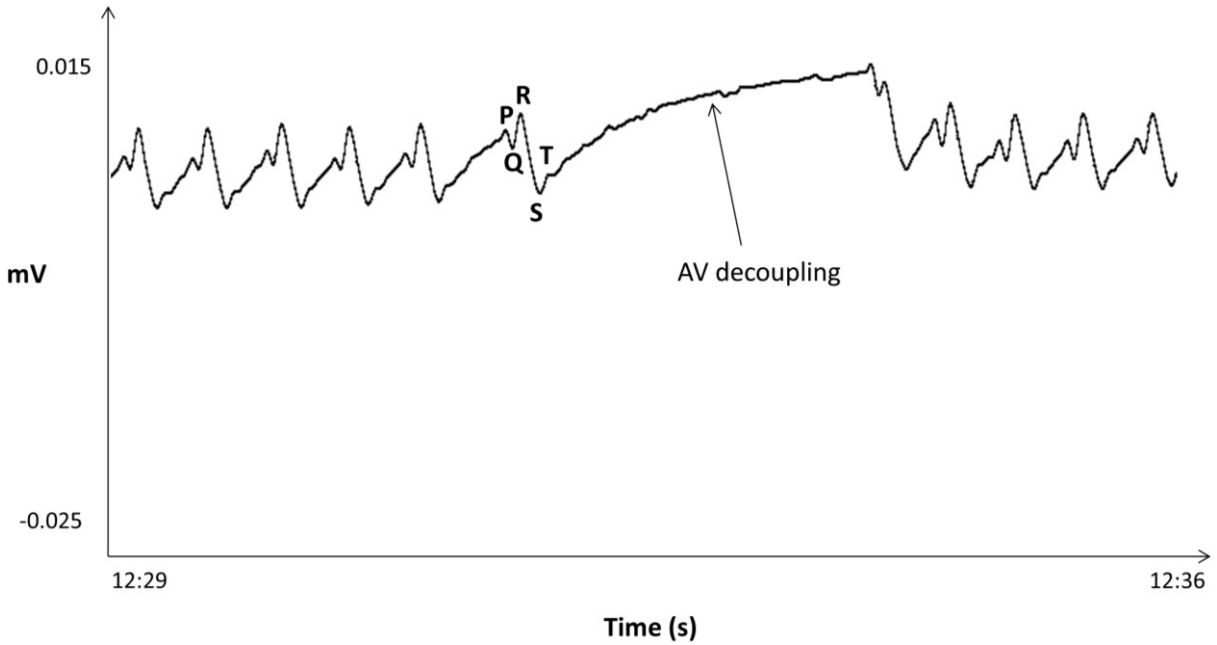

Figure 3.29 – AV block in zebrafish larvae treated with verapamil. *ECG trace displaying possible AV block in a 3 dpf zebrafish larva after one hour and 20 minutes of exposure to 1 mM verapamil.*

3.5 Discussion

3.5.1 Optimisation of a zebrafish embryo and larval ECG recording set-up

An ECG recording set-up capable of producing reliable and reproducible ECG recordings from zebrafish embryos and larvae aged between 2 and 5 dpf using a similar technique to that previously developed for 5 dpf zebrafish larvae was optimised and refined (Forouhar et al., 2004). Compared to previous documented zebrafish ECG studies where only P and R waves were recorded (Forouhar et al., 2004)(Yu et al., 2010)(Dong et al., 2012) our ECG recording set-up was able to detect all the components of an ECG waveform including P, QRS and T waves. This opened up the way for measuring QT intervals and thus determining the effect of QT prolonging drugs on 3 dpf zebrafish larvae. Additionally, the ECGs obtained using our ECG set-up were also found to be much more similar to human and adult zebrafish ECGs

(**Figure 3.30**), highlighting potentially that our set-up was much more sensitive compared to previously-developed larval zebrafish ECG set-ups.

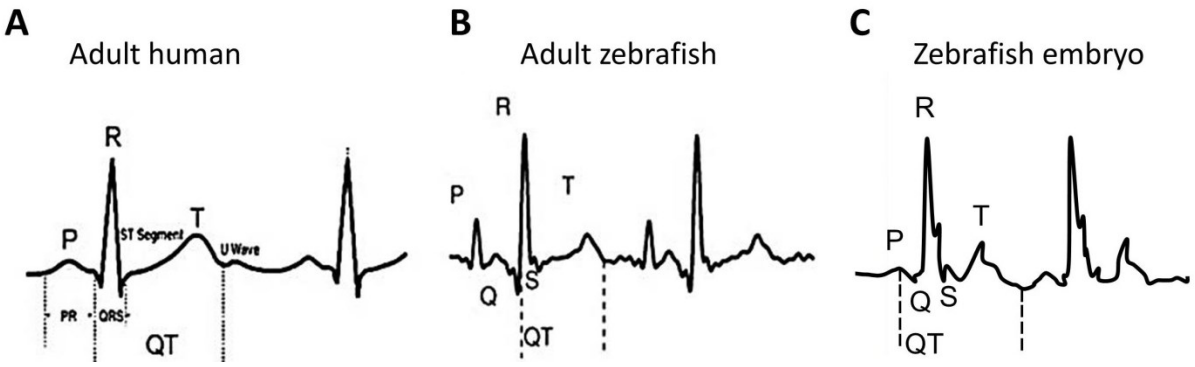

Figure 3.30 – Comparison of ECG signals between human adults, adult zebrafish and zebrafish embryos. *A) Basic outline of an adult human ECG (taken from Li et al., 2008), B) Basic outline of an adult zebrafish ECG (taken from Li et al., 2008), C) Basic outline of a zebrafish embryo ECG.*

To optimise our zebrafish embryo and larval ECG recording set-up, various factors were addressed such as motion artefact, immobilization method, electrode positioning, recording temperature and developmental stage of the zebrafish embryo used.

By performing invasive ECG recordings we were able to show that our surface ECG recording set-up was capable of recording ECG signals that represented the true electrical activity of the zebrafish embryo and larval heart. Using drugs such as cromakalim, blebbistatin and BDM could not confirm this finding due to technical issues that were experienced. The ineffectiveness of cromakalim may have been due to reduced penetration into the zebrafish or due to tested drug concentrations being too low. BDM and blebbistatin on the other hand affected the ECG waveform morphology, as well as causing zebrafish mortality. BDM is well known to have electrophysiological side effects, which have been documented in several species and also in explanted zebrafish embryo hearts (Jou et al., 2010)(Lou et al., 2012).

Blebbistatin on the other hand has not been documented to produce any notable electrophysiological side effects such as those seen with BDM or cytochalasin D, even in explanted zebrafish embryo hearts (Lou et al., 2012). The reason for the observed side effects with blebbistatin may have been due to toxic decomposition products being produced after exposure of blebbistatin to light during ECG recordings, as blebbistatin has been documented to be sensitive to light (Kolega, 2004).

For immobilization of zebrafish embryos and larvae MS222 was chosen, as tubocurarine was found to be effective only when the zebrafish were continuously exposed, limiting its use, as it could potentially interact with other drugs in solution whilst performing drug treatments. Tubocurarine has been documented to undergo drug-drug interactions, specifically with anti-arrhythmics (Harrah et al., 1970). However, compared to MS222 tubocurarine did not affect the heart rate. MS222 at very high concentrations induced bradycardia, as it impairs ion transport in excitable cells by blocking the conductance of potassium and sodium ions (Rombough, 2007). Despite the unwanted side effects at higher concentrations of MS222, at a concentration of 0.3 mg/mL no significant side effects were observed, which agrees with what has been documented in the literature (Denvir et al., 2008). Additionally, treatment of zebrafish larvae with QT prolonging drugs in the absence of any anaesthesia produced the same effects on ECG recordings (data not shown); providing further support that MS222 does not significantly influence the QTc interval at 0.3 mg/mL. Based on this, MS222 at 0.3 mg/mL was used as the immobilization agent of choice for all ECG recordings.

ECG recordings were found to be heavily influenced by the recording temperature. A temperature between 21°C and 22°C was found to be optimal for taking ECG recordings. At lower temperatures the ECG waveform was found to be prolonged whereas at higher temperatures the opposite was found to occur.

The calculated Q_{10} values over the 10°C range were found to be 2.7, reflecting the temperature effects (Barrionuevo and Burggren, 1999). These values closely resemble those documented for trout larvae with a Q_{10} of around 2.4 over a 5-15°C temperature range (Mirkovic and Rombough, 1998).

The increase in RR, QRS, QT and QTc interval durations seen in zebrafish larvae with a decrease in temperature was found to be similar to that seen in other teleosts including the Nile tilapia (*Oreochromis niloticus)* as well as in humans with therapeutic hypothermia (Maricondi-Massari et al., 1998)(Amin et al., 2008). At lower temperatures biochemical processes are slowed leading to slower heart activity (Gillis and Tibbits, 2002)(Schwerte and Fritsche, 2003). At higher temperatures the opposite occurs with the ECG waves becoming narrower and the QTc interval durations shortening due to increased heart activity (Khan et al., 2010). As zebrafish embryos obtain oxygen through dermal diffusion, the effect of temperature on oxygen levels in the water only becomes important at around 7-14 dpf (Jacob et al., 2002)(Rombough, 2002).

ECG recordings could be obtained from zebrafish embryos as young as 2 dpf, which has previously never been done. Overall, zebrafish embryo and larval ECG recordings were found

to be similar at all stages of development tested, which included 2, 3, 4 and 5 dpf. The heart of the zebrafish embryo is an evolutionary antecedent of the mammalian four chambered heart (Simões-Costa et al., 2005). On an anatomical level, despite the obvious difference in heart structure between zebrafish and humans, even at an early embryonic stage the zebrafish has an immature conduction system (Arrenberg et al., 2010)(Tessadori et al., 2012). The primary pacemaking site is situated in the dorsal right quadrant of the sinoatrial ring and is characterised by islet-1 expression (Arrenberg et al., 2010)(Tessadori et al., 2012). Furthermore, during development a fast ventricular conduction system develops alongside ventricular trabeculation (Kirchmaier et al., 2012). The ventricular trabeculation and thickening is highly dependent on the presence of a cardiac specific L-type calcium channel (Rottbauer et al., 2001). At 5 dpf the ventricle has thickened substantially due to a gradual increase in the number of ventricular cardiomyocytes, so that it is in its mature adult configuration (Taneda et al., 2010)(Huang et al., 2013). Therefore, at 5 dpf it is much easier to detect T waves.

3.5.2 Comparison of our ECG recording set-up to other zebrafish ECG recording set-ups

The ECG recording set-up we developed was found to be comparable to other zebrafish ECG recording set-ups but also showed some differences. For example, the ECG recording set-up developed by Yu and colleagues for recording larval zebrafish ECGs above 7 dpf differed somewhat in that a suction electrode and a micropipette with a bigger tip were used, which might have had an influence on the quality of recordings obtained (Yu et al., 2010). Additionally, the recording time used was very short (one minute) and the R waves were found to be very wide, which could have been due to incorrect annotation of the waveform

as possibly the recording was inverted (Yu et al., 2010). This may have also been the case for the recordings obtained by Forouhar and colleagues where the ECG recordings from 5 dpf zebrafish larvae showed very wide R waves as well (Forouhar et al., 2004).

The ECG recording set-up used by Dong and colleagues on the other hand differed in that an invasive approach was used with micropipettes of an unknown tip length but these recordings on 3 dpf zebrafish larvae showed more similarity to our and adult zebrafish ECG recordings than the previous studies mentioned (Dong et al., 2012). The annotation of R waves on these ECG recordings may also have been incorrect, as the values quoted for various ECG parameters such as the QRS interval (0.305 seconds) and QT interval (0.786 seconds) were almost two times higher in comparison to our calculated values.

ECG recordings performed by Rottbauer and colleagues also on 3 dpf zebrafish larvae showed the greatest resemblance to our recordings with clear P, QRS and possibly T waves evident (Rottbauer et al., 2001). The ECG recording methodology used was not described in detail but based on the description provided it seemed to be similar to our recording method; hence confirming that it is possible to obtain high quality ECG signals from 3 dpf zebrafish larvae.

3.5.3 A larval zebrafish model for QT prolongation

In this chapter the three known human QT prolonging drugs tested (terfenadine, haloperidol and pimozide) along with the anti-arrhythmic (verapamil) were found to cause QTc prolongation in 3 dpf zebrafish larvae, similar to that seen in adult zebrafish and also humans

(Milan et al., 2006). QT prolongation is something that has previously never been demonstrated before in zebrafish larvae. Terfenadine QTc prolongation in zebrafish larvae was found to be dose-dependent and broadly sigmoidal, which is similar to what is seen in dogs treated with terfenadine (Salata et al., 1995). Haloperidol and pimozide on the other hand did not show any dose-dependency in their QT prolonging effects.

Structurally all compounds inducing QT prolongation were found to be different, however it has been shown that compounds with molecular weights >250 and clogP values >3.7 are likely to be potent hERG blockers (Aronov, 2005). This is most probably to do with the large pore size of the hERG channel as well as the highly lipophilic nature of the pore lining (Aronov, 2005). All three compounds tested, namely terfenadine, haloperidol and pimozide meet these criteria (DrugBank, 2013a)(DrugBank, 2013b)(DrugBank, 2013d). Interestingly, verapamil also meets the above criteria (DrugBank, 2013e).

Verapamil is a calcium channel blocker that specifically binds to the alpha 1c subunit of the L-type calcium channel, which prevents it from opening and thereby decreases the influx of calcium ions (Rottbauer et al., 2001). In the larval zebrafish ECG studies verapamil was found to reduce myocardial contractility, inducing mild bradycardia and most surprisingly QT prolongation. This is contrary to what has been reported in mammalian models and humans at therapeutic concentrations (Hondeghem et al., 2003)(Cheng et al., 2006). This result however is consistent with data obtained in *in vitro* hERG cell assays (e.g. human embryonic kidney cells) (Martin et al., 2004) and *Xenopus laevis* oocytes (Duan et al., 2007). Additionally, in humans in overdose conditions verapamil has been shown to cause QT

prolongation (Fossa et al., 2002). It is possible that the observed QTc prolongation in zebrafish embryos with verapamil is due to greater sensitivity of zERG to block compared to hERG (Langheinrich et al., 2003).

Penicillin was used as a negative control in the ECG drug treatment studies as it is known not to prolong the QT interval in humans or adult zebrafish (Milan et al., 2006). In 3 dpf larval zebrafish it was also found to have no effect on the QTc interval duration at any of the tested concentrations.

3.5.4 A larval zebrafish model for atrioventricular block and arrhythmia

With verapamil, terfenadine, haloperidol and pimozide AV block was observed as a secondary cardiotoxic condition after prolonged drug exposure, which could be related to the uptake of these drugs and the time course of internal concentrations. With verapamil the AV block was characterised by prolongation of the PR interval, resembling changes seen in humans and mammals following verapamil exposure at concentrations above the therapeutic limit (Enyeart et al., 1983)(Thomas et al., 1996). AV block has also been previously reported in zebrafish larvae exposed to verapamil (Berghmans et al., 2008)(Rottbauer et al., 2001).

With terfenadine at 30 and 50 µM and with all concentrations of haloperidol and pimozide the AV block observed was similar to that seen in humans with this condition and induced by terfenadine in adult zebrafish (Clarke et al., 1976)(Milan and MacRae, 2005).

It is known that when hERG is inhibited in mammals and zERG is inhibited in zebrafish AV block is observed (Haverkamp et al., 2000)(Langheinrich et al., 2003). At the moment there is no evidence indicating that blocking other cardiac ion channels produces the same effect (Letamendia et al., 2012). In humans the occurrence of AV block is rare; occurring mostly in neonates and newborns due to the effects of cardiotoxic drugs or due to a genetic condition (Langheinrich et al., 2003). In neonates and newborns AV block is found to occur alongside QT prolongation (Langheinrich et al., 2003), which is also the case in 3 dpf zebrafish larvae. Therefore, this suggests that the results obtained for the ECG drug treatment studies in 3 dpf zebrafish may be more relevant to human neonates and newborns than to human adults. Additionally, zERG has been shown to be more sensitive to developing block than hERG (Langheinrich et al., 2003). It has been postulated that the reason behind this is that the zebrafish ventricle depends more heavily on the I_{Kr} current for repolarisation than the atrium (Langheinrich et al., 2003).

Another secondary cardiotoxic effect observed primarily with terfenadine was the development of a ventricular arrhythmia. The ventricular arrhythmia was characterised by premature ventricular contractions and ectopic beats, similar to what is seen in humans (Guilleminault et al., 1983). In humans terfenadine is found to induce ventricular arrhythmias at plasma concentrations between 30-300 nM, concentrations at which hERG can be blocked *in vitro* (Taglialatela et al., 1998). In canine and rabbit models arrhythmia development (particularly TdP) has been found to be difficult to reproduce (Carlsson et al., 1993)(Chézalviel-Guilbert et al., 1995)(Hoffmann and Warner, 2006). Current *in vitro* methods are based predominantly on measuring the effects on the I_{kr} current either directly

or indirectly using cell-based systems without considering the effect of proteins found downstream or considering possible effects of drug-drug interactions (Milan and MacRae, 2005). Thus, the zebrafish embryo presents a promising alternative model to study this condition in an *in vivo* scenario. This is backed up by the recent findings that adult zebrafish also develop arrhythmia as well as TdP after terfenadine treatment (Milan and MacRae, 2005).

3.5.5 The zebrafish larva as a preclinical model for cardiotoxicity

At the moment for investigating QT prolongation and associated cardiac disorders there is no gold standard animal model. The current animal models (e.g. beagle dogs and rabbits) show a lot of variability and have low reproducibility (Langheinrich et al., 2003). A number of readouts for cardiotoxicity are obtainable using zebrafish embryos and larvae which do not require any specialized equipment, such as bradycardia, AV block, atrial fibrillation and arrhythmias which can all be observed using a simple stereomicroscope (Langheinrich et al., 2003). However, the detail that can be obtained by taking *in vivo* ECG recordings is far greater than that which can be obtained just through simple microscopic observations, optical mapping (Peal et al., 2011), high throughput transgenic screens (Letamendia et al., 2012) or photocardiography (Yoshida et al., 2009) alone. ECG recordings are able to detect in real time various cardiac dysfunctions including QT prolongation, QRS prolongation, PR prolongation, AV block, bradycardia, arrhythmia and atrial fibrillation, along with possibly many other conditions that still need to be uncovered. Apart from compound screening the ECG recording set-up could also be applied to studying cardiac-specific mutations and their associated manifestations.

3.5.6 Current limitations of the zebrafish embryo and larval ECG recording set-up and future perspectives

The current ECG set-up presents an exciting tool for future studies. The next step would be to develop the ECG recording set-up further by increasing the throughput. Preliminary work in this area has already shown that multi-electrode recordings can be taken from the same fish simultaneously. ECG measurements along with the other techniques mentioned before could comprise a battery of tests to identify drugs that present with cardiotoxicity during drug development. However, the main limitation that still needs to be addressed not just for this ECG screening tool but for all types of zebrafish compound screening are drug uptake and metabolism.

With this current ECG set-up drug uptake and internal drug concentrations cannot be quantified in the zebrafish larvae. However, such a step could be introduced as an additional test accompanying the ECG measurements. For example, one approach could be to calculate the body burden of the drug inside the zebrafish larva by using liquid chromatography-mass spectrometry (LC-MS) technology, which could be done immediately after taking zebrafish larval ECG recordings (Diekmann and Hill, 2013)(McGrath, 2012). Hence, using such an approach the exact internal concentrations of the parent drug or metabolite could be determined. This would also help to uncover species-specific differences. For example, it was recently shown that terfenadine metabolism in zebrafish is different to that in humans with azacyclone and terfenadine alcohol the main metabolites in zebrafish and fexofenadine the main metabolite in humans (Diekmann and Hill, 2013).

The exposure times that were applied in this study were relatively short. This may have led to some drugs failing to approach equilibrium in order to induce an effect. A way around this would be to perform a time-course analysis (i.e. using different exposure times), as it would indicate whether equilibrium has been reached. However, using such an approach on a whole embryo basis may not be representative of what is occurring at the target organ (the heart). Therefore, results obtained in this way would need to be interpreted with care.

For the QT prolongation studies only one negative control was tested. Therefore, for future studies it would be important to test further negative controls to ensure that the baseline responses of zebrafish larvae to negative drugs can be compared against those causing QT prolongation. Additionally, in the ECG drug treatment studies performed it was assumed that any electrophysiological effects observed were due to a direct action on cardiac ion channels. However, QT prolongation does not solely occur via blockade of cardiac ion channels but also by non-ion channel mechanisms, such as through disturbances to pumps, exchangers, calcium storage/release mechanisms, caveolin-3 (membrane protein) and ankyrin B (adapter protein found in brain and muscles) (Milan and MacRae, 2005). Therefore, these effects must also be taken into consideration when interpreting drug-induced QT prolongation results especially for compounds not known or expected to affect cardiac ion channels, such as hERG.

One further limitation of the work performed in this chapter was that the analysis of ECG waveforms had to be done manually in our case as it was not possible to do this automatically using the existing LabChart 7 Pro software. Therefore, this issue would need to

be addressed for future studies and also when up-scaling this technology in order to reduce the variability introduced by human error.

3.6 Conclusion

The zebrafish larva presents a promising model for investigating drug-induced cardiotoxicity, particularly QT prolongation which has not been previously demonstrated in early stage zebrafish larvae. Further studies using other classes of cardiotoxic drugs, such as QRS prolonging agents would need to be performed in order to validate this set-up as a screening tool and to show that it has applications beyond screening for QT prolongation. Testing of further controls would also help to determine the specificity and sensitivity of the set-up. Additionally, the characterisation of cardiac specific mutants using the ECG recording set-up would be a further step to show its versatility. Finally, development of the set-up into high throughput with automated analysis and additional studies on drug uptake and metabolism would help to promote this system as an *in vivo* pre-clinical screening tool for evaluating cardiotoxic potential of candidate drugs during drug development, an area in which a gold standard is still lacking.

Chapter Four: CHARACTERISATION OF THE BIOLOGICAL ACTIVITY OF NOVEL AZETIDINE AND Y-LACTAM COMPOUNDS USING THE ZEBRAFISH EMBRYO

Foreword:

The work presented in this chapter was a joint collaboration with the chemistry department at the University of Birmingham. For the azetidines all biological work including analysis and interpretation of results was performed solely by me under the supervision of Professor Ferenc Müller. All chemical work for the azetidines was performed solely by Dr. Antonio Feula. In the case of the Y-lactams, the compounds were provided by Dr. John S. Fossey and Mariwan H. Salih from their ongoing research. The general morphology and toxicity assessments for the Y-lactams were performed equally between me and Mariwan H. Salih. All fluorescence microscopy and stainings were performed by me with some contribution from Mariwan H. Salih. All data analysis and interpretation of results was performed by me. The work was supervised jointly by Professor Ferenc Müller and Dr. John S. Fossey.

4.1 Introduction and Overview

4.1.1 Zebrafish as a model for testing of novel small molecules

The assessment of the biological activity of small molecules has been mainly based on using targeted *in vitro* assays such as cell-based or purified protein assays (MacRae and Peterson, 2003). Such assays can be done quickly in high throughput formats. However, they are not as informative as whole organism assays, where the interaction of a small molecule with different cell types, tissues and proteins can be followed and the effects on the whole organism observed (MacRae and Peterson, 2003). Additionally, *in vitro* assays are restricted due to their selectivity. For example, in the case of protein-based assays the screens that are performed are biased towards a small selection of molecules, i.e. those that will inhibit a particular protein (MacRae and Peterson, 2003).

In the case of whole organism screening, small molecules may elicit a range of different observable phenotypes via previously unknown pathways or mechanisms (MacRae and Peterson, 2003). Additionally, using a whole organism to probe for biological activity of small molecules can also give an indication of toxicity. For example, a compound that may be toxic to an individual cell may not be toxic in a whole organism due to various factors including metabolism and plasma protein binding. This is also true the other way round. Toxicity is particularly important when assessing the biological activity of novel compounds. It is important to identify the dose ranges where a small molecule is effective/potent but has low toxicity. This is commonly done by calculating EC50 (concentration of a compound producing a response in 50% of the tested population) and LC50 (concentration of a compound causing mortality in 50% of the tested population) values. Additionally, LOEC (lowest observed effect

concentration) and NOEC (no observed effect concentration) values can also be calculated as additional toxicity endpoints.

Zebrafish embryos are particularly useful for assessing the biological activity of novel compounds as the disruption of any one of the many genes that are found in zebrafish may lead to the development of an observable phenotype (MacRae and Peterson, 2003). These include developmental, physiological and behavioural phenotypes (MacRae and Peterson, 2003). Therefore, many large scale chemical screens are being performed using zebrafish embryos in order to determine the effects of small molecules, as these can be carried out in large numbers with small quantities of compound in a very short period of time (MacRae and Peterson, 2003)(Langheinrich et al., 2003)(Spring et al., 2002). In addition to this, the acute toxicity of small molecules can be easily recorded using zebrafish embryos, thereby enabling the relationship between efficacy and acute toxicity of a compound to be explored.

4.1.2 The zebrafish larva as a model for hepatotoxicity

Toxicity can manifest itself in various forms, including organ-specific toxicities such as hepatotoxicity. Hepatotoxicity accounts for most of the drug withdrawals both during the drug development process and also post-marketing showing the lowest correlation in animal testing to humans (Olson et al., 2000). Drug-induced liver injury (DILI) is often manifested as an idiosyncratic response occurring in 1 in 10,000 patients treated with certain drugs and accounting for around 10% of drug-induced liver failure cases (Jaeschke, 2007).

Many of the conditions that can occur as a result of liver damage, infection or drug toxicity often present with similar pathological features, hence making it sometimes difficult to define the underlying cause (Shin and Fishman, 2002). However, acute liver failure is predominantly attributed to DILI (Ostapowicz and Lee, 2000).

Although, there a number of *in vitro* assays which perform very well in detecting hepatotoxicity (e.g. liver microsomes, primary hepatocyte cell cultures, hepatocyte/kupffer cell co-cultures, bioreactors and immortalised hepatoma cell lines), many candidate drugs are only found to be hepatotoxic when they are tested in strongly regulated models like macaque monkeys or in humans in clinical trials (Soldatow et al., 2013). Therefore, there is a big demand to find a suitable model to detect hepatotoxicity early on in drug development.

The zebrafish larva represents a good model for investigating drug-induced hepatotoxicity, as it has a separate liver and pancreas and not a hepatopancreas like other teleosts (Fischer and Dietrich, 2000). Additionally, the zebrafish larva has orthologues of human CYP enzymes, therefore having the capability to replicate CYP-mediated hepatotoxicity seen in humans (Goldstone et al., 2010).

Recent zebrafish assays that have been developed to assess hepatotoxicity include: 1) a brightfield microscopy method where changes in liver size and extent of necrosis are quantified through semi-automated analysis (He et al., 2013) and 2) a fluorescence-based microscopy method where a transgenic zebrafish line with a fluorescently labelled liver is used to determine changes in liver size after drug exposure (Zhang et al., 2014). Additionally,

gene expression, histology and liver-specific stainings have also been used to assess hepatotoxicity in zebrafish embryos and larvae (Driessen et al., 2013)(Driessen et al., 2014)(Lam et al., 2013). Stainings that have been used include Oil Red O (ORO) staining which can be used to identify hepatic steatosis (accumulation of fat in the liver) (Braunbeck et al., 1990) (Amali et al., 2006). Such assays in zebrafish specific for liver toxicity should advance lead compounds and reduce costs for pharmaceutical companies.

4.1.3 Zebrafish liver development

The zebrafish liver is formed in two phases, namely phase 1 (budding) and phase 2 (growth). In the first phase, there are three sub-phases. In the first sub-phase endodermal cells located caudal to the pharyngeal region aggregate to form a rod by 24 hpf (Tao and Peng, 2009). At 28 hpf the part of the rod underneath the first somite starts thickening and this continues to thicken during the second sub-phase until it reaches a certain size and bends to the left forming the liver primordium (Horne-Badovinac et al., 2003). At 34 hpf in sub-phase three, a trough develops between the liver primordium and the adjacent lying oesophagus (Tao and Peng, 2009). This trough continues to grow and the hepatic duct is formed connecting the liver to the intestine (Field et al., 2003). In phase 2 (growth phase), rapid on-going cell proliferation causes changes in liver shape, size and position, as well as differentiation of hepatoblasts into specific liver cell types (Tao and Peng, 2009). By 96 hpf the liver is fully formed consisting of two liver lobes, which are positioned just above the yolk (Field et al., 2003). By 5 dpf the liver is situated posterior to the pericardium and anterior to the gut. Two important genes involved in liver development include *prox1* (required for the migration of the hepatoblasts and the outgrowth of the liver bud) and *hhex* (required for controlling liver

progenitor initiation and development) (Tao and Peng, 2009). The whole liver development process is outlined in **Figure 4.1**.

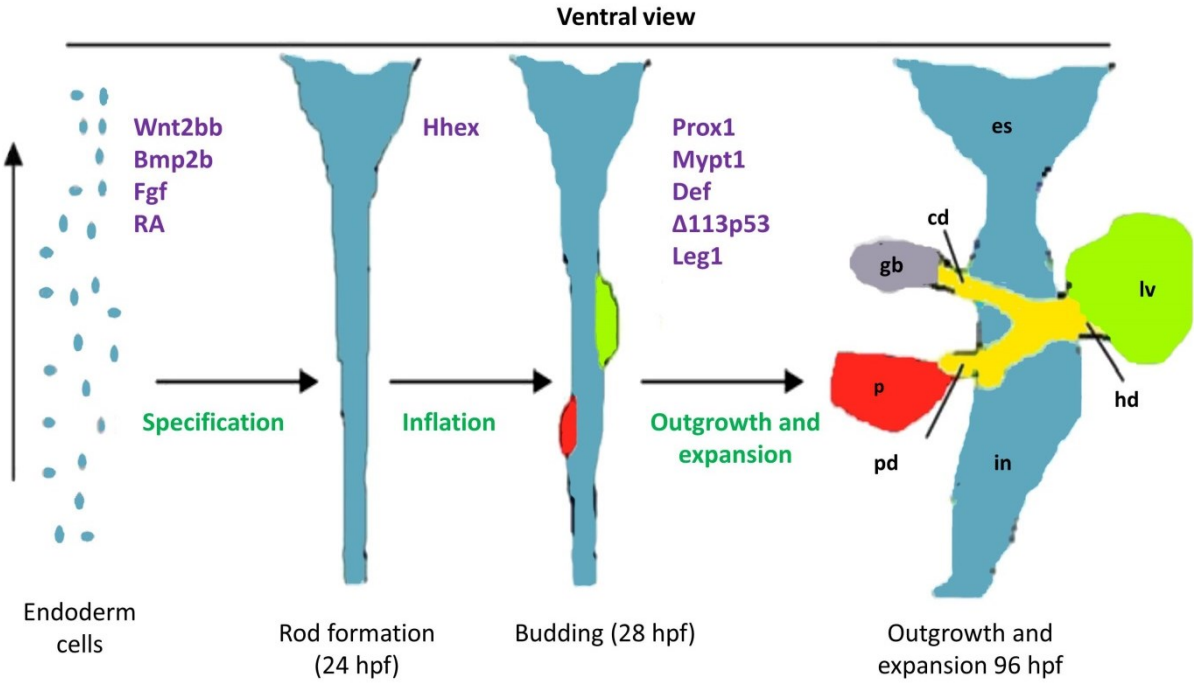

Figure 4.1 – Overview of zebrafish liver development. *Genes important in liver development are coloured purple. Images are shown as ventral views with anterior at the top. Key: gb = gall bladder, cd = cystic duct, es = esophagus, p = pancreas, pd = pancreatic duct, in = intestine, hd = hepatic duct, lv = liver*
Source: Figure adapted from (Tao and Peng, 2009)

4.1.4 Zebrafish liver structure

The liver is the main organ involved in: 1) metabolism/detoxification of various endogenous and exogenous substances, 2) creation of vital blood protein/clotting factors, 3) synthesis of enzymes required for digestion, 4) detoxification of ammonia through the urea cycle and 5) production of bile that is secreted by the gall bladder (Tao and Peng, 2009).

In 4 dpf zebrafish the hepatocytes of the liver are hexagonal in shape but are arranged in tubules and not in plates like in mammals (Strmac and Braunbeck, 1999). The hepatocytes have a nucleolus with some heterochromatin, the mitochondria are arranged around the

nucleus and cisternae of rough endoplasmic reticulum (RER) form sheaths around these structures (Strmac and Braunbeck, 1999). Smooth endoplasmic reticulum (SER) and golgi fields are concentrated in the peribiliary area with peroxisomes dispersed in the cytoplasm (Strmac and Braunbeck, 1999). The hepatic arteries, bile ducts and portal veins show a random distribution in zebrafish, whereas in humans they are organised in portal tracts (Vliegenthart et al., 2014).

4.2 Aims

In this chapter novel compounds were probed for biological activity using the zebrafish embryo. This was done in order to gain an insight into how structural differences between the compounds produced different biological effects. The compounds that were tested in this chapter included a selection of azetidines and Y-lactams, which represent novel compounds previously not tested in zebrafish embryos. These compounds have potential applications in agricultural or pharmaceutical industries, as insecticides or treatments for alcohol use disorders. The rate-limiting step in the synthesis of these compounds is producing enough starting material to make a 1, 3, 5-trisubstituted pyrrolidin-2-one (Katritzky et al., 2000). This rate-limiting step has been overcome by the John Fossey group using a novel synthesis method, which involves using a homoallylamine (**1**) as a starting material to form azetidines (**2**) and Y-lactams (**3**) (see **Figure 4.2**) (Feula et al., 2010).

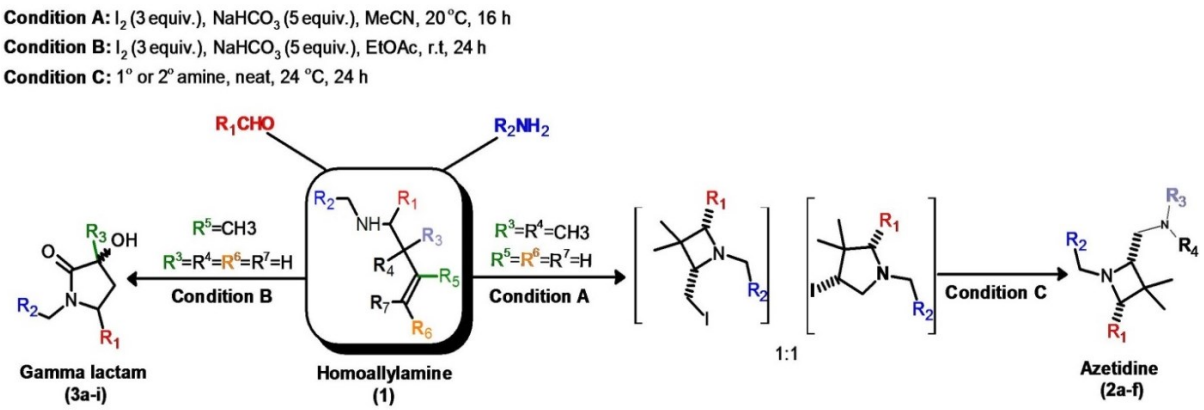

Figure 4.2 – Scheme of azetidine and Y-Lactam synthesis.
Source: Adapted from data provided by Mariwan H. Salih

From the azetidines synthesized six were selected for biological activity testing including racemic *cis*-**2a**, **2b**, **2c**, **2d**, **2e** and **2f** representing a chemically diverse set of azetidines with aromatic, heteroaromatic, benzyclic and aliphatic moieties in their structures (**Table 4.1**).

Table 4.1 – Chemical structures of tested azetidines. *Key: Bn = Benzene*
Source: Chemical structures provided by Dr. Antonio Feula

Compound	Chemical structure	LogP
2a	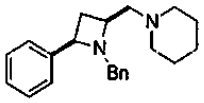	3.61
2b	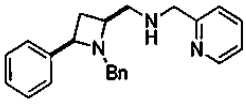	2.84
2c	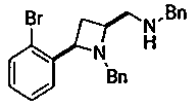	-1.6
2d	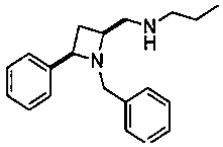	2.55
2e	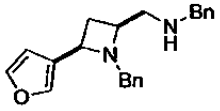	5.3
2f	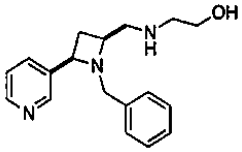	0.66

The Y-lactam compounds created on the other hand were not individual isomers like the azetidines but instead mixtures of the two diastereoisomers and associated enantiomers in varying ratios (**Table 4.2**).

Table 4.2 – Chemical structures and diastereoisomer ratios for tested Y-lactams.
Source: Chemical structures and data provided by Mariwan H. Salih

Compound	Diastereoisomer ratio (DR)	Chemical structure	LogP
3a	58:42	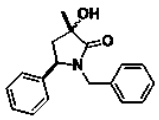	2.81
3b	56:44	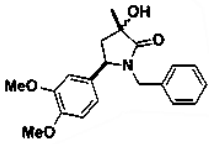	2.48
3c	24:76	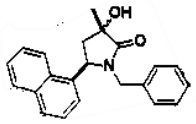	4.53
3d	60:40	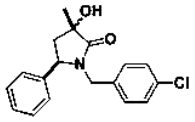	3.52
3e	61:39	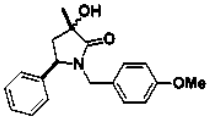	2.73
3f	54:46	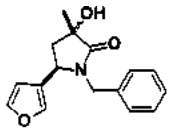	1.98
3g	36:64	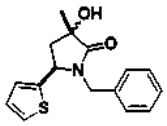	2.45
3h	45:55	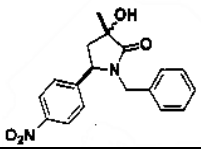	1.05
3i	67:33	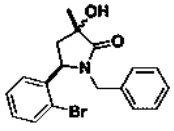	3.67

The chemical structures of both sets of compounds implied that they could have potential insecticidal or therapeutic properties. Hence, the aim as mentioned before was to assess

these compounds for biological activity (acute toxicity and development of morphological effects) using the zebrafish embryo as a model. Biological activity was evaluated by performing general toxicity assessments where zebrafish embryo mortality after exposure to these drugs was recorded. Additionally, morphological assessments were performed to characterise the biological effects of these compounds. Interesting phenotypes that developed were then selected for further analysis in order to determine whether the development of a particular phenotype was due to certain features of the compound chemical structure. For the Y-lactams a much broader dose range was tested, as the closely related β-lactams were shown to elicit effects in zebrafish embryos only at relatively high doses (Oliveira et al., 2013). A selection of Y-lactams which showed particularly interesting phenotypes (e.g. liver toxicity) was also selected for further testing. The responses observed with the Y-lactams in zebrafish embryos were compared against those documented with the β-lactams in zebrafish embryos to see if there were any similarities. Azetidines on the other hand are analogues of nicotine; hence the effects of the selected azetidines on zebrafish embryo development, as well as any neurotoxic effects were compared to effects reported with nicotine.

Finally, the responses observed with the azetidines and Y-lactams were also compared with one another in order to see if any phenotypes were similar between them and in instances where this was the case whether this was due to structural similarities.

4.3 Methods

4.3.1 Toxicity and morphology testing of novel Y-lactams

Nine diverse compounds from the Y-lactam family were tested for toxicity in zebrafish embryos. Zebrafish embryos were tested in 96 well plates with one zebrafish embryo placed in each well. One row was allocated to each tested concentration, in total six concentrations were tested per drug. One row per plate was also assigned to the solvent control (0.1% DMSO) and one row per plate to the E3 embryo medium control. Treatments were initiated at the 75% epiboly stage and zebrafish embryos were treated with compound over five days without compound renewal. Compound stock solutions were prepared using DMSO and subsequent dilutions were prepared using E3 embryo medium. Oxygen levels were not measured.

In the first part of the toxicity testing zebrafish embryos were exposed to each compound at six different concentrations (0.01, 0.1, 1, 10, 100 and 1000 µM). For compound **3c** however, the range was adjusted to 0.001, 0.01, 0.1, 1, 10 and 100 µM due to solubility problems at 1000 µM. In this first phase mortality was recorded daily over a five day exposure period. Using the mortality data, the percentage cumulative mortality over the five day exposure period was calculated. The logarithm of the tested concentrations was then plotted against percentage mortality to produce concentration mortality plots. From these plots LC50 values were calculated using GraphPad Prism 5.0 (GraphPad Software Incorporation, USA) by determining the concentration at which 50% mortality was observed (see **Figure 4.3**). Additionally, NOEC and LOEC values were also determined (see **Supplementary Table 8.1** for model parameters in Appendix).

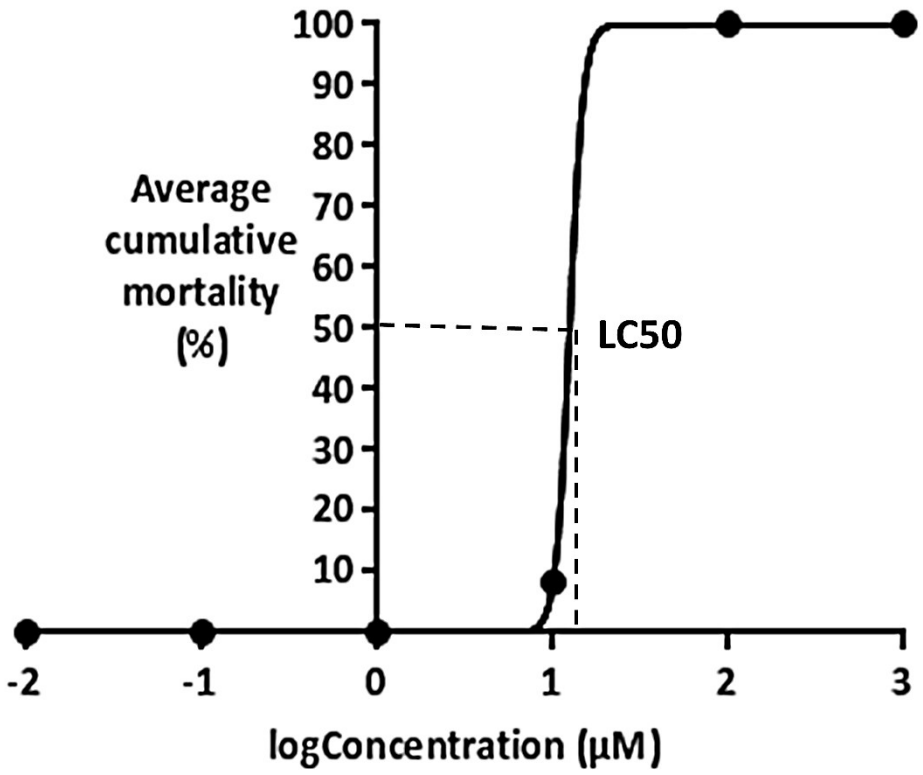

Figure 4.3 – Example of a log concentration mortality plot for Y-lactam 3a. *The LC50 value represents the concentration at which 50% mortality is observed.*

For the second phase a narrower concentration range was used to score a wide variety of morphological effects with 20 features scored for severity, as shown in **Table 4.3**.

Table 4.3 – Morphology features scored and their associated abbreviations.

Feature	**Abbreviation**
Reduced circulation	CR
Reduced movement	MO
Hatching	HA
Reduced heart rate	HR
Developmental delay	DD
Deformation	DF
Notochord	NO
Trunk curvature	TC
Protruding mouth	PM
Pectoral fin	PF
Somites	SO
Jaw malformations	JM
Yolk edema	YE
Yolk size	YS
Heart edema	HE
Liver necrosis	LN
Brain hemorrhage	BH
Hydrocephalus	HYD
Reduced pigmentation	PI
Mortality	MORT

In this chapter and also in **chapter 5**, a scoring system was used to assign severity scores to the features observed where 0 = normal, 1 = within normal range, 2 = mild, 3 = moderate, 4 = severe and 5 = very severe. Using such a quantitative morphometric approach eliminated the possibility of bias, which may have occurred if a personal scoring system had been used. Using the morphology data, the percentage of zebrafish embryos presenting with morphological effects over the five day exposure period was determined. The logarithm of the tested concentrations was then plotted against the percentage of zebrafish embryos presenting with morphological effects to produce concentration effect plots. From these plots EC50 values were calculated using GraphPad Prism 5.0 (GraphPad Software Incorporation, USA) by determining the concentration at which 50% of zebrafish embryos

presented with morphological effects. Additionally, NOEC and LOEC values were also determined (see **Supplementary Table 8.2** for model parameters in Appendix).

By dividing the LC50 by the EC50 teratogenic index values were calculated in order to determine the potency of the compounds with a ratio >2 indicating specific effects and therefore teratogenicity. Additionally, excess toxicity in the form of toxic ratio (TR) was also determined for each of the compounds using the experimentally derived LC50 values and predicted LC50 values. Predicted LC50 values were obtained using the following equation:

log(1/LC50) = 0.871logP – 4.87 (n=50, r=0.998, s=0.237) (Könemann, 1981)

The toxic ratio was calculated from these predicted and experimentally derived LC50 values using the following equation:

logTR = log(1/LC50 experimental) – log(1/LC50 predicted) (Zhang et al., 2013)

The threshold for the logTR was set at 1. Compounds with a logTR value <1 were considered to show baseline toxicity, whereas compounds with a logTR value >1 were considered to show excess toxicity.

4.3.2 Fluorescence imaging of vasculature/red blood cells in Y-lactam-treated embryos

In order to determine the effects of the Y-lactam **3a** on blood vessel stability, red blood cell circulation and red blood cell clotting the double transgenic zebrafish line Tg(*gata-1:DsRed*);Tg(*fli-1:EGFP*) was used. Zebrafish embryos from this line were treated with the Y-lactam **3a** at the 75% epiboly stage and then observed at 72 and 96 hpf using the GFP and

DsRed filter of a Nikon SMZ1500 stereomicroscope with an epi-fluorescence illuminator (Nikon, UK).

4.3.3 Toxicity and morphology testing of novel azetidines

To assess the toxicity and morphological effects induced by a selection of azetidines in zebrafish embryos, 10 zebrafish embryos at the 75% epiboly stage were transferred to each well of a 24 well plate. Zebrafish embryos were then exposed continuously to the six selected azetidines (**2a**-**2f**) in a total volume of 1.5 mL with three wells assigned to each compound/control (0.1% DMSO and E3 embryo medium) over a five day period. All zebrafish embryos were observed daily and a selection of morphological defects were recorded. These included tail curvature (TC), abnormal jaw formation (JM), delayed development (DD), hypopigmentation (PI), slowed heart rate (HR), tail necrosis (TN), heart edema (HE), brain edema (BE) and reduced circulation/blood clots (CR). Additionally, the number of mortalities was also recorded daily over the five day exposure period. Mortality was defined based on the OECD guidelines TG 236 for the fish embryo toxicity (FET) test as coagulation, lack of heartbeat after 48 hpf and lack of detachment of the tail bud from the yolk sac (OECD, 2013). One well per treatment group was used for imaging zebrafish embryos daily over the five day period. All dilutions were prepared fresh on the day using E3 embryo medium. All plates were kept at 28°C and covered in kitchen foil to prevent possible photodegradation of the compounds. Treatments with the azetidines at concentrations of 10 and 25 µM were started at the 75% epiboly stage, whereas treatments with a 30 µM concentration were started at the prim-5 stage to determine whether the azetidines also produced similar effects when treated at late stages. Stages were determined using the staging series outlined

by Kimmel and colleagues (Kimmel et al., 1995). The experiment was carried out in triplicate and the results were then averaged.

4.3.4 Fluorescence imaging of vasculature/red blood cells in azetidine-treated embryos

In order to determine the effects of azetidine **2a** on blood vessel stability, the transgenic zebrafish line Tg(*fli-1:EGFP*) was employed. To assess red blood cell circulation and clotting the double transgenic zebrafish line Tg(*gata-1:DsRed*);Tg(*fli-1:EGFP*) was used. Zebrafish embryos from these lines were treated with compound **2a** at the 75% epiboly stage and then observed at 72 and 96 hpf using the GFP and DsRed filter of a Nikon SMZ1500 stereomicroscope with an epi-fluorescence illuminator (Nikon, UK).

4.3.5 Oil Red O staining

Oil Red O (ORO) staining was performed in order to stain lipids. For ORO staining fixed zebrafish embryos and larvae were utilised. Before staining with ORO solution (Sigma-Aldrich, Germany) fixed samples were infiltrated with propylene glycol (Sigma Aldrich, UK) in a graded series (25%, 50%, 75% and 100%). Samples were then stained with 0.5% ORO solution in 100% propylene glycol overnight at room temperature. The following day the samples were washed with decreasing concentrations of propylene glycol (100%, 75%, 50% and 25%) before being washed twice with PBS. After the final wash, the samples were first transferred to 25% glycerol for five minutes before finally being transferred to 80% glycerol for final storage and imaging. Samples were imaged on a Nikon SMZ800 stereomicroscope (Nikon, UK).

4.3.6 Acridine orange staining

Acridine orange staining was used to visualise dead cells. Firstly, a 1000X stock solution (5 mg/mL) of acridine orange was made using distilled water and stored at 4°C. From this initial stock solution, a 1 in 1000 dilution was performed using E3 medium to create a final working dilution of 5 µg/mL. Drug-treated and untreated zebrafish larvae at 3 dpf were then exposed to 3 mL of 5 µg/mL of acridine orange for 30 minutes in the dark. The zebrafish larvae were then rinsed with 20 mL of E3 embryo medium to wash off the stain. The zebrafish larvae were immediately imaged using the GFP filter on a SMZ1500 Zoom stereomicroscope with an epi-fluorescence illuminator (Nikon, UK) and the number of dead cells was quantified. Dead cells were identified as those brightly fluorescing.

4.3.7 Sudan black staining

Sudan black staining was performed to stain leukocytes. Zebrafish larvae were firstly fixed in PFA and then stained with 60 µL Sudan black reagent before a final washing step was performed in a graded series of ethanol to remove excess stain. The stained zebrafish larvae were then stored in PBS and the number of leukocytes located in and around the liver were counted using a stereo microscope. The experiment was repeated three times and final results were averaged.

4.3.8 Brightfield liver image analysis

Zebrafish embryos that had been treated with 1000 and 2000 µM Y-lactam **3h** at the 75% epiboly stage were evaluated for changes in liver size at 5 dpf compared to untreated controls. Raw brightfield images of livers were processed using ImageJ version 4.2

(http://rsbweb.nih.gov/ij/) to obtain values for the liver area. These values were then averaged for each treatment group and used for final comparisons. In total 12 zebrafish larvae from three independent experiments were tested.

4.3.9 Motility assays

Motility assays with the six selected azetidines (**2a**-**2f**) were performed to determine the effects of these compounds on the neurobehavioral responses of 6 dpf zebrafish larvae. All experiments were carried out in the laboratory of Biotecont Ltd. in accordance with Hungarian law for animal experimentation.

Azetidines were administered at a concentration of 20 µM to 6 dpf zebrafish larvae and the distances moved by the larvae were recorded for 30 minutes. The assays were carried out in a four well plate (Thermo Fisher Scientific, Germany) with two wells allocated per compound and two wells allocated per control (1% DMSO) with the total volume in each well totalling 20 mL. To each well 10 zebrafish larvae were added, which were allowed to acclimatize in the recording plate for 30 minutes before the plate was inserted into the FLIPR Tetra locomotion measurement system (Richter Gedeon Nyrt., Hungary). This locomotion measurement system was able to take pictures of every well every second whilst shining blue light repeatedly at 999 ms. The images taken were processed using custom-made software (KomiPL) provided by to Pictron Ltd. (Budapest, Hungary). The software automatically identified individual zebrafish larvae and then used changes in pixel intensity over the whole time frame as a measure of how much each zebrafish larva had moved

during that time period (shown in **Figure 4.4**) with greater pixel changes indicating greater movement.

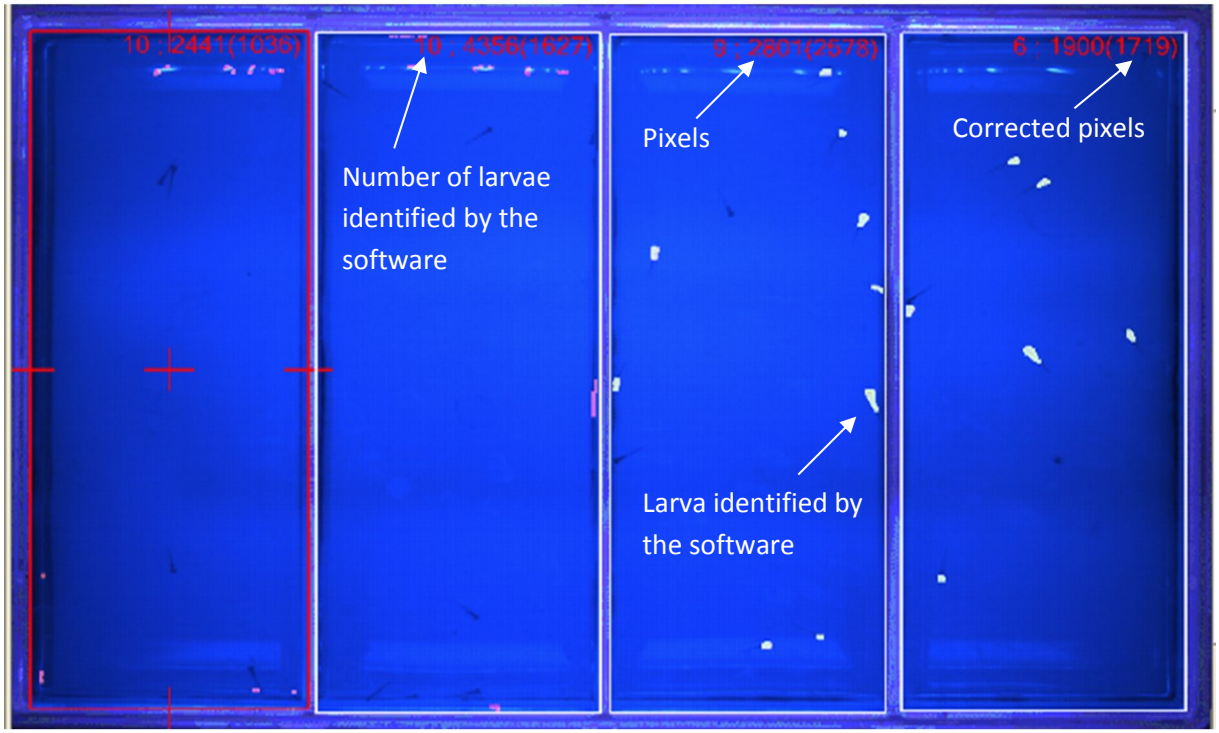

Figure 4.4 – Screenshot from KomiPL software showing tracking of individual zebrafish larvae by the software (highlighted in white). *Values found at the top of each well indicate number of zebrafish larvae successfully tracked and the number of pixels detected.*

The corrected pixel changes obtained every minute over the 30 minute time period were then used for further data analysis. The corrected pixel changes were used because they corrected the pixel intensity for the number of zebrafish larvae correctly identified by the software. The corrected pixel changes were then averaged for the three independent repeats and plotted against time. The results for the azetidine-treated zebrafish larvae were then compared against their respective 1% DMSO controls.

4.4 Results

4.4.1 Y-Lactam dose-range finding study

The Y-lactams were evaluated for biological activity by determining their effects on zebrafish embryo development. The Y-lactams represent a class of compounds particularly important in the field of synthetic organic chemistry. Several biologically active natural products contain a Y-lactam core including the cotinine alkaloid and the anti-fungal agent (-)-pramanicin (Dübon et al., 2009)(Schwartz et al., 1994).

A two phase study was performed with the Y-lactams. Phase 1 was used to determine the toxicity of the compounds using a logarithmic concentration series (0.01, 0.1, 1, 10, 100 and 1000 μM) by recording mortality daily over five days (see section **4.3.1** for further details). For compound **3c** due to solubility problems at 1000 μM, the concentration range was adjusted (0.001, 0.01, 0.1, 1, 10 and 100 μM).

The results for phase 1 (**Figure 4.5**) showed that over the 120 hour exposure period all compounds except compound **3h** caused 100% mortality at the highest tested concentration. Compound **3c** was found to be the most toxic compound causing high mortality even at concentrations as low as 10 μM.

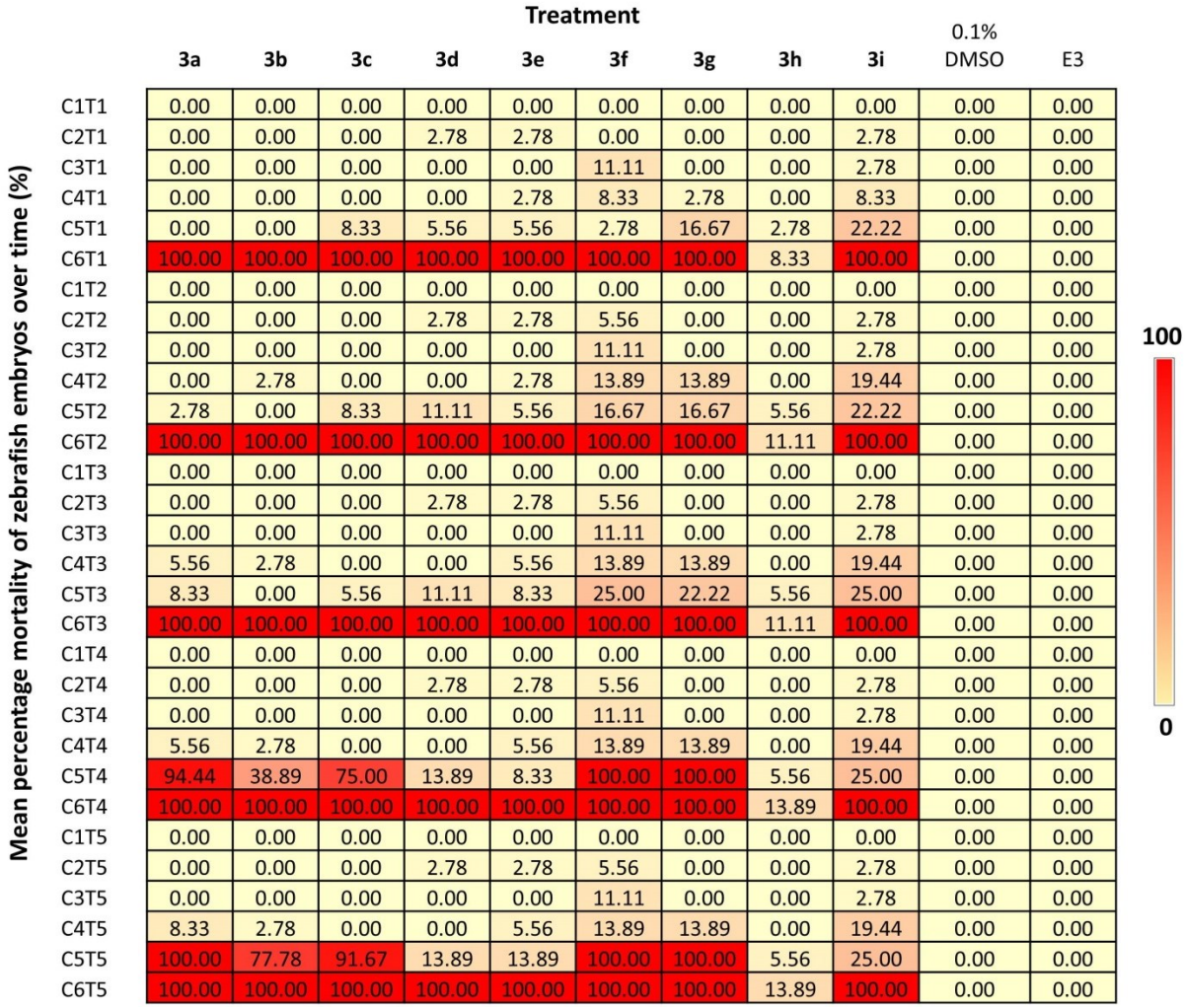

Figure 4.*5 – Heat map showing the mean cumulative percentage mortality of zebrafish embryos treated with Y-lactams at different concentrations over time. In total 36 zebrafish embryos were tested per concentration/control (SD range +/- 0-11.12%). Key: T1-T5 = 24, 48, 72, 96 and 120 hpf, C1-C6 = 0.01, 0.1, 1, 10, 100 and 1000 µM (except 3c where C1-C6 = 0.01, 0.1, 1, 10, 100 and 1000 µM). Colour key: light pink* ***= 0%, red = 100%***

Using these results log concentration mortality curves were plotted and from these toxicity endpoints such as LC50, NOEC and LOEC values were calculated (**Table 4.4**). Compound **3c** was found to have the lowest calculated LC50, LOEC and NOEC values and compound **3h** the highest.

Table 4.4 – Calculated toxicological endpoints for tested Y-lactams.

Compound	LOEC (µM)	NOEC (µM)	LC50 (µM)	LogP
3a	100	10	27.98	2.81
3b	100	10	55.08	2.48
3c	10	1	8.07	4.53
3d	1000	100	140.28	3.52
3e	1000	100	142.28	2.73
3f	100	10	17.99	1.98
3g	100	10	11.86	2.45
3h	2000	1000	1584.89	1.05
3i	1000	100	484.17	3.67

4.4.2 Evaluation of the morphological effects induced by Y-lactams

For the second phase of the study, a narrower concentration range was used to score a large number of morphological features for severity every day over a five day period (see **Table 4.3** for full list of features). This was done in order to see how the Y-lactams affected zebrafish embryo development and if there was any dose-dependency in the phenotypes produced. For the scoring of morphological effects the concentration at which 100% mortality was observed in the first study was used as the highest tested concentration in this study. For the remaining concentrations a geometric range was used. The concentration range (C1-C6) used for compounds **3a**, **3b**, **3d**, **3e**, **3f**, **3g** and **3i** was 31.25, 62.5, 125, 250, 500 and 1000 µM. For compound **3c** a concentration range of 3.125, 6.25, 12.5, 25, 50 and 100 µM was used. For compound **3h** a concentration range of 62.5, 125, 250, 500, 1000 and 2000 µM was used, as 100% mortality was not observed at 1000 µM. For the scoring of morphological features a scoring system was used to assign severity where 0 = normal, 1 = within normal range, 2 = mild, 3 = moderate, 4 = severe and 5 = very severe. Following treatment of zebrafish embryos with a selection of Y-lactams a number of phenotypes were observed as can be seen in **Figure 4.6**.

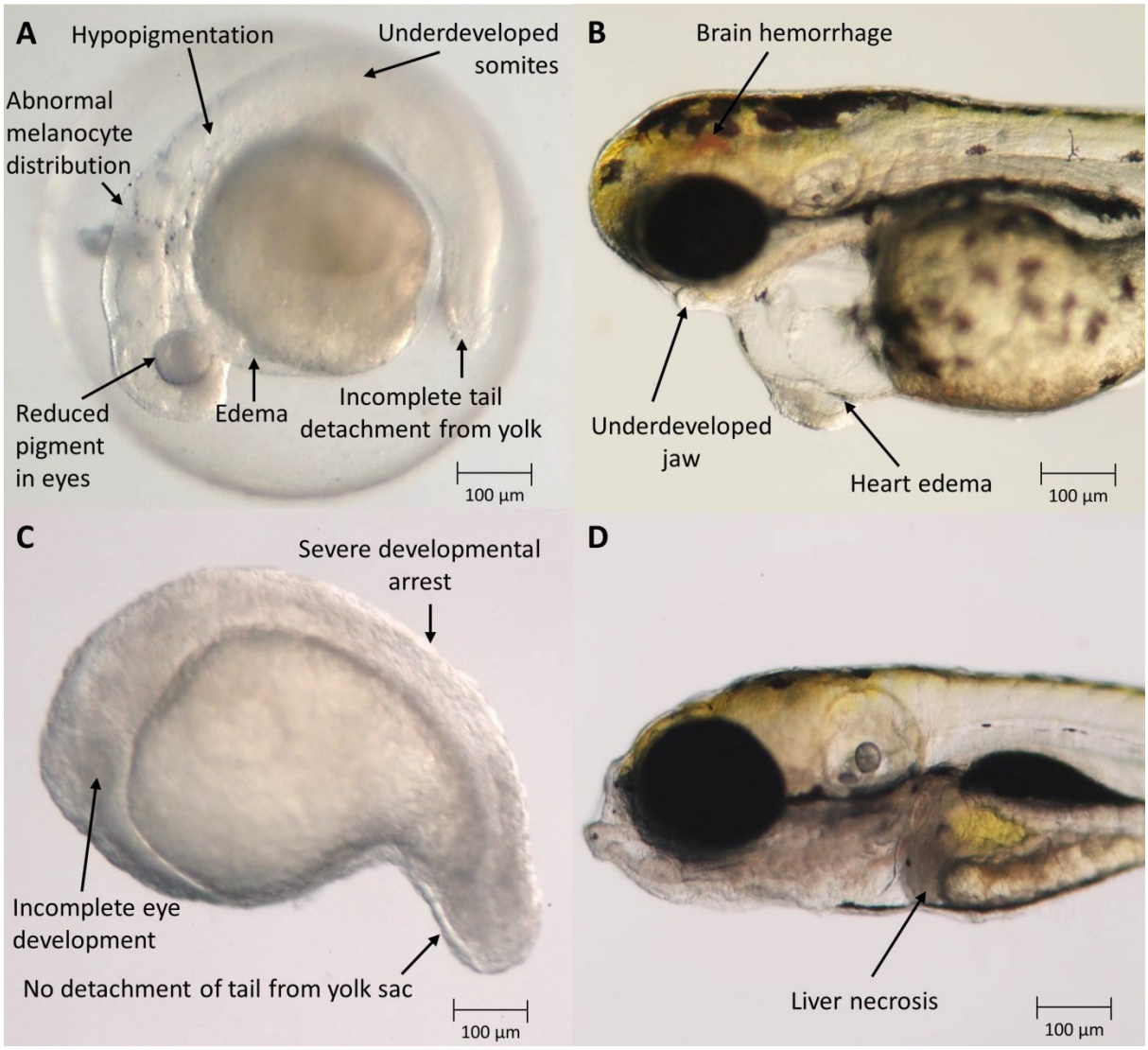

Figure 4.6 – Selection of phenotypes observed following treatment of zebrafish embryos with Y-lactams. *A) Delayed development and hypopigmentation after 48 hours of treatment with 1000 µM compound* ***3b****, B) Brain hemorrhage, delayed development and heart edema after 72 hours of treatment with compound* ***3g****, C) Severe developmental arrest after 24 hours of exposure with 1000 µM compound* ***3d****, D) Liver necrosis after 120 hours of treatment with 10 µM compound* ***3f****. All images are lateral views.*

It was found that with a few of the compounds, specific phenotypes developed at certain concentrations. For example with compound **3a** there was a dose-dependency in the development of brain hemorrhage (62.5-500 µM). With compound **3f** on the other hand liver toxicity was found to occur at specific doses (31.25 and 10 µM). Additionally, with

compound **3h** only at the highest and second highest tested concentrations (2000 and 1000 µM) liver toxicity was observed.

Using the morphology data log concentration response curves were plotted and EC50 values were calculated (**Table 4.5**). EC50 values were found to be highest for compound **3d** and lowest for compound **3c**. In addition to this the ratio between LC50 and EC50 values was calculated in order to obtain a value for the teratogenic index (**Table 4.5**). The Y-lactams **3a, 3b**, **3f** and **3g** were found to have LC50/EC50 ratio values <2, suggesting that the phenotypes observed with these compounds were secondary effects of generic primary effects. The remaining Y-lactams were found to have LC50/EC50 ratio values >2, especially Y-lactam **3h** which was found to have a ratio value of around 25 suggesting that this compound was provoking specific effects at sub-lethal concentrations. Additionally, compound **3c** was also found to be highly teratogenic.

Table 4.5 - EC50 and teratogenic index values for the nine tested Y-lactams. *Teratogenic index values >2 indicate specific effects.*

Compound	EC50 (µM)	Teratogenic index (LC50/EC50)
3a	15.07	1.86
3b	31.33	1.76
3c	3.13	2.58
3d	65.01	2.16
3e	17.58	8.09
3f	17.99	1.00
3g	31.33	0.38
3h	62.66	25.29
3i	57.94	8.36

As a next step, a PCA model was generated to determine if there was any relationship between physiochemical descriptors of the Y-lactams (logP, MW, HBA, HBD and HB) and the

biological responses (LOEC, NOEC, EC50, LC50 and morphological feature scores). The PCA model that was generated was found to be of good quality (R^2X=0.687, Q^2=0.433, four significant components). From the PCA scores plot (**Figure 4.7A**) it could be seen that the scores (observations) for Y-lactam **3h** at different concentrations were separated away from the rest of the scores. When looking at the loading plot (**Figure 4.7B**) which shows the variables it could be seen that this compound showed the least mortality, as well as the least severity in terms of morphological responses, which explains why it is placed so far apart from the rest of the scores on the scores plot. The further a score is on the scores plot from other scores the more different it is.

The scores for the remainder of the Y-lactams at the highest tested concentration were found to be clustered close together in the top right quadrant of the PCA plot (circled) based on their high mortality rates and severity scores for the morphological features reduced heart rate (HR), reduced circulation (CR) and reduced movement (MO), which are indicators of lethality. These features were found to have the most influence on the location of the scores. A high logP value was found to have some influence on the development of certain morphological features, such as yolk edema, heart edema, jaw malformations, notochord abnormalities and yolk size.

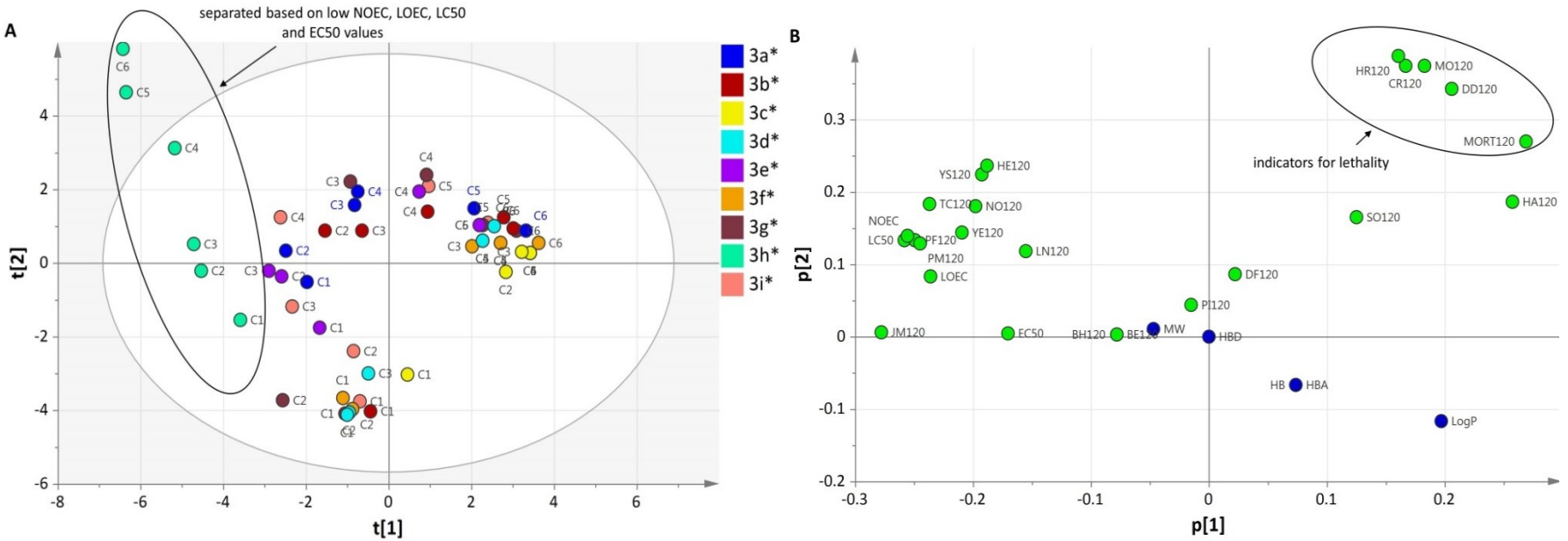

Figure 4.7 - A two-component PCA model of zebrafish embryo biological responses (observations) against morphological features, toxicity endpoints and physiochemical descriptors (variables) following treatment with Y-lactams over a 120 hour exposure period. *Only the morphological features scored at 5 dpf were used to create the model. A) Scores plot, B) Loading plot. Biological features = HR (slowed heart rate), HE (heart edema), CR (reduced circulation), JM (jaw malformations), TC (tail curvature), DD (delayed development), BE (brain edema), BH (brain hemorrhage) and PI (hypopigmentation), MO (reduced movement), HA (hatching), DF (deformation), NO (abnormal notochord), PM (abnormal protruding mouth), PF (abnormal pectoral fin), SO (abnormal somites), YE (yolk edema), YS (increased yolk size), LN (liver necrosis) and MORT (mortality). Toxicological endpoints = EC50, LC50, LOEC and NOEC. Chemical descriptors = logP, MW, HB, HBA and HBD. The loading vector (p) and the scores vector (t) are displayed as vectors p and t. The numbers beside p and t indicate the PCA component (1 or 2). The observations for tested Y-lactams are denoted by coloured circles with different concentrations labelled. Coloured circles also denote the location of the variables within the loading plot with differences in colour indicating whether the variables are biological (green) or chemical (blue).The further scores or variables are from one another the more different they are.*

To confirm that effects observed with certain Y-lactams (e.g. **3h**) were specific and not a result of baseline toxicity logP values were plotted against log(1/EC50) values (**Figure 4.8**). From this graph no strong correlation could be seen between increased logP values and decreased log(1/EC50) values.

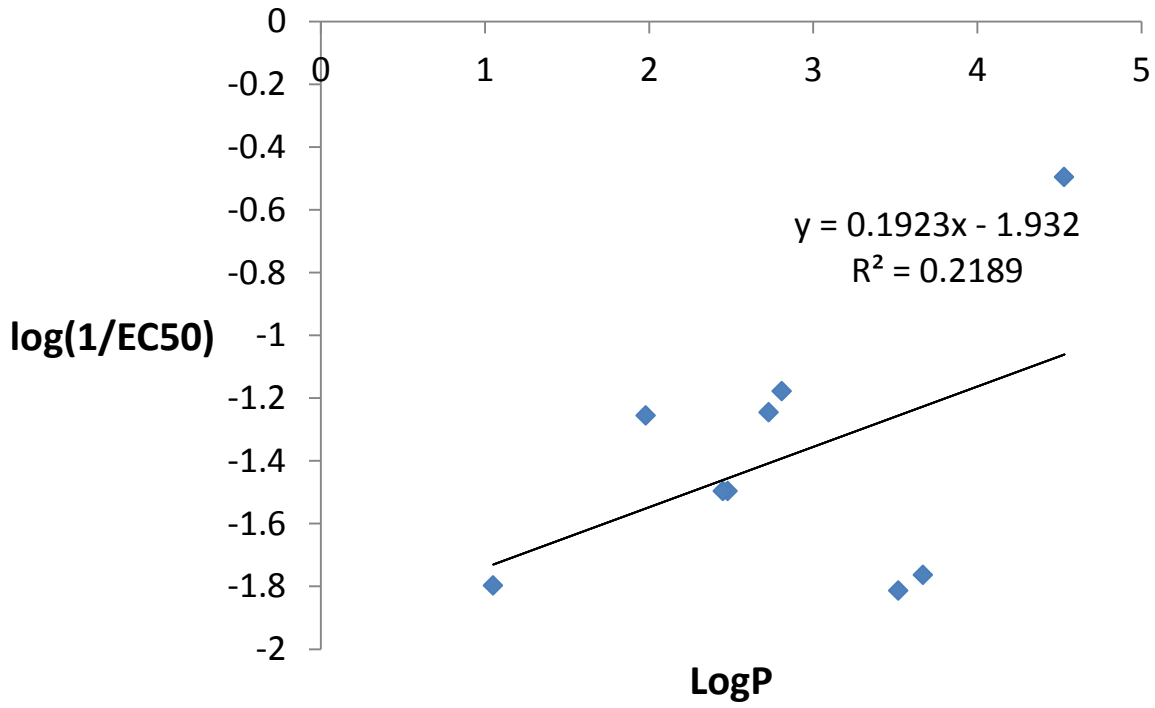

Figure 4.8 – LogP values plotted against log(1/EC50) values for tested Y-lactams. *Line of best fit and correlation coefficient (r^2) are also shown on graph.*

Another approach was then taken to determine whether the biological responses observed with the Y-lactams were a result of specific activity or baseline toxicity. Toxic ratio (TR) values were calculated for each of the Y-lactams using predicted and experimental LC50 values (see **Table 4.6**). It could be seen that for the Y-lactams **3g** and **3h** the logTR values were >1 suggesting that the toxicity observed was due to a specific mechanism of action rather than baseline toxicity. However, with the remaining Y-lactams the logTR values were

found to be <1 suggesting that the toxicity observed was due to baseline toxicity. This was most evident for Y-lactam **3c**.

Table 4.6 – Toxic ratio (TR) values for toxicity observed with Y-lactams. *LogTR>1 = specific toxicity, logTR<1 = baseline toxicity.*

Y-lactam	LogP	log(1/LC50) predicted (mmol/L)	log(1/LC50) experimental (mmol/L)	logTR (toxic ratio)
3a	2.81	-2.43	-1.45	0.98
3b	2.48	-2.71	-1.74	0.97
3c	4.53	-0.93	-0.91	0.02
3d	3.52	-1.81	-2.15	-0.34
3e	2.73	-2.49	-2.15	0.34
3f	1.98	-3.15	-1.26	1.89
3g	2.45	-2.74	-1.07	1.66
3h	1.05	-3.96	-3.20	0.76
3i	3.67	-1.68	-2.69	-1.01

4.4.3 Specific characterisation of Y-lactams 3a, 3f and 3h

After the biological activity of the Y-lactams had been determined, compounds **3a**, **3f** and **3h** were selected for further testing, as with these three compounds specific phenotypes were observed. With Y-lactam **3a** and in some cases with Y-lactam **3g** brain hemorrhage and hydrocephalus was observed. With compounds **3f** and **3h** liver toxicity was observed.

Brain hemorrhage and hydrocephalus are particularly interesting, as they present life-threatening conditions that are not very well understood (Aronowski and Hall, 2005)(Huang et al., 2002). Brain hemorrhage phenotypes have been observed in other zebrafish embryo studies as a result of targeted block of a specific gene involved in maintaining blood vessel stability in the brain (Liu et al., 2007)(Buchner et al., 2007)(Zou et al., 2011). It was therefore

of interest to investigate whether the brain hemorrhage phenotype observed with **3a** occurred by the same or different mechanism. Liver toxicity on the other hand represents a condition that can have many underlying causes. It was therefore of interest to find out the causes of the liver toxicity observed with **3f** and **3h**.

4.4.3.1 Specific characterisation of Y-lactam 3a

The brain hemorrhage phenotype observed with Y-lactam **3a** was further investigated to see which part of the brain it was targeted to and what could be the underlying cause without going into molecular detail. It was found that brain hemorrhage development with **3a** was specifically confined to the brain ventricle (**Figure 4.9A**). Additionally, hydrocephalus (accumulation of cerebrospinal fluid) was found to accompany the brain hemorrhage induced by **3a** (**Figure 4.9A**). No such conditions were observed in untreated controls (**Figure 4.9B**). All the zebrafish embryos that were treated with 100 µM **3a** from the 75% epiboly stage were found to develop ventricular brain hemorrhage (VBH) by 3 dpf (**Figure 4.9C**, n=30 zebrafish larvae at 3 dpf per compound treatment/control, $P<0.05$). However in some cases, the hemorrhage also spread to other parts of the brain including the midbrain, which was found to occur in about 50% of cases and also the forebrain in around 25% of cases (**Figure 4.9D**). Hemorrhage formation in the brain ventricle and in the mid-brain was found to be significant, whereas this was not the case for the forebrain (n=30 zebrafish larvae per compound treatment/control at 3 dpf, $P<0.05$ for brain ventricle and mid-brain, $P>0.05$ for forebrain). Compound **3g** was also found to induce hemorrhage formation but only in 25% of cases and the localization of the hemorrhage was not as consistent as with compound **3a**.

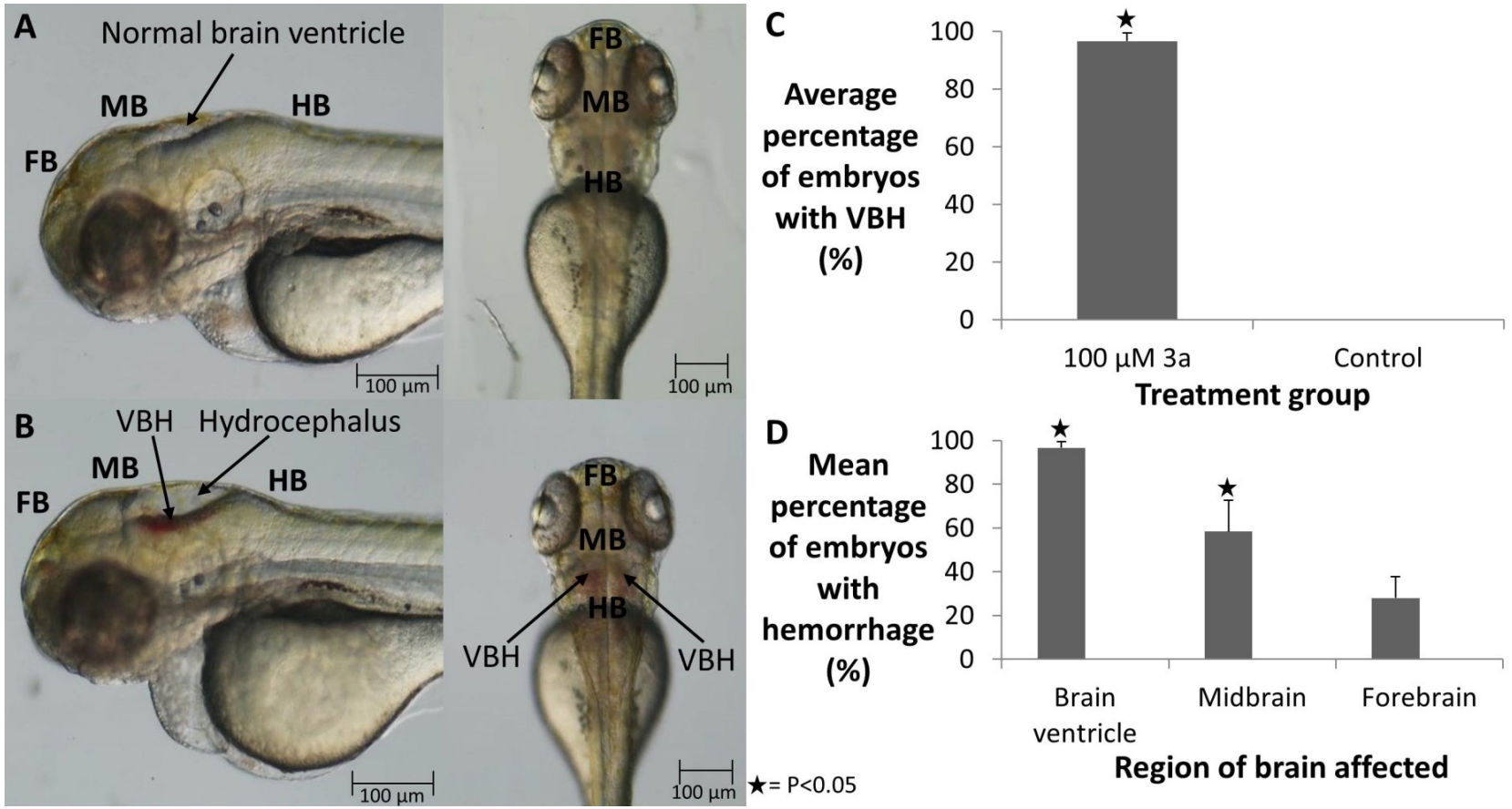

Figure 4.9 – Ventricular brain hemorrhage (VBH) formation in zebrafish larvae after treatment with Y-lactam 3a. *A) Untreated zebrafish larva at 3 dpf (lateral view (left) and dorsal view (right)), B) 100 µM compound* ***3a****-treated zebrafish larva at 3 dpf (lateral view (left) and dorsal view (right)), C) Percentage of zebrafish larvae at 3 dpf presenting with ventricular brain hemorrhage (VBH) (n=30 zebrafish at 3 dpf per compound treatment/control, P<0.05) and D) Percentage of zebrafish larvae presenting with hemorrhage in different areas of the brain (n=30 zebrafish at 3 dpf per compound treatment/control, P<0.05 for brain ventricle and midbrain, P>0.05 for forebrain). Key: VBH = ventricular brain hemorrhage, FB = forebrain, MB = midbrain, HB = hindbrain*

To further explore the brain hemorrhage phenotype observed with **3a** a transgenic zebrafish line Tg(*gata-1:DsRed*);Tg(*fli-1:EGFP*) was employed to visualise red blood cells and blood vessels (**Figure 4.10**). It could be clearly seen that an accumulation of red blood cells occurred in the brain ventricle of the 100 µM **3a**-treated zebrafish larvae, which was not present in the controls (**Figure 4.10A**,**B**). Additionally, it was observed that bleeding was predominantly restricted to the basement membrane underlying the brain ventricle (**Figure 4.10C**,**D**). The brain hemorrhage was also seen to be confined only to the brain ventricle with the surrounding vasculature undamaged (**Figure 4.10E**,**F**). At 4 dpf the brain angiogenesis in the 100 µM **3a**-treated zebrafish larvae was found to be reduced compared to controls and signs of cell death in this region were also apparent (**Figure 4.10G**,**H**). Additionally, the number of zebrafish larvae treated with 100 µM **3a** displaying blood cell pooling in the brain and reduced overall circulation was found to be significant (**Figure 4.10I**,**J**, n=30 zebrafish larvae at 3 dpf per treatment/control, $P<0.05$).

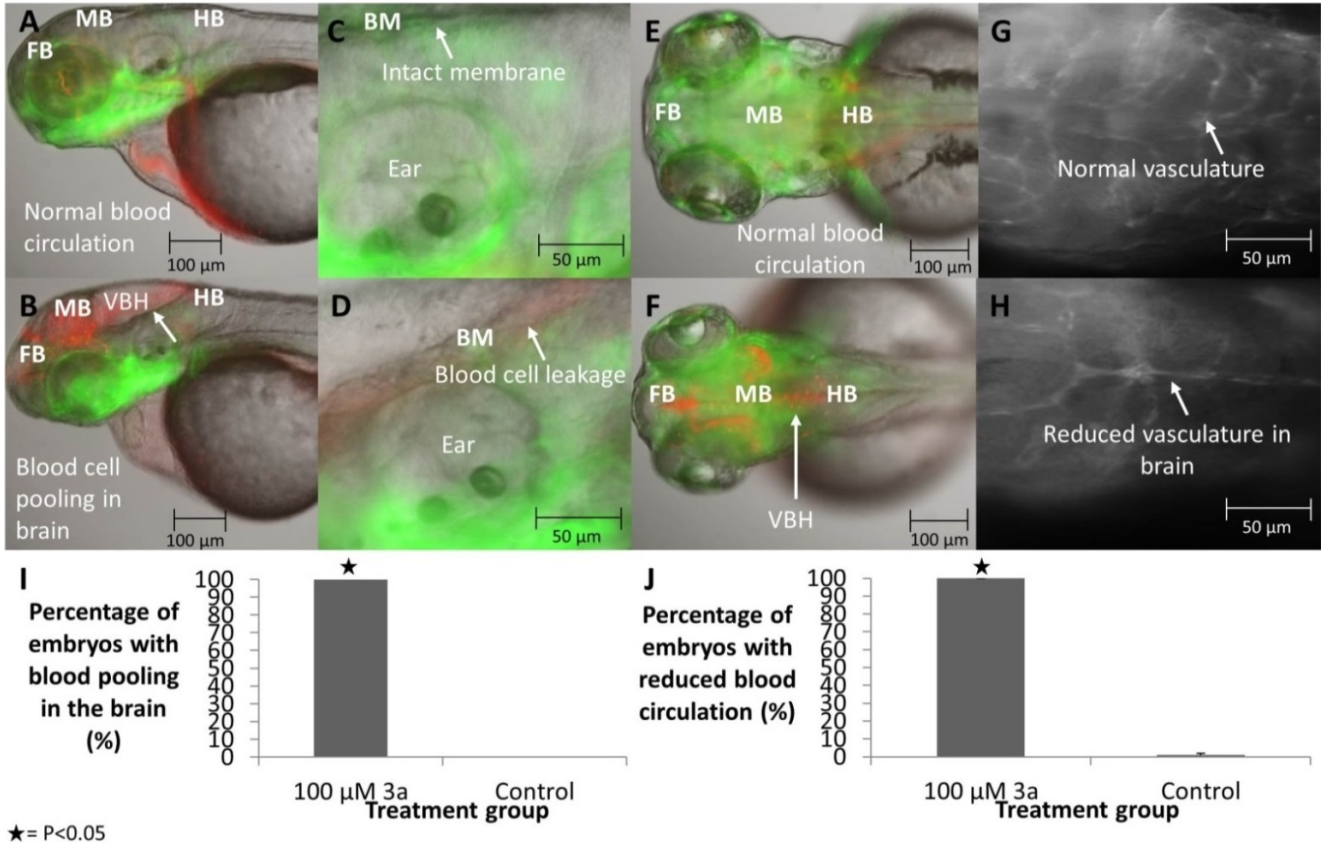

Figure 4.10 – Red blood cell localization and blood vessel architecture of 100 µM 3a-treated zebrafish embryos visualised using Tg(gata-1:DsRed);Tg(fli-1:EGFP). *Images (A-F) are shown as Brightfield, GFP and DsRed overlays. A) Lateral overlay of an untreated and B) a 100 µM **3a**-treated zebrafish at 3 dpf, C) Lateral overlay of an untreated and D) a 100 µM **3a**-treated zebrafish at 3 dpf zoomed in, E) Dorsal overlay of an untreated and F) a 100 µM **3a**-treated zebrafish at 3 dpf, G) Black and white image showing GFP expression in an untreated and H) a 100 µM **3a**-treated zebrafish at 4 dpf, I) Percentage of zebrafish with blood pooling in the brain (n=30 zebrafish at 3 dpf per compound treatment/control, P<0.05), J) Percentage of zebrafish with reduced blood circulation (n=30 zebrafish at 3 dpf per compound treatment/control, P<0.05). Key: VBH = ventricular brain hemorrhage, FB = forebrain, MB = midbrain, HB = hindbrain*

Based on the previous experiment where cell death in the brains of 100 µM **3a**-treated 4 dpf zebrafish larvae was seen, acridine orange staining was performed (see section **4.3.6**) to determine whether this cell death was mediated by apoptosis. It was found that in the 100 µM **3a**-treated zebrafish larvae compared to the controls there was extensive apoptotic cell death visible in the hindbrain and also around the midbrain part of the brain ventricle characterized by brightly fluorescing cells (**Figure 4.11**). The number of apoptotic cells in this region was found to be significant (**Figure 4.11**, n=12 zebrafish larvae at 4 dpf per compound treatment/control, $P<0.05$). Additionally, this region was also found to coincide with the region where hemorrhage was observed. This finding agrees with the literature where neural cell death due to apoptosis in the brain ventricles of premature human infants born with intraventricular hemorrhage (IVH) is observed (Dummula et al., 2011).

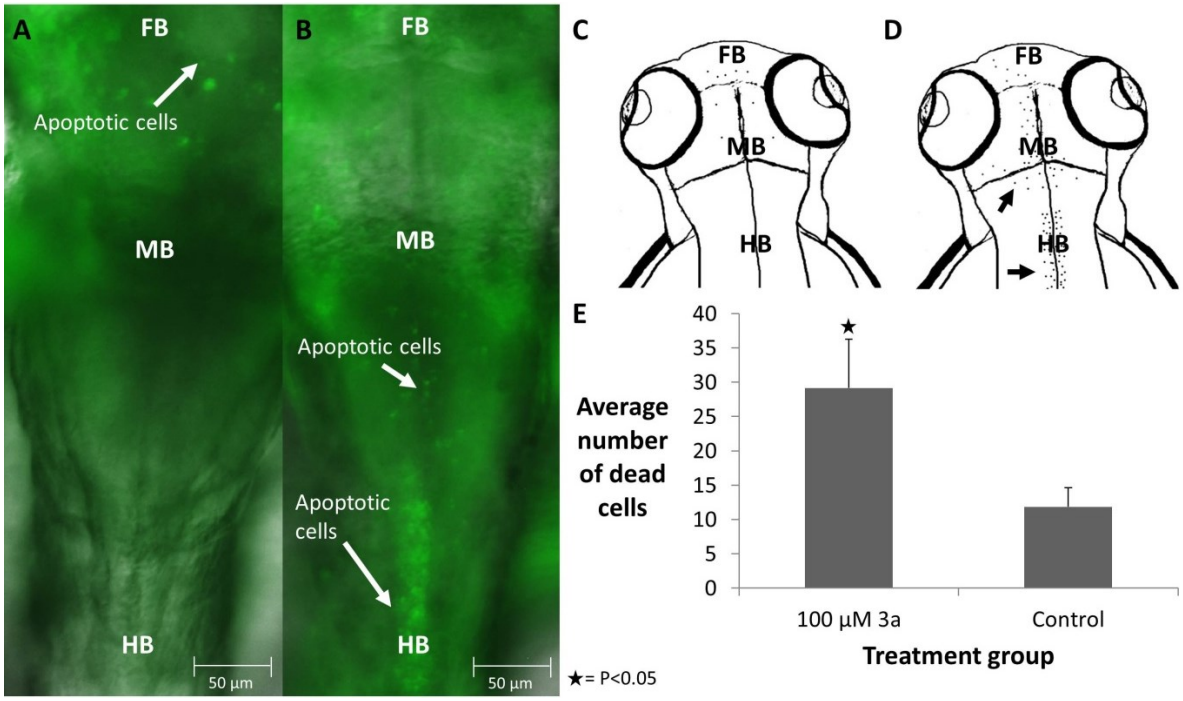

Figure 4.11 – Acridine orange staining of dead cells in zebrafish larvae presenting with ventricular brain hemorrhage. *A) Acridine orange staining of an untreated zebrafish larva at 4 dpf viewed under the GFP channel (dorsal view), B) Acridine orange staining of a 100 µM compound **3a**-treated zebrafish larva at 4 dpf viewed under the GFP channel (dorsal view), C) Drawing of dead cell localization in an untreated zebrafish larva at 4 dpf (dorsal view), D) Drawing of dead cell localization in a 100 µM compound **3a**-treated zebrafish larva at 4 dpf (dorsal view), E) Average number of dead cells counted in the brains of untreated (control) and 100 µM **3a**-treated zebrafish larvae (n=12 zebrafish larvae at 4 dpf per compound treatment/control, P<0.05). Key: FB = forebrain, MB = midbrain, HB = hindbrain*

4.4.3.2 Specific characterisation of Y-lactams 3f and 3h

The next aim was to characterize Y-lactams **3f** and **3h** further, as with both of these compounds liver toxicity was observed in the initial morphology studies. Liver toxicity is difficult to detect and has led to a number of drug withdrawals from the market. Between 1994 and 2006, 14 out of 38 drugs approved by the US Food and Drug Administration (FDA) had to be removed due to safety concerns regarding potential liver toxicity (Dykens and Will, 2007).

With compound **3f** liver necrosis was observed only at a concentration of 10 μM after 120 hours of exposure (**Figure 4.12A**,**B**). This phenotype was also found to occur specifically in the absence of any other morphological effects. After performing ORO staining to stain lipids (see section **4.3.5**), it was found that the zebrafish larvae with liver necrosis had abnormal lipid accumulation in the liver indicative of steatosis (**Figure 4.12C**,**D**). Steatosis, also known as fatty liver can occur due to impairment of triglyceride excretion and synthesis (Leclercq et al., 1998). To determine whether the steatosis observed was also accompanied by inflammation, untreated zebrafish larvae and those presenting with liver necrosis were fixed and stained with Sudan black reagent (see section **4.3.7**). This was done in order to see whether leukocytes were localized in and around the liver region as this would be indicative of hepatitis (inflammation of the liver). However, it was found that both the untreated zebrafish larvae and those with liver necrosis did not to have any leukocyte localization in and around the liver (**Figure 4.12E**,**F**). This therefore suggested that the liver necrosis and steatosis observed with **3f** was independent of an inflammatory response. In addition, liver size was also assessed and was found to be unchanged in both treated and untreated zebrafish larvae (data not shown).

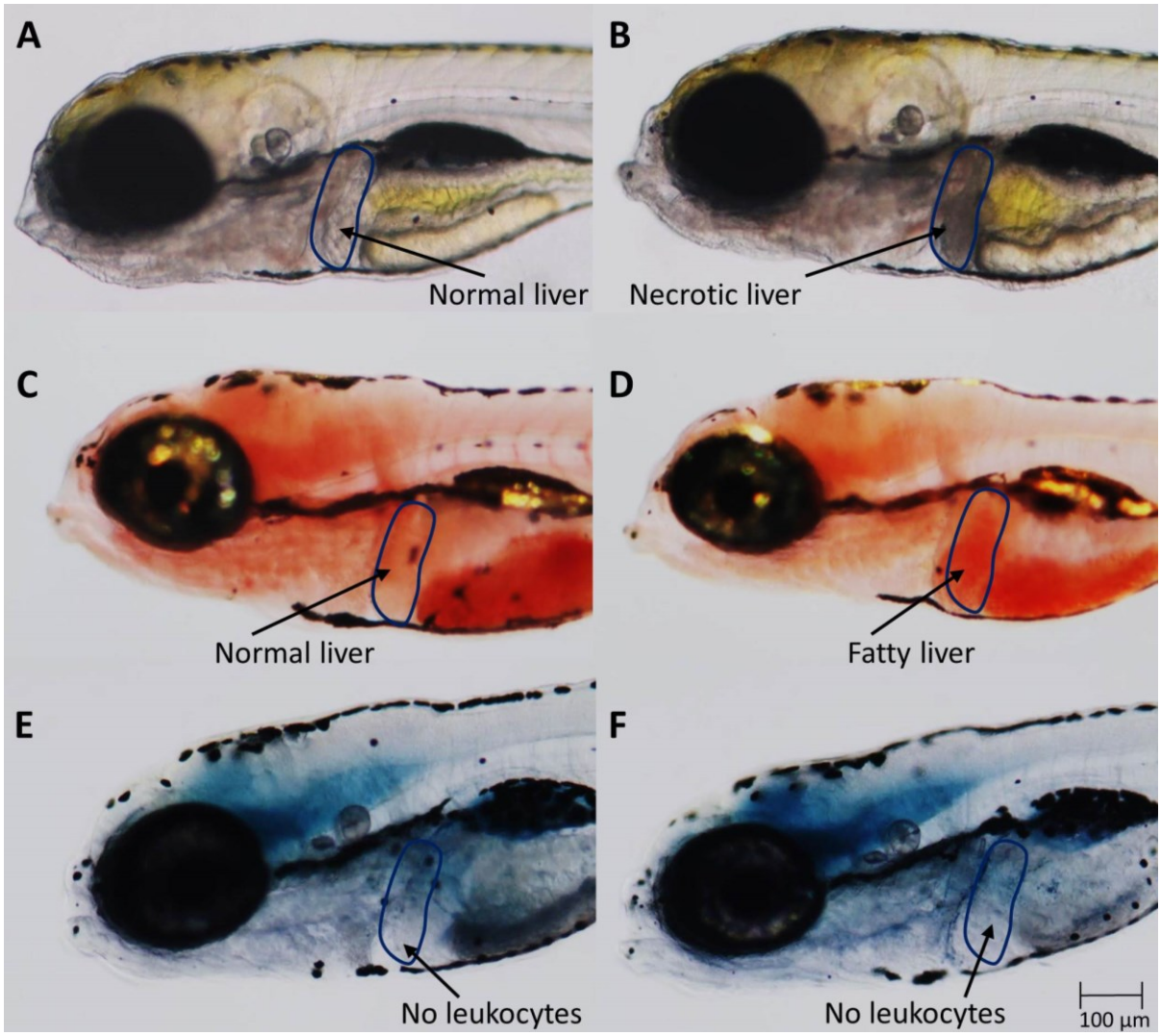

Figure 4.12 – Liver necrosis and steatosis in zebrafish larvae treated with 10 µM Y-lactam 3f. *A) Untreated zebrafish larva at 5 dpf, B) 10 µM **3f**-treated zebrafish larva at 5 dpf, C) Untreated zebrafish larva at 5 dpf stained with Oil red O, D) 10 µM **3f**-treated zebrafish larva at 5 dpf stained with Oil red O, E) Untreated zebrafish larva at 5 dpf stained with Sudan black, F) 10 µM **3f**-treated zebrafish larva at 5 dpf stained with Sudan black.*

The Y-lactam **3h** was then also characterized in a similar way to **3f** to see whether it caused liver necrosis by the same mechanism. Exposure to compound **3f** resulted in an enlarged necrotic liver (**Figure 4.13A**,**B**). This was accompanied by steatosis characterized by large lipid droplets in and around the liver, as shown by ORO staining (**Figure 4.13C**,**D**). Additionally, after performing Sudan black staining it was apparent that an inflammatory response was also involved with leukocytes found to infiltrate the liver (**Figure 4.13E**,**F**).

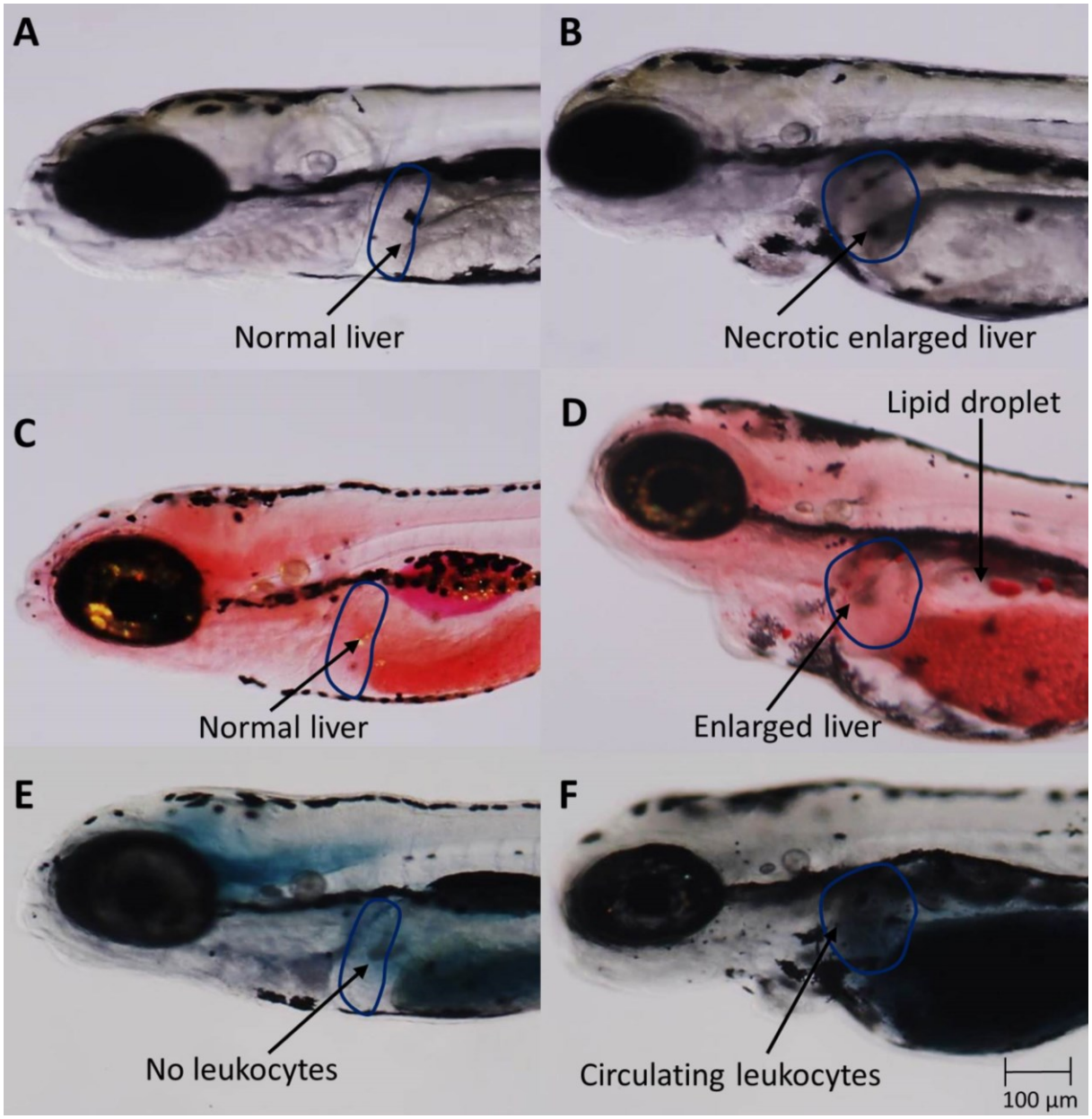

Figure 4.13 – Liver necrosis and steatohepatitis in zebrafish larvae treated with Y-lactam 3h at 2000 µM. *A) Untreated zebrafish larva at 5 dpf, B) 2000 µM **3h**-treated zebrafish larva at 5 dpf, C) Untreated zebrafish larva at 5 dpf stained with Oil red O, D) 2000 µM **3h**-treated zebrafish larva at 5 dpf stained with Oil red O, E) Untreated zebrafish larva at 5 dpf stained with Sudan black, F) 2000 µM **3h**-treated zebrafish larva at 5 dpf stained with Sudan black.*

Additionally, with compound **3h** the extent of liver necrosis and steatosis was found to be concentration dependent, occurring at two concentrations, namely 1000 and 2000 µM (**Figure 4.14**).

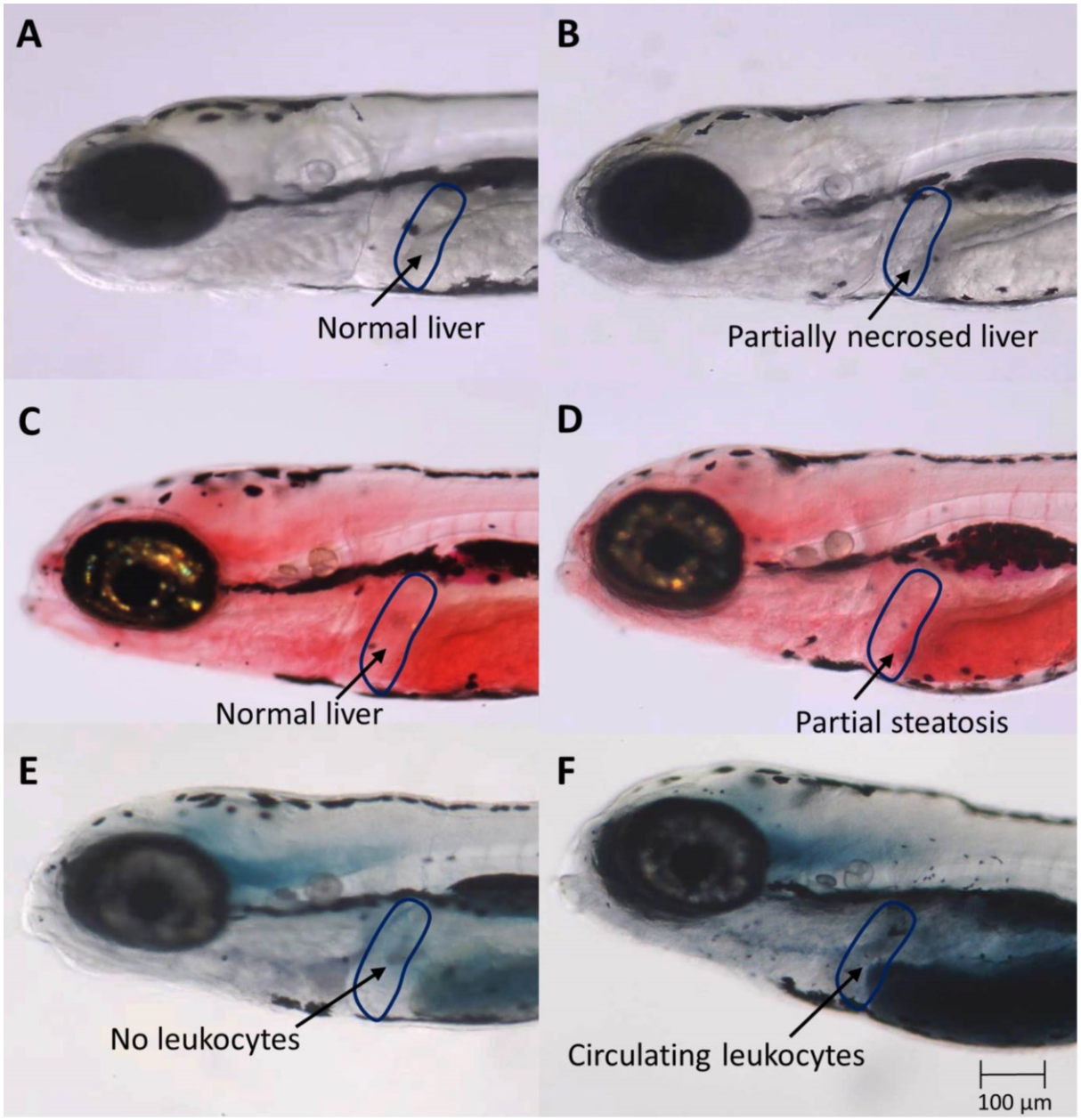

Figure 4.14 – Partial liver necrosis and steatohepatitis in zebrafish larvae treated with Y-lactam 3h at 1000 µM. *A) Untreated zebrafish larva at 5 dpf, B) 1000 µM* ***3h****-treated zebrafish larva at 5 dpf, C) Untreated zebrafish larva at 5 dpf stained with Oil red O, D) 1000 µM* ***3h****-treated zebrafish larva at 5 dpf stained with Oil red O, E) Untreated zebrafish larva at 5 dpf stained with Sudan black, F) 1000 µM* ***3h****-treated zebrafish larva at 5 dpf stained with Sudan black.*

The leukocyte number as well as the percentage increase in liver size was determined for both concentrations of Y-lactam **3h** (**Figure 4.15**). With both concentrations of Y-lactam **3h** a significant increase in the leukocyte number localized around the liver was observed (**Figure**

4.15A, n=12 zebrafish larvae at 5 dpf per compound treatment/control, P<0.05). Additionally, the average liver size was found to be significantly increased after treatment with Y-lactam **3h** at 2000 µM but not at 1000 µM (**Figure 4.15B**, n=12 zebrafish larvae at 5 dpf per compound treatment/control, P<0.05 for 2000 µM **3h**, P>0.05 for 1000 µM **3h**).

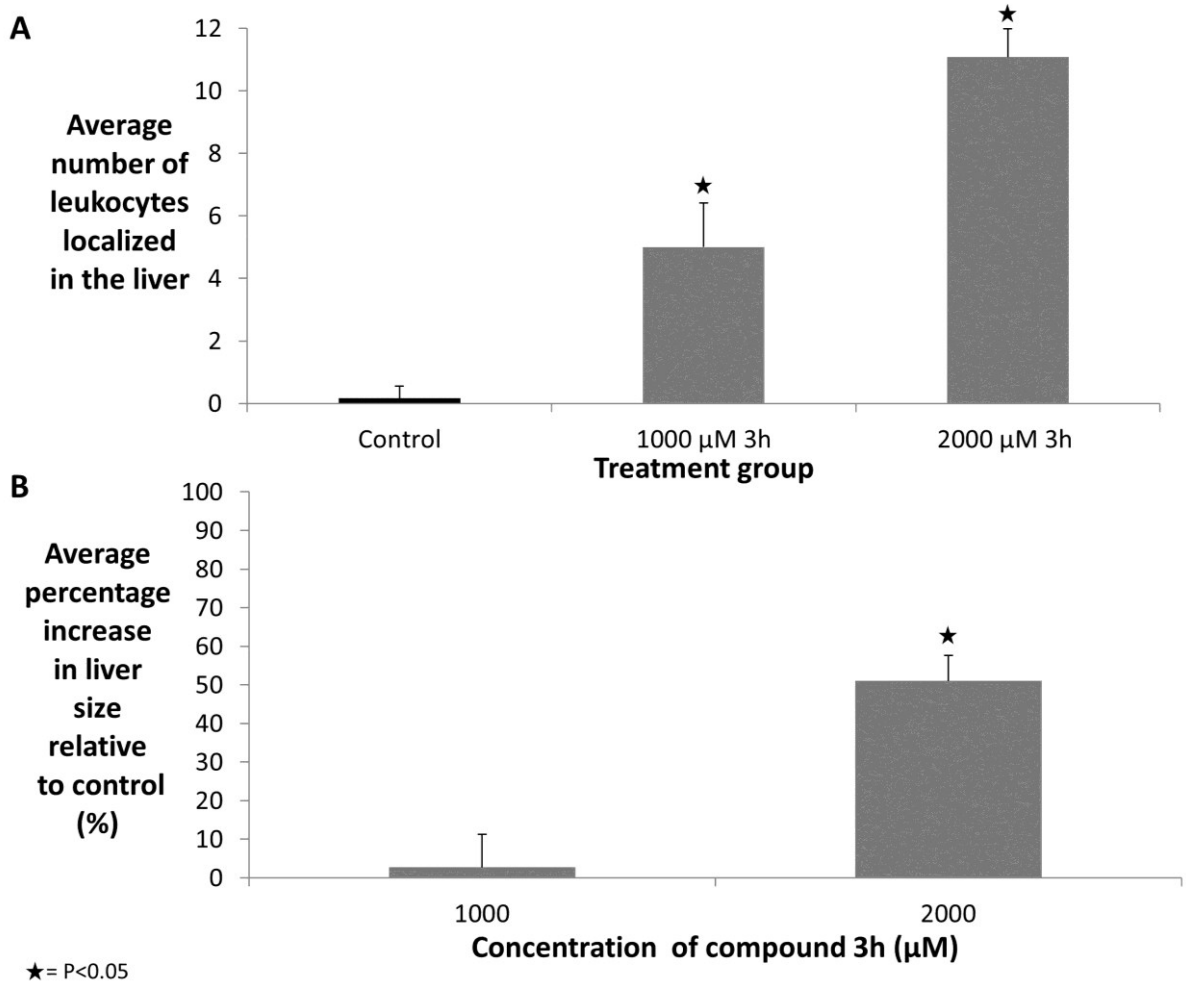

Figure 4.15 – Increase in circulating leukocytes in and around the liver and increase in liver size after treatment of zebrafish larvae with Y-lactam 3h. *A) Average leukocyte number in livers of control, 1000 µM and 2000 µM compound **3h**-treated zebrafish (n=12 zebrafish larvae at 5 dpf per compound treatment/control, P<0.05 for 1000 and 2000 µM **3h**), B) Average percentage increase in liver size relative to control for 1000 and 2000 µM compound **3h**-treated zebrafish (n=12 zebrafish larvae at 5 dpf per compound treatment/control, P<0.05 for 2000 µM).*

4.4.4 Morphology analysis of azetidine-treated zebrafish embryos

The initial aim was to explore the biological activity of six selected azetidines by observing how they affected zebrafish embryo development. Due to time constraints three different treatment regimens were utilised (treatments with each azetidine at a concentration of 10 and 25 µM commencing at the 75% epiboly stage up until 120 hpf and treatments with each azetidine at 30 µM beginning at 24 hpf up until 120 hpf). The latter treatment regimen was employed in order to see whether the selected azetidines also affected later stages of zebrafish embryo development once the major cellular processes had been completed.

The percentage of zebrafish embryos presenting with particular morphological effects were quantified and averaged from three separate repeats over a five day exposure period for all three treatment regimens (**Figure 4.16**, n=30 zebrafish larvae at 5 dpf per compound/control [0.1% DMSO and E3 embryo medium]). Morphological features recorded included tail curvature (TC), abnormal jaw formation (JM), delayed development (DD), hypopigmentation (PI), slowed heart rate (HR), tail necrosis (TN), heart edema (HE), brain edema (BE) and reduced blood circulation (CR).

All tested azetidines at 10 µM except azetidine **2f** showed significant differences in the morphological effects they produced compared to the controls ($P>0.05$ for **2f**, $P<0.05$ for the rest). At 25 µM, all tested azetidines showed significant differences compared to the controls ($P>0.05$ for all). When zebrafish embryos were treated at 24 hpf at a concentration of 30 µM, azetidines **2b**, **2d** and **2f** were found to show no significant differences in the

morphological effects they produced compared to the controls (P>0.05). However, azetidines **2a**, **2c** and **2e** were found to show significant differences (P<0.05).

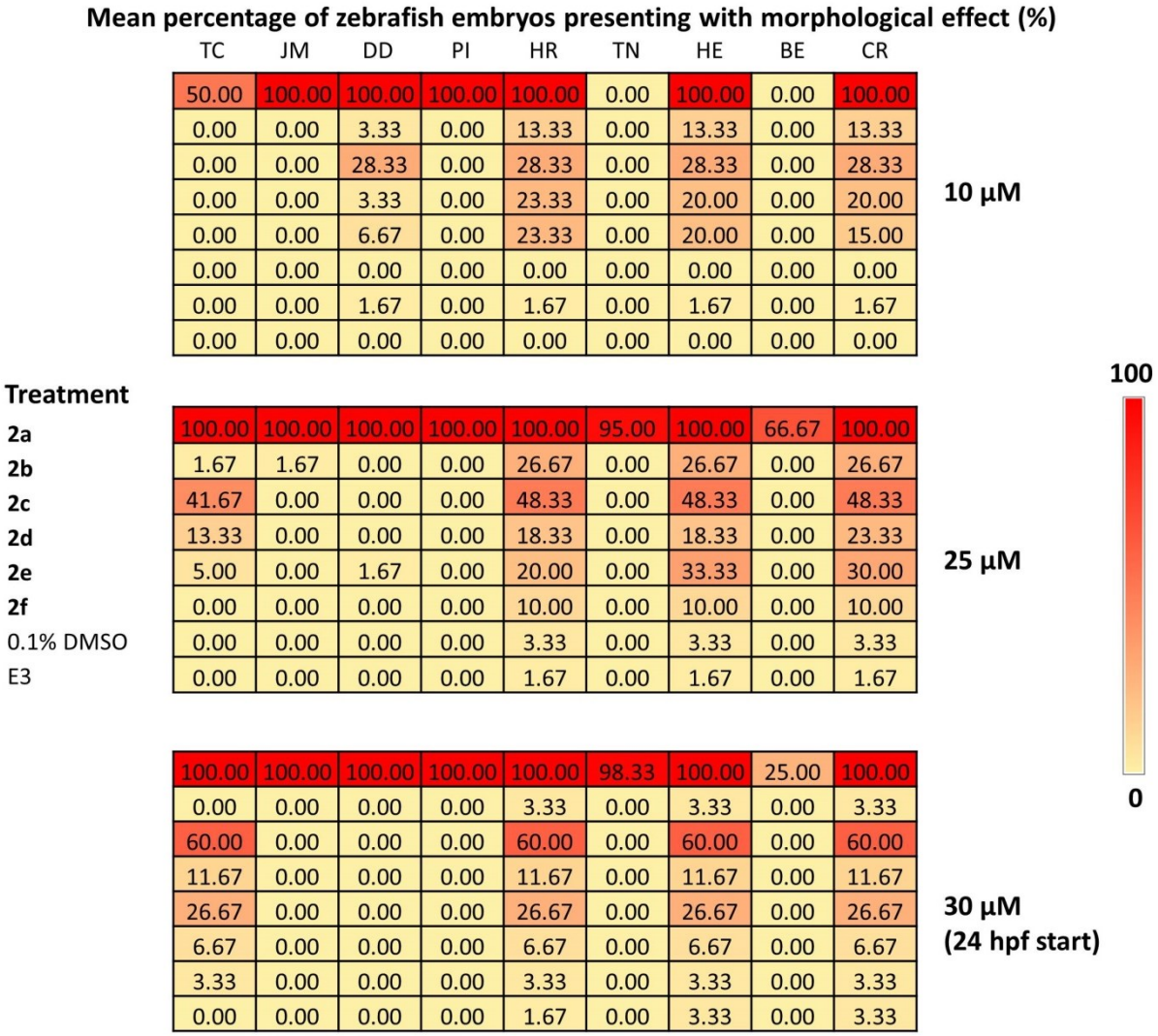

Figure 4.16 – Heat map showing morphological effects observed in zebrafish larvae after exposure to the six selected azetidines. *Top) Mean percentage of zebrafish larvae presenting with morphological defects after 120 hours of 10 µM azetidine treatment initiated at the 75% epiboly stage (n=30 zebrafish larvae at 5 dpf per compound/control, SD range +/- 0-31.75%, P>0.05 for **2f**, P<0.05 for rest), Middle) Mean percentage of zebrafish larvae presenting with morphological defects after 120 hours of 25 µM azetidine treatment initiated at the 75% epiboly stage (n=30 zebrafish larvae at 5 dpf per compound/control, SD range +/- 0-46.19%, P<0.05 for all), Bottom) Mean percentage of zebrafish larvae presenting with morphological defects after 96 hours of 30 µM azetidine treatment initiated at the prim-5 stage (n=30 zebrafish larvae at 5 dpf per compound/control, SD range +/- 0-30.41, P>0.05 for **2b**, **2d**, **2f**, P<0.05 for rest). Key: TC = tail curvature, JM = abnormal jaw formation, DD = delayed development, PI = hypopigmentation, HR = slowed heart rate, TN = tail necrosis, HE = heart edema, BE = brain edema and CR = reduced circulation. Colour key: light yellow = 0%, red = 100%*

Compound **2a** at all tested concentrations and exposure times was found to be the most biologically active producing various morphological effects in zebrafish embryos including hypopigmentation, delayed development, reduced circulation, reduced heart rate, trunk curvature, pericardial edema, scoliosis, hydrocephalus and abnormal somite development (U-shaped somites). Some of these effects including abnormal somite development, delayed development, scoliosis and pericardial edema have also been observed in zebrafish embryos after nicotine treatment (Welsh et al., 2009).

Compound **2c** (containing an ortho-bromophenyl substituent) was found to be the next most active compound producing a variety of morphological effects including reduced heart rate, slowed circulation, pericardial edema and trunk curvature. Compound **2e** (containing a furan group) was also found to cause similar effects such as pericardial edema, reduced heart rate, slowed circulation and delayed development. The remaining azetidines **2b**, **2d** and **2f** were found to have little or no effect on zebrafish embryo development.

Mortality of zebrafish embryos after exposure to the six selected azetidines was also recorded over the 120 hour exposure period. Mortality was defined as coagulation of the zebrafish embryo, lack of somite development, non-detachment of the tail and after 48 hours lack of a heartbeat based on the OECD guidelines (OECD, 2013).

It was found that azetidine **2a** caused the highest mean cumulative percentage mortality in all of the different treatment regimens and this was found to be significantly different from the controls (0.1% DMSO and E3 embryo medium) (**Figure 4.17**, n=30 zebrafish embryos,

P<0.05). Mortality with azetidine **2a** was found to occur relatively early (100% mortality by 72 hpf) when the zebrafish embryos were treated at 25 µM. Azetidine **2c** was also found to cause a significantly high number of mortalities leading to 100% mortality at 120 hpf when zebrafish embryos were treated with a 30 µM concentration (n=30 zebrafish embryos, P<0.05). The mortality rates observed for the other tested azetidines were found to be comparable to the controls with little mortality observed (n=30 zebrafish embryos, P>0.05). Based on these results it was evident that azetidine **2a** caused the most number of mortalities followed by azetidine **2c**. The remaining azetidines were found to cause little or no mortality.

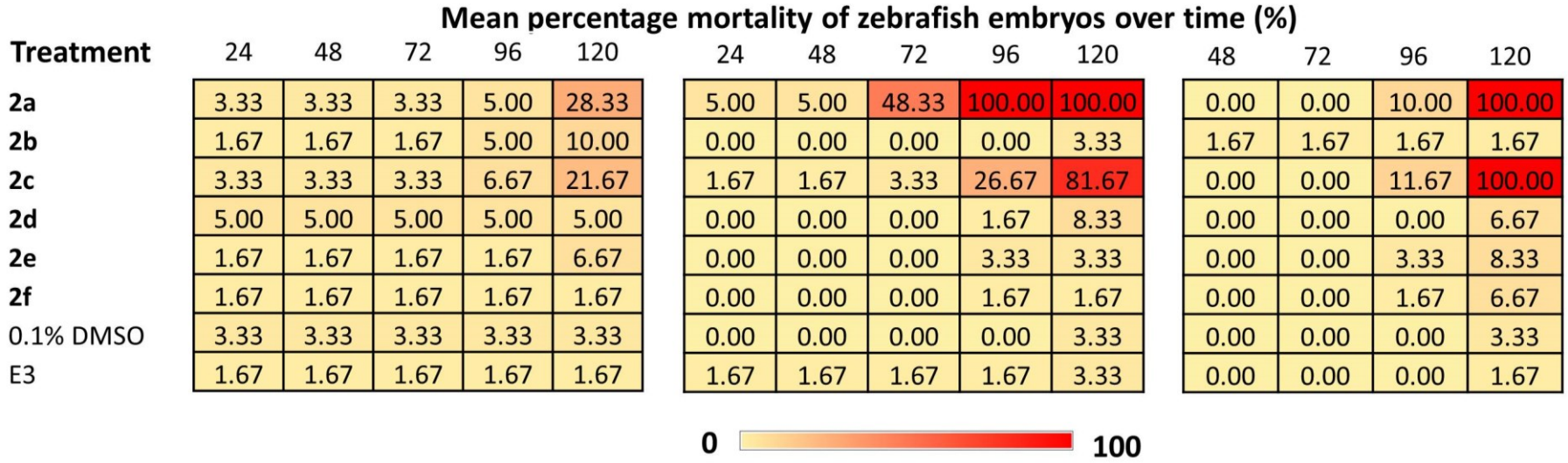

Figure 4.17 – Heat map showing the mean mortality rate of zebrafish embryos after treatment with the six selected azetidines over time. *Time is indicated on the top of each heat map in hours (24, 48, 72, 96 and 120). Left) Mean cumulative percentage mortality of zebrafish embryos treated at the 75% epiboly stage with azetidines at a concentration of 10 µM (n=30 zebrafish embryos per compound/control, SD range +/- 0-11.35%, P<0.05 for **2a** and **2c**, P>0.05 for rest), Middle) Mean cumulative percentage mortality of zebrafish embryos treated at the 75% epiboly stage with azetidines at a concentration of 25 µM (n=30 zebrafish embryos per compound/control, SD range +/- 0-10.41%, P<0.05 for **2a** and **2c**, P>0.05 for rest), Right) Mean cumulative percentage mortality of zebrafish embryos treated at the prim-5 stage with azetidines at a concentration of 30 µM (n=30 zebrafish embryos per compound/control, SD range +/- 0-10%, P<0.05 for **2a** and **2c**, P>0.05 for rest). Colour key: light yellow = 0%, red = 100%*

Using the biological data (mean percentage of zebrafish larvae at 5 dpf presenting with a particular morphological defect after treatment at 25 μM) and a few chemical descriptors, such as logP (lipophilicity of a compound), MW (molecular weight), HB (sum of hydrogen bond donors and acceptors), HBA (number of hydrogen bond acceptors) and HBD (number of hydrogen bond donors) a PCA model (R^2X=0.992, Q^2=0.619, two significant components) was created (**Figure 4.18**).

Using the PCA model the relationship between the physiochemical properties of the compounds and their biological activities could be investigated to a certain extent. From the PCA model it was observed that azetidine **2a** was separated from the rest of the group as it showed the most biological activity producing various morphological effects. Compared to the other azetidines azetidine **2a** also had the least number of hydrogen bond donors, as well as a relatively high logP with a low molecular weight, suggesting that it may have been able to penetrate into the zebrafish embryo better than the other compounds. The remaining azetidines were found to cluster relatively close together as they produced no or little morphological effects in comparison to azetidine **2a**.

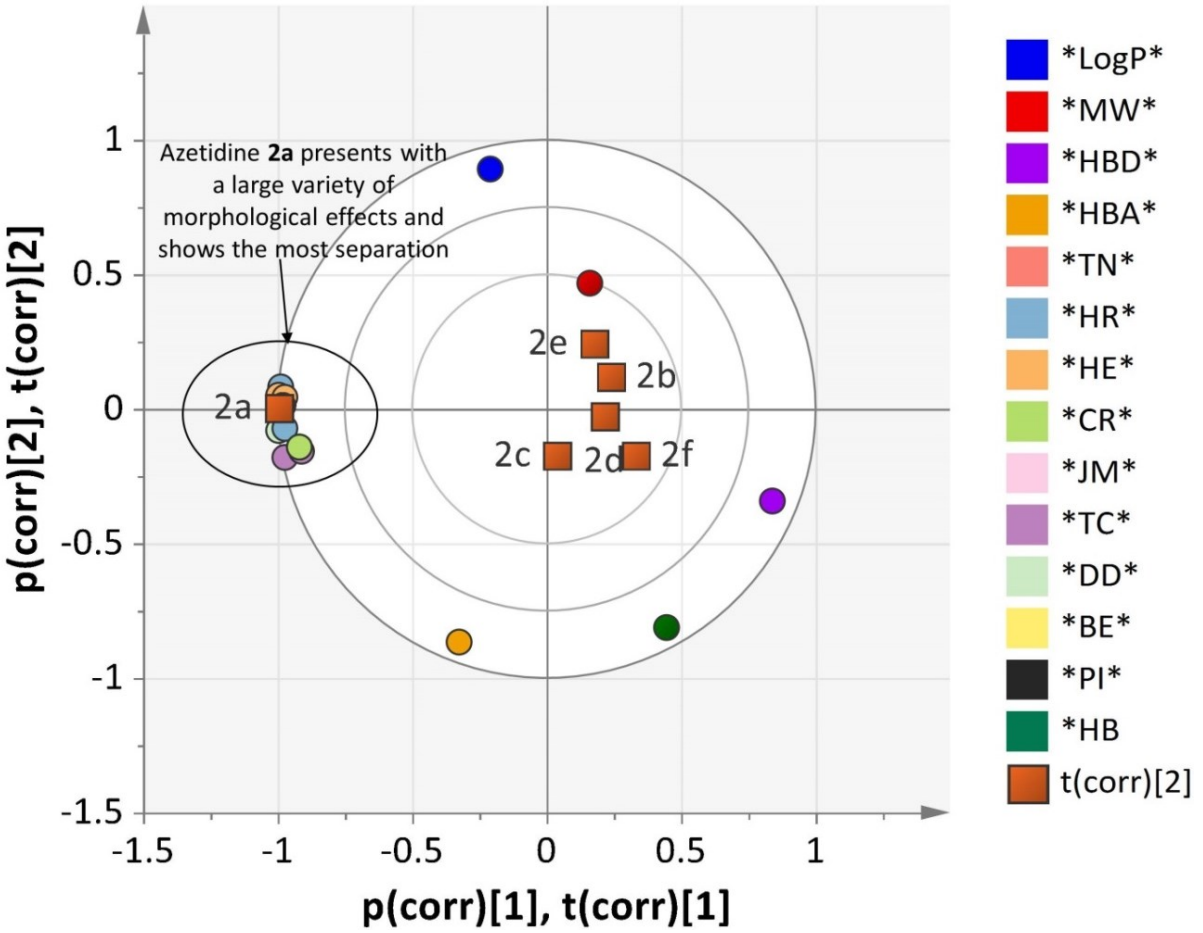

Figure 4.18 – A combined biplot two-component PCA model of zebrafish embryo biological responses (observations) against morphology features and physiochemical descriptors (variables) following treatment with a selection of azetidines over a 120 hour exposure period. *Biological features = TN (tail necrosis), HR (slowed heart rate), HE (heart edema), CR (reduced circulation), JM (jaw malformations), TC (tail curvature), DD (delayed development), BE (brain edema) and PI (hypopigmentation). Results presented after treatment at 25 µM. Chemical descriptors = logP (lipophilicity), MW (molecular weight), HB (sum of hydrogen bond donors and acceptors), HBA (number of hydrogen bond acceptors) and HBD (number of hydrogen bond donors). The loading vector (p) and the scores vector (t) are displayed correlation scaled as vector p(corr) and t (corr). The numbers beside p(corr) and t(corr) indicate the PCA component (1 or 2). All points are distributed within the correlation circle of radius and thus everything is contained within the model. The observations (scores) for tested azetidines are denoted by brown squares. The different coloured circles denote the location of the variables within the loading plot.*

4.4.5 Neurobehavioural effects of azetidines

As the biological activity of the tested azetidines had been evaluated by determining their effects on zebrafish embryo development the next step was to see how these compounds affected zebrafish behavioural responses as a second readout for biological activity. Due to the structural similarities of the tested azetidines to nicotine it was of interest to see whether they would potentially also induce neurobehavioural effects similar to those observed with nicotine (Petzold et al., 2009).

To investigate this, a locomotor activity assay was employed where the swimming behaviour of zebrafish larvae was investigated. In brief, zebrafish larvae at 6 dpf were acclimatized for 30 minutes in the recording plate consisting of 4 wells (Thermo Fisher Scientific, Germany) with each well containing 20 mL of E3 embryo medium and 10 larvae each. The medium in two of the wells was then replaced with a selected azetidine at a concentration of 20 µM, whereas the medium in the other two wells was replaced with control solution (1% DMSO). The locomotor activity was then assessed by inserting the recording plate into the FLIPR Tetra locomotion measurement system (Richter Gedeon Nyrt., Hungary). This locomotion measurement system was able to take pictures of every well every second whilst shining blue light repeatedly at 999 ms. The images taken were processed using custom-made software (KomiPL) provided by to Pictron Ltd. (Budapest, Hungary). The software automatically identified individual zebrafish larvae and then used changes in pixel intensity over the whole time frame as a measure of how much each zebrafish larva had moved during that time period with greater pixel changes indicating greater movement. For each azetidine the experiment was performed three times at a concentration of 20 µM.

The corrected pixel changes over the recording period were used as a readout to determine the extent of movement of the zebrafish larvae, as these values were corrected for the number of zebrafish larvae that had been correctly identified by the software (see **Figure 4.19**). It was found that azetidines **2a**, **2c** and **2e** all significantly decreased the locomotor activity of zebrafish larvae compared to controls (n=60 zebrafish larvae at 6 dpf per compound/control, $P<0.05$ for **2a**, **2c** and **2e**). This was also in line with what has been reported with high nicotine concentrations (Thomas et al., 2009a). Azetidines **2b**, **2d** and **2f** however were found to have no significant effect on larval zebrafish locomotor activity producing comparable results to the controls (n=60 zebrafish larvae at 6 dpf per compound/control, $P>0.05$ for **2b**, **2d** and **2f**).

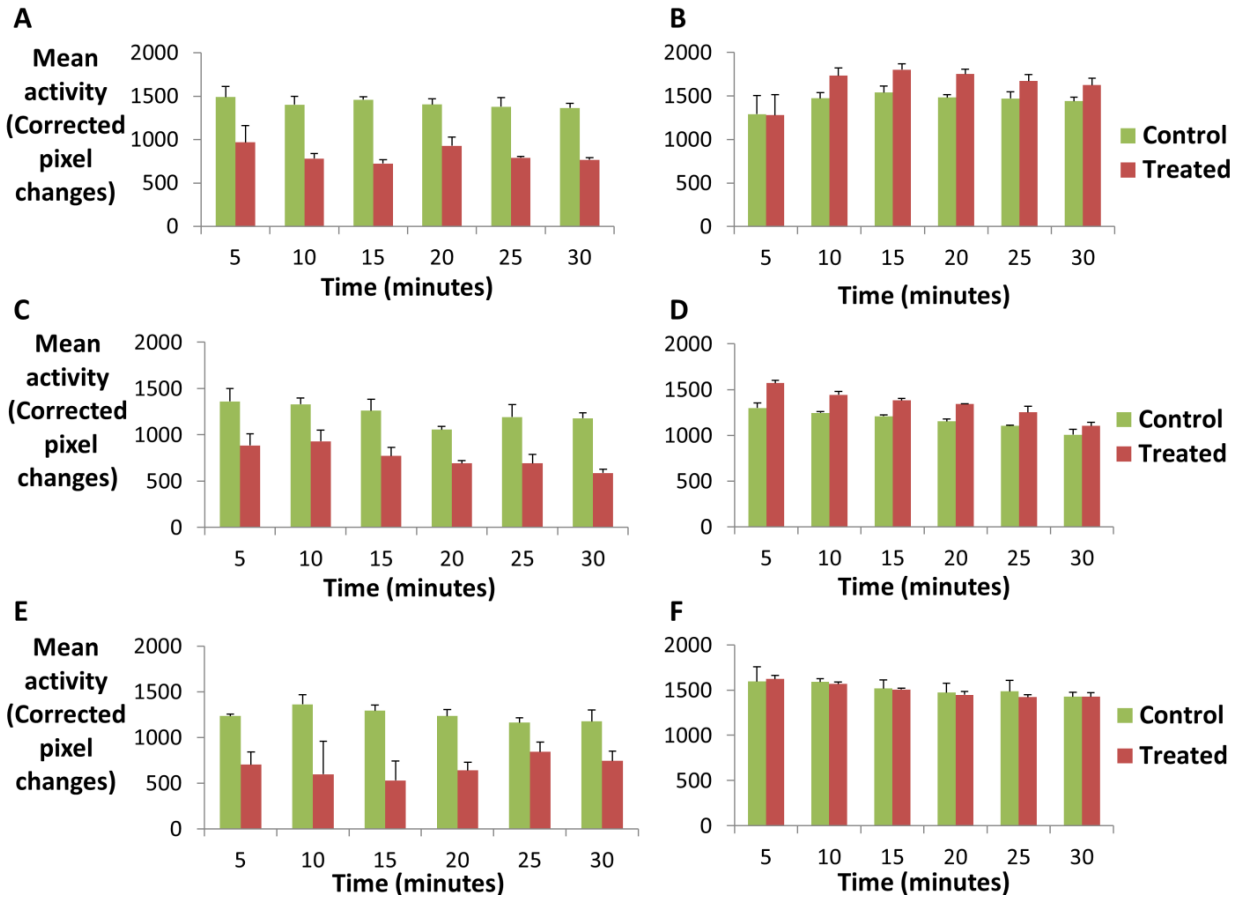

Figure 4.19 – Effects of six selected azetidines on 6 dpf zebrafish larval locomotor activity. *A)* ***2a*** *and 1% DMSO control (P<0.05), B)* ***2b*** *and 1% DMSO control (P>0.05), C)* ***2c*** *and 1% DMSO control (P<0.05), D)* ***2d*** *and 1% DMSO control (P>0.05), E)* ***2e*** *and 1% DMSO control (P<0.05), F)* ***2f*** *and 1% DMSO control (P>0.05). Corrected pixel changes represent mean locomotor activity of azetidine-treated (20 µM) and untreated 6 dpf zebrafish larvae over a 30 minute recording period with averages for each five minute segment shown (n=60 zebrafish larvae at 6 dpf per azetidine/control).*

4.4.6 Specific characterization of azetidine 2a

As azetidine **2a** was found to cause various biological effects in the initial studies it was investigated further. Treatment of zebrafish embryos with azetidine **2a** as mentioned previously produced a variety of morphological effects including reduced blood circulation, hypopigmentation, tail curvature, brain edema/hydrocephalus, cardiac edema, enlarged yolk sac and abnormal somite development (see **Figure 4.20**).

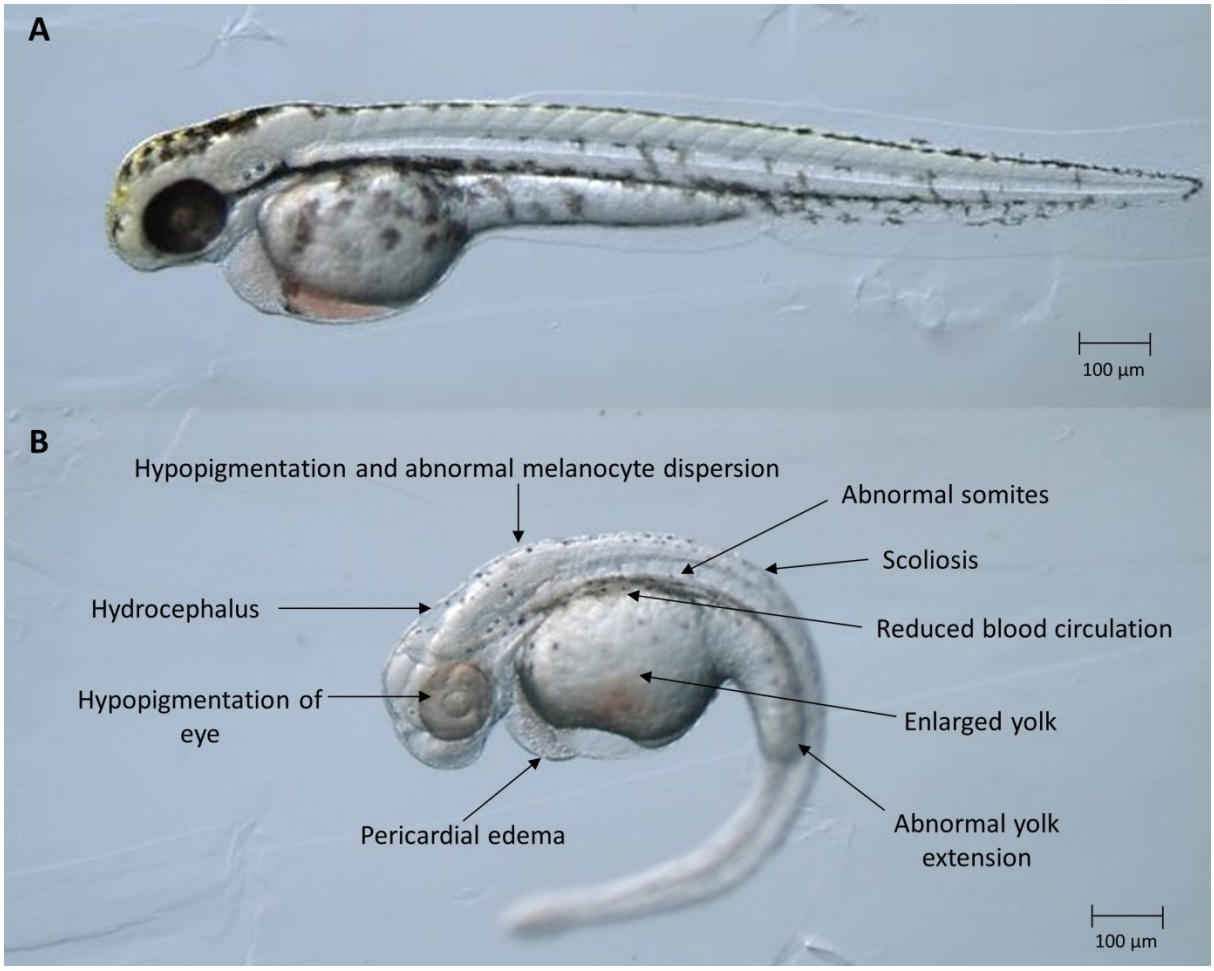

Figure 4.20 – Morphological effects observed after treatment of zebrafish embryos with azetidine 2a. *A) Brightfield image (lateral view) of a control (untreated) zebrafish embryo at 2 dpf, B) Brightfield image (lateral view) of a 25 µM **2a**-treated zebrafish embryo at 2 dpf.*

Reduced blood circulation was the main effect observed after azetidine **2a** treatment contributing to the development of a wide variety of secondary phenotypes including blood clotting. Using a transgenic zebrafish line *Tg(fli-1:EGFP)* the vasculature was studied in further detail to identify any blood vessel damage in azetidine **2a**-treated zebrafish embryos (**Figure 4.21**). It was found that after treatment of 75% epiboly stage zebrafish embryos for 36 hours with 50 µM azetidine **2a** the vasculature in the tips of the tails was not fully formed with tail necrosis evident (**Figure 4.21A**,**B**,**C**,**D**). This was significantly different to what was seen in controls (**Figure 4.21E**, n=40 zebrafish embryos at 36 hpf per drug/control, $P<0.05$).

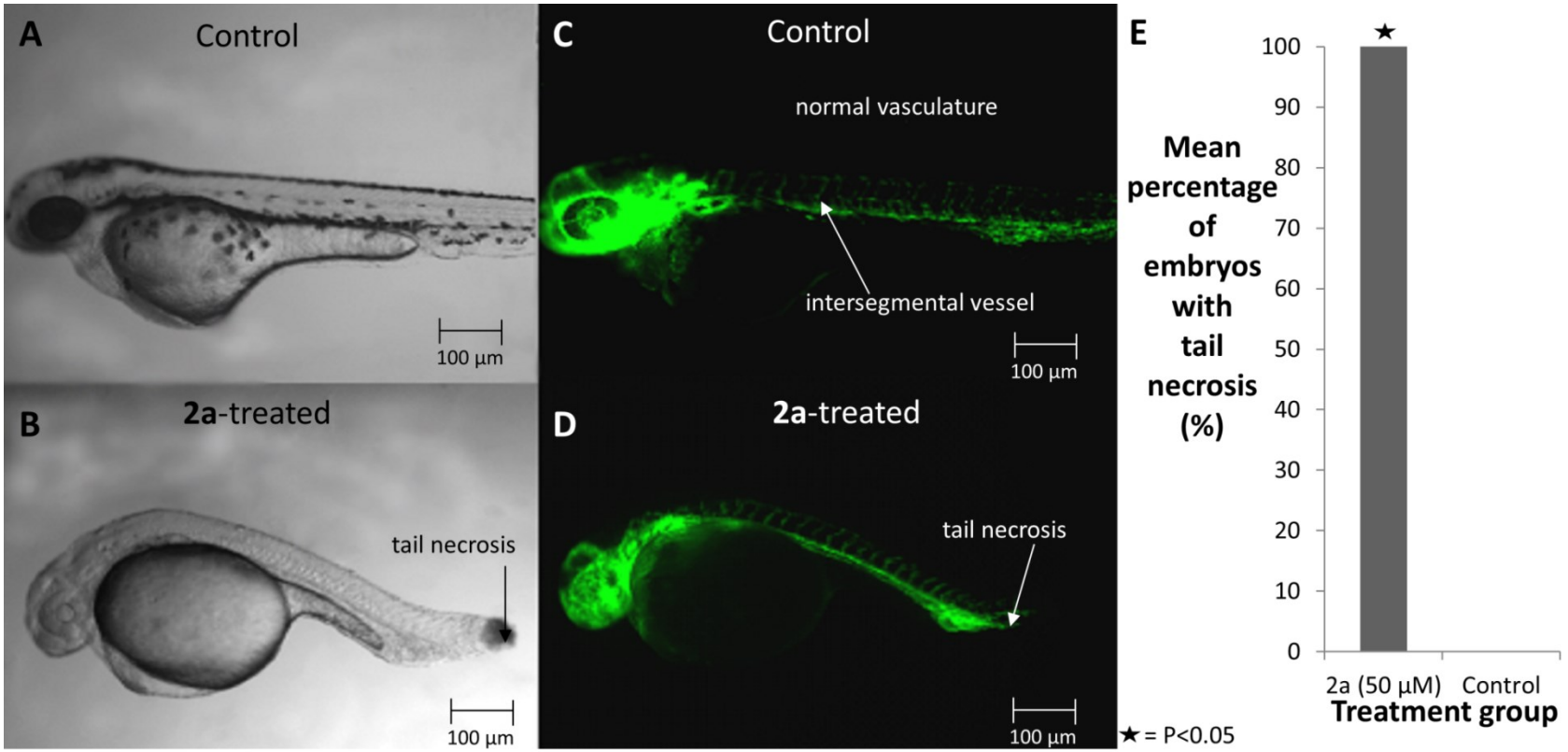

Figure 4.21 – Specific characterization of azetidine 2a vasculature effects using the Tg(fli-1:EGFP) transgenic zebrafish line. *A) Brightfield image (lateral view) of a control (untreated) zebrafish embryo at 36 hpf, B) Brightfield image (lateral view) of a 50 µM* ***2a****-treated zebrafish embryo at 36 hpf, C) Fluorescence GFP image (lateral view) displaying the vasculature of a control (untreated) zebrafish embryo at 36 hpf, D) Fluorescence GFP image (lateral view) displaying the vasculature of a 50 µM* ***2a****-treated zebrafish embryo at 36 hpf, E) Mean percentage of zebrafish embryos displaying tail necrosis at 36 hpf after treatment with 50 µM of azetidine* ***2a*** *compared to untreated controls (n=40 zebrafish embryos at 36 hpf per drug/control, P<0.05).*

Using a double transgenic line Tg*(fli-1:EGFP)(gata-1:DsRed)*, red blood cells were then assessed for clotting and perturbed circulation. It was found that after initial treatment of zebrafish embryos from this transgenic line at the 75% epiboly stage with 50 µM azetidine **2a** until 36 hpf the blood circulation was severely reduced compared to controls with blood clots evident in the tail (**Figure 4.22A**,**B**,**C**,**D**). The occurrence of blood clots was also found to be significant compared to the untreated controls (**Figure 4.22E**, n=40 zebrafish embryos at 36 hpf per drug/control, $P<0.05$).

A brain hemorrhage phenotype was observed in 10% of zebrafish embryos at 2 dpf after treatment with 25 µM azetidine **2a** at the 75% epiboly stage. This phenotype was particularly interesting, as it was specific to azetidine **2a**. By performing ORO staining to stain lipids it was found that the hemorrhage was specifically confined to the brain ventricle, causing ventricular brain hemorrhage (VBH) (**Figure 4.23**). Out of the 40 zebrafish embryos treated with azetidine **2a** only four showed this phenotype with none of the controls displaying such a phenotype (n=40 zebrafish embryos at 2 dpf per drug/control, $P<0.05$).

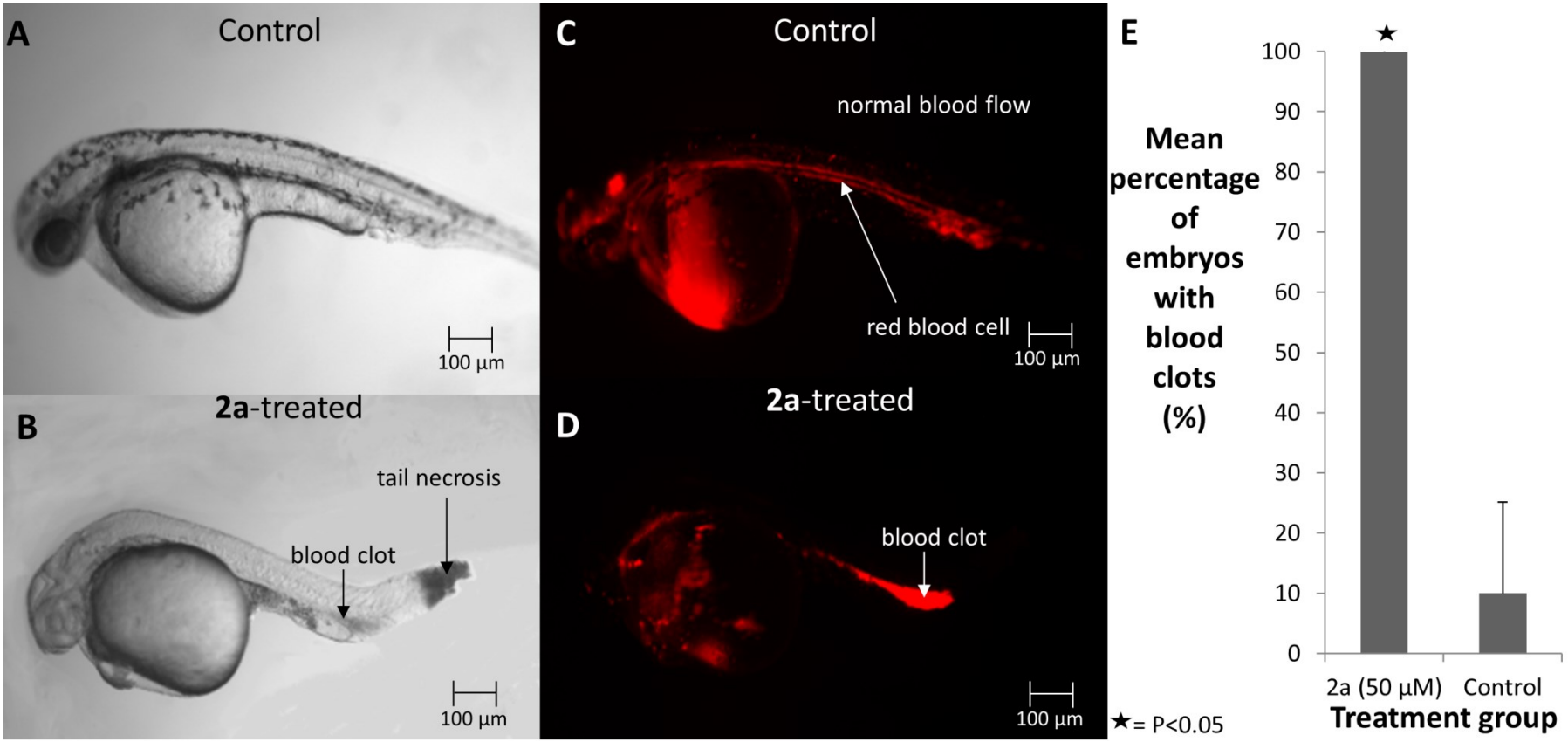

Figure 4.22 – Specific characterization of azetidine 2a blood circulation effects using the* Tg*(fli-1:EGFP)(gata-1:DsRed) transgenic zebrafish line*. A) Brightfield image (lateral view) of a control (untreated) zebrafish embryo at 36 hpf, B) Brightfield image (lateral view) of a 50 µM **2a**-treated zebrafish embryo at 36 hpf, C) Fluorescence DsRed image (lateral view) displaying the red blood cells of a control (untreated) zebrafish embryo at 36 hpf, D) Fluorescence DsRED image (lateral view) displaying the red blood cells of a 50 µM **2a**-treated zebrafish embryo at 36 hpf, E) Mean percentage of zebrafish embryos presenting with blood clots at 36 hpf after treatment with 50 µM azetidine **2a** compared to untreated controls (n=40 zebrafish embryos at 36 hpf per drug/control, P<0.05).*

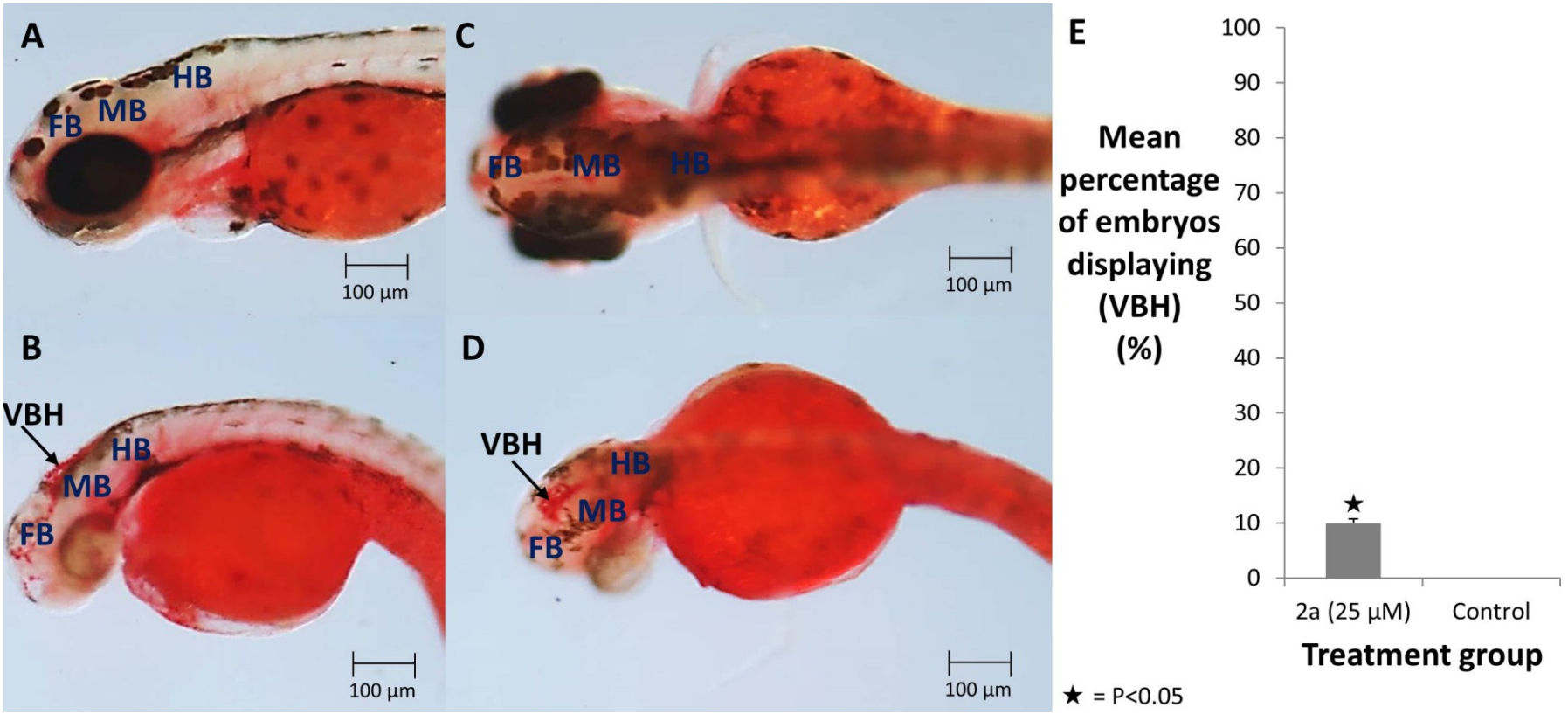

Figure 4.23 – Ventricular brain hemorrhage (VBH) phenotype observed with azetidine 2a. *Oil Red O staining images of: A) Untreated 2 dpf control zebrafish embryo (lateral view), B) Azetidine **2a**-treated zebrafish embryo at 2 dpf (lateral view), C) Untreated 2 dpf control zebrafish embryo (dorsal view), D) Azetidine **2a**-treated zebrafish embryo at 2 dpf (dorsal view), E) Mean percentage of embryos presenting with ventricular brain hemorrhage (n=40 zebrafish embryos at 2 dpf, P<0.05). Key: VBH = ventricular brain hemorrhage, FB = forebrain, MB = midbrain, HB = hindbrain*

4.5 Discussion

4.5.1 Toxicity and morphological effects of Y-lactams on zebrafish embryos

A diverse set of Y-lactams were evaluated for biological activity in the zebrafish embryo using a two phase approach. The results from phase 1 (dose-range finding) showed that compound **3c** was the most toxic and compound **3h** was the least toxic of the nine Y-lactams tested. Toxicity observed with Y-lactam **3c** was most probably due to its methoxy groups, which have been extensively documented in the literature to cause high toxicity due to radical formation (Smith et al., 2002).

All nine compounds were found to produce morphological effects with effects most pronounced for **3a**, **3f**, **3g** and **3h**. Treatment of zebrafish embryos with all nine compounds was also repeated using dechorionated embryos (data not shown) where the observations were found to be the same, suggesting that the chorion was not acting as a barrier to drug uptake.

4.5.2 Possible mechanisms for hemorrhage formation with Y-lactam 3a

The Y-lactam **3a** was chosen for further investigation following the initial toxicity studies, as it caused hemorrhage formation in the brain ventricle from 3 dpf onwards, which was not evident in controls (**Figure 4.24A**,**B**). Hemorrhage formation was also found to occur with compound **3g**, but at a lower frequency and with less specificity compared to compound **3a**, so it was not considered for further investigation (**Figure 4.24C**).

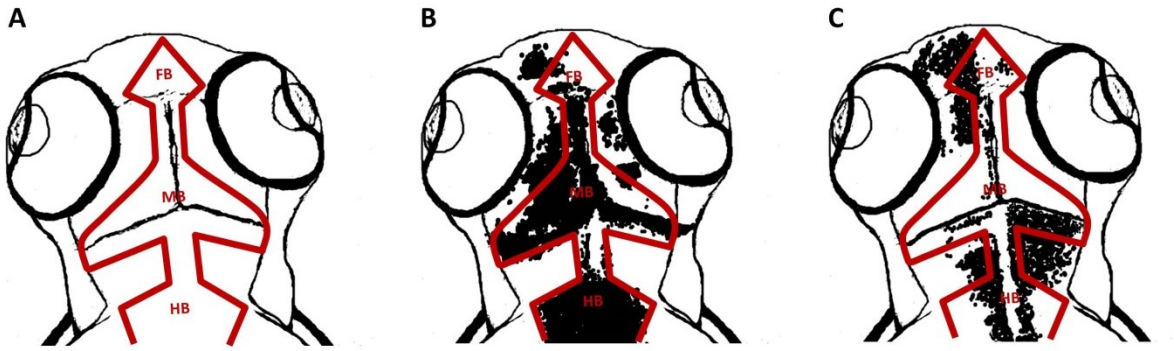

Figure 4.24 – Depiction of hemorrhage localization in the brain ventricles of 3 dpf zebrafish larvae. *Annotated drawings of 4 dpf zebrafish larvae brain ventricles: A) Untreated control, B) 100 µM compound **3a**-treated, C) 100 µM compound **3g**-treated. Key: FB = forebrain, MB = midbrain, HB = hindbrain*

The development of ventricular brain hemorrhage and hydrocephalus after exposure to Y-lactam **3a** was possibly caused by knockdown of the *βPix* gene. The *βPix* gene is highly expressed in the neuroepithelial lining of the brain ventricle in zebrafish embryos and has two splice variants *βPixA* and *βPixB* (Liu et al., 2007). Knockdown of both splice variants results in hydrocephalus and hemorrhage, whereas knockdown of splice variant B only leads to hemorrhage formation and knockdown of splice variant A only leads to hydrocephalus formation (Liu et al., 2007). As both hydrocephalus and hemorrhage formation was apparent after Y-lactam **3a** treatment it is possible that this compound affects both splice variants of the *βPix* gene. Additionally, zebrafish mutants with a *βPix* gene knockdown have a less complex vascular pattern in the brain compared to their wild-type siblings (Liu et al., 2007), a feature also observed with Y-lactam **3a**. These similarities in features suggest that disruption of the βPix-Pak pathway most likely is responsible for the development of ventricular brain hemorrhage observed with Y-lactam **3a**. However, synergistic effects with other genes (*pak2a*, *ccm1* and *rap1)* cannot be ruled out, as all of these produce a hemorrhage phenotype in zebrafish (Gore et al., 2008). Hence, analysis on a genetic level would be the

next step to identify which genes have an altered expression pattern in zebrafish embryos presenting with brain hemorrhage after treatment with Y-lactam **3a** and whether knockdown of the *βPix* gene is the main cause.

In terms of clinical relevance, in human pre-term and low birth weight babies intraventricular hemorrhage (IVH) and hydrocephalus can lead to morbidity (cognitive impairment) and mortality (Kazan et al., 2005). The specific intraventricular hemorrhage/hydrocephalus induced by compound **3a** could be utilized as a drug-induced zebrafish disease model for intraventricular hemorrhage/hydrocephalus where drugs could be screened to identify those that can reverse this condition.

4.5.3 Liver toxicity with Y-lactams 3f and 3h

The Y-lactam **3f** was selected for further investigation due to the development of a specific liver necrosis and steatosis phenotype in the absence of any other morphological abnormalities. The liver necrosis observed with Y-lactam **3f** was most likely due to the action of the furan side group, which is known to induce liver toxicity and carcinogenicity (Cordelli et al., 2010). For example, female mice fed furans develop elevated liver enzyme levels and liver necrosis (Fransson-Steen et al., 1997). It has been recently found that the highly reactive oxidation product of furans *cis-2-butene-1,4-dial* (BDA) is produced predominantly by CYP2E1 oxidation in human microsomes (Gates et al., 2012). This metabolite has been shown to be conjugated to glutathione in rat hepatocytes to form 2-(S-glutathionyl)succinaldehyde which can then form pyrrole cross-links with lysine, glutamine, ornithine, putrescine and spermidine (Peterson et al., 2011). These polyamines are thought

to be the main culprits of furan toxicity as they will bind to negatively charged molecules like DNA, RNA or proteins to form adducts (Minois et al., 2011). Hence, protein adduct formation with liver proteins could explain the liver necrosis observed after treatment with Y-lactam **3f**. Steatosis which was also observed could be explained by impaired synthesis and elimination of triglycerides by the liver.

With compound **3h** the liver necrosis phenotype was only found to develop late during zebrafish development and at relatively high tested concentrations 2000 and 1000 µM suggesting that compound **3h** was not able to penetrate very well into the zebrafish embryo, most probably due to its very low logP value.

At 2000 µM liver necrosis was accompanied by delayed development, trunk curvature, lipid droplet formation, severe pericardial edema, reduced heart rate and reduced circulation. Additionally, the hatching gland was still present at 5 dpf and the liver was found to be enlarged compared to controls. At 1000 µM the zebrafish was morphologically normal with partial liver necrosis. However, in both cases liver necrosis was accompanied by steatosis and inflammatory infiltration.

Compound **3h** has a nitroxy group which is known to be liver toxic and possibly carcinogenic in humans (Rickert et al., 1983). For example, male Sprague-Dawley CD rats treated with nitrobenzene develop enlarged hepatocytes with big nucleoli and inflammation (Tyl et al., 1987). This phenotype seems to show similarities to the phenotype observed with Y-lactam **3h**. Liver toxicity of nitrobenzene is attributed to its metabolism. Nitrobenzene metabolism

can produce a large variety of metabolites, including phenolic metabolites by CYP1A2 oxidation, e.g. p-aminophenol, p-nitrophenol, m-nitrophenol and p-hydroxyacetanilide (Rickert et al., 1983). These metabolites mainly undergo sulphation before they are excreted from the body (Rickert et al., 1983). Nitrobenzene can also form free radicals (Rickert et al., 1983). The nitroanion is the first free radical formed, which can react with oxygen to form the superoxide radical (Jw, 1999). These superoxide radicals can in turn interact with nitric oxide to form peroxynitrite as well as hydrogen peroxide (Knight et al., 2003). Peroxynitrite and hydrogen peroxide can cause lipid peroxidation by reacting with unsaturated lipids to form lipid radicals and also lipid peroxyl radicals (Knight et al., 2003). This ultimately can lead to necrosis of liver cells, as well as other cell types (Knight et al., 2003). The formation of lipid droplets could be attributed to the disruption of regulatory networks involved in regulating intracellular lipid storage and also possibly due to decreased fatty acid metabolism (Zitting et al., 1982).

Another effect documented with compound **3h** was the presence of an inflammatory infiltrate in and around the liver. In humans it has been shown that toxic hepatitis can occur following nitrobenzene exposure (Kaplowitz, 2004). This is likely due to one of the nitrobenzene metabolites forming adducts with cellular proteins (Kaplowitz, 2004). In turn, these macromolecules could act as haptens resulting in an autoimmune reaction (Kaplowitz, 2004). Thus, the above described mechanisms are likely to be responsible for the liver toxicity observed with compound **3h**, because zebrafish have the capacity to metabolize aromatic amines through a CYP1A family orthologue, therefore being able to potentially

form the same metabolites found in rodents and humans after nitrobenzene exposure (Scornaienchi et al., 2010).

4.5.4 Toxicity and morphological effects of azetidines on zebrafish embryos

A small selection of structurally diverse azetidines was assessed for biological activity using the zebrafish embryo as a model. The azetidine **2a** which possesses a piperidine (secondary amine) fragment was found to be the most biologically active, producing a vast array of phenotypes including hypopigmentation, delayed development, reduced blood circulation, scoliosis and U-shaped somites. It was also found to be the most toxic. Azetidine **2a** is structurally similar to azetidine **2b**. Azetidine **2b** however was found to be relatively non-toxic in the zebrafish embryo assays suggesting that the piperidine fragment of **2a** was important in conferring toxicity. Additionally, azetidines **2c** and **2e** which are structurally similar to one another were both found to induce similar biological responses, although azetidine **2c** was found to be the more active. Azetidines **2d** and **2f** also structurally similar to one another produced little biological effects. These results showed that slight differences in chemical structure greatly influenced the biological activity of these compounds.

By using multivariate analysis it was found that the biologically active azetidine **2a** had a very high logP value with reduced hydrogen bond donor sites, thus making it very cell permeable. This may have contributed to its potency and high toxicity. Azetidine **2c** on the other hand was found to have a very low logP value and this might explain why it was only found to have an effect on zebrafish embryos late during development, as it may have not penetrated into zebrafish embryos at earlier stages. The remaining azetidines (**2b**, **2d**, **2e** and **2f**) were

found to have lower toxicity and produced fewer morphological effects despite having comparable logP values to azetidine **2a**. Thus, logP may have not been the only factor contributing to biological activity. For azetidine **2a** it is possible that release of the piperidine fragment by metabolism may have been responsible for its effects as well as conversion into an ionised form.

4.5.5 Azetidine locomotor effects and similarities to nicotine

The six selected azetidines were also investigated for their effects on the nervous system by performing locomotor activity assays. Reduced locomotor activity was observed after treatment of 6 dpf zebrafish larvae with azetidines **2a**, **2c** and **2e**. This reduction in locomotor activity was found to be similar to that observed with high nicotine concentrations in zebrafish (Thomas et al., 2009a).

Nicotine at low concentrations acts as a stimulant causing an increase in locomotor activity as binding of nicotine to nACh receptors stimulates the release of acetylcholine, whereas at high concentrations nicotine acts as a depressant by reducing this activity leading to desensitization of nACh receptors so that they are no longer responsive (Petzold et al., 2009)(Silvette et al., 1962). It has been demonstrated that zebrafish larvae (above 4 dpf) can be sensitized to nicotine, as re-exposure to nicotine following prior exposure increases the locomotor activity much more than that of zebrafish larvae exposed to nicotine for the first time (Petzold et al., 2009). This effect on locomotor activity is also seen in rats exposed to nicotine (Cohen et al., 1991). Additionally, over-excitation of muscle cells and mechanical

forces also contribute to reduced locomotor activity, effects which are commonly observed with acetylcholinesterase inhibitors (Behra et al., 2002).

4.5.6 Similarities between azetidine and nicotine phenotypes

Nicotine represents the structurally most similar compound to the tested azetidines. Nicotine is a naturally occurring alkaloid and in its pure form is extremely toxic to humans and mammals (mouse oral LD50 = 24 mg/kg) (Ujváry, 1999)(Yamamoto and Casida, 1999). Nicotine has been previously tested in zebrafish embryos and has been documented to be a potent teratogen inducing a number of morphological effects (Welsh et al., 2009). These include reduced notochord length, jaw malformations, reduced somite number, apoptotic death of brain cells and muscle paralysis (Parker and Connaughton, 2007)(Klee et al., 2011)(Thomas et al., 2009b). The morphological effects observed with a few of the tested azetidines were found to resemble those reported with nicotine. For example, treatment of zebrafish embryos with azetidines **2a**, **2c** and **2e** led to the development of curved tails, reduced heart rate, slowed circulation and cardiac edema.

4.5.7 Similarities between azetidine 2a and nicotine phenotypes

Azetidine **2a** was found to show the greatest resemblance to nicotine in terms of its chemical structure and the morphological effects it produced in zebrafish embryos. Nicotine like azetidine **2a** has no hydrogen bond donors but two hydrogen bond acceptors, which may be an important factor in azetidine **2a** toxicity. In regards to lipophilicity, azetidine **2a** however has a higher logP value than nicotine (DrugBank, 2013c). Despite nicotine having a

low logP value it has been shown to be readily absorbed at neutral pH when it is in its unionized state (Hukkanen et al., 2005).

The morphological effects observed with azetidine **2a** which were found to be similar to nicotine included the formation of U-shaped somites, muscular bends, reduced notochord length and jaw malformations (summarised in **Table 4.7**) (Parker and Connaughton, 2007). U-shaped somites are a characteristic feature of nicotine toxicity in zebrafish embryos. This phenotype occurs due to disruption of the hedgehog signalling pathway which is important for ensuring the correct development of slow muscles (Woods and Talbot, 2005). The associated muscular bends develop early in zebrafish embryos due to incorrect growth of motor neurons leading to disorganization of the slow muscle fibres (Welsh et al., 2009). As zebrafish embryos treated with azetidine **2a** were unable to hatch out of their chorions, the weakened muscular development can be partially attributed to this. However, inhibition of the chorionase enzyme or osmotic disturbances may have also contributed to the development of this particular phenotype, hence further investigation would be required to identify the exact cause (He et al., 2012). The slow movement of muscles could also be related to over-excitation of muscles (Parker and Connaughton, 2007).

Table 4.7 - Comparison of the effects observed after nicotine and azetidine 2a treatment of zebrafish embryos.

Source: Data on nicotine treatments in zebrafish embryos obtained from (Klee et al., 2011) and (Welsh et al., 2009).

Morphology features	**Nicotine**	**Azetidine 2a**
Delayed development	√	√
Jaw malformations	√	√
Curved tail	√	√
U-shaped somites	√	√
Bradycardia	√	√
Reduced circulation	√	√
Pericardial edema	√	√
Reduced locomotion	√	√
Short stature	√	√
Hypopigmentation	X	√
Brain hemorrhage	X	√

Azetidine **2a** was found to lead to the development of hydrocephalus and also ventricular brain hemorrhage, an effect which has not been documented with nicotine. It is likely that this phenotype developed due to vascular stability in the brain being compromised through vessel or membrane rupture. It has been documented that effects on the βPix Pak2a signalling pathway in zebrafish embryos can result in the formation of ventricular brain hemorrhage (Liu et al., 2007).

An additional effect observed with azetidine **2a** and not with nicotine included hypopigmentation. The hypopigmentation phenotype observed with azetidine **2a** was found to be similar to that observed with anti-thyroid agents such as thiamazole (Elsalini and Rohr, 2003), which indicate that azetidine **2a** possibly affects thyroid signalling. It has been reported that pigmentation effects in zebrafish embryos may be linked to reduced levels of cyclic adenosine monophosphate (cAMP) and disruptions to the function of microtubules, which are both important in ensuring the dispersion and aggregation of the pigment melanin

(Logan et al., 2006). At later stages of zebrafish embryonic development disturbances to the function of xanthophores can also contribute to the development of a hypopigmentation phenotype (Odenthal et al., 1996). Recently, it was discovered that the zebrafish melanosomes (organelles involved in melanin production) are sensitive to light and at 3 dpf start to aggregate via stimulation from the eyes (Nguyen et al., 2013). This optical stimulation may have been perturbed in azetidine **2a**-treated zebrafish embryos and therefore contributed to abnormal dispersion of melanin.

Many of the features observed with azetidine **2a** such as hypopigmentation, delayed development, craniofacial abnormalities and pericardial edema are also observed after treatment of zebrafish embryos with piperidines, e.g. 2-methylpiperidine (Schulte and Nagel, n.d.). Therefore, it seems more likely that the piperidine fragment is responsible for the morphological effects observed with azetidine **2a**. Additionally, ionisation of azetidine **2a** may also contribute to its toxicity.

4.5.8 Similarities in responses between Y-lactams and azetidines

When comparing the biological responses observed with the Y-lactams to those observed with the azetidines it was interesting to note that the azetidine **2a** and the Y-lactam **3a** produced similar phenotypes. These included hydrocephalus, brain hemorrhage and a cardiac phenotype (AV block). The main difference between them was that azetidine **2a** also caused hypopigmentation, which was not seen with **3a**. However, the brain hemorrhage phenotype observed was found to be very similar between both **2a** and **3a**, suggesting that azetidine **2a** also affects brain vasculature stability in the same way as Y-lactam **3a**, so it

would be interesting to carry out further work on both compounds to see whether they indeed have a similar mode of action. Both of these compounds were also found to have low molecular weights compared to the other compounds in their respective groups as well as logP values above 2 which may have contributed to their high potency.

Two other compounds with structural similarities are the azetidine **2c** and the Y-lactam **3i**, which both contain bromine in their chemical structures. Both compounds were found to be biologically active and produced similar morphological effects such as trunk curvature, pericardial edema, yolk edema, slowed circulation and a reduced heart rate. Such effects have also been reported in zebrafish embryos treated with brominated phenols and indoles (Kammann et al., 2006). The toxicity of these brominated compounds in zebrafish embryos is likely to be attributed to the metabolism of the bromobenzene constituent. In humans bromobenzene is metabolized by CYP2B to a reactive bromobenzene 3,4-epoxide but also forms a stable 2,3-epoxide (Ioannides, 1996)(Lau and Zannoni, 1981). The reactive 3,4-epoxide can bind to protein thiol groups resulting in protein adducts and the 2,3-epoxide can form covalent bonds with haemoglobin (Koen et al., 2000)(Lau and Zannoni, 1981).

The azetidine **2e** and the Y-lactam **3f** were also found to be structurally similar with both compounds containing a furan group. Additionally, morphological effects including pericardial edema, slowed circulation and reduced heart rate were observed with both of these compounds. However, liver necrosis that was observed with the Y-lactam **3f** was not observed with azetidine **2e**, which could be due to the structural differences between them or the concentrations tested for azetidine **2e** being too low to induce a similar effect.

4.5.9 Limitations of current study and future work

In the current study, azetidines were tested using three treatment regimens at three different concentrations and one azetidine was selected for further investigation. If more time had been available, the mortality and morphology studies could have been improved by testing a wider range of concentrations, so as to make sure that all six azetidines were tested at a concentration at which they would be active. As more time was available when investigating the Y-lactams, a two phase study was performed where initially a dose-range finding and then a morphology study was performed. This approach would have also been useful when testing the azetidines. Additionally, for the azetidines it would be useful in the future to perform assays specifically targeting the mode of action which nicotine employs. This could be done by performing receptor binding studies for example.

For azetidine **2a** and the Y-lactam **3a** cellular or molecular studies should be performed in the future in order to understand their exact modes of action and to determine the exact causes behind the hydrocephalus/brain hemorrhage phenotypes. Similarly, identifying the exact causes behind liver necrosis observed with Y-lactams **3f** and **3h** would also be particularly useful. Performing bioanalysis or metabolomic studies may be one way this could be done, as information on the metabolites formed could help to identify the metabolic pathways leading to toxicity.

Further characterisation of these compounds in terms of their physiochemical properties would also be useful in order to link the observed biological effects to their chemical structures. Particularly, the acid dissociation constant (pKa) would be useful in

understanding the kinetics of the compounds and whether they are more cell permeable in an ionised or unionised state at physiological pH. Furthermore, the stability of the compounds would need to be investigated as well as exposure concentration profiles.

Another limitation of the studies performed in this chapter was that a limited amount of compound was available for testing. Also, the compounds that were tested were mixtures of isomers in the case of the Y-lactams and so it is not known whether all the isomers or one isomer of each compound represent the active component/s responsible for the observed effects. Therefore, currently all of the isomers of each of the Y-lactam compounds are being isolated and will be tested for biological activity in zebrafish embryos in the near future. It would be particularly interesting to find out the results for compound **3a** as it could be that only a single isomer of this compound can induce brain hemorrhage formation.

4.6 Conclusions

Despite the small range of compounds tested, a variety of biological effects were observed with slight changes in chemical structure having a profound impact on activity. Additionally, the morphology analysis performed enabled clustering of compounds providing a first indication as to which compounds share a similar mode of action. The studies performed also gave an indication of what structural properties may be desired when synthesising compounds in the future. The compounds tested in this chapter which were designed based on Lipinski's rule of five for drug-likeness evoked a large variety of biological effects and through further work particularly on compound **2a** and **3a** possible therapeutic benefits could be unveiled or disease models established. Additionally, the liver toxicity observed

with compound **3f** and compound **3h** showed that the zebrafish larva presents a good model for investigating hepatotoxicity, particularly drug-induced hepatitis for which no gold standard animal model exists at the moment.

Chapter Five: DEVELOPMENT OF A DRUG TOXICITY PREDICTION TOOL USING THE ZEBRAFISH EMBRYO

FOREWORD

The results presented in this chapter were obtained through collaboration with Professor Torbjörn Lundstedt, Associate Professor Katrin Lundstedt-Enkel and Professor Johan Trygg from AcurePharma AB, Uppsala University and AcureOmics AB, respectively who provided the data for the physiochemical descriptors. All biological work was carried out by me under the supervision of Professor Ferenc Müller. Training in multivariate analysis was provided by Associate Professor Katrin Lundstedt-Enkel. All subsequent multivariate analysis was performed by me. Associate Professor Katrin Lundstedt-Enkel, Professor Torbjörn Lundstedt and Professor Johan Trygg aided in the interpretation of multivariate models. Additional interpretation of results in terms of biological context was performed solely by me.

5.1 Introduction and Overview

5.1.1 Zebrafish embryo as a model for toxicological studies

The zebrafish embryo as mentioned in the previous chapters has numerous advantages over conventional mammalian animal models for drug testing and toxicology studies. The rapid development of zebrafish embryos and the large numbers that can be tested mean that many experiments can be performed in a short period of time (Langheinrich, 2003). Experiments that are performed with rodents on the other hand involve much smaller numbers and are also more time consuming with rodent development relatively slow in comparison (Langheinrich, 2003). However, rodents do have an advantage in that they are genetically more similar to humans than zebrafish embryos are. It is also possible to utilise the same dosage route intended for human use when performing tests in rodents, which can provide useful information on the ADME properties of a compound.

For drug screening purposes the zebrafish embryo has several advantageous features including the ability to absorb chemicals dermally or orally 3 dpf onwards, the ability to survive in minimal quantities of liquid and tolerance to DMSO concentrations of up to 1.5%, which is useful when using drugs not particularly soluble in water (Goldsmith, 2004). For rodents the quantities of chemicals required for dosing are much larger and exposure times are also longer (Hill et al., 2005). As zebrafish embryos are small in size, they can be tested in 96 well or even 384 well plates which are amenable to automation, thus automated high throughput assays can be performed by utilising zebrafish embryo sorting robots, liquid handling robots and automated imaging microscopes (d' Alençon et al., 2010).

Additionally, as the zebrafish embryo is optically transparent throughout development it is possible to study the effects of drugs on various morphology features including the heart using a simple stereomicroscope (Burns et al., 2005). Thus, scoring these features for severity after drug exposure can be used as endpoints in addition to classical toxicology endpoints such as LC50 (concentration that kills 50% of the population), EC50 (concentration that produces an effect in 50% of the population), NOEC (no observed effect concentration) and LOEC (lowest observed effect concentration) values (Hermsen et al., 2011)(Panzica-Kelly et al., 2010).

Currently, *in vivo* toxicology studies involve using rodents, which as mentioned previously is expensive, requires large amounts of compound and takes a relatively long time to perform. The zebrafish embryo could present a cheaper and quicker alternative. It has already been demonstrated that the zebrafish embryo shares many similarities with humans in terms of toxic responses and that it is possible to perform large scale toxicity screens (Padilla et al., 2012)(Weigt et al., 2011)(Goldsmith, 2004)(Hill et al., 2005)(Ali et al., 2011). Hence, the zebrafish embryo offers the opportunity to test compounds first cheaply and inexpensively in an *in vivo* setting, whilst at the same time achieving a similar throughput to *in vitro* assays.

5.1.2 Using biological data to create predictive models

As mentioned in **Chapter 1**, in drug development large compound libraries need to be screened to identify potential candidate drugs. These candidate drugs then undergo further testing in *in vitro* and *in vivo* models. However, in order to save resources and time, predictive models can be utilised either in the initial drug candidate selection process or

after candidate drugs have been selected. For example, predictive models can be created to predict the ADME properties of compounds, as well as their biological activity, potency, accumulation and toxicity (Hansch et al., 1995)(Yoshida and Topliss, 2000)(Nendza, 1998). This enables those compounds with unfavourable properties to be removed before further testing is done.

Predictive models are based on structure activity relationships (SARs), where the aim is to identify substituents in the chemical structure of a compound that could potentially cause toxicity or unfavourable ADME properties. These substituents are referred to as structural alerts and will be flagged up when a compound containing such a structural alert is introduced into the model. More recently, quantitative structure activity relationship (QSAR) models are being increasingly explored. QSAR models are used to relate the physiochemical properties of a compound to its biological activity (Lessigiarska et al., 2006) (Hansch et al., 1995). QSAR models not only provide information on toxicity but can also give some indication on the mechanism of toxicity of a compound (Lessigiarska et al., 2006). QSAR models generated today heavily rely on using multivariate analysis techniques such as principal component analysis (PCA), partial least squares (PLS) and orthogonal partial least squares (OPLS) (see **Chapter 1** for further details).

5.1.3 Problems encountered with predictive models and how these can be overcome

QSAR modelling is particularly useful for predicting toxicity and ADME of new drugs undergoing development. However, many QSAR models that are generated are based on experimental datasets obtained from different sources, where experiments are performed

under different conditions and with different drugs, therefore making them not directly comparable to one another (Sköld et al., 2006). This can therefore affect the quality of the models generated.

To overcome such problems a study was performed by Sköld and colleagues (Sköld et al., 2006). The aim of the study was to start the experimental characterisation of a reference 'benchmark' group of compounds that were drug-like, low-cost, commercially available, physiochemically diverse and amenable to analytical measurements (Sköld et al., 2006). In this study, firstly all the available information on 691 pharmaceuticals marketed in Sweden at the time was collated (Sköld et al., 2006). A filtering step was then introduced to remove those compounds which were not commercially available and had unusual administration routes leaving only 284 pharmaceuticals (Sköld et al., 2006). Multivariate analysis in the form of PCA was then performed on these 284 compounds using 28 chemical descriptors (Sköld et al., 2006). From this PCA model 24 drugs were selected which showed the greatest chemical and spatial diversity, i.e. drugs which were most distantly spaced from one another on the PCA scores plot. These 24 drugs designated reference drugs were then characterised and experimentally-derived values for lipophilicity, solubility and permeability were determined and combined with the existing physiochemical data (**Table 5.1**) (Sköld et al., 2006). By using this approach, a high quality benchmark dataset for a group of reference drugs that cover the whole chemical spectrum and which are readily available has been developed ready to be used by other groups for further characterisation.

Table 5.1 - Chemical descriptors with explanation of terms.
Source: Adapted from (Sköld et al., 2006)

Chemical descriptor	**Explanation**
MW	molecular weight
V	molecular volume
S	molecular surface area
O	ovality
E_{LUMO}	energy of lowest unoccupied molecular orbital
E_{HOMO}	energy of highest occupied molecular orbital
H	hardness
DM	dipole moment
NPSA	nonpolar surface area
PSA	polar surface area
PSA/NPSA	ratio of polar to non-polar surface area
logP	log *P* values taken from http://www.drugbank.ca/
logP_{Cr}	log *P* calculated according to the method developed by Ghose and Crippen
logP_{Mor}	log *P* calculated according to the method developed by Moriguchi et al.
logP_{ACD}	log *P* calculated with ACD/Labs
log$D_{ACD_6.5}$	log *D* at pH 6.5 calculated with ACD/Labs
log$D_{ACD_7.4}$	log *D* at pH 7.4 calculated with ACD/Labs
Q_H	highest partial charge on a hydrogen atom
HBD	number of hydrogen-bond donors
ΣQ_H (SQH)	sum of the partial charge of all hydrogen atoms attached to an O, N, or S atom,
$CWPSA_{HBD}$	sum of absolute charge-weighted surface area of all hydrogen atoms attached to an O, N, or S atom
Q_{MN}	absolute value of lowest partial charge of a non-hydrogen atom
HBA	number of hydrogen-bond acceptors
ΣQ_{MN} (SQMN)	sum of absolute partial charge of all negatively charged O, N, S, and F atoms
$CWPSA_{HBA}$	sum of absolute charge-weighted surface area of all negatively charged N, O, S, F, Cl, Br, and I atoms
HB	sum of HBD and HBA, PSA = molecular surface area of all N, O, S, and attached H atoms
PSA_{NO}	molecular surface area of all N, O, and attached H atoms
PSArel	PSA/S × 100, PSA/NPSA
PSA_{cw}	sum of (absolute) charge-weighted surface area of all N, O, halogen, and attached H atoms

5.2 Aims

The aim of this study was to use the reference drug set derived by Sköld and colleagues to determine the association between the physiochemical properties of these drugs and their biological effects in zebrafish embryos. In this study toxicity was used as a measure of biological effects. Therefore, various indicators of toxicity were determined such as LC50, EC50, LOEC and NOEC values, which could then be used as biological outputs. Additional biological outputs measured included morphological effects that developed during zebrafish embryo development, which were assigned severity scores.

The ideal situation would be that predictions for the biological effects of new compounds could be made based solely on chemical descriptors. However, in practice this would be difficult to do and may only be possible for specific groups of compounds. Therefore, using the biological outputs determined for the reference drug set the aim in this chapter was to create a QSAR model that could be used as a predictive tool in order to identify similarities between compounds and relate them to their physiochemical properties. This could support read-across in mammalian toxicology for compounds that share significant similarities in the zebrafish model. Hence, the overall objective was to create a QSAR model which had the potential to be implemented in pre-clinical testing regimes to predict the toxicity of compounds undergoing development.

5.3 Methods

In this chapter the reference drug set derived by Sköld and colleagues was biologically characterised in zebrafish embryos (Sköld et al., 2006). However, two of the 24 reference drugs namely carisoprodol and tinidazole were not tested due to problems in shipping and poor availability. Hence, six additional drugs were selected from the initial PCA model that had been developed by Sköld and colleagues to maintain the spatial and chemical diversity of the drug set tested (Sköld et al., 2006). In total 28 reference drugs with varied therapeutic indications (**Table 5.2**) and diverse chemical structures (**Figure 5.1**) were tested in this chapter and also in **Chapter 6**.

Table 5.2 - 28 reference drug set.
Reference drugs derived from the study performed by Sköld and colleagues. They are representative of marketed drugs in terms of their chemical structures and functions. Terfenadine is no longer marketed due to QT prolonging effects (Woosley RL et al., 1993).

Compound	Function	Compound	Function
flupenthixol dihydrochloride	*anti-psychotic*	**metoclopramide hydrochloride**	*anti-emetic*
fenofibrate	*anti- cholesterol*	**tetracycline**	*antibiotic*
sulindac	*anti-inflammatory*	**thiamazole**	*anti-thyroid*
glipizide	*anti-diabetic*	**erythromycin**	*antibiotic*
hydrochlorothiazide	*anti-hypertensive*	**carbamazepine**	*anti-epileptic*
amantadine hydrochloride	*anti-Parkinson's*	**folic acid**	*required in diet*
amiloride hydrochloride	*anti-hypertensive*	**levodopa**	*anti-Parkinson's*
bendroflumethiazide	*anti-hypertensive*	**terfenadine**	*anti-histamine*
d-penicillamine	*anti-rheumatic*	**metformin**	*anti-diabetic*
chlorprothixene hydrochloride	*anti-psychotic*	**enalapril**	*anti-hypertensive*
chlorzoxazone	*muscle relaxant*	**liothyronine**	*anti-thyroid*
levothyroxine	*anti-thyroid*	**tioguanine**	*anti-cancer*
meclizine dihydrochloride	*anti-emetic*	**malathion**	*OP insecticide*
prednisone	*immunosuppressant*	**captopril**	*anti-hypertensive*

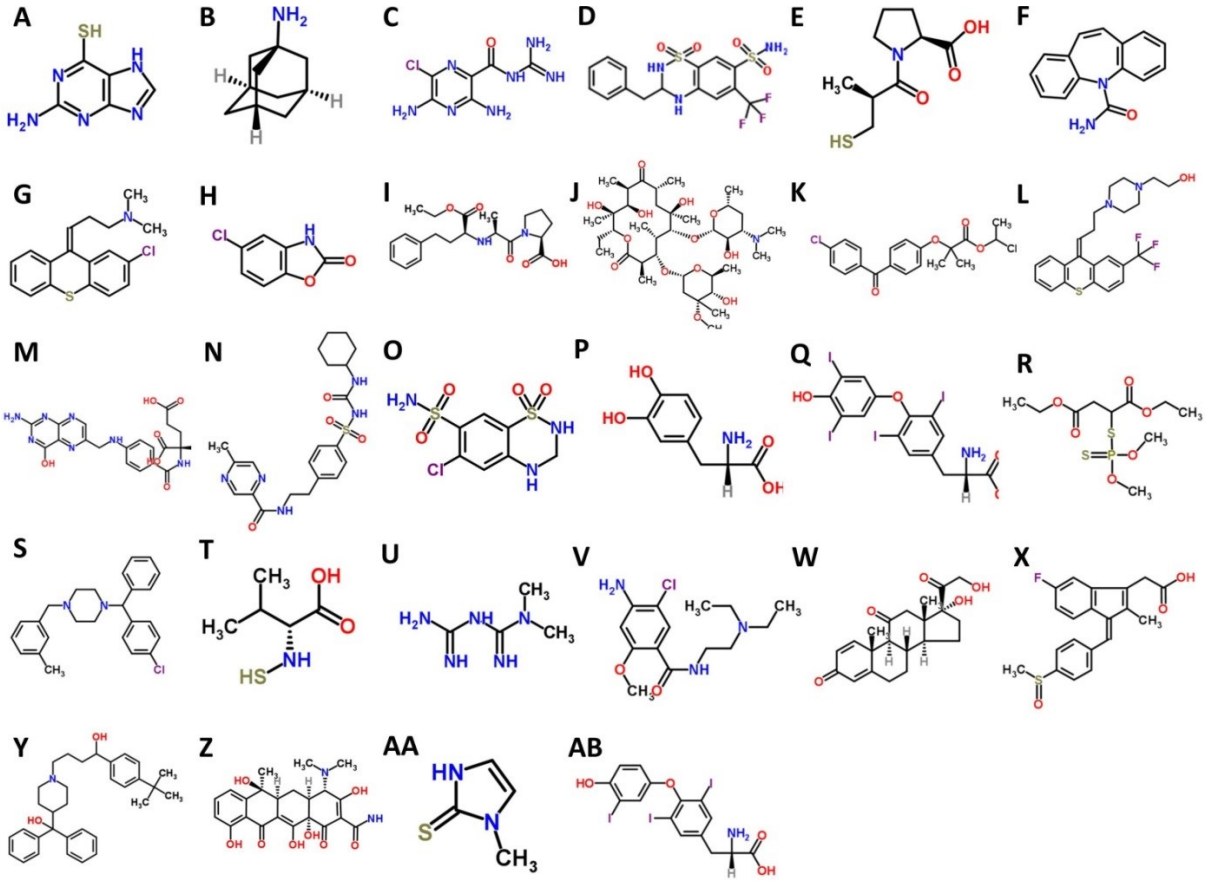

Figure 5.1 – Chemical structures of the 28 reference drugs. *A) 6-thioguanine, B) Amantadine, C) Amiloride, D) Bendroflumethiazide, E) Captopril, F) Carbamazepine, G) Chlorprothixene, H) Chlorzoxazone, I) Enalapril, J) Erythromycin, K) Fenofibrate, L) Flupenthixol, M) Folate, N) Glipizide, O) Hydrochlorothiazide, P) Levodopa, Q) Levothyroxine, R) Malathion, S) Meclizine, T) Mercaptovaline, U) Metformin, V) Metoclopramide, W) Prednisone, X) Sulindac, Y) Terfenadine, Z) Tetracycline, AA) Thiamazole, AB) Liothyronine.*
Source: www.chemspider.com

5.3.1 Toxicity and morphology assessment of 28 reference drugs in zebrafish embryos

The biological characterisation of the 28 reference drugs was done by determining the toxicity of these drugs in the zebrafish embryo. Beneficial or therapeutic effects of these drugs were not investigated in this chapter, but were investigated in **Chapter 6**.

Toxicity was investigated using two studies. In the first study (dose-range finding) zebrafish embryos were treated with six different concentrations (0.1, 1, 10, 100, 1000 and 10000 µM) of each drug along with two controls (0.1% DMSO and E3 embryo medium). Treatments were performed in 96 well plates with one zebrafish embryo placed in each well containing 150 µL of liquid. Treatments were initiated at the 75% epiboly stage and in total for each concentration 36 zebrafish embryos were tested (12 zebrafish embryos per repeat). Zebrafish embryos were observed using a Leica MZF10 fluorescence stereo microscope (Leica, Germany). Mortality was recorded every 24 hours over the 120 hour exposure period. Mortality was defined as coagulation of the zebrafish embryo, lack of somite development, non-detachment of the tail and after 48 hpf lack of a heartbeat based on the OECD guidelines outlined for the FET test (OECD, 2013). The mortality data was then used to plot logarithmic concentration-mortality curves from which toxicity endpoints such as LC50, LOEC and NOEC values were calculated using GraphPad Prism 5.0 (GraphPad Software Incorporation, USA).

In the second part of the study, visible morphological effects induced in zebrafish embryos by the 28 reference drugs were recorded and scored for severity. Morphological features were scored for every 24 hours over the 120 hour exposure period. The features scored

included reduced circulation (Circ), reduced movement (Movement), hatching (Hatch), reduced heart rate (Hrate), developmental delay (DelDev), deformation (Deformed), notochord (Notoch), tail curvature (TailCurv), protruding mouth (Pmouth), pectoral fin (Pfin), somites (Somites), jaw malformation (JawMal), yolk edema (Yedem), yolk size (Ysize), heart edema (Hedem), liver necrosis (LiverNec), brain hemorrhage (BrainHem), brain edema (Bedem) and overall health (Health). For the scoring of morphological features a scoring system was used to assign severity where 0 = normal, 1 = within normal range, 2 = mild, 3 = moderate, 4 = severe and 5 = very severe. EC50 was used as an additional toxicity indicator and was calculated for each drug from log concentration-response curves using GraphPad Prism 5.0 (GraphPad Software Incorporation, USA).

By dividing the LC50 by the EC50 teratogenic index values were calculated in order to determine the potency of the compounds with a ratio >2 indicating specific effects and therefore teratogenicity. Additionally, excess toxicity in the form of toxic ratio (TR) was also determined for each of the compounds using the experimentally derived LC50 values and predicted LC50 values. Predicted LC50 values were obtained using the following equation:

$\log(1/LC50) = 0.871\log P - 4.87$ (n=50, r=0.998, s=0.237) (Könemann, 1981)

The toxic ratio was calculated from these predicted and experimentally derived LC50 values using the following equation:

$\log TR = \log(1/LC50\ \text{experimental}) - \log(1/LC50\ \text{predicted})$ (Zhang et al., 2013)

The threshold for the logTR was set at 1. Compounds with a logTR value <1 were considered to show baseline toxicity, whereas compounds with a logTR value >1 were considered to show excess toxicity due to a specific mechanism of action.

To determine whether the chorion acted as a barrier preventing certain drugs from producing an effect in zebrafish embryos, a test was performed using a selection of 10 drugs (metformin, riboflavin, erythromycin, glipizide, 6-thioguanine, d-penicillamine, folate, prednisone, levodopa and hydrochlorothiazide) that did not show a response in either the dose-range finding study or the morphological effect study. These drugs were evaluated for toxicity and morphological effects in 75% epiboly stage zebrafish embryos that had been dechorionated. The drug concentrations used were the same as those used in the study for zebrafish embryos in their chorions. As before, morphological defects and mortality were recorded daily over a five day exposure period. Results were then averaged and compared.

5.4 Results

5.4.1 Zebrafish embryo mortality induced by 28 reference drugs

In the first study, the aim was to determine the toxicity of the 28 reference drugs in zebrafish embryos. This was done by recording zebrafish embryo mortality after exposure to each reference drug every 24 hours over a 120 hour exposure period. A logarithmic concentration series was used (0.1, 1, 10, 100, 1000 and 10000 µM) to ensure that all drugs were tested at concentrations at which they would induce an effect, as well as to uncover any relationships between concentration and mortality. An E3 embryo medium control and a solvent control (0.1% DMSO) were also included in the experiments.

To find out whether there was any difference between the E3 embryo medium and 0.1% DMSO controls orthogonal partial lest squares discriminant analysis (OPLS-DA) modelling was performed (data not shown). Using this modelling no significant difference was found between the two groups (R^2Y=0.007, Q^2=0.006). Therefore, for subsequent analysis the E3 embryo medium and 0.1% DMSO controls were considered as one control group.

To determine which drugs were highly toxic and teratogenic a PCA model of the zebrafish embryo mean cumulative percentage mortality for each drug over the 120 hour exposure period at each tested concentration was created (**Figure 5.2**). In the PCA model the tested concentrations were denoted by C1-C6 (0.1, 1, 10, 100, 1000 and 10000 μM) and the exposure times by T1-T5 (24, 48, 72, 96 and 120 hours).

The PCA model generated was found to be of good quality (R^2X=0.899, Q^2=0.533, two significant components) and from the scores plot (**Figure 5.2A**) it could be seen that bendroflumethiazide, terfenadine and chlorprothixene (coloured red) were outside of the model, i.e. not located within the white circle. These three compounds could not be explained by the model due to their values being erroneous or very different. Upon further inspection and by looking at the loading plot (**Figure 5.2B**) it was found that these three drugs were extremely toxic and teratogenic causing high mortality at almost all tested concentrations, which was not the case with any of the other drugs tested. In contrast, erythromycin, d-penicillamine and folate (coloured green) showed little toxicity similar to the controls (coloured blue) over the whole exposure period. Additionally, a cluster of drugs including carbamazepine, malathion and amantadine located in the bottom left quadrant of

the scores plot were found to cause high mortality only at the highest tested concentration. From this initial PCA model already differences could be seen between the drugs based on their propensity to cause mortality with drugs associated close to the controls showing little or no mortality and drugs located towards the right hand side of the scores plot demonstrating high mortality.

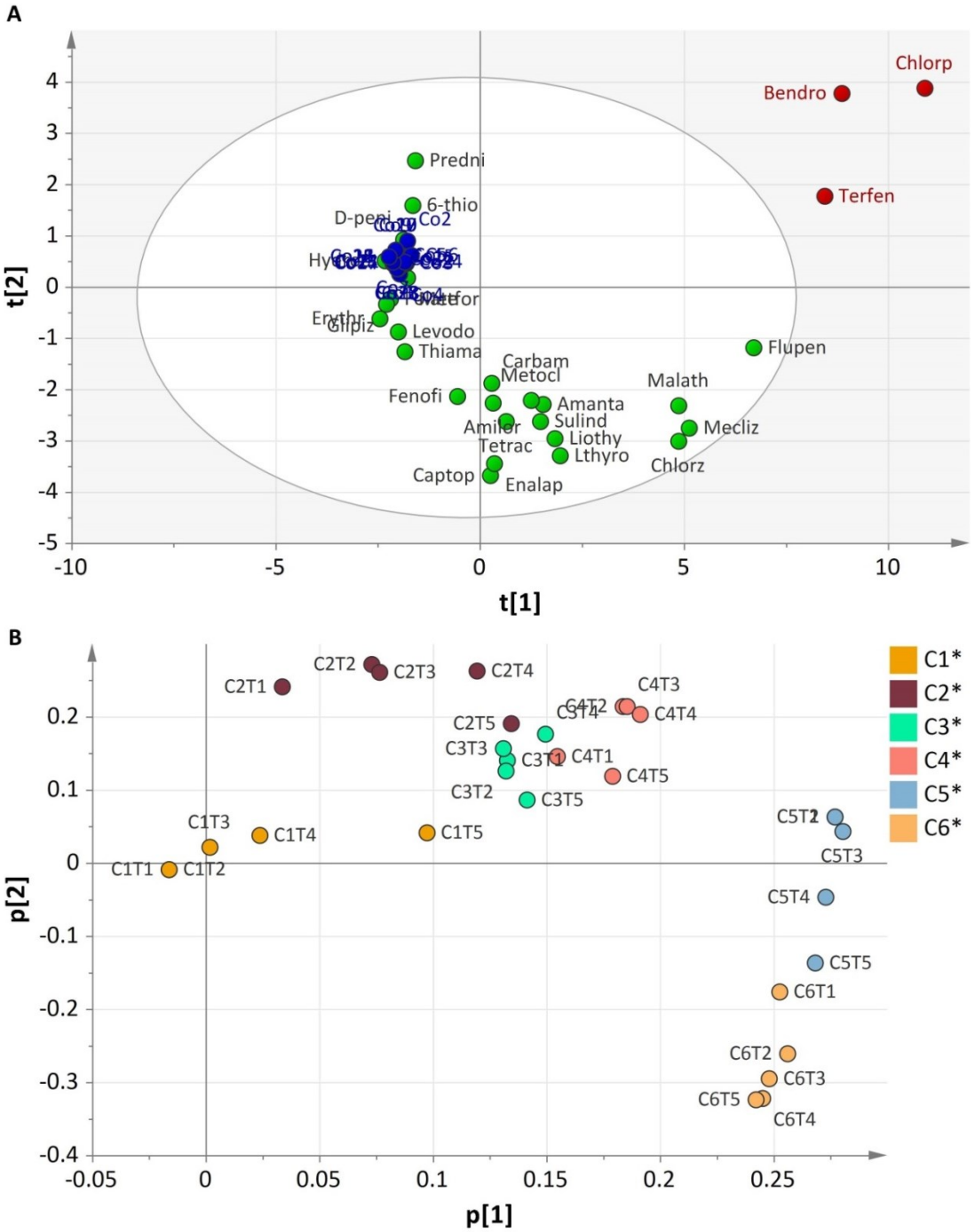

Figure 5.2 – A two-component PCA model of zebrafish embryo mortality (observations) against concentrations and exposure times (variables) following treatment with 28 reference drugs over a 120 hour exposure period. *A) Scores plot showing biological responses, B) Loading plot showing variables. The loading vector (p) and the scores vector (t) are displayed as vectors p and t. The numbers beside p and t indicate the PCA component (1 or 2). On the scores plot, the observations for the 28 reference drugs are denoted by coloured circles (green = drugs contained within the model, blue = controls [E3 and 0.1% DMSO] and red = outliers [show high toxicity]). On the loading plot the different concentration/exposure time combinations are denoted by coloured circles. Key: C1-6 = concentrations tested (0.1, 1, 10, 100, 1000 and 10000 µM), T1-5 = exposure period (24, 48, 72, 96 and 120 hours).*

From the data LC50, NOEC and LOEC values were calculated (**Table 5.3**). Chlorprothixene was found to have the lowest LC50 and one of the highest logP values. For nine reference drugs (6-thioguanine, d-penicillamine, erythromycin, folate, glipizide, hydrochlorothiazide, levodopa, metformin and prednisone) LC50 values could not be calculated.

Table 5.3 – Toxicological endpoints (LC50, NOEC and LOEC) calculated for each of the 28 reference drugs during phase 1 after 120 hours of exposure. *The physiochemical descriptors logP and pKa are also shown for each of the compounds.*

Compound	**LC50 (µM)**	**NOEC (µM)**	**LOEC (µM)**	**LogP**	**pKa**
6-thioguanine	N/A	10000	N/A	-0.1	10.5
Amantadine	290	100	1000	2.5	10.7
Amiloride	7430	1000	10000	-0.3	8.7
Bendroflumethiazide	18	10	100	1.9	8.5
Captopril	2113	1000	10000	0.3	4.0
Carbamazepine	304	100	1000	2.5	16.0
Chlorprothixene	4	1	10	5.2	9.8
Chlorzoxazone	186	100	1000	1.6	9.4
D-penicillamine	N/A	10000	N/A	-1.8	-1.8
Enalapril	7142	1000	10000	0.1	3.0
Erythromycin	N/A	10000	N/A	3.1	8.9
Fenofibrate	7027	1000	10000	5.3	-4.9
Flupenthixol	32	10	100	4.5	15.6
Folate	N/A	10000	N/A	-2.5	3.4
Glipizide	N/A	10000	N/A	1.9	5.9
Hydrochlorothiazide	N/A	10000	N/A	-0.1	7.9
Levodopa	N/A	10000	N/A	-2.4	2.3
Liothyronine	43	1	10	2.9	0.3
L-thyroxine	7	1	10	4.0	0.3
Malathion	129	100	1000	2.4	-6.8
Meclizine	228	100	1000	5.8	8.1
Metformin	N/A	10000	N/A	-0.5	12.4
Metoclopramide	184	100	1000	2.6	9.3
Prednisone	N/A	10000	N/A	1.5	12.6
Sulindac	185	100	1000	3.4	4.7
Terfenadine	9	1	10	7.1	13.2
Tetracycline	5605	1000	10000	-1.3	3.3
Thiamazole	4515	1000	10000	-0.3	10.4

5.4.2 Morphological effects of 28 reference drugs on zebrafish embryos during development

The next aim was to investigate the toxicity and teratogenicity induced by the 28 reference drugs further by recording and scoring morphological phenotypes that developed during zebrafish embryo development. To address this aim a study was performed with a geometric concentration series consisting of six concentrations along with two controls (E3 embryo medium and solvent control). A narrower geometric concentration series was used so that the development of phenotypes could be investigated. The concentrations tested in this study were based on those where an effect was observed in the first study (**Table 5.4**).

For the second study mortality along with the number of zebrafish embryos presenting with morphological effects was recorded every 24 hours over the whole 120 hour exposure period. Log-concentration response curves were then plotted and from this EC50 values for each of the 28 reference drugs over the 120 hour exposure period were calculated, as well as NOEC and LOEC values named NOEC2 and LOEC2, so as not to confuse them with NOEC and LOEC values calculated in the first study (**Table 5.5**). Morphological features were also scored for severity daily over the 120 hour exposure period (see section **5.3.1** for further details). In addition to this the teratogenic index (LC50/EC50) was calculated for each of the drugs (**Table 5.5**). It was found that a large number of drugs (amantadine, captopril, carbamazepine, chlorprothixene, chlorzoxazone, enalapril, liothyronine, l-thyroxine, meclizine, sulindac, terfenadine, tetracycline and thiamazole) were teratogenic with teratogenic index values >2. However, for a small number of drugs a teratogenic index value

could not be calculated, as for these drugs LC50 values could not be determined due to low or no toxicity.

Table 5.4 – Concentration ranges of 28 reference drugs used in study 2.

Compound	**Concentration (µM)**
6-thioguanine	1000-32000
Amantadine	400-12800
Amiloride	400-12800
Bendroflumethiazide	5-160
Captopril	400-12800
Carbamazepine	400-12800
Chlorprothixene	0.5-16
Chlorzoxazone	40-1280
D-penicillamine	1000-32000
Enalapril	31.25-1000
Erythromycin	31.25-1000
Fenofibrate	1000-32000
Flupenthixol	4-128
Folate	500-16000
Glipizide	6.25-200
Hydrochlorothiazide	31.25-1000
Levodopa	15.625-500
Liothyronine	400-12800
L-thyroxine	0.5-16
Malathion	50-1600
Meclizine	35-1120
Metformin	1000-32000
Metoclopramide	400-12800
Prednisone	25-800
Sulindac	300-9600
Terfenadine	1.25-40
Tetracycline	400-12800
Thiamazole	400-12800

Table 5.5 – Toxicological endpoints (EC50, NOEC2 and LOEC2) and teratogenic index values calculated for each of the 28 reference drugs from study 2. *Teratogenic index values >2 indicate specific effects.*

Compound	**EC50 (µM)**	**NOEC2 (µM)**	**LOEC2 (µM)**	**Teratogenic index (LC50/EC50)**
6-thioguanine	19952.62	2000.00	4000.00	N/A
Amantadine	48.19	N/A	N/A	6.02
Amiloride	3784.43	3200.00	6400.00	1.96
Bendroflumethiazide	29.24	10.00	20.00	0.62
Captopril	807.24	400.00	800.00	2.62
Carbamazepine	88.72	40.00	80.00	3.43
Chlorprothixene	0.68	0.50	1.00	5.88
Chlorzoxazone	83.75	80.00	160.00	2.22
D-penicillamine	16368.17	16000.00	32000.00	N/A
Enalapril	644.17	625.00	1250.00	11.09
Erythromycin	2588.21	2500.00	5000.00	N/A
Fenofibrate	3564.51	2000.00	4000.00	1.97
Flupenthixol	17.82	16.00	32.00	1.80
Folate	18492.69	16000.00	32000.00	N/A
Glipizide	105.44	100.00	200.00	N/A
Hydrochlorothiazide	5420.01	5000.00	10000.00	N/A
Levodopa	997.70	500.00	1000.00	N/A
Liothyronine	1.21	N/A	N/A	35.54
L-thyroxine	0.11	N/A	N/A	63.64
Malathion	81.10	80.00	160.00	1.59
Meclizine	35.08	35.00	70.00	6.50
Metformin	9120.11	1000.00	2000.00	N/A
Metoclopramide	855.07	800.00	1600.00	0.22
Prednisone	414.95	400.00	800.00	N/A
Sulindac	54.58	0.00	0.00	3.39
Terfenadine	1.25	1.25	2.50	7.20
Tetracycline	80.35	80.00	160.00	69.76
Thiamazole	400.87	400.00	800.00	11.26

To confirm that effects observed with a sub-set of 28 reference drugs were specific and not a result of baseline toxicity the logP values of the 28 reference drugs were plotted against their respective log(1/EC50) values (**Figure 5.3**). From this graph a weak correlation was observed between high logP values and high log(1/EC50) values.

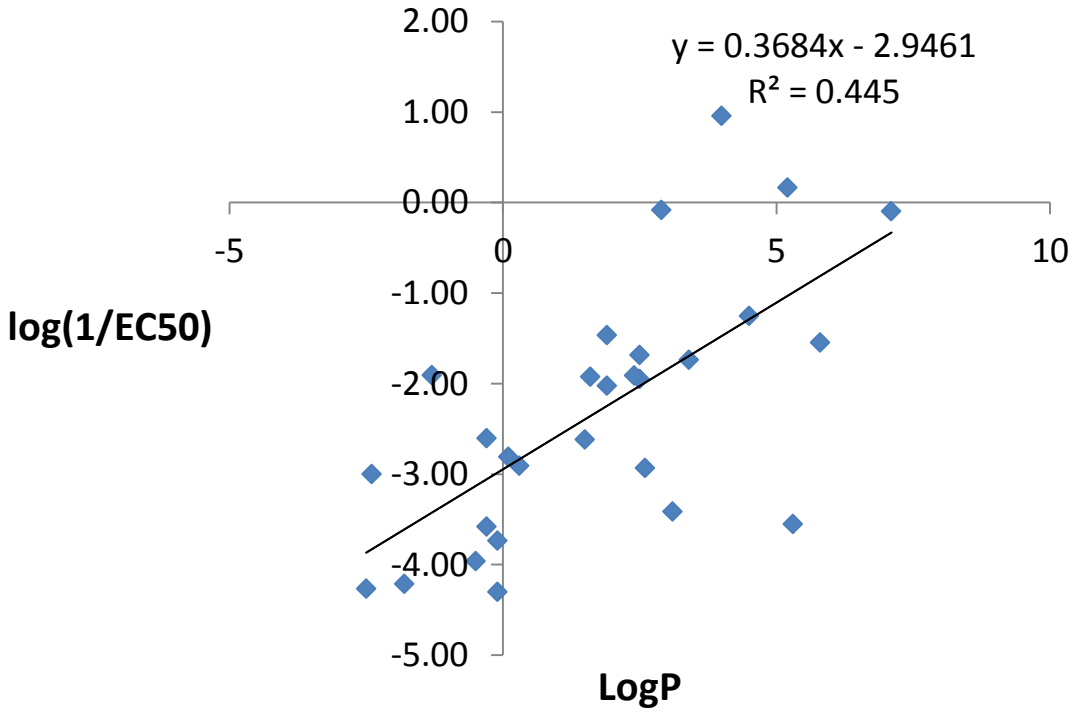

Figure 5.3 – LogP values plotted against log(1/EC50) values for the 28 reference drugs. *Line of best fit and correlation coefficient (r^2) are also shown on graph.*

Another approach was then taken to determine whether the biological responses observed with the 28 reference drugs were a result of specific activity or baseline toxicity. Toxic ratio (TR) values were calculated for each of the 28 reference drugs using predicted and experimental LC50 values (see Table 5.6). It could be seen that for a sub-set of the 28 reference drugs (amiloride, bendroflumethiazide, captopril, chlorzoxazone, tetracycline and thiamazole) the logTR values were >1 suggesting that the toxicity observed was due to a specific mechanism of action rather than baseline toxicity. However, with the remaining

drugs the logTR values were found to be <1 suggesting that the toxicity observed was due to baseline toxicity and therefore caused by narcosis (membrane interaction).

Table 5.6 – Toxic ratio (TR) values for toxicity observed with 28 reference drugs. *LogTR>1 = specific toxicity, logTR<1 = baseline toxicity.*

Drug	LogP	log(1/LC50p) (mmol/L)	log(1/LC50e) (mmol/L)	logTR (toxic ratio)
6-thioguanine	-0.1	-4.96	N/A	N/A
Amantadine	2.5	-2.70	-2.46	0.23
Amiloride	-0.3	-5.13	-3.87	1.26
Bendroflumethiazide	1.9	-3.22	-1.26	1.96
Captopril	0.3	-4.61	-3.32	1.28
Carbamazepine	2.5	-2.70	-2.48	0.21
Chlorprothixene	5.2	-0.35	-0.60	-0.26
Chlorzoxazone	1.6	-3.48	-2.27	1.21
D-penicillamine	-1.8	-6.44	N/A	N/A
Enalapril	0.1	-4.78	-3.85	0.93
Erythromycin	3.1	-2.17	N/A	N/A
Fenofibrate	5.3	-0.26	-3.85	-3.59
Flupenthixol	4.5	-0.96	-1.51	-0.55
Folate	-2.5	-7.05	N/A	N/A
Glipizide	1.9	-3.22	N/A	N/A
Hydrochlorothiazide	-0.1	-4.96	N/A	N/A
Levodopa	-2.4	-6.96	N/A	N/A
Liothyronine	2.9	-2.35	-1.63	0.71
L-thyroxine	4	-1.39	-0.85	0.54
Malathion	2.4	-2.78	-2.11	0.67
Meclizine	5.8	0.18	-2.36	-2.53
Metformin	-0.5	-5.31	N/A	N/A
Metoclopramide	2.6	-2.61	-2.26	0.34
Prednisone	1.5	-3.57	N/A	N/A
Sulindac	3.4	-1.91	-2.27	-0.36
Terfenadine	7.1	1.31	-0.95	-2.26
Tetracycline	-1.3	-6.00	-3.75	2.25
Thiamazole	-0.3	-5.13	-3.65	1.48

A variety of phenotypes were found to develop in zebrafish embryos after exposure to the 28 reference drugs. Some of these phenotypes were found to be common between many

drugs such as cardiac effects, including pericardial edema, reduced heart rate and reduced circulation. These common phenotypes were found to occur close to lethality and therefore represent secondary unspecific events. Other phenotypes were found to be more specific, e.g. brain edema/hydrocephalus observed with thiamazole. The specific phenotypes observed were found to be generalised between particular classes of drugs with reduced pigmentation for example observed with those drugs affecting the thyroid gland (l-thyroxine, liothyronine and thiamazole) (**Table 5.7**). This would make sense based on the function of these compounds, as compounds with similar pharmacological actions and shared biological pathways would be expected to produce similar toxic effects.

Table 5.7 – Specific phenotypes associated with drug classes from the 28 reference drug set.

Compound class	**Phenotype**
Anti-histamines (meclizine, terfenadine)	Cardiac toxicity (reduced HR, pericardial edema, AV block)
Anti-thyroid (l-thyroxine, liothyronine, thiamazole)	Reduced pigmentation, brain edema/hydrocephalus (thiamazole at highest tested concentration only)
Antibiotics (erythromycin, tetracycline)	Little/no toxicity
Anti-lipemics (fenofibrate)	Little/no toxicity
Anti-convulsants (carbamazepine)	Craniofacial abnormalities (jaw malformations)
Anti-diabetics (glipizide, metformin)	Little/no toxicity
Muscle relaxants (chlorzoxazone)	Reduced movement and developmental arrest
Diuretics (captopril, enalapril)	Enlarged yolk
Dietary supplement (folate)	Little/no toxicity
Anti-psychotics (flupenthixol, chlorprothixene)	Craniofacial abnormalities (jaw malformations)
Insecticides (malathion)	Reduced pigmentation
Anti-rheumatics (D-penicillamine)	Little/no toxicity
Anti-neoplastic (6-thioguanine)	Little/no toxicity
Anti-Parkinson's (amantadine)	Craniofacial abnormalities (jaw malformations)
Anti-hypertensives (bendroflumethiazide)	Developmental arrest
Anti-inflammatory (sulindac)	Black yolk

In order to distinguish those drugs producing severe morphological effects and toxicity from those drugs producing no or little effects a PCA model was generated. The model was created using the severity scores for the morphological features at only one time point and concentration, namely after 120 hours of exposure and at the highest tested concentration (C6T5) along with mortality (Dead) and the toxicity endpoints (LC50, EC50, LOEC1, NOEC1, LOEC2, NOEC2) that had been previously calculated. This model was found to be of good quality (R^2X=0.716, Q^2=0.48, three significant components) showing a clear separation between the highly toxic drugs and those causing little toxicity (**Figure 5.4**). On the scores plot (**Figure 5.4A**) drugs showing no or little toxicity were found to be clustered on the left hand side (circled), whereas toxic drugs were found to be clustered on the right hand side (circled). Additionally, from the scores plot it was evident that folic acid (circled and coloured in red) was outside of the model, i.e. outside of the white circle. This was because it caused the least mortality and the least morphological effects compared to the other drugs tested.

When looking at the loading plot (**Figure 5.4B**) it could be seen that the drugs situated in the top left quadrant of the scores plot were those that had high LC50, LOEC1 and NOEC1 values and were most similar in these variables. In contrast, the drugs situated in the top right quadrant of the scores plot were those drugs that produced various morphological effects, such as jaw malformations, tail curvature, abnormal somite development, etc. These drugs were found to be the same selection of drugs that caused high mortality in the first study (e.g. chlorprothixene). Additionally, features indicative of mortality, i.e. no movement (Movement), no heart rate (Hrate) and no circulation (Circ) were found to cluster close together on the loading plot.

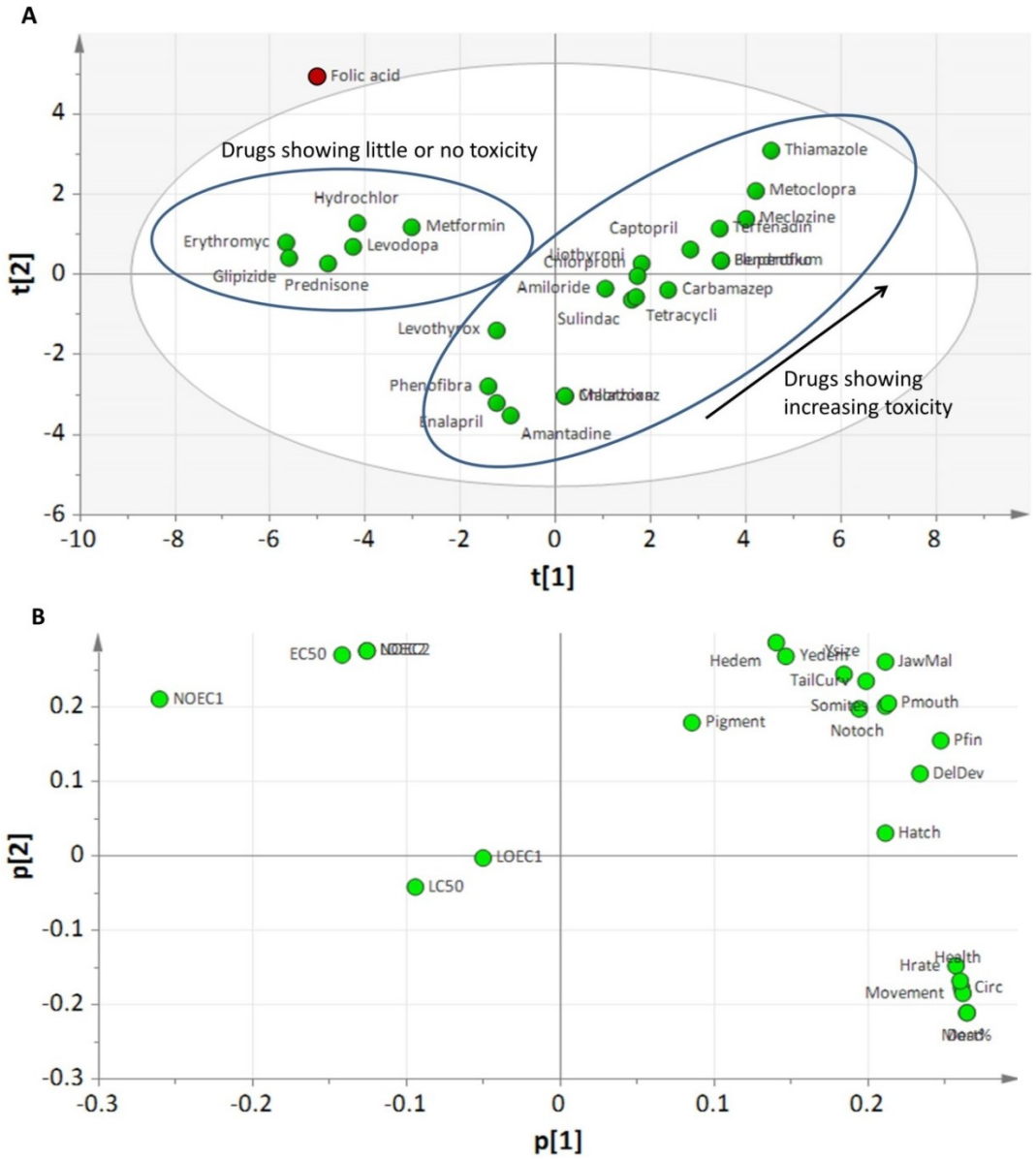

Figure 5.4 – A three-component PCA model of zebrafish embryo responses (observations) against variables (toxicity endpoints and morphological features) following treatment with 28 reference drugs over a 120 hour exposure period. *A) Scores plot showing biological responses, B) Loading plot showing variables. The loading vector (p) and the scores vector (t) are displayed as vectors p and t. The numbers beside p and t indicate the PCA component (1 or 2). On the scores plot, the observations for the 28 reference drugs are denoted by coloured circles (green = drugs contained within the model and red = outliers). On the loading plot the variables (toxicity endpoints and morphology features) are denoted by green circles. Toxicity endpoints = LC50, EC50, NOEC1, LOEC1, NOEC2 and LOEC2. Morphological features = reduced circulation (Circ), reduced movement (Movement), hatching (Hatch), reduced heart rate (Hrate), developmental delay (DelDev), deformation (Deformed), notochord (Notoch), tail curvature (TailCurv), protruding mouth (Pmouth), pectoral fin (Pfin), somites (Somites), jaw malformation (JawMal), yolk edema (Yedem), yolk size (Ysize), heart edema (Hedem), liver necrosis (LiverNec), brain hemorrhage (BrainHem), brain edema (Bedem), mortality (Dead) and overall health (Health).*

5.4.3 Development of a QSAR model based on zebrafish embryo toxicity endpoints and morphological features

To determine whether there was any relationship between the physiochemical properties of the 28 reference drugs and the induction of biological effects in zebrafish embryos a QSAR model was generated. To generate the model the principal components from the initial PCA model of the 28 reference drugs (refer back to **Figure 5.4**) were used as the Y variables on a hierarchical OPLS regression. In a standard PLS the Y vector can be anywhere relative to X. In OPLS modelling however the Y vector is placed in alignment with the first component in the X matrix enabling separation of the correlated and uncorrelated variables. A hierarchical OPLS regression enables a clear distinction to be made between the non-correlating variables on the Y axis and the correlating variables on the X axis.

The hierarchical OPLS model generated was found to be of very good quality (R^2X=0.729, Q^2=0.975, three significant components). From the scores plot (**Figure 5.5A**) a clear distinction could be made between the drugs showing little or no toxicity located in the top right quadrant (circled) to those which increased in toxicity starting from the bottom right quadrant working up towards the top left quadrant (circled). Additionally, on the scores plot folic acid (circled red) was found to be outside of the model. This was because it caused no mortality and produced little or no morphological effects even at the highest tested concentration.

From the loading plot (**Figure 5.5B**) it was evident that many physiochemical descriptors were clustered close together with the morphological features. One of these physiochemical descriptors included logP (determinant of lipophilicty and drug cell permeability). High logP values were found to be associated with increased toxicity (i.e. decreased LC50, EC50, NOEC and LOEC values) and increased severity scores for the morphological features heart rate, movement and circulation (all indicators of death). The same relationship was also seen with $logD_{ACD\_6.5}$ and $logD_{ACD\_7.4}$ values, which describe the lipophilicty for both the ionised and unionised form of a drug. A low polar surface area (PSA) was also found to be an important determinant for toxicity. A high EHOMO also contributed to increased toxicity and was found to have a very big influence on the model. Additionally, low ELUMO and low hardness (H) values were also found to be associated with increased toxicity.

Overall from the model it could be seen that several chemical features of the drugs were associated with the development of morphology phenotypes and also mortality. Particularly, logP which is an indicator of hydrophobicity and EHOMO which is an indicator of the electron releasing ability of a drug were found to be important toxicity determinants.

However, the QSAR model generated also needs to be interpreted with caution, as it may be biased due to scores for the phenotypes at one concentration only being used to generate the model.

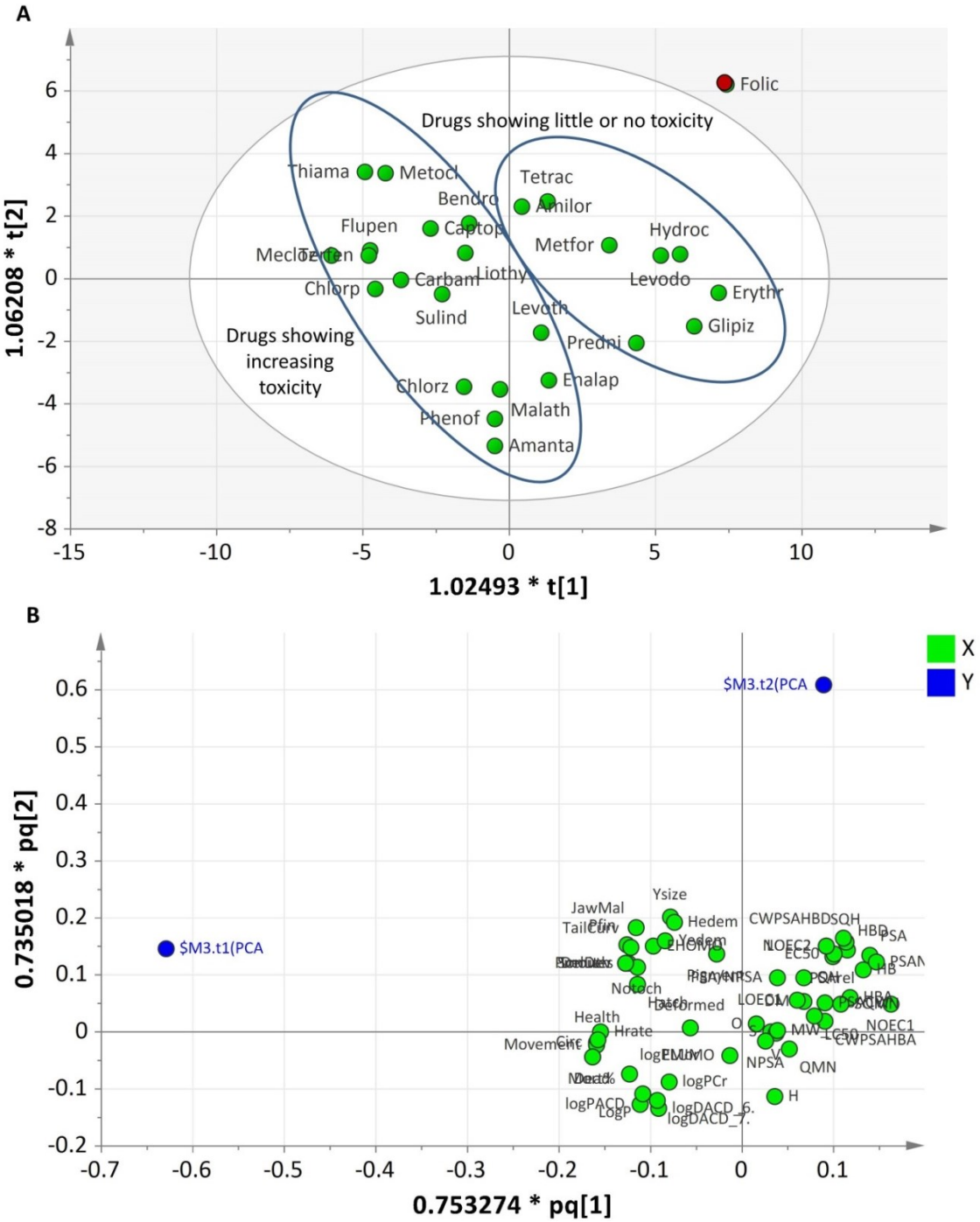

Figure 5.5 – Three-component hierarchical OPLS model of physiochemical descriptors and biological endpoints (variables) against biological responses (observations). *A) Scores plot, B) Loading plot. On the scores plot the scores vector is displayed as t with the number next to it indicating the OPLS component (1 or 2). The scores of PCA components 1 and 2 are labelled on the X and Y axis, respectively. The scores for each drug are labelled and enclosed within green circles with a clear separation seen between those that are toxic and non-toxic. On the loading plot the X and Y loadings are represented by p and q, respectively. The biological variables and chemical descriptors (X) are enclosed in green circles. The PCA components (Y) are enclosed in blue circles. The loadings of PCA components 1 and 2 are labelled on the X and Y axis, respectively.*

From the variable importance plot (VIP) plot shown in **Figure 5.6** which shows the most important variables contributing to mortality it can also be seen that logP is the most important physiochemical descriptor for mortality, closely followed by a high EHOMO value.

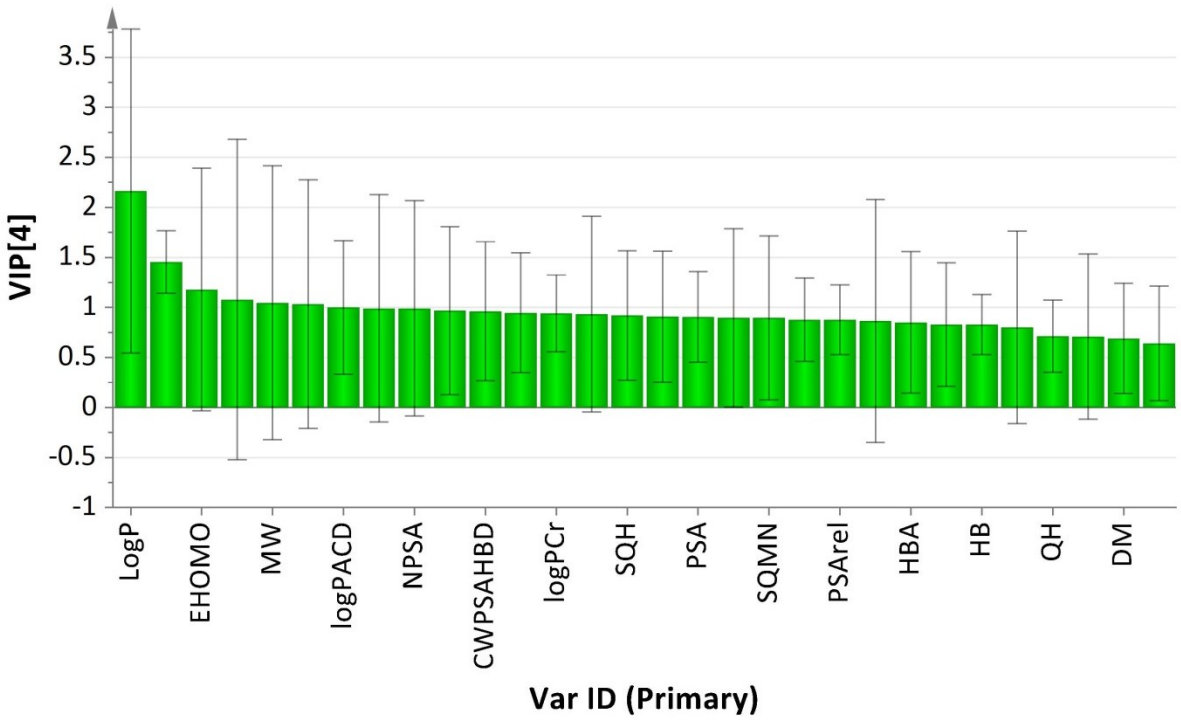

Figure 5.6 – VIP plot showing the most important physiochemical properties contributing to zebrafish embryo mortality after exposure to the 28 reference drugs. *The VIP scores which are a measure of the importance of each variable in modelling X and Y are displayed on the Y axis with the name of each individual variable displayed along the x axis. The error bars indicate standard deviation.*

The next objective of the study was to validate the QSAR model generated by making predictions for the biological outputs of similar structured compounds. In order to validate the QSAR model, biological data for a validation drug set (diclofenac, doxorubicin, ibuprofen, glutamate, hydroxyurea and riboflavin) was acquired in the same way as for the 28 reference drug set. These six validation drugs were selected due to their functional and physiochemical diversity (**Figure 5.7**).

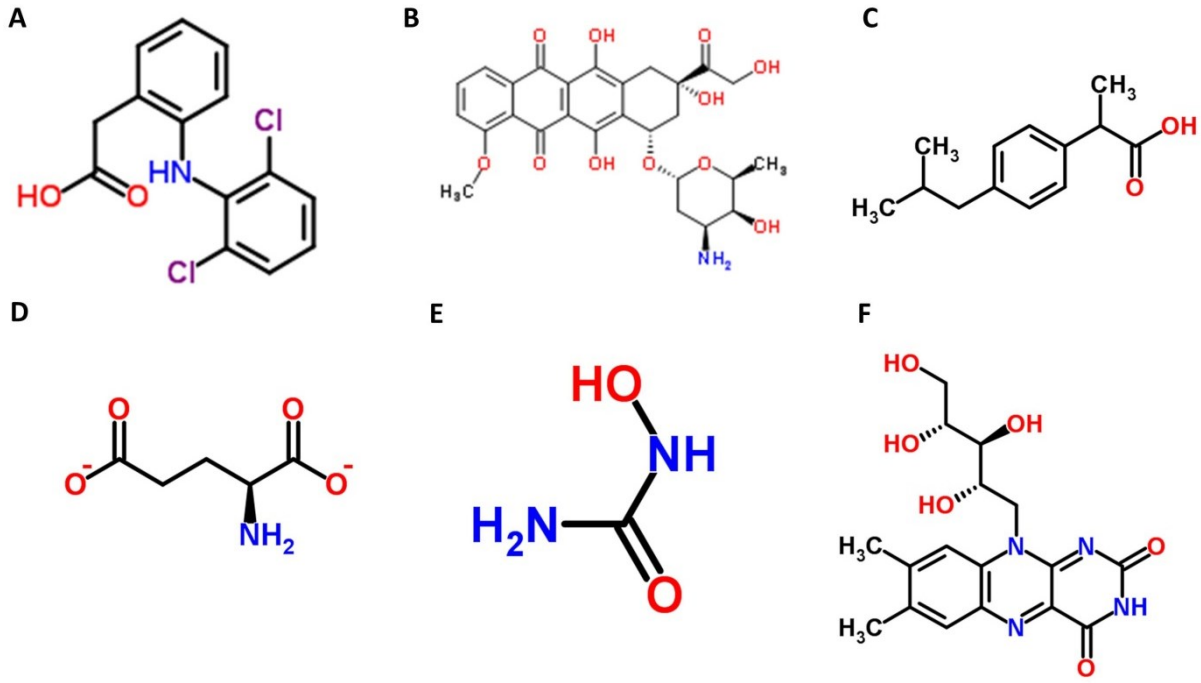

Figure 5.7 – Chemical structures of six validation drugs. *A) Diclofenac, B) Doxorubicin, C) Ibuprofen, D) L-glutamate, E) Hydroxyurea, F) Riboflavin.*
Source: www.chemspider.com

For the six validation drugs firstly a dose-range finding study was performed with log-concentration mortality curves plotted for each drug based on the mortalities observed over a 120 hour exposure period. From the log-concentration mortality curves LC50, NOEC1 and LOEC1 values were calculated (**Table 5.8**). In the second study, zebrafish embryos were treated with the six validation drugs over a 120 hour exposure period and mortality was recorded daily (**Table 5.8**). The concentration ranges used for the drugs in the second study are shown in **Table 5.8**. Morphological features were also scored for severity (see section **5.3.1** for further details). From this EC50 values were also calculated (**Table 5.8**). In addition to this the teratogenic index was calculated for the six validation drugs (**Table 5.9**). It was found that ibuprofen, diclofenac and doxorubicin were particularly teratogenic to zebrafish embryos presenting with teratogenic index values >2. Furthermore, the calculated logTR (toxic ratio) values showed that ibuprofen and glutamate most probably operated via a

specific mechanism of action and not via narcosis (membrane interaction) which is the case for the other four drugs (**Table 5.9**).

Table 5.8 – Calculated toxicological endpoints for validation drug set and concentration ranges used for phase 2 study.
All values listed are in µM.

Compound	EC50	LC50	NOEC1	LOEC1	NOEC2	LOEC2	Phase 2
Diclofenac	1.21	5.53	1.00	10.00	N/A	N/A	2.5-80
Doxorubicin	93.97	173.56	100.00	1000.00	50.00	100.00	25-800
Glutamate	272.27	259.53	100.00	1000.00	125.00	250.00	62.5-2000
Hydroxyurea	12705.70	N/A	10000.00	N/A	6250.00	12500.00	3125-100000
Ibuprofen	9.98	27.85	10.00	100.00	5.00	10.00	5-160
Riboflavin	798.00	N/A	N/A	N/A	N/A	N/A	50-1600

Table 5.9 – Teratogenic index values, logTR (toxic ratio) values and physiochemical descriptors (logP and pKa) for validation drug set. *Teratogenic index values >2 indicate specific effects. LogTR>1 = specific toxicity, logTR<1 = baseline toxicity.*

Compound	LogP	pKa	Teratogenic index (LC50/EC50)	log(1/LC50p) (mmol/L)	log(1/LC50e) (mmol/L)	logTR (toxic ratio)
Diclofenac	4.51	4.15	4.57	-0.95	-0.74	0.20
Doxorubicin	3.97	4.91	1.85	-1.42	-2.24	-0.82
Glutamate	-1.80	10.14	0.95	-6.44	-2.41	4.02
Hydroxyurea	-1.46	10.20	N/A	-6.14	N/A	N/A
Ibuprofen	1.27	9.53	2.79	-3.77	-1.44	2.32
Riboflavin	-3.69	2.23	N/A	-8.08	N/A	N/A

To assess the predictivity of the QSAR model the mean severity scores of a selection of morphological features for diclofenac at the highest tested concentration and the longest exposure time (C6T5) were predicted and compared to the observed values (**Figure 5.8A**). It was found that the predictions made were almost identical to the observed values. When using the model to predict the mean cumulative mortality for the six validation drugs at the

highest tested concentration and the longest exposure time (C6T5) (**Figure 5.8B**) the mortalities predicted for diclofenac, doxorubicin, glutamic acid and riboflavin were close to the observed values with the exception of hydroxyurea where mortality was under-predicted by 33%.

In general the QSAR model generated shows good predictivity, despite a small number of drugs having been used to generate it. Further drugs would need to be introduced into the model to further optimise it. Based on the current results the model seems to be good for predicting the biological responses for highly toxic compounds; however a larger drug set would need to be validated in order to test the limits of the model sufficiently. Additionally, the high predictive capacity could be biased by many of the compounds acting as narcotics in zebrafish embryos.

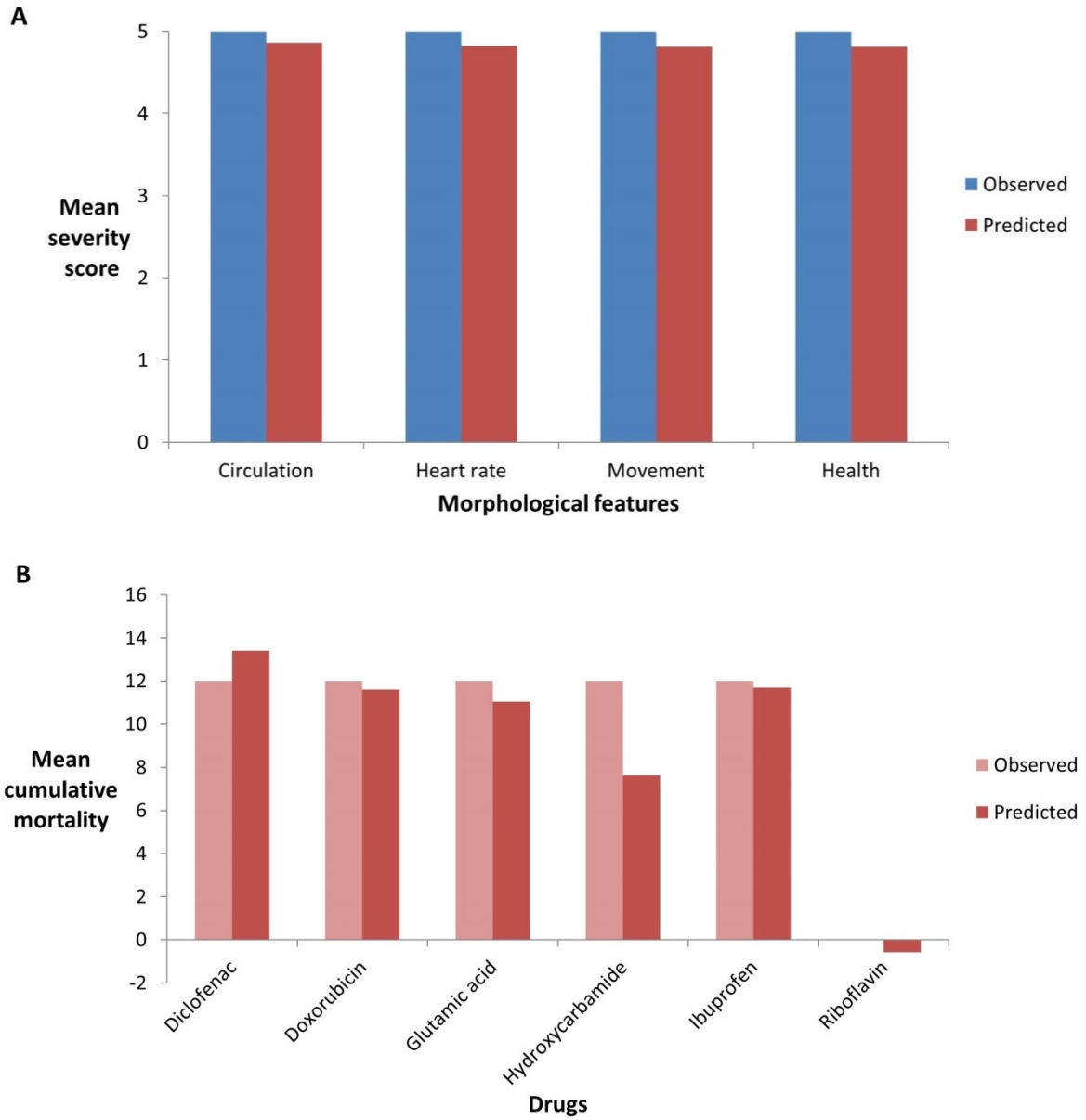

Figure 5.8 – Predictivity of the hierarchical OPLS regression model. *A) Observed and predicted zebrafish embryo mean severity scores for a selection of morphology features following diclofenac treatment at one time point and concentration (C6T5), B) Observed and predicted values for the zebrafish embryo mean cumulative mortality following treatment with the six validation drugs at one time point and concentration (C6T5).*

5.4.4 Effect of dechorionation on the morphological responses of the 28 reference drugs

In some studies it has been reported that the chorion of the zebrafish embryo could act as a barrier to drug penetration (Henn and Braunbeck, 2011)(Mandrell et al., 2012)(Ali et al., 2011)(King Heiden et al., 2007)(Truong et al., 2011). Therefore, a study was performed to

determine whether penetration of drugs into the zebrafish embryo chorion affected their ability to produce a morphological response. Particularly, for the drugs that were found to be non-responsive in the initial studies this was an issue that needed to be addressed. A selection of 10 drugs taken from the 28 reference and validation drug set (metformin, 6-thioguanine, d-penicillamine, folate, prednisone, levodopa, hydrochlorothiazide, glipizide, riboflavin and erythromycin) were re-examined for mortality and the generation of morphological responses by using dechorionated zebrafish embryos. The zebrafish embryos were dechorionated immediately after fertilisation (see **Chapter 2** for further details) and then treated at the 75% epiboly stage using the drug concentrations outlined in **Table 5.4** and **Table 5.8**. Morphological responses and mortality were recorded daily over the 120 hour exposure period.

OPLS-DA modelling was performed to determine whether removal of the chorion had an effect on the toxicity of these drugs. By assigning a class to each treatment method, i.e. still in chorion (class 1) and dechorionated (class 2); the two groups could be discriminated. Using this modelling (**Figure 5.9**, R^2X=0.0622, Q^2=-1.94) it was found that there was no significant difference between the two treatment methods (n=36 zebrafish larvae at 5 dpf per drug concentration/control, P>0.05). When looking at the scores plot (**Figure 5.9A**) it could be seen that the dechorionated drug treatments (blue circles) and the drug treatments with zebrafish in their chorions (green circles) produced similar morphological responses and mortalities, clearly identifiable by overlapping of the scores for each drug using both treatment methods.

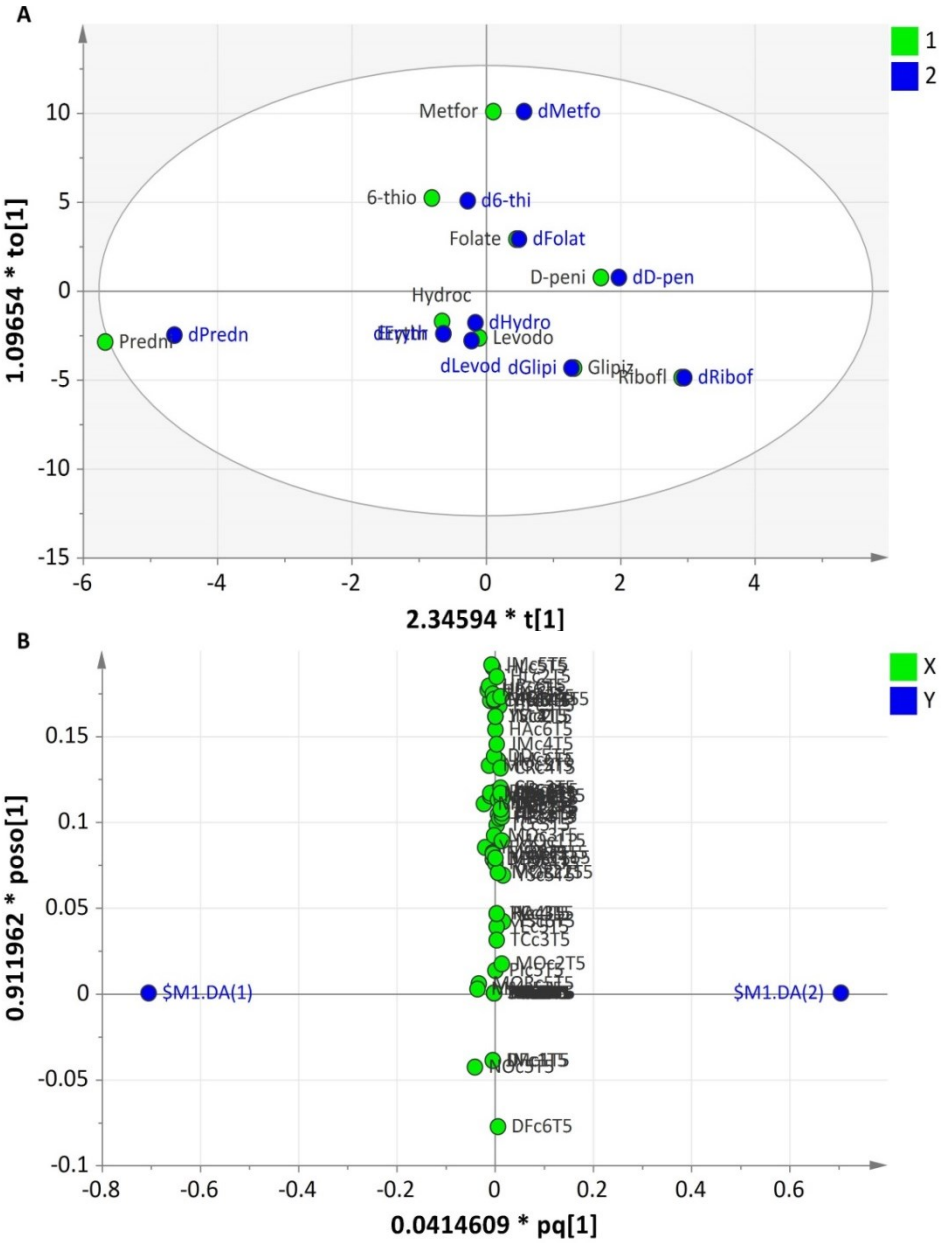

Figure 5.9 – A two-component OPLS-DA model of biological responses (observations) against morphological features and mortality (variables) following drug treatment of zebrafish embryos with or without chorion. *A) Scores plot, B) Loading plot. On the scores plot the scores vectors are displayed as t and to with the number next to them indicating the OPLS-DA component (1 or 2). The scores of the OPLS-DA classes 1 and 2 are labelled on the X and Y axis, respectively. The scores for the responses observed for each drug after treatment with embryos in their chorions are labelled and enclosed within green circles. The scores for the responses observed for each drug after treatment of dechorionated embryos are labelled and enclosed within blue circles and marked with a small letter d in front of the drug name. The numbers on the axes represent the scores for each class. On the loading plot the X and Y loadings are represented by p and q and po and so, respectively for each class. The morphological features are displayed as X variables and are enclosed in green circles. The two treatment methods (classes 1 and 2) are displayed as Y variables and enclosed in blue circles. Key: Morphological features labelled with concentration (c1-c6) and exposure time.*

5.4.5 Comparison of the toxicity of the 28 reference drug set between zebrafish embryos and rodents

In order to evaluate the applicability of the zebrafish embryo as a toxicological model the logLC50 values calculated for the 28 reference and six validation drugs from the zebrafish embryo toxicity studies were compared to existing logLD50 values for rodents from the literature. This has also been done in other studies (Ali et al., 2011). Ideally, a better comparison would have been mammalian embryo data; however this is scarce and not readily available.

By performing a simple regression analysis between zebrafish embryo logLC50 and rat logLD50 values there was found to be a weak correlation (R^2=0.12) (**Figure 5.10A**). The same was seen when comparing zebrafish embryo logLC50 and mice logLD50 values (R^2=0.08) (**Figure 5.10B**). Despite the weak correlation, the logLC50/LD50 values for some drugs were similar between all three species, such as in the case of sulindac and doxorubicin. A few drugs on the other hand showed big differences between the three species. For example, l-thyroxine was found to be extremely toxic in zebrafish embryos compared to rodents. Additionally, amiloride was found to be less toxic in zebrafish than in rodents. It could also be seen that the more lipophilic drugs were the ones that were more toxic in zebrafish embryos than in rodents. Based on this data it seems that toxicity endpoints such as LC50 may not be the best parameter when comparing toxicity between different species.

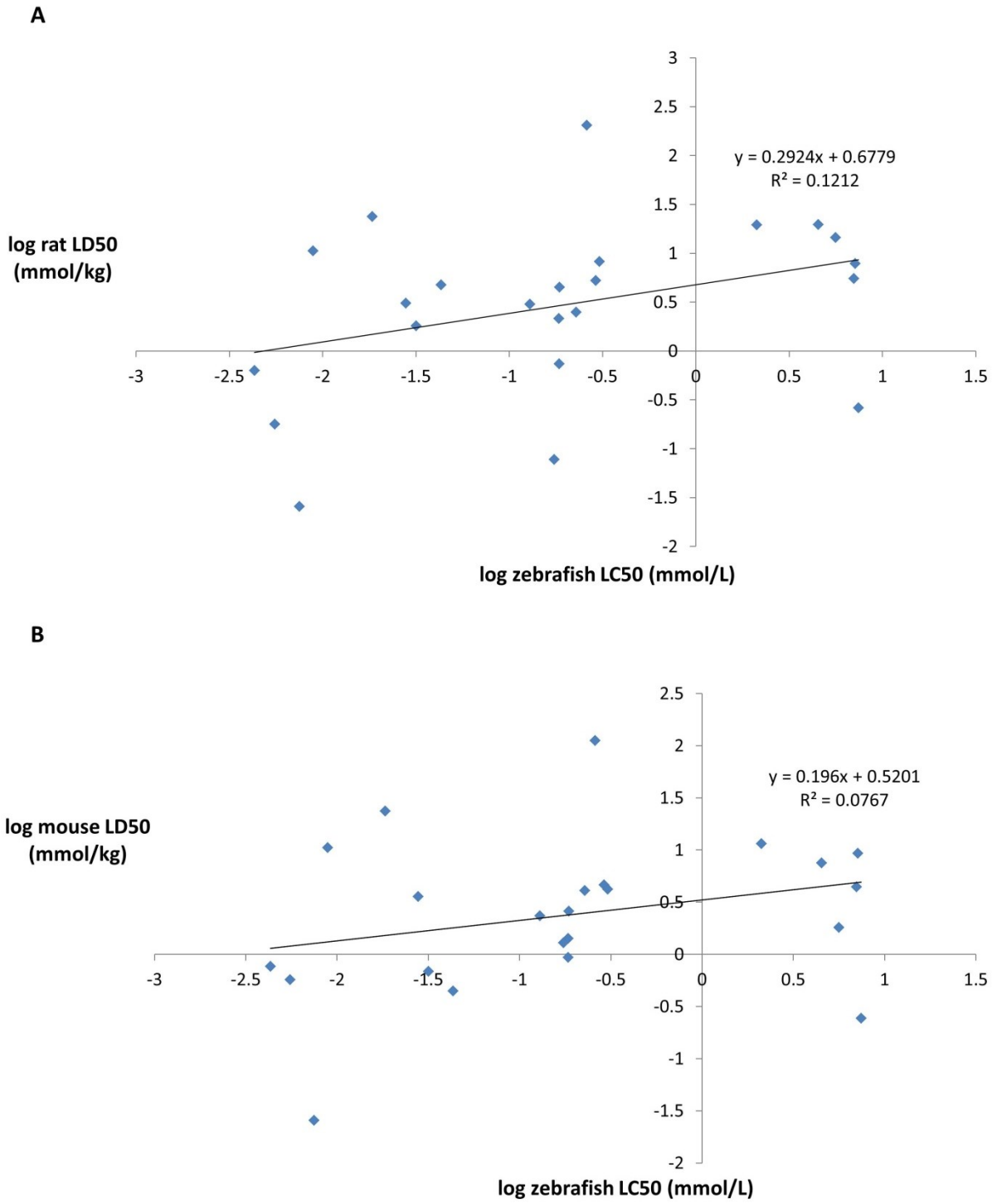

Figure 5.10 – Correlation between zebrafish logLC50 and rodent logLD50 values for 28 reference drugs and six validation drugs. *A) Correlation between zebrafish logLC50 and rat logLD50 values (R^2=0.12), B) Correlation between zebrafish logLC50 and mouse logLD50 values (R^2=0.08).*

5.5 Discussion

5.5.1 Relationship between toxicity and physiochemical descriptors

The 28 reference drugs were evaluated for toxicity in zebrafish embryos by performing dose-range finding and morphology studies using a similar approach to other zebrafish embryo toxicity studies (Scholz et al., 2013)(Panzica-Kelly et al., 2010)(Hermsen et al., 2011)(Ali et al., 2011). Out of the 28 compounds tested nine were found to show little or no toxicity. The remaining 19 compounds were all found to cause significant levels of mortality with five particularly toxic. These included flupenthixol, chlorprothixene, l-thyroxine, terfenadine and bendroflumethiazide which were found to cause high mortality at several concentrations. Additionally, by calculating toxicity endpoints such as LC50, EC50, NOEC and LOEC values, as well as scoring morphological features for severity and determining teratogenic index and toxic ratio values it was found that chlorprothixene showed the most toxicity out of the 28 reference drugs tested.

From the QSAR model generated of the toxicity endpoints and morphological feature scores against the physiochemical properties of the drugs it was found that logP was an important physiochemical descriptor. A high logP value was found to correlate with increased toxicity and the development of severe morphological defects. This relationship has also been reported in other zebrafish studies (Padilla et al., 2012)(Berghmans et al., 2008)(Weimin et al., 2001)(Chen et al., 2012), as well as in other organisms (Wayne Schultz et al., 1991)(Newsome et al., 1991)(Landis et al., 1993). As logP gives an indication of how well a drug can penetrate through the cell membrane, a drug with a higher logP value will be able to get into cells more easily to induce an effect than a drug which has a low logP value. The

logP value for a chemical can be calculated directly from its chemical structure therefore making it a useful indicator in predicting drug uptake and drug toxicity in zebrafish embryos (Petersen and Kristensen, 1998). Additionally, logP is inversely correlated to the number of hydrogen bond acceptors (HBA) and hydrogen bond donors (HBD) (Kamlet et al., 1987). A high logP value is also associated with increased cell membrane permeability across the blood brain barrier, which might explain the high toxicity observed with chlorprothixene, terfenadine and flupenthixol.

High $logD_{ACD\_6.5}$ and $logD_{ACD\_7.4}$ values were also found to be associated with toxicity and increased severity of morphological features. This is because $logD_{ACD\_6.5}$ and $logD_{ACD\_7.4}$ values indicate the lipophilicity of a drug at a given pH compensated for ionisation, whereas logP only indicates the lipophilicty of a drug in its neutral state.

A low polar surface area (PSA) was also found to be an important determinant for toxicity in conjunction with high logP, $logD_{ACD\_6.5}$ and $logD_{ACD\_7.4}$ values. This is because compounds with a low polar surface area can cross biological membranes more easily and thus distribute to various tissues, which can result in off target effects and therefore cause toxicity (Hughes et al., 2008).

Molecular weight was not found to have a very big influence on toxicity, as even large molecular weight compounds like l-thyroxine were highly toxic. In the case of erythromycin however molecular weight was found to be important. Despite erythromycin having a fairly high logP, it also has a very high molecular weight thus affecting its ability to penetrate into

cells. It has been documented that erythromycin has to be injected into the zebrafish embryo in order for it to have an effect (Milan et al., 2003). This probably explains why erythromycin produced little or no effects in the zebrafish embryo studies.

A high EHOMO value was also associated with increased toxicity and was found to have a very big influence on the QSAR model that was generated. As EHOMO gives an indication of the electron-releasing capabilities of a drug, a drug with a higher EHOMO value would be able to release electrons more easily. These released electrons could ionise the drug making it more reactive, so that it has the potential to interact with cells and tissues causing damage. Additionally, low ELUMO and low hardness (H) values were also found to be associated with increased toxicity, as the electronic structure of the molecules in drugs with low ELUMO and hardness values can be changed more easily thus increasing their reactivity (Cronin, 2004).

A small molecular volume (V), molecular surface area (S) and ovality (O) were also associated with increased toxicity, as these properties enable greater drug uptake together with a high logP value and a low PSA value (Cronin, 2004). All of these parameters intercorrelate with logP as they increase the hydrophobic character of drugs thereby increasing their toxic potential.

Overall from the QSAR model generated it could be seen that a high logP value (high hydrophobicity) was the main driving force behind increased toxicity. For the majority of

drugs toxicity was caused by baseline toxicity, i.e. narcosis (membrane interaction) and only in a very few cases a specific mechanism of toxicity was involved.

5.5.2 Novelty of QSAR model based on zebrafish embryo developmental toxicity

QSAR models are an important part of toxicity testing today. Particularly, in the pharmaceutical industry when selecting candidate drugs to take forward in the drug development process testing each individual compound for toxicity is not feasible. Therefore, QSAR models are created that can predict the toxicity of compounds based on structural alerts such as the presence of functional groups associated with toxicity.

In the past many different approaches were used when generating QSAR models for predicting toxicity of compounds (Wayne Schultz et al., 1991)(Newsome et al., 1991)(Landis et al., 1993)(Weimin et al., 2001)(Chen et al., 2012). Originally, QSAR models were developed to predict toxicity of compounds from the same chemical class, however this was found to impair model quality, as compounds even from the same chemical class may have different toxicity mechanisms (Ren, 2002). QSAR models in use today are more targeted and predict the toxicity of compounds with a similar mechanism of action to increase the predictive power of the model (Ren, 2002)(Hansch et al., 1995). This in itself has drawbacks as the mechanism of action of the untested compounds needs to be known before a QSAR model can be made, which is not always possible. Additionally, when performing QSAR modelling it is assumed that a compound's properties can be defined based on its structure, its charge density and molecular composition implying that similar structured compounds

have similar activity based on these properties, which may not always be the case and needs to be taken into consideration (Nendza, 1998).

QSAR models that are generated based on *in vitro* results do not provide adequate enough information on their own on the hazard potential of a compound in an *in vivo* scenario (Elmore et al., 2014). This is mainly because, it is difficult to extrapolate effects seen *in vitro* such as non-specific cytotoxicity to an *in vivo* scenario (Elmore et al., 2014).

QSAR models have been previously created using biological data derived from zebrafish assays (Chen et al., 2012)(Ding et al., 2011)(Weimin et al., 2001)(Aldeco et al., 2011). However, these models have been restricted to particular biological endpoints and particular classes of compounds, such as triazoles or chloroanilines (Ding et al., 2011)(Weimin et al., 2001). Therefore, so far no QSAR model has been generated to cover compounds from different chemical classes with different mechanisms of action.

In this study a QSAR model was created using drugs from various chemical classes with different functions in order to cover the whole chemical space of pharmaceuticals. By including biological data derived from zebrafish embryo assays into the model the quality and also the predictive power of the model was increased. Using this approach, the aim was to generate a model where the general toxicity could be determined for any pharmaceutical regardless of its pharmacological class or chemical structure. This has not been done before and presents the real novelty of the QSAR model that was generated. In time, further zebrafish embryo assays could be performed using this 28 reference drug set to collect

further biological data that could be incorporated into the model, so as to increase its quality and also predictivity.

5.5.3 Influence of the zebrafish embryo chorion on drug penetration

In the zebrafish embryo toxicity and morphology studies performed it was found that ten compounds including erythromycin, hydrochlorothiazide, d-penicillamine, glipizide, levodopa, metformin, 6-thioguanine, prednisone, folate and riboflavin produced no or little toxicity.

In order to address the question whether the chorion presented a barrier to diffusion of these drugs into the zebrafish embryo preventing the generation of any morphological effects these drugs were re-examined for biological effects by dechorionating the zebrafish embryos before treatment. It was found there was no difference in the results obtained with or without the chorion. This shows that the non-responsiveness of these ten drugs was not due to the chorion acting as a barrier to drug diffusion.

The chorion represents an under-studied aspect of zebrafish embryo physiology. However, slowly more and more research is being done on it. A few zebrafish embryo studies have shown that with some types of compounds (particularly those with large molecular weights) the chorion can present a barrier to the diffusion of a drug into the zebrafish embryo (Henn and Braunbeck, 2011)(Kim et al., 2004)(Hagedorn et al., 1998). Particularly, in one of these studies it was shown that a high molecular weight cationic polymer Luviquat HM 522 only caused toxicity in dechorionated zebrafish embryos and not in zebrafish embryos with a

chorion (Henn and Braunbeck, 2011). However, in some cases a compound may not be able to diffuse into the zebrafish embryo even when it is dechorionated. This is seen with erythromycin which has to be injected directly into the zebrafish embryo in order for it to have an effect (Milan et al., 2003). These reported findings highlight that a bioanalysis test would be useful to determine whether compound uptake does occur in zebrafish embryos with or without a chorion.

As manual dechorionation or enzyme-mediated dechorionation using pronase is often time consuming and has low survival rates (Henn and Braunbeck, 2011), implementing dechorionation into large scale zebrafish drug screens has remained relatively unexplored. However, the latest advances in technology have meant that even automated zebrafish chorion removal is now possible, so that in the future dechorionation could be implemented into zebrafish embryo drug screens (Mandrell et al., 2012).

5.5.4 Comparability of zebrafish embryo toxicity data to rodent toxicity data

When comparing calculated logLC50 values to published rodent logLD50 values for the 28 reference drugs the correlation was found to be weak. Possibly if a larger number of drugs had been tested the correlation may have been stronger, as demonstrated in the study by Ali and colleagues where 60 drugs were tested (Ali et al., 2011). However, a difference in exposure routes between zebrafish embryos and mammals is probably the main reason for the weak correlation. Zebrafish embryos undergo constant water-borne drug exposure and receive drugs mainly by dermal diffusion, whereas rodents are exposed to drug as a single dose orally. This means in zebrafish embryos the liver is by-passed and the drug directly

enters the systemic circulation. This could lead to differences in internal drug concentrations between the two species. Therefore, determining the plasma drug concentrations at the LC50 may be more representative, as has been shown when *in vitro* LC50 values are compared to plasma concentrations at the LC50 (LC50plasma) (Ekwall et al., 1998) (Sjöström et al., 2008).

Additional reasons for the weak correlation between zebrafish logLC50 and rodent logLD50 values could be due to differences in metabolism, particularly species specific sensitivity with zebrafish embryos more sensitive to certain types of drugs compared to rodents and vice versa (Ali et al., 2011).

Despite the weak correlation, some drugs did show similar toxicities between the three species, such as in the case of sulindac and doxorubicin. However, a few drugs showed big differences between species. These included for example, l-thyroxine which was found to be extremely toxic in zebrafish embryos compared to rodents and amiloride which was found to be less toxic in zebrafish embryos than in rodents. Particularly, compounds containing a carboxylic acid (COOH) functional group with the exception of folate and fenofibrate were found to be more toxic to zebrafish embryos than rodents. Amines, particularly chlorprothixene were found to be extremely toxic to zebrafish embryos compared to rodents. Overall, it could be seen that the more lipophilic drugs were the ones that were more toxic in zebrafish embryos than in rodents, presumably due to their ability to penetrate into the zebrafish embryo more efficiently to cause an effect.

5.5.5 Limitations of study and future perspectives

Despite the QSAR model generated using zebrafish embryo toxicity endpoints and morphology severity scores showing good predictivity for a validation drug set, the study used to create the model could have been improved. Particularly, the study design could have been improved by including a bioanalysis step. This could have involved performing a time course analysis to determine whether an equilibrium concentration has been reached. There is not enough known at the moment about the metabolism of different drugs in zebrafish embryos, hence bioanalysis could help in determining whether there are species-specific differences in metabolism and whether there are significant differences in the metabolism of certain drugs between zebrafish and humans. Additionally, the model could be improved in the future by characterising more drugs and by incorporating more biological data from other zebrafish embryo assays into the model. Including additional physiochemical descriptors such as rotatable bonds and metabolic stability may also improve the predictivity of the model in the future (Abraham et al., 2002). Additionally, as the QSAR model was generated using the severity scores only at one time point and concentration it may be biased. Therefore, the model could be improved in the future by including EC50 values for the severity scores.

The logLC50 values that were determined from the zebrafish embryo studies were found to show a weak correlation with published logLD50 values for rodents. As mentioned previously, the main reason for the weak correlation was probably the difference in exposure route between zebrafish embryos and rodents. Other reasons include differences in metabolism, exposure time, developmental stage and study design.

It also has to be said that the zebrafish embryo may not present the best model for predicting toxicity for all types of drugs and that a combination of different species may be needed to determine the toxicity of specific drug types. For example, to test the safety and efficacy of antibiotics rodents do not present a good model due to differences in intestinal flora which can result in outcomes not representative of the human situation (Billstein, 1994). Therefore, larger mammals (e.g. primates) are normally used for testing antibiotics. This supports the idea that the QSAR model generated using zebrafish embryo data should serve as a complementary model to existing techniques already in place. It can be envisaged that the QSAR model is implemented early on in drug development to exclude those compounds showing very high toxicity, as those are also likely to show toxicity in rodents and higher mammals. For compound classes where it is known that the zebrafish shows species-specific differences to mammals the results from the QSAR model would need to be evaluated with caution and preferably double-checked *in vivo* in an appropriate animal model where a species-specific difference is known not to occur.

5.6 Conclusion

A QSAR model which was developed by characterising a reference drug set in zebrafish embryos could be used as a predictive tool to predict the toxicity of similar structured compounds in zebrafish embryos. Additionally, due to the many similarities between zebrafish and humans particularly in terms of toxic responses, this model could also be used to predict human toxicity.

Despite the model showing limitations with further refinement it has the potential in the future to be implemented into pre-clinical testing routines for hazard risk assessment where it could save money, time, reduce the number of animals tested and in the long-term potentially also save lives by excluding those drugs with toxicity potential early on in the drug development process.

Chapter Six: CHARACTERISATION OF THE ANTI-INFLAMMATORY RESPONSES OF A 28 REFERENCE DRUG SET IN ZEBRAFISH LARVAE

Foreword:

All the work presented in this chapter was performed by me with supervision from Dr. Clemens Grabher and Dr. Urban Liebel. Christine Wittmann provided initial support with carrying out ChIn assays and Dr. Luke Pase provided initial support with carrying out HyPer assays. All analysis was performed solely by me. The automated image analysis tool was developed by Dr. Urban Liebel and Dr. Markus Reischl.

6.1 Introduction and Overview

6.1.1 Zebrafish immune system

The zebrafish presents a good model for investigating the immune system and its responses, particularly as the innate and adaptive immune system are conserved between mammals and teleosts (Meeker and Trede, 2008). In adult zebrafish the kidney is the functional equivalent of the human bone marrow generating all the components of a functioning immune system (Meeker and Trede, 2008)(Lieschke et al., 2001).

6.1.2 Zebrafish innate immune system

The innate immune system which is the first line of defence against infection or mechanical damage mainly comprises leukocytes (white blood cells) which consist of macrophages and neutrophils (Meeker and Trede, 2008)(Lieschke et al., 2001). At around 15 hpf embryonic macrophages are present which originate from the rostral blood compartment and travel to the yolk expressing the marker *pu.1*; at later stages the marker lysozyme C is expressed (Meeker and Trede, 2008)(Hall et al., 2007). Once the circulatory system has formed, macrophages spread to several tissues phagocytising cell debris and clearing bacteria from the circulation (Herbomel et al., 2001). Neutrophils are produced at around 48 hpf and originate from the intermediate cell mass (ICM) (Hall et al., 2007). Neutrophils which are from the heterophil lineage have a multi-lobed nucleus and express a neutrophil specific protein myeloperoxidase (zMPO) (Meeker and Trede, 2008). In fully developed adult zebrafish there are two main granulocyte lineages; the heterophil lineage and the eosinophil lineage (Lieschke et al., 2001). Eosinophils (involved in combating parasites) have a non-segmented nucleus and have only been identified in adult zebrafish (Lieschke et al., 2001).

6.1.3 Zebrafish adaptive immune system

In zebrafish the adaptive immune system which is the second line of defence against infection or mechanical damage develops late after around 4-6 weeks (Meeker and Trede, 2008). The adaptive immune system is comprised of T cells, B cells and natural killer (NK) cells. T cells which are involved in mediating the immune response and directly getting rid of infected cells undergo differentiation in the thymus before migrating to various tissues, such as the skin (Meeker and Trede, 2008). T cell receptors, MHC class I, II and III proteins have all been identified in zebrafish and the T cell receptors have been shown to undergo V(D)J recombination like in mammals (Meeker and Trede, 2008). In zebrafish B cells are initially produced in the pancreas and later produced in the kidney (Meeker and Trede, 2008). B cells produce antibodies against various antigens (Meeker and Trede, 2008). Zebrafish B cells are able to undergo V(D)J rearrangements like in mammals and can produce the mammalian antibody subtypes IgD and IgM (Meeker and Trede, 2008). In zebrafish the complement system and homologs of toll-like receptors have also been identified (Meeker and Trede, 2008). The NK cells which also form part of the innate immune response eliminate diseased cells (Goldsmith and Jobin, 2012).

6.1.4 Zebrafish as a model for studying inflammation

Inflammation is a natural mechanism that ensues following damage to tissue by either a physical wound or infection. Inflammation is characterised by infiltration of immune cells such as macrophages and granulocytes by chemotaxis to the wound site following release of pro-inflammatory mediators. These pro-inflammatory mediators include hydrogen peroxide, chemokines and cytokines (d' Alençon et al., 2010)(Nomiyama et al., 2008)(Lieschke, 2001).

The inflammatory processes are well conserved between zebrafish and humans (Meeker and Trede, 2008). For example, orthologues of the human chemokine CXCL12 and the human cytokine interleukin 1β are present in zebrafish (d' Alençon et al., 2010)(Nomiyama et al., 2008)(Lieschke, 2001).

To study the inflammatory process in zebrafish, wounding of the tail-fin can be carried out which attracts inflammatory cells to the wound site (Meeker and Trede, 2008). Macrophages which are located in perivascular locations will travel to the wound site due to chemotaxis and phagocytise cell debris (Meeker and Trede, 2008). Neutrophils will undergo morphology changes as they migrate to the wound site by producing a pseudopod (Mathias et al., 2006). After arriving at the wound some neutrophils will move around the wound site, whereas others will stop and take on a globular structure (Mathias et al., 2006). During resolution of inflammation, the leukocytes will migrate back to the vasculature; this differs from humans where normally neutrophils are apoptosed following resolution (Meeker and Trede, 2008).

Using fluorescently labelled macrophages and neutrophils; migration of immune cells can be visualised in real time in zebrafish (Meeker and Trede, 2008). Inflammation can be induced in zebrafish larvae through chemical treatment (e.g. copper sulphate) or mechanical damage (e.g. tail-fin wounding) (Mathias et al., 2006). The zebrafish therefore enables inflammation to be studied down to cellular resolution offering many advantages over other animal models where tissues are not transparent hampering the possibility of imaging immune cells and *in vitro* assays where only individual components of the immune response can be studied at one time.

6.1.5 Chemically induced inflammation (ChIn) assay

By inducing inflammation in zebrafish larvae therapeutic drug screens can be performed to detect anti-inflammatory compounds. Particularly, the zebrafish tail-fin wounding assay has been extensively used for this purpose (Mathias et al., 2006)(Ellett et al., 2011)(Loynes et al., 2010)(Mathias et al., 2009). Despite the many advantages of the tail-fin wounding assay it does have its drawbacks in that it is low throughput, takes a lot of time and requires some technical ability to perform consistently (Renshaw and Ingham, 2010). With this in mind a chemically induced inflammation (ChIn) screening assay was generated using zebrafish larvae (d' Alençon et al., 2010). In this assay, hair cells which are located in neuromasts and form the lateral line of the zebrafish are damaged to induce an inflammatory response (d' Alençon et al., 2010)(Williams and Holder, 2000)(Ghysen and Dambly-Chaudière, 2004). A double transgenic zebrafish line Tg(*cldnB:GFP*);Tg(*lysC:DsRed2*) where the neuromasts fluoresce green under GFP and the leukocytes fluoresce red under DsRed is utilised in the ChIn assay (Williams and Holder, 2000)(d' Alençon et al., 2010)(Hall et al., 2007). For the ChIn assay zebrafish larvae at 3 dpf are used, as they have established a primitive lateral line at this stage of development (d' Alençon et al., 2010).

To induce hair cell damage in the Chin assay copper sulphate is used, which induces oxidative stress and causes leukocytes to migrate to neuromasts (Olivari et al., 2008)(Yoong et al., 2007). Once arrived there, the leukocytes will remain there for several hours (d' Alençon et al., 2010). After around 6 hours following the removal of copper leukocytes start to migrate away from the neuromasts (d' Alençon et al., 2010).

In brief, the ChIn assay involves using 3 dpf zebrafish larvae from the transgenic line Tg(*cldnB:GFP*);Tg(*lysC:DsRed2*) where the neuromasts and leukocytes are fluorescently labelled (see section **6.3.3** for full method). The zebrafish larvae are incubated with compound for one hour before subsequent incubation in copper sulphate for one hour (d' Alençon et al., 2010). Copper is then washed off and the zebrafish larvae are anaesthetised before being individually positioned laterally in wells of a 384 well plate for subsequent automated fluorescence imaging. Images are analysed automatically enabling the quantification of leukocytes within neuromasts. Compounds with anti-inflammatory properties will reduce the number of leukocytes occupying the neuromasts. Hence, the ChIn assay can be used to perform large scale screens for the detection of anti-inflammatory compounds.

6.1.6 Role of hydrogen peroxide in inflammation

Hydrogen peroxide belongs to the reactive oxygen species (ROS) group and is generated as a side product of metabolism or deliberately produced by cells (e.g. neutrophils) to initiate a respiratory burst to kill bacteria (Wittmann et al., 2012). Recently using zebrafish, hydrogen peroxide was found to play a vital role in the recruitment of inflammatory cells to a site of injury by forming a gradient, which attracts immune cells to the site of injury (Niethammer et al., 2009). The gradient is formed by the activity of a specific class of the nicotinamide dinucleotide monophosphate (NADPH) oxidases known as dual oxidase (Duox), which is able to generate hydrogen peroxide directly (Wittmann et al., 2012). In zebrafish neutrophils a kinase from the Src family known as Lyn was discovered and was found to have a role in guiding neutrophils to wound sites by detecting the levels of hydrogen peroxide (Yoo et al.,

2011)(Wittmann et al., 2012). Additionally, it was found that when the Duox enzyme was inhibited and no hydrogen peroxide was generated by epithelial cells Lyn could not perform its function preventing the migration of neutrophils to wound sites (Yoo et al., 2011). These studies showed that hydrogen peroxide plays an important role in initiating inflammation by guiding neutrophils to sites of damage.

6.1.7 *In vivo* visualisation of leukocytes and hydrogen peroxide levels following acute inflammation in zebrafish larvae

As mentioned above hydrogen peroxide performs an important function in initiating inflammation. The zebrafish transgenic line Tg*(lyz.HyPer)* which has the hydrogen peroxide sensor fluorophore HyPer can be used to monitor hydrogen peroxide levels *in vivo* (Belousov et al., 2006). HyPer has two excitation maxima at 420 and 500 nm with high hydrogen peroxide levels emitting more light when excited at 500 nm compared to 420 nm (Pase et al., 2012). The ratio between these two can be calculated to determine differences in hydrogen peroxide levels over time (Pase et al., 2012). Using this approach, the HyPer assay can be used to screen for anti-oxidants.

In brief, the zebrafish HyPer assay is performed by inducing inflammation in 3 dpf Tg*(lyz.HyPer)* zebrafish larvae by cutting the caudal fins (see section **6.3.4** for full method). Following cutting of the caudal fins, the zebrafish larvae are anaesthetised and immobilised in low melting point agarose and imaged using an automated fluorescence microscope. Ratiometric analysis (determination of the ratio between two fluorescence intensities) is then performed to quantify changes in the levels of hydrogen peroxide over time.

6.2 Aims

Anti-inflammatories represent a large market worldwide due to their many disease indications, as a large number of diseases have an inflammatory component (Masferrer and Needleman, 2000). There is continually ongoing research to identify novel compounds with anti-inflammatory properties (Ehrman et al., 2010). However, there has also been growing interest to identify existing marketed compounds which have been marketed for other indications to see if they have possible anti-inflammatory effects not previously documented (Nath et al., 2009).

Based on this the main aim of this work was to determine the potential anti-inflammatory activity of the 28 reference drug set characterised in **Chapter 5** firstly using a manual assay and secondly a high throughput automated fluorescence-based assay (d' Alençon et al., 2010).

6.3 Methods

The anti-inflammatory activity of the 28 reference drugs was firstly characterised by performing a manual tail-fin wounding assay followed by an automated high throughput chemically induced inflammation (ChIn) assay. Positive hits from these assays were then verified by performing SYTOX® blue staining. Additionally, these hits were also tested for anti-oxidant activity using the HyPer assay.

6.3.1 Sudan black staining

Sudan black staining was used to visualise leukocytes. To perform Sudan black staining zebrafish larvae at 3 dpf were firstly exposed to drug for one hour before being anaesthetised in 0.02% MS222. The caudal fin tips were then cut and the zebrafish larvae were allowed to recover in E3 embryo medium for three hours. After the recovery period the zebrafish larvae were fixed in 4% PFA in PBS (1 mL) for two hours at room temperature. The zebrafish larvae were then washed twice with PBST (1 mL) and stained with 60 µL Sudan black reagent (Sigma-Aldrich, Germany) for 20 minutes. After 20 minutes, the stain was washed off thoroughly with 70% ethanol (1 mL) in three washes of 1, 5 and 10 minutes. The zebrafish larvae were then washed twice with PBST (1 mL). To remove pigment and aid counting of cells, the stained zebrafish larvae were treated with 1% hydrogen peroxide and 1% potassium hydroxide solution for 15 minutes at room temperature. After this time the solution was replaced with PBST and the samples were stored at 4°C until required for use. To quantify the number of neutrophils at the wound site, the end of the notochord until the site of the tail cut was used as the region for counting (see **Figure 6.1**).

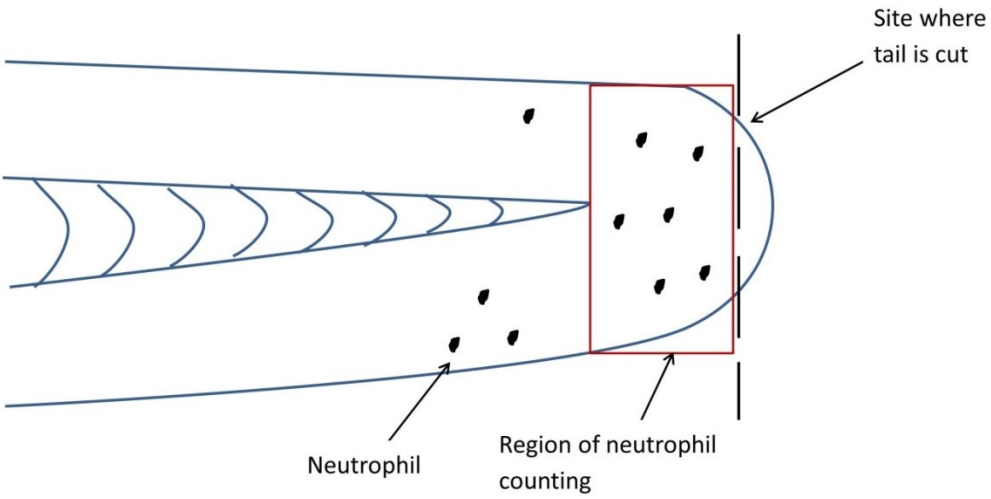

Figure 6.1 – Depiction of the area used for counting the number of leukocytes after cutting the tail fins of 3 dpf zebrafish larvae. *Neutrophils are represented by black dots and dashed lines mark area of cut. Tail is shown from left to right with the tail tip on the right.*

Leukocytes were counted at the wound site using a Leica MZF10 fluorescence stereo microscope (Leica, Germany). The experiment was repeated three times for each concentration and final results were averaged.

6.3.2 SYTOX® blue staining

SYTOX® blue staining was performed to detect copper chelation that could occur due to interaction of copper with certain drugs resulting in the formation of a copper-drug complex. To test for copper chelation, 15 zebrafish larvae at 3 dpf were tested per drug/control.

All 28 drugs were prepared at a concentration of 10 µM along with a control solution (1% DMSO). The zebrafish larvae were first cleaned and then separated into wells of a six well plate with 60 zebrafish larvae placed in each well. SYTOX® blue stain (Sigma-Aldrich, Germany) at a concentration of 5 µM was prepared using E3 embryo medium from an initial stock solution of 5 mM. The stain was then added to each well at a volume of 5 mL and then left to incubate for two hours at 28°C. After incubation, the stain was washed off three times with E3 embryo medium and the zebrafish embryos were transferred in groups of 15 to one well of a 24 well plate. To each well a different drug at a concentration of 10 µM was added at a volume of 1 mL. To one of the wells a control solution of 1% DMSO was added and to the other E3 embryo medium was added. The plate was then left to incubate for one hour at 28°C. After incubating for one hour, 1 mL of 20 µM copper sulphate (Merck Millipore, Germany) solution was added to each well except to one of the 1% DMSO control wells to give a final concentration of 10 µM of copper in each well. The whole plate was then left to incubate for one hour at 28°C. After this time the zebrafish larvae in each individual well

were observed using the CFP filter on a Leica MZF10 fluorescence stereo microscope (Leica, Germany) with set exposure parameters (brightness=26%, pseudo-colours=511 nanometres (nm), gain=X1 and exposure time=1000 milliseconds (ms)).

The same procedure outlined above was then repeated for three drugs (sulindac, chlorzoxazone and tetracycline) at a concentration of 100 µM. In each case the experiment was repeated three times and the fluorescence intensity was noted.

6.3.3 Chemically induced inflammation (ChIn) assay

The chemically induced inflammation (ChIn) assay was performed in order to determine the anti-inflammatory potential of the 28 reference drugs. Zebrafish larvae at 3 dpf from the transgenic line Tg*(cldnB:GFP)(lyz:DsRed2)nz50* were separated into batches of 16 zebrafish larvae and distributed into a six well plate. To the wells E3 + 1% DMSO (4 mL) was added. Drugs were made up to a concentration of 30 µM from their initial stock solutions using E3 embryo medium. Drugs were then added at 2 mL to each of the wells giving a final dilution of 10 µM in each well. To four of the wells only 2 mL of 1% DMSO was added. These wells served as the controls. The plates were then incubated at 28°C for one hour. After one hour, copper sulphate stock solution (20 mM) was diluted in E3 embryo medium to make 20 mL of a 70 µM dilution. To each well except to two of the 1% DMSO control wells 1 mL of the 70 µM copper sulphate stock solution was added to give a final copper sulphate concentration of 10 µM in each well. The plates were then incubated for another hour at 28°C.

After incubation for one hour, all the wells were washed with E3 embryo medium and replaced with a solution consisting of E3 embryo medium, 1% DMSO and 0.02% MS222. A multipette® plus multi-pipette (Eppendorf, Germany) was then used to fill each well of a 384 well plate (Greiner Bio-One GmbH, Germany) with 20 µL of the above solution. The zebrafish larvae were then transferred individually in a volume of 80 µL to a well in the 384 well plate. One drug was allocated one column on the 384 well plate. Two columns were assigned to the 1% DMSO controls (columns 1 and 24) and two to the positive copper controls (columns 2 and 23). After transferring all the zebrafish larvae to the 384 well plate, each individual zebrafish larva was positioned laterally in the well within an hour of removal of copper sulphate to make sure the inflammatory response did not diminish before imaging was performed.

Imaging of each well was performed using a Scan^R screening microscope (Olympus Biosystems, Germany) with images taken under brightfield (25 ms), cyanine 3 (300 ms) and GFP (350 ms) every hour over six hours with a 4X objective (ULAPO). Images were acquired in four dimension z-slices with a distance of 50 µm. The detection of the zebrafish larvae in the wells was automated using an autofocus algorithm. After image collection, the images were processed using LabView Vision (National Instruments, Germany) with scripts written in ImageJ version 4.2 (http://rsbweb.nih.gov/ij/) by Markus Reischl (KIT, Germany). This enabled sorting of brightfield and fluorescence images of each well into red-green-blue (RGB) overlay images as extended focus projections. Using these sorted images the number of leukocytes (coloured red) occupying the neuromasts (coloured green) was automatically quantified (**Figure 6.2**). This was used as a measure of the inflammatory response.

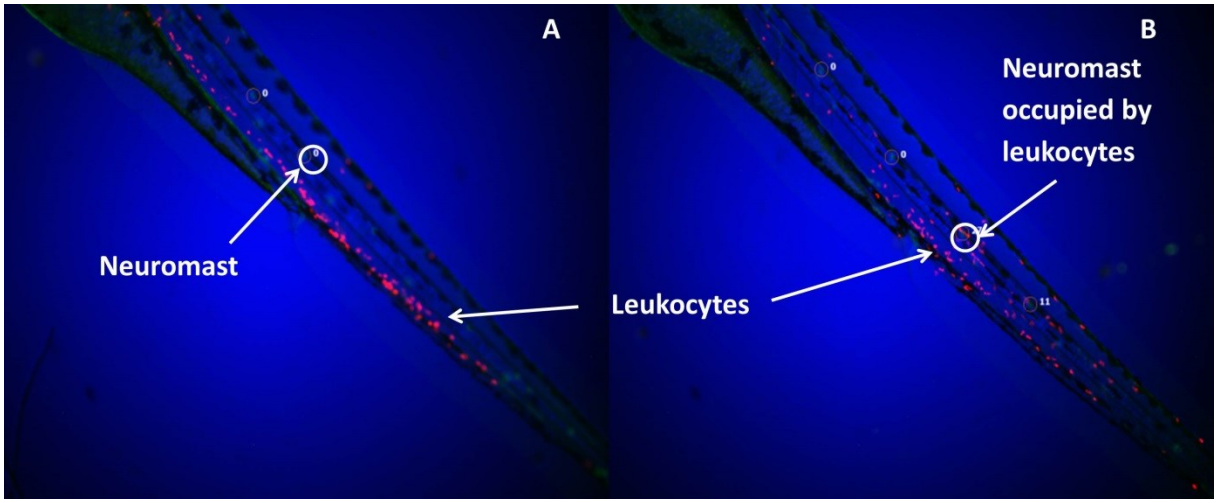

Figure 6.2 – Fluorescence analysis of leukocyte localization within neuromasts using the Tg(cldnB:GFP)(lyz:DsRed2)nz50 transgenic zebrafish line. *Lateral overlays (brightfield, GFP, DsRed) of: A) 3 dpf zebrafish larva treated with 1% DMSO only (negative control) and B) 3 dpf zebrafish larva treated with copper (positive control).*

Additionally, using MATLAB 7.11 R2010b (MathWorks, Germany) plots of the inflammatory response over time (**Figure 6.3**) were automatically generated from the sorted data.

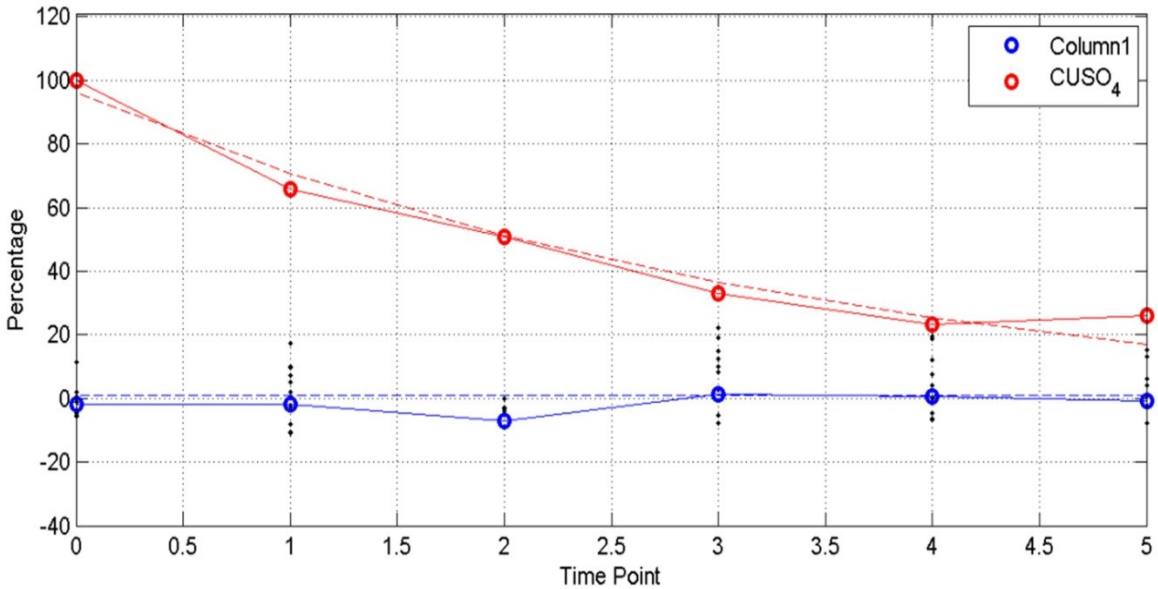

Figure 6.3 – Plot of inflammatory response over time for 1% DMSO control zebrafish larvae at 3 dpf. *Red line = percentage increase in inflammatory response after treatment of zebrafish larvae with copper, blue line = percentage increase in inflammatory response after treatment of zebrafish larvae with 1% DMSO.*

Tabulated values were also generated which were used to solve the equation $e^{(a0 + a1x)}$ with a0 representing the initial inflammatory response, a1 the resolution of inflammation (slope of the curve) and x the time point. By substituting x for 0, the initial inflammatory response (%) = e^{a0} X 100 could be calculated by inserting the value for a0 into the equation.

The threshold for the initial anti-inflammatory response was set at ≤50%. Drugs with initial anti-inflammatory responses above this threshold were considered not to present with significant anti-inflammatory activity.

6.3.4 HyPer zebrafish assay (*In vivo* quantification of hydrogen peroxide levels)

To quantify the levels of hydrogen peroxide produced during an acute inflammatory response in 3 dpf zebrafish larvae, a Tg*(lyz.HyPer)* transgenic zebrafish line containing the hydrogen peroxide sensor fluorophore HyPer was utilised. Zebrafish larvae obtained from this line were first sorted so as to ensure that only those zebrafish larvae showing expression throughout the whole body were chosen for experimentation. After sorting, two zebrafish larvae were incubated in 4 mL of either 1% DMSO or drug solution at a specified concentration for one hour before adding 200 µL of 0.4% MS222 to give a final concentration of 0.02% MS222 in each well. The caudal fins were then cut and the zebrafish larvae were then transferred to a PELCO® clear well glass bottom dish (PLANO GmbH, Germany) with 500 µL of liquid. The zebrafish larvae were then sucked up in a Pasteur pipette together with molten 1.5% low melting point agarose (PEQLAB, Erlangen, Germany). The two zebrafish larvae were then arranged laterally with the tail tips positioned opposite one another. The Scan^R screening microscope (Olympus Biosystems, Munich, Germany)

was then used to take brightfield images (25 ms) and fluorescence images with the FITC-Hyper channel (150 ms) using the excitation filter FF01-425-/30-25 for HyPer low and the FF01-482/35-25 excitation filter for HyPer high every minute over 60 minutes.

ImageJ version 4.2 (http://rsbweb.nih.gov/ij/) was then used to perform a ratiometric analysis on the captured images by calculating ratios for HyPer low/HyPer high. This was done by firstly opening the image sequence for a specific dataset in non-numerical order. The channels were then split into brightfield, HyPer low and HyPer high and saved separately as TIFF files. For each channel an area in the background was then selected (area without tail in view) and subtracted using a scaling factor of one. Both the HyPer low and HyPer high channels were then converted to 32 bit images and thresholding was performed using the default settings on ImageJ and a NaN background. Using this function, only the tails themselves were outlined excluding background artefacts and saturated pixels. The image calculator function was then used to divide the HyPer high by the HyPer low channel. The resulting stack was then thresholded as before and the brightness and contrast were set to values in the range of 0.6 and 2.2, respectively. The lookup table function was then used to produce a 16 colour stack where different colours indicated different pixel intensities.

In most cases before ratiometric analysis could be performed tail movement had to be corrected for as the tail tip needed to be fixed in the same place to perform accurate analysis. To correct for tail movement, each tail was analysed individually by first drawing a box around the tail tip and then duplicating this part of the stack. The duplicated stack was then multiplied by 1000 before being converted to a 16 bit stack in order to retain the pixel

values. The rigid body function on the stackreg plug-in was then used to correct for tail movement. Once this was done, the stack was converted back to 32 bit and divided by 1000.

For the ratiometric analysis a small box was drawn around the tail tip at the site of the cut. Using the T-functions plug-in an intensity time monitor plot was generated to show the changes in pixel intensity values over the 60 minute time period. The pixel values obtained from this plot were averaged for each drug treatment. For each drug in total eight zebrafish larvae were tested. An outline of the whole image analysis process is shown in **Figure 6.4**.

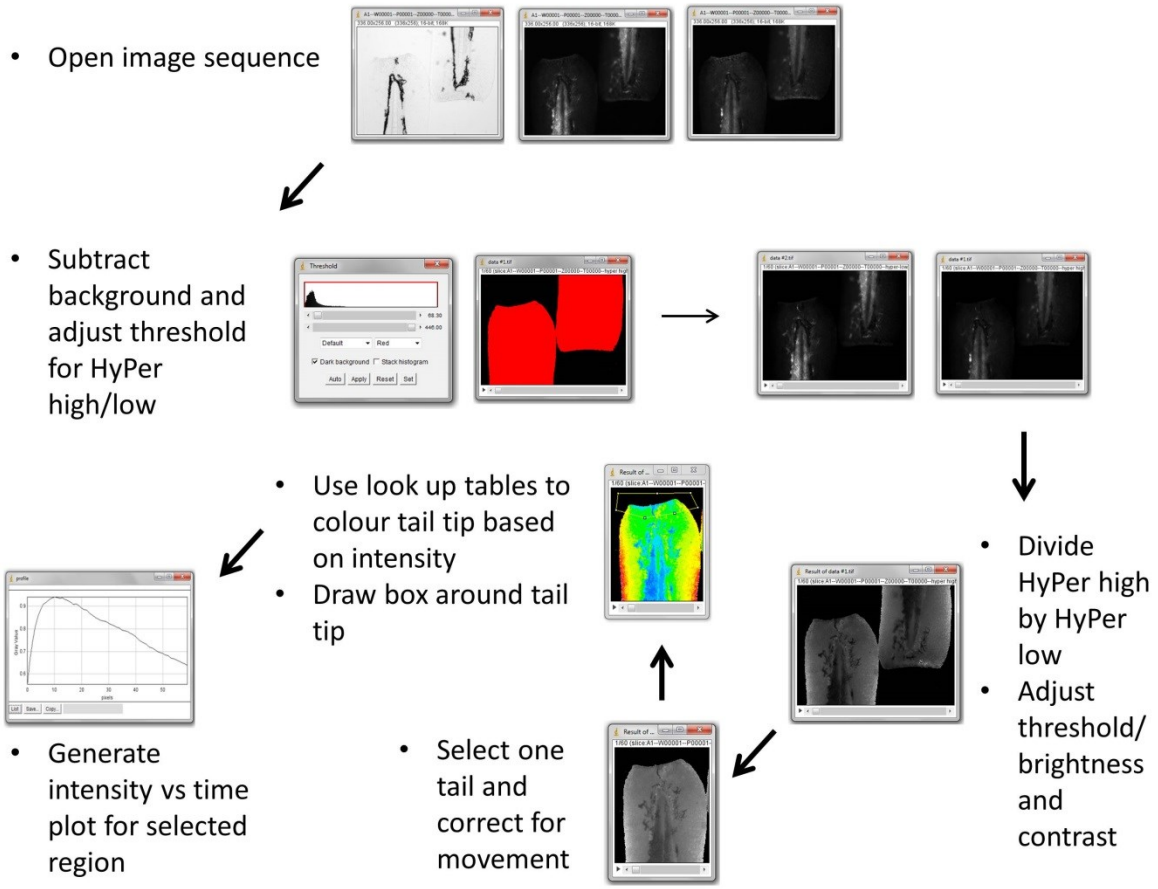

Figure 6.4 – Outline of image analysis process for hydrogen peroxide ratiometric analysis.

For the HyPer assay only malathion (10 µM), meclizine (100 µM), chlorzoxazone (100 µM) and d-penicillamine (100 µM) were tested out of the 28 reference drug set.

6.4 Results

6.4.1 Tail-fin wounding

To determine the anti-inflammatory activity of the 28 reference drugs, initially a tail-fin wounding assay was carried out in order to get a broad overview of the possible anti-inflammatory responses of these drugs.

Manual tail-fin wounding for all 28 reference drugs was initially carried out at a concentration of 10 µM for each drug. This involved treatment of 3 dpf zebrafish larvae with each drug at a concentration of 10 µM followed by cutting of caudal tail fins, fixation and staining with Sudan black, as outlined in section **6.3.1**. The experiment was repeated three times and the average leukocyte count for each treatment/control group was calculated (**Figure 6.5**). It was observed that malathion, metformin, terfenadine, meclizine and thiamazole all significantly decreased the mean number of leukocytes compared to the cut control (**Figure 6.5**, n=45 zebrafish larvae at 3 dpf per drug/control, $P<0.05$). The uncut control showed staining of leukocytes mainly in the caudal vein as expected (Herbomel et al., 1999). Both of the positive controls in this assay sulindac and prednisone (known anti-inflammatory agents) on the other hand had no significant effects on reducing leukocyte number at the wound site (**Figure 6.5**, n=45 zebrafish larvae at 3 dpf per drug/control, $P>0.05$). This may have been due to the concentration of drug used being too low to induce an effect or due to ineffective penetration of the drugs into the zebrafish larvae.

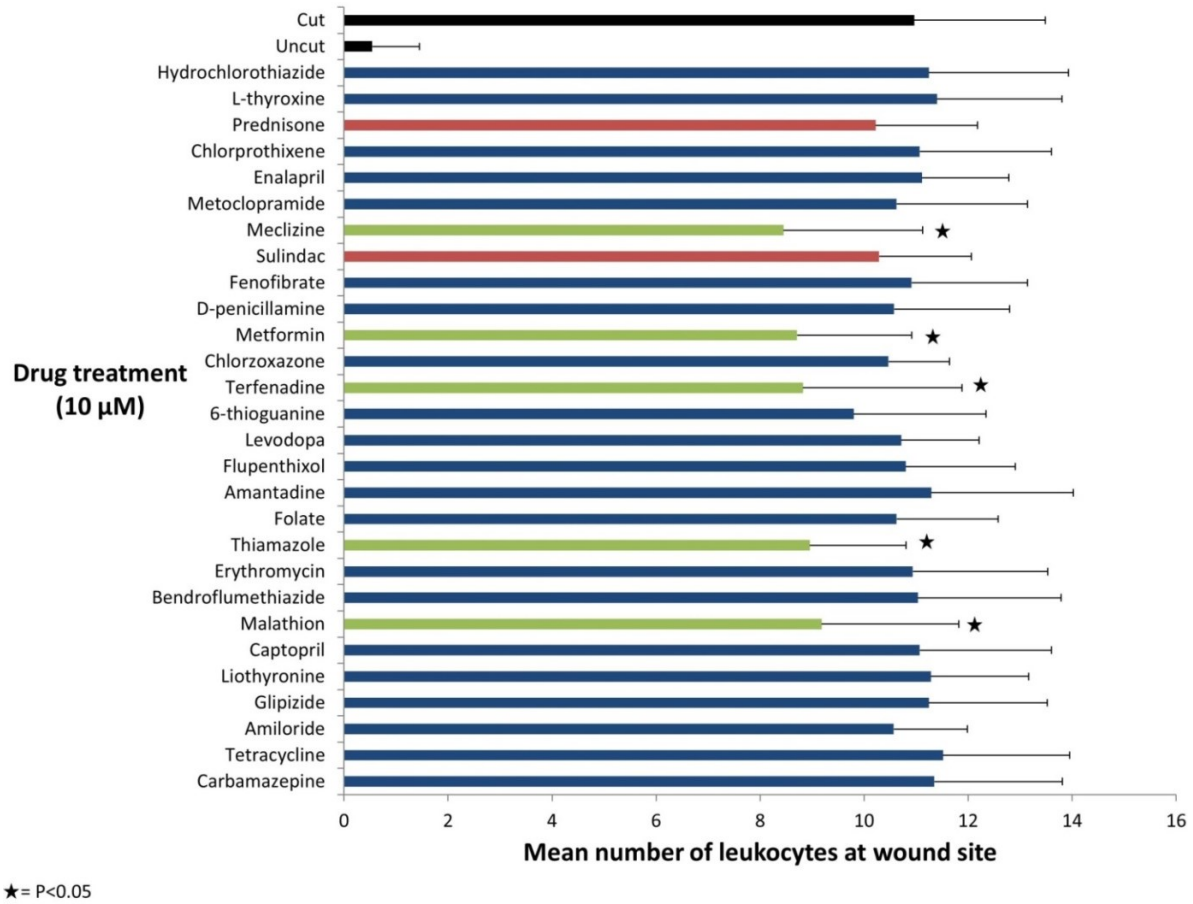

Figure 6.5 – Anti-inflammatory responses of 28 reference drugs at 10 µM after tail-fin wounding of zebrafish larvae. *Treatments were initiated at 3 dpf (n=45 zebrafish larvae at 3 dpf per drug/control, P<0.05 for meclizine, metformin, terfenadine, thiamazole and malathion, P>0.05 for rest). Key: red = positive controls, green = drugs that significantly reduce the leukocyte count at the wound site, black = untreated cut and uncut controls*

Manual tail-fin wounding was also performed at a higher concentration of 100 μM (**Figure 6.6**). Terfenadine, chlorprothixene, flupenthixol and malathion could not be evaluated at the higher concentration as they caused toxicity (heart edema, cellular necrosis and hypoxia), so they were therefore not included in the results.

It was found that thiamazole, chlorzoxazone, meclizine and metformin at 100 μM all significantly reduced leukocyte number at the wound site compared to the cut control (**Figure 6.6**, n=45 zebrafish larvae at 3 dpf per drug/control, $P<0.05$). The staining in the uncut control was as expected (mainly in the caudal vein). Additionally, one of the positive controls (sulindac) was also found to significantly reduce the leukocyte number at the wound site (**Figure 6.6**, n=45 zebrafish larvae at 3 dpf per drug/control, $P<0.05$), whilst the other (prednisone) was found to have no effect (**Figure 6.6**, n=45 zebrafish larvae at 3 dpf per drug/control, $P>0.05$).

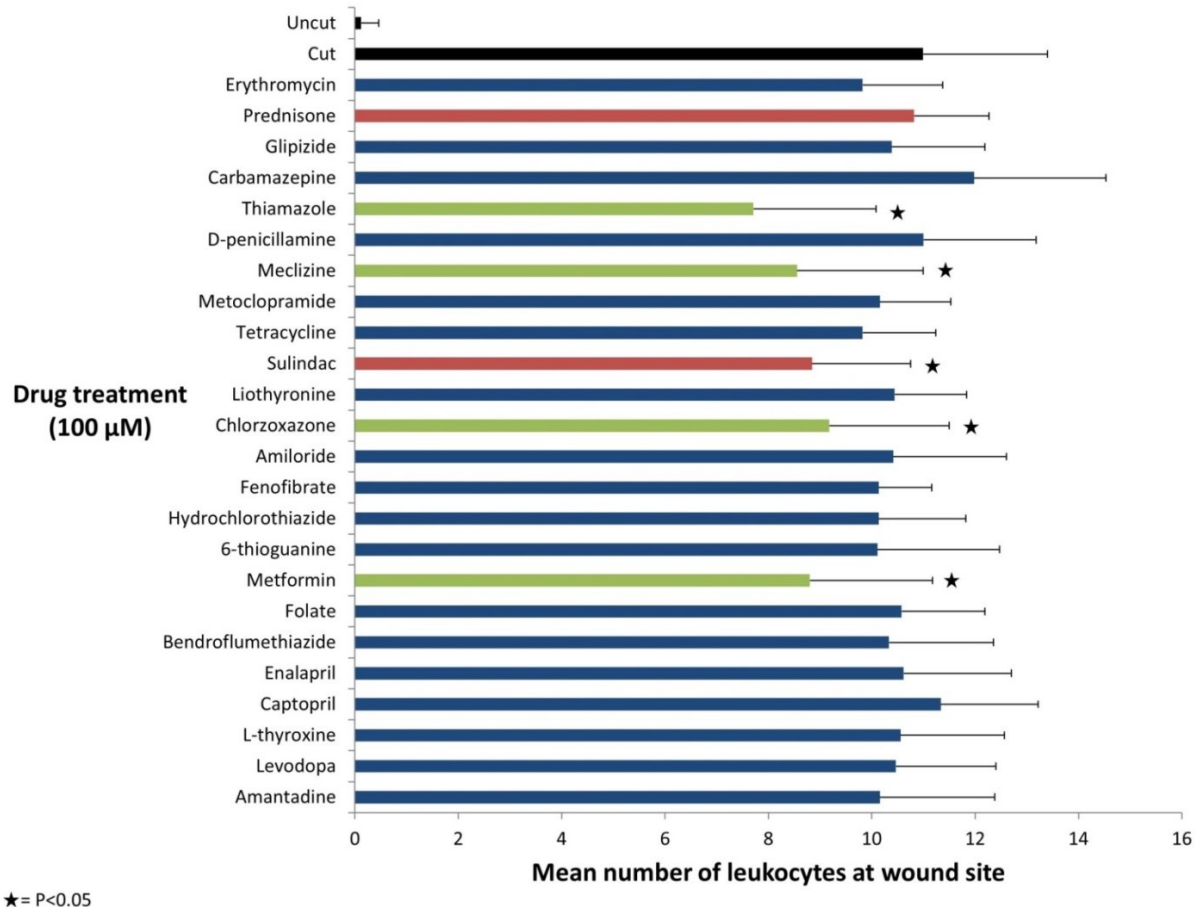

Figure 6.6 – Anti-inflammatory responses of 28 reference drugs at 100 µM after tail-fin wounding of zebrafish larvae. *Treatments were initiated at 3 dpf (n=45 zebrafish larvae at 3 dpf per drug/control, P<0.05 for d-penicillamine, meclizine, chlorzoxazone and metformin, P>0.05 for rest). Key: red = positive controls, green = drugs that significantly reduce the leukocyte count at the wound site, black = untreated cut and uncut controls*

6.4.2 Automated chemically induced inflammation assay (ChIn)

The next aim was to determine the anti-inflammatory activity of the 28 reference drugs via the automated ChIn assay. In brief, this was done by treating 3 dpf zebrafish larvae from the Tg*(cldnB:GFP)(lyz:DsRed2)nz50* transgenic line with drug for one hour, followed by treatment with copper sulphate for one hour to induce inflammation before subsequent imaging of the inflammatory response using an automated fluorescence microscope. Using the processed images the initial inflammatory response was calculated with a cut-off point for significant anti-inflammatory activity set at ≤50%.

As in the manual tail-fin wounding assay, all 28 reference drugs were initially tested at a concentration of 10 µM (**Figure 6.7**). It was observed that malathion, 6-thioguanine and thiamazole all caused a significant reduction in the inflammatory response under the cut-off point of 50% (**Figure 6.7**, n=48 zebrafish larvae at 3 dpf per drug/control, $P<0.05$ for malathion and thiamazole, $P<0.005$ for 6-thioguanine). One of the positive controls sulindac was also found to significantly reduce the inflammatory response below the cut-off point (**Figure 6.7**, n=48 zebrafish larvae at 3 dpf per drug/control, $P<0.05$). The other positive control prednisone however had no effect (**Figure 6.7**, n=48 zebrafish larvae at 3 dpf per drug/control, $P>0.05$). Terfenadine caused serious malformations (cardiac edema, reduced circulation, reduced heart rate and tail necrosis) of zebrafish larvae at 10 µM in the presence of copper sulphate, therefore its anti-inflammatory activity could not be evaluated using the ChIn assay.

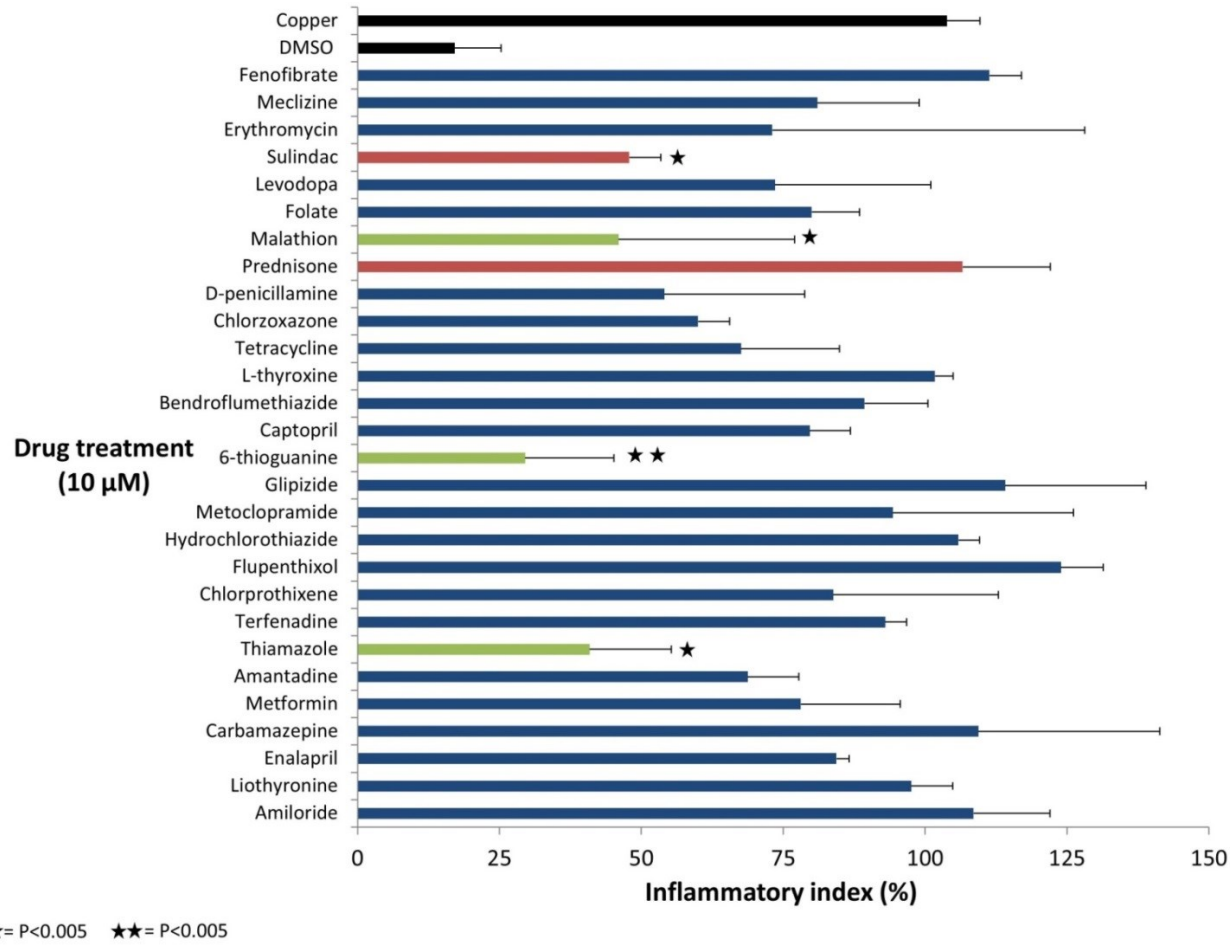

Figure 6.7 – Anti-inflammatory responses of the 28 reference drugs at 10 µM using the zebrafish ChIn assay. *Treatment was initiated at 3 dpf (n=48 zebrafish larvae at 3 dpf per drug/control, P<0.05 for thiamazole, malathion and sulindac, P<0.005 for 6-thioguanine). Key: red = positive controls, green = drugs significantly reducing the inflammatory response, black = DMSO and copper controls*

Similarly, at 100 µM all 28 reference drugs except terfenadine, chlorprothixene, flupenthixol and malathion were evaluated for anti-inflammatory activity using the ChIn assay (**Figure 6.8**). These drugs were excluded as they caused toxicity (cellular necrosis). It was found that levodopa, 6-thioguanine, d-penicillamine, thiamazole, chlorzoxazone, meclizine and tetracycline all significantly reduced the inflammatory response below the cut-off point of 50% (**Figure 6.8**, n=48 zebrafish larvae at 3 dpf per drug/control, $P<0.0005$ for levodopa, chlorzoxazone, 6-thioguanine, d-penicillamine, meclizine and tetracycline, $P<0.005$ for thiamazole). The positive control sulindac was also found to significantly reduce the inflammatory response below the cut-off point of 50% (**Figure 6.8**, n=48 zebrafish larvae at 3 dpf per drug/control, $P<0.0005$), whereas the other positive control prednisone again had no effect (**Figure 6.8**, n=48 zebrafish larvae at 3 dpf per drug/control, $P>0.05$).

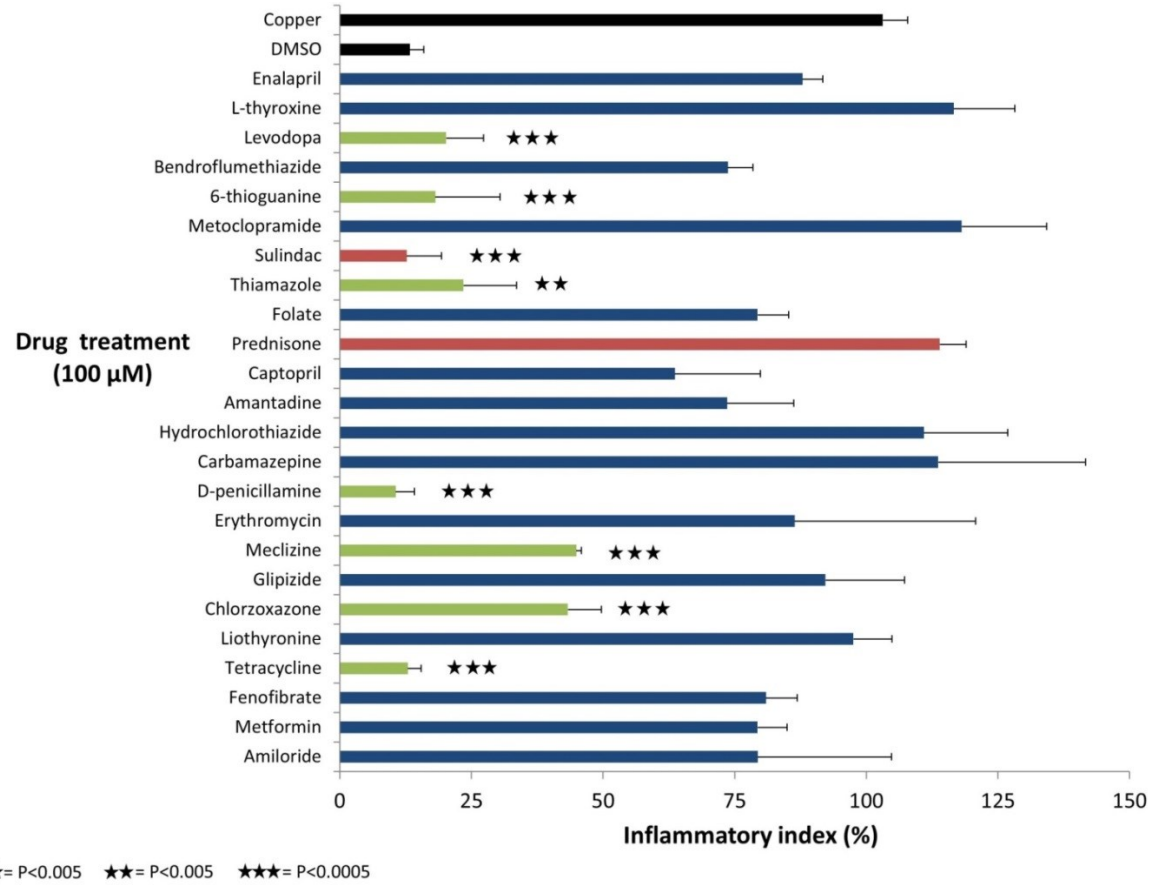

Figure 6.8 - Anti-inflammatory responses of the 28 reference drugs after treatment at 100 µM evaluated using the zebrafish ChIn assay. *Treatments were initiated at 3 dpf (n=48 zebrafish larvae at 3 dpf per drug/control, P<0.0005 for levodopa, 6-thioguanine, sulindac, d-penicillamine, meclizine, chlorzoxazone and tetracycline, P<0.005 for thiamazole). Key: red = positive controls, green = drugs significantly reducing the inflammatory response, black = DMSO and copper controls*

6.4.3 SYTOX® blue staining

To confirm the results obtained in the automated ChIn assay SYTOX® blue staining was performed. The SYTOX® blue nuclear stain which fluorescently labels neuromasts was used to exclude false positives that may have been generated after performing the ChIn assay. False positives may have arisen through the interaction of a drug with copper generating a drug/copper complex, thereby preventing an inflammatory response from being generated and thus exhibiting a negative control phenotype with reduced localization of leukocytes in neuromasts.

Initially, all 28 reference drugs were tested for copper chelation ability at a concentration of 10 µM using the SYTOX® blue stain (**Table 6.1**, n=15 zebrafish larvae at 3 dpf per drug/control). In brief, SYTOX® blue staining was performed by staining zebrafish larvae at 3 dpf for two hours with 5 µM SYTOX® blue, followed by washing off the stain, treating with drug solution for one hour before final incubation with copper sulphate for one hour. The neuromasts of the zebrafish larvae were then visualised using a fluorescence microscope and the extent of fluorescence was noted for each drug treatment group. Based on this each drug was classified as a strong copper chelator, a weak copper chelator or no copper chelator. It was found that thiamazole, 6-thioguanine and d-penicillamine were strong copper chelators (strong neuromast fluorescence still present), whereas levodopa, enalapril and captopril were weak copper chelators (weak neuromast fluorescence still present) (**Table 6.1**, n=15 zebrafish larvae at 3 dpf per drug/control).

Table 6.1 – SYTOX® blue staining results for 28 reference drugs at 10 µM.

Compound	Copper chelation
Thiamazole	√√
6-thioguanine	√√
D-penicillamine	√√
Levodopa	√
Enalapril	√
Captopril	√
Tetracycline	X
Erythromycin	X
Bendroflumethiazide	X
Hydrochlorothiazide	X
Metformin	X
Glipizide	X
Fenofibrate	X
Prednisone	X
Sulindac	X
Liothyronine	X
L-thyroxine	X
Amantadine	X
Carbamazepine	X
Amiloride	X
Malathion	X
Chlorzoxazone	X
Folate	X
Flupenthixol	X
Chlorprothixene	X
Metoclopramide	X
Terfenadine	X

Key: X = no response, √ = weak response, √√ = strong response

Tetracycline, sulindac and chlorzoxazone were also tested for copper chelation ability at 100 µM. It was found that tetracycline was an intermediate copper chelator at 100 µM contrary to what was seen at 10 µM. However, both sulindac and chlorzoxazone showed no copper chelation ability even at 100 µM.

After having performed the SYTOX® blue staining it was determined that out of the nine drugs showing a positive response in the ChIn assay (6-thioguanine, levodopa, thiamazole, tetracycline, sulindac, d-penicillamine, meclizine, malathion and chlorzoxazone) only four were true positives and did not interact with copper (malathion, sulindac, meclizine and chlorzoxazone). After having filtered out the false positives; the next step was to see whether there was a relationship between the drug concentration and the extent of inhibition of inflammation for these four drugs. Hence, malathion, sulindac, meclizine and chlorzoxazone were tested for anti-inflammatory activity using the ChIn assay at 50 µM. it was also of interest to determine whether there was a relationship between the drug concentration and the extent of copper chelation, so therefore thiamazole and tetracycline were also tested at 50 µM using the ChIn assay.

The results from the ChIn assay showed that both malathion and sulindac at 50 µM had anti-inflammatory index values below the cut-off point of 50% (**Figure 6.9A**, n=48 zebrafish larvae at 3 dpf per drug, $P<0.05$ for malathion, $P<0.005$ for sulindac). Chlorzoxazone and meclizine on the other hand were both found to have anti-inflammatory index values above the 50% cut-off point (**Figure 6.9A**, n=48 zebrafish larvae at 3 dpf per drug, $P<0.05$). Thiamazole at 50 µM was found to show strong copper chelation (anti-inflammatory index value ≤50%), whereas tetracycline at 50 µM was found to show weak copper chelation (anti-inflammatory index value >50%). When combining this data with the previous ChIn data at 10 µM and 100 µM for these drugs, it could be seen that even when using only three concentrations all six drugs showed some concentration-dependency (**Figure 6.9B**).

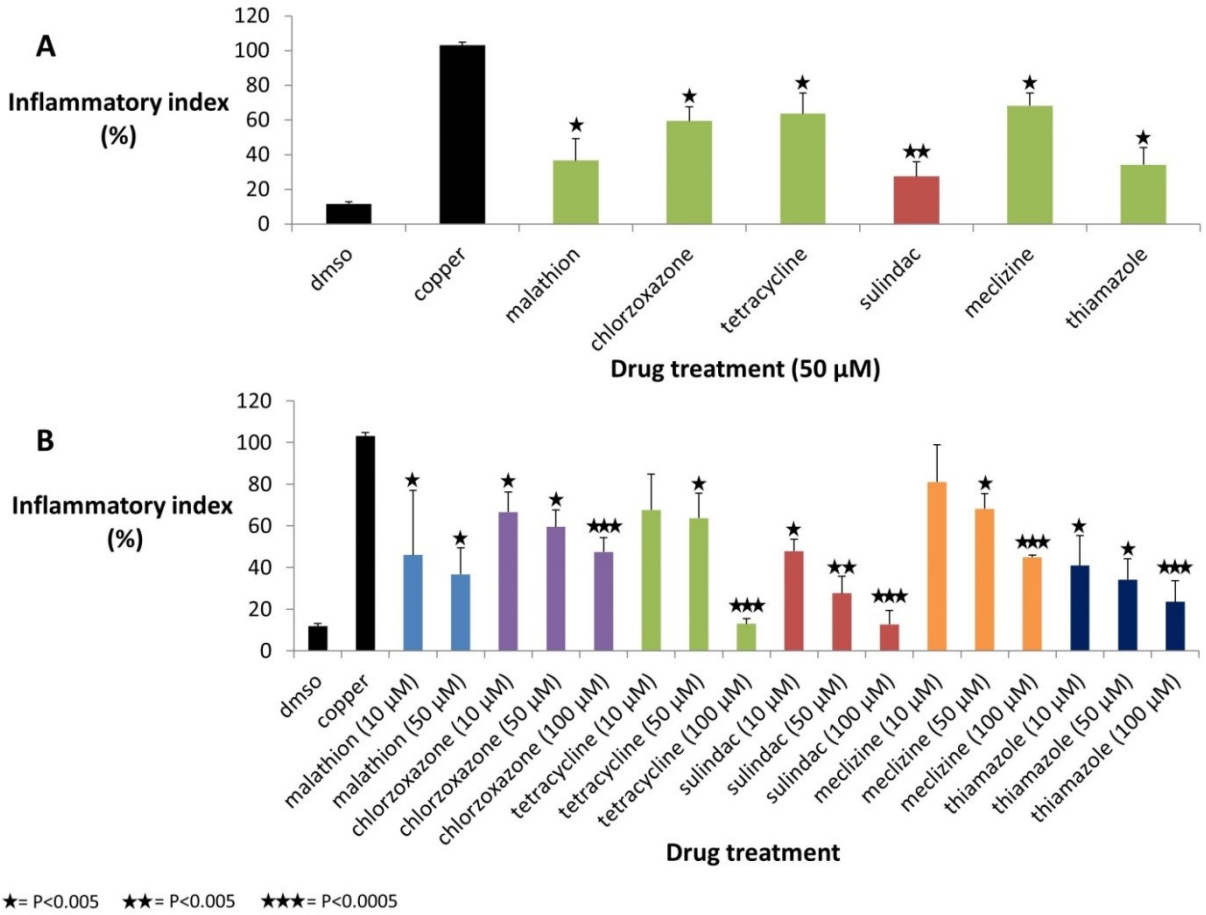

Figure 6.9 – Anti-inflammatory activity and extent of copper chelation observed with a selection of the 28 reference drugs evaluated using the zebrafish ChIn assay at 50 µM. *A) Responses observed with malathion, chlorzoxazone, tetracycline, sulindac, meclizine and thiamazole at 50 µM in the ChIn assay (n=48 zebrafish larvae at 3 dpf per drug/control, P<0.05 for malathion, chlorzoxazone, tetracycline, meclizine, thiamazole and P<0.005 for sulindac). Key: red = positive controls, green = drugs significantly reducing the inflammatory response, black = DMSO and copper controls. B) Overview of the responses observed in the ChIn assay for malathion, chlorzoxazone, tetracycline, sulindac, meclizine and thiamazole at 10, 50 and 100 µM (n=48 zebrafish larvae at 3 dpf per drug concentration/control, P<0.05 for 10 µM thiamazole, malathion and sulindac, P<0.005 for 10 µM 6-thioguanine, P<0.0005 for 100 µM levodopa, 6-thioguanine, sulindac, d-penicillamine, meclizine, chlorzoxazone and tetracycline, P<0.005 for 100 µM thiamazole, P<0.05 for 50 µM malathion, chlorzoxazone, tetracycline, meclizine, thiamazole and P<0.005 for 50 µM sulindac). Key: red = positive control, green = tetracycline, light blue = malathion, purple = chlorzoxazone, orange = meclizine, dark blue = thiamazole, black = DMSO and copper controls*

Based on the results obtained from all three assays (manual tail-fin wounding assay, ChIn assay and SYTOX® blue staining) it was found that sulindac, chlorzoxazone, meclizine and malathion all showed positive responses in the tail-fin wounding and ChIn assays and

showed no response in the SYTOX® blue staining assay (**Table 6.2**). Thiamazole was found to be a copper chelator which was confirmed by SYTOX® blue staining despite showing an effect in the tail-fin wounding assay. This is because, thiamazole is known to have inherent anti-inflammatory activity, as well as being able to chelate copper (Alturfan et al., 2007)(Lagorce et al., 1997). Drugs which were only found to show a response in the ChIn assay (levodopa, tetracycline, 6-thioguanine, d-penicillamine) were all found to be copper chelators, which was confirmed by SYTOX® blue staining (**Table 6.2**). Metformin only displayed a response in the tail-fin wounding assay and had no effect in the ChIn assay or the SYTOX® blue staining. It is unclear why metformin did not show a response in the ChIn assay, despite metformin being documented to have anti-inflammatory properties (Isoda et al., 2006)(Logie et al., 2012). It is possible that the concentrations tested may have been too low.

Table 6.2 – Overview of the responses of the 28 reference drugs in the zebrafish tail-fin wounding assay, ChIn assay and SYTOX® blue staining.

Drugs	Assay		
	Tail-fin wounding	ChIn	SYTOX® blue
Malathion	**decrease**	**decrease**	**no effect**
Liothyronine	no effect	no effect	no effect
Amiloride	no effect	no effect	no effect
Glipizide	no effect	no effect	no effect
Terfenadine	**toxicity**	**toxicity**	**no effect**
Fenofibrate	no effect	no effect	no effect
Meclizine	**decrease**	**decrease**	**no effect**
L-thyroxine	no effect	no effect	no effect
D-penicillamine	**no effect**	**decrease**	**interacts with copper**
Carbamazepine	no effect	no effect	no effect
Tetracycline	**no effect**	**decrease**	**interacts with copper**
Prednisone	no effect	no effect	no effect
Folate	no effect	no effect	no effect
Chlorzoxazone	**decrease**	**decrease**	**no effect**
Enalapril	**no effect**	**slight decrease**	**interacts with copper**
Metformin	**decrease**	**no effect**	**no effect**
Bendroflumethiazide	no effect	no effect	no effect
Flupenthixol	no effect	no effect	no effect
Thiamazole	**decrease**	**decrease**	**interacts with copper**
Sulindac	**decrease**	**decrease**	**no effect**
Metoclopramide	no effect	no effect	no effect
Chlorprothixene	**no effect**	**toxicity**	**no effect**
6-thioguanine	**no effect**	**decrease**	**interacts with copper**
Hydrochlorothiazide	no effect	no effect	no effect
Amantadine	no effect	no effect	no effect
Levodopa	**no effect**	**decrease**	**interacts with copper**
Captopril	**no effect**	**slight decrease**	**Interacts with copper**
Erythromycin	no effect	no effect	no effect

*Key: **green** = reduce inflammation in tail-fin wounding and ChIn assays + no copper chelation, **black** = cause toxicity, **purple** = reduce inflammation in ChIn assay + chelate copper, **blue** = reduce inflammation in tail-fin wounding and ChIn assays + chelate copper, **brown** = reduce inflammation in tail-fin wounding assay but no effect in ChIn assay + no copper chelation*

6.4.4 Evaluation of the anti-oxidant properties of a selection of the 28 reference drugs

As malathion, chlorzoxazone and meclizine were found to show anti-inflammatory activity despite not being documented in the literature to have such effects they were also investigated for possible anti-oxidant activity. This was done by carrying out a HyPer assay to quantify the levels of hydrogen peroxide produced during an acute inflammatory response in zebrafish larvae treated with these drugs. In brief, Tg*(lyz.HyPer)* zebrafish larvae at 3 dpf were firstly treated with drug for one hour, followed by cutting of caudal fin tips before performing automated fluorescence imaging using the Scan^R screening microscope. Images were taken every minute over 60 minutes with ImageJ used to perform a ratiometric analysis of the images by calculating ratios for HyPer low/HyPer high. The results obtained from the HyPer assay showed that 10 μM malathion reduced the levels of hydrogen peroxide significantly during acute inflammation compared to the 1% DMSO control (**Figure 6.10**, n=8 zebrafish larvae at 3 dpf per drug/control, $P<0.05$). Meclizine and chlorzoxazone at 100 μM on the other hand showed no significant differences when compared to the 1% DMSO control (**Figure 6.10**, n=8 zebrafish larvae at 3 dpf per drug/control, $P>0.05$). Additionally, d-penicillamine was also tested in this assay as it is a known anti-oxidant and therefore served as a positive control. D-penicillamine at 100 μM was found to significantly reduce the levels of hydrogen peroxide and this reduction was found to be much greater than that achieved by malathion (**Figure 6.10**, n=8 zebrafish larvae at 3 dpf per drug/control, $P<0.0001$).

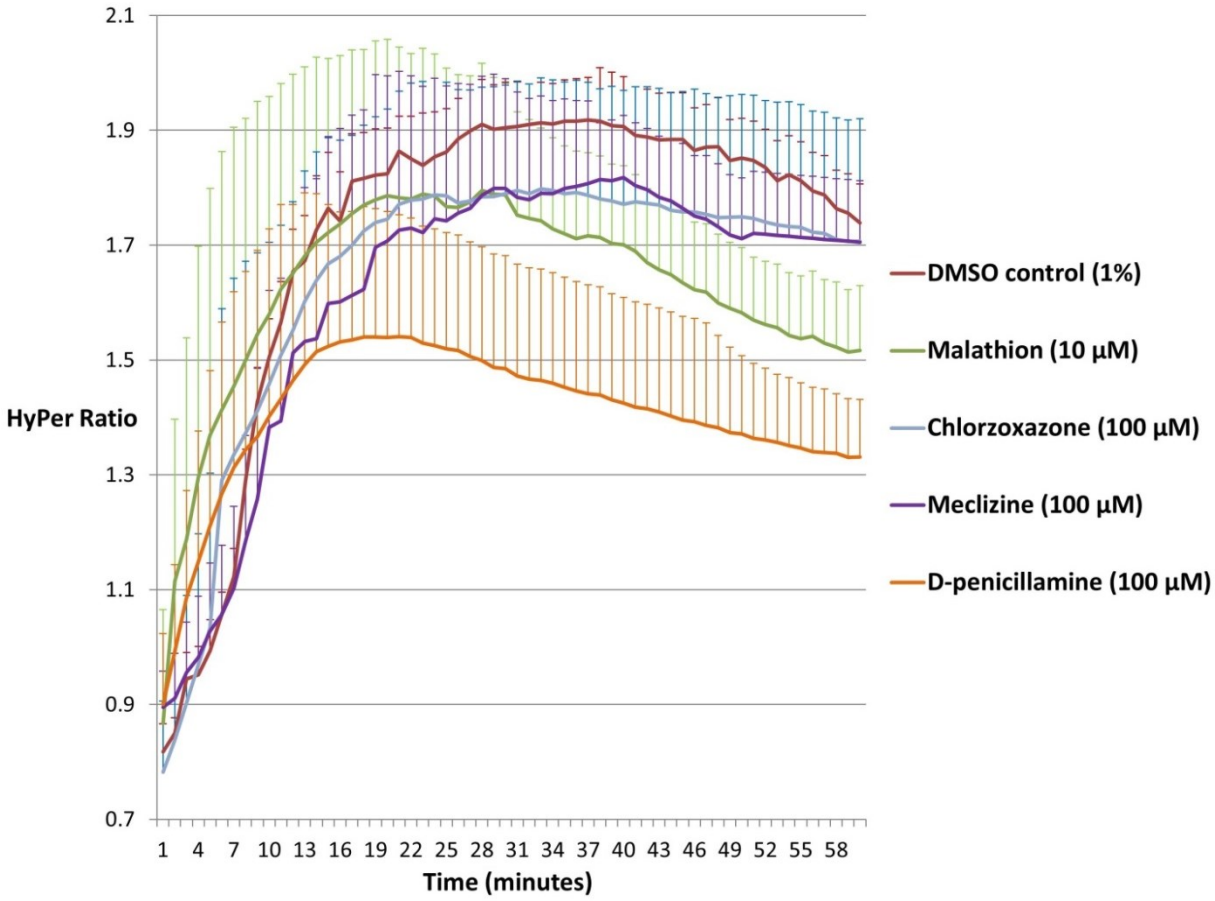

Figure 6.10 – Change in HyPer ratio after treatment of 3 dpf zebrafish larvae with a selection of the 28 reference drugs following initial acute inflammation by cutting of tail-fins. *Zebrafish larvae at 3 dpf were treated with 1% DMSO, 10 µM malathion, 100 µM chlorzoxazone, 100 µM meclizine and 100 µM d-penicillamine (n=8 zebrafish larvae at 3 dpf per drug/control, P<0.05 for 10 µM malathion, P<0.0001 for 100 µM d-penicillamine, P>0.05 for rest)*

6.5 Discussion

6.5.1 Anti-inflammatory responses of 28 reference drugs

Out of the 28 reference drugs tested for anti-inflammatory activity in zebrafish larvae it was found that only sulindac, chlorzoxazone, meclizine and malathion represented true hits. Thiamazole was found to be a copper chelator in the SYTOX® blue staining but still showed a strong anti-inflammatory response in the tail-fin wounding assay. Levodopa, tetracycline, 6-thioguanine and d-penicillamine were all found to be false positives in the ChIn assay and

were confirmed as copper chelators following SYTOX® blue staining. Metformin was found to show an anti-inflammatory response in the tail-fin wounding assay but not in the ChIn assay. Terfenadine showed a response only in the tail-fin wounding assay at the lower concentration of 10 µM but could not be evaluated at the higher concentration of 100 µM due to toxicity. Additionally, due to toxicity terfenadine could not be evaluated for anti-inflammatory activity in the ChIn assay.

Malathion, not previously documented to have anti-inflammatory effects was found to show strong anti-inflammatory effects in zebrafish larvae. Malathion which is an acetylcholinesterase inhibitor is known to induce oxidative stress, which has been demonstrated in rats where it was found to reduce the activity of superoxide dismutase, catalase and glutathione S-transferase (Selmi et al., 2013)(Ruckmani et al., 2011). However, malathion has also been shown at sub-chronic and sub-lethal doses to reduce the neutrophil counts in rats (Bhatia et al., 1996). Hence, it could be that malathion also reduces the leukocyte count in zebrafish larvae. This would make sense with the above argument, as both the tail-fin wounding assay and ChIn assay are based solely on quantifying leukocyte number and no other inflammation parameter. Therefore, if malathion does reduce the leukocyte count it would be identified as a positive hit in both assays. Further studies however would be required to verify this.

The second generation anti-histamine terfenadine was found to display anti-inflammatory effects in zebrafish larvae at 10 µM in the tail-fin wounding assay. Terfenadine has been documented *in vitro* to down-regulate the generation of superoxide radicals by neutrophils

(Hayashi and Hashimoto, 1999) and suppress neutrophil chemotactic responses (Eda et al., 1994). Recently, it has been discovered that inhibition of zERG which is predominantly expressed in the zebrafish heart but is also expressed in leukocytes leads to reduced leukocyte migration (Brown et al., 2007). It is thought that zERG plays an important role in leukocyte adhesion (Brown et al., 2007). This could therefore explain the reduced leukocyte number observed in the zebrafish tail-fin wounding assay, as terfenadine is a known zERG inhibitor. Further detailed investigation of this drug would be needed though to verify this as a mechanism for its anti-inflammatory action.

Meclizine which reduced inflammation in both the zebrafish tail-fin wounding and ChIn assay is a first generation anti-histamine reported to protect against oxidative damage and reactive oxygen species by inhibiting mitochondrial respiration (Gohil et al., 2011). Although zERG block has not been reported so far with meclizine it is possible that like terfenadine meclizine causes reduced leukocyte migration due to zERG block (Simons, 2004). Further studies would be needed to verify this.

Metformin was found to be positive in the tail-fin wounding assay but not in the ChIn assay. Metformin has been shown to inhibit NF-KB and TNF-α IL-6 production in endothelial cells in the vasculature (Isoda et al., 2006). It is unclear why metformin showed a response in the tail-fin wounding assay and not the Chin assay. This would require further investigation.

Thiamazole was found to reduce inflammation both in the ChIn and the tail-fin wounding assays. It was also found to strongly chelate copper. Thiamazole is a powerful chelator of the

cuprate ion being able to inhibit many copper-dependent enzymes, such as tyrosinases (Hanlon and Shuman, 1975). Thiamazole has been documented to have anti-inflammatory properties independent of its copper chelating effects including the ability to inhibit prostaglandin H synthase, reduce the levels of prostaglandin E2 and scavenge superoxide radicals (Lagorce et al., 1997)(Komosinska-Vassev et al., 2000).

Chlorzoxazone which is a muscle relaxant and analgesic also displayed anti-inflammatory effects in zebrafish larvae (Abdel-Azeem et al., 2009). Chlorzoxazone specifically inhibits SK2 channels, which are a sub-type of calcium activated potassium channels mainly expressed in neurons of the brain (Sah, 1996)(Cao et al., 2001). The effect of chlorzoxazone on SK channels is responsible for its muscle relaxant properties; however it could be that this is also related to its anti-inflammatory effects. Further studies would be needed to verify this.

Sulindac the positive control for both the zebrafish tail-fin wounding and ChIn assays was found to show strong anti-inflammatory activity, agreeing with reported effects (d' Alençon et al., 2010). Sulindac is an NSAID that blocks the cyclooxygenase (COX) enzymes COX-1 and COX-2, preventing the synthesis of prostaglandins (**Figure 6.11**) (Cryer and Feldman, 1998). The anti-inflammatory effects of sulindac are mediated by its metabolite sulindac sulphide, which has poor selectivity for COX-2 and is therefore associated with gastrointestinal toxicity due to inhibition of COX-1 (Cryer and Feldman, 1998).

Prednisone the other positive control for the zebrafish tail-fin wounding and ChIn assays was found to show no anti-inflammatory activity. Prednisone is a glucocorticoid that attenuates

an inflammatory response by decreasing vascular permeability and reducing prostaglandin synthesis (**Figure 6.11**) (Coutinho and Chapman, 2011). Prednisone can also alter cellular inflammatory responses through glucocorticoid receptor (GR) antagonism or suppression of genes involved in initiating inflammation (Coutinho and Chapman, 2011). The reason for prednisone showing no anti-inflammatory activity in zebrafish larvae could be due to weak penetration.

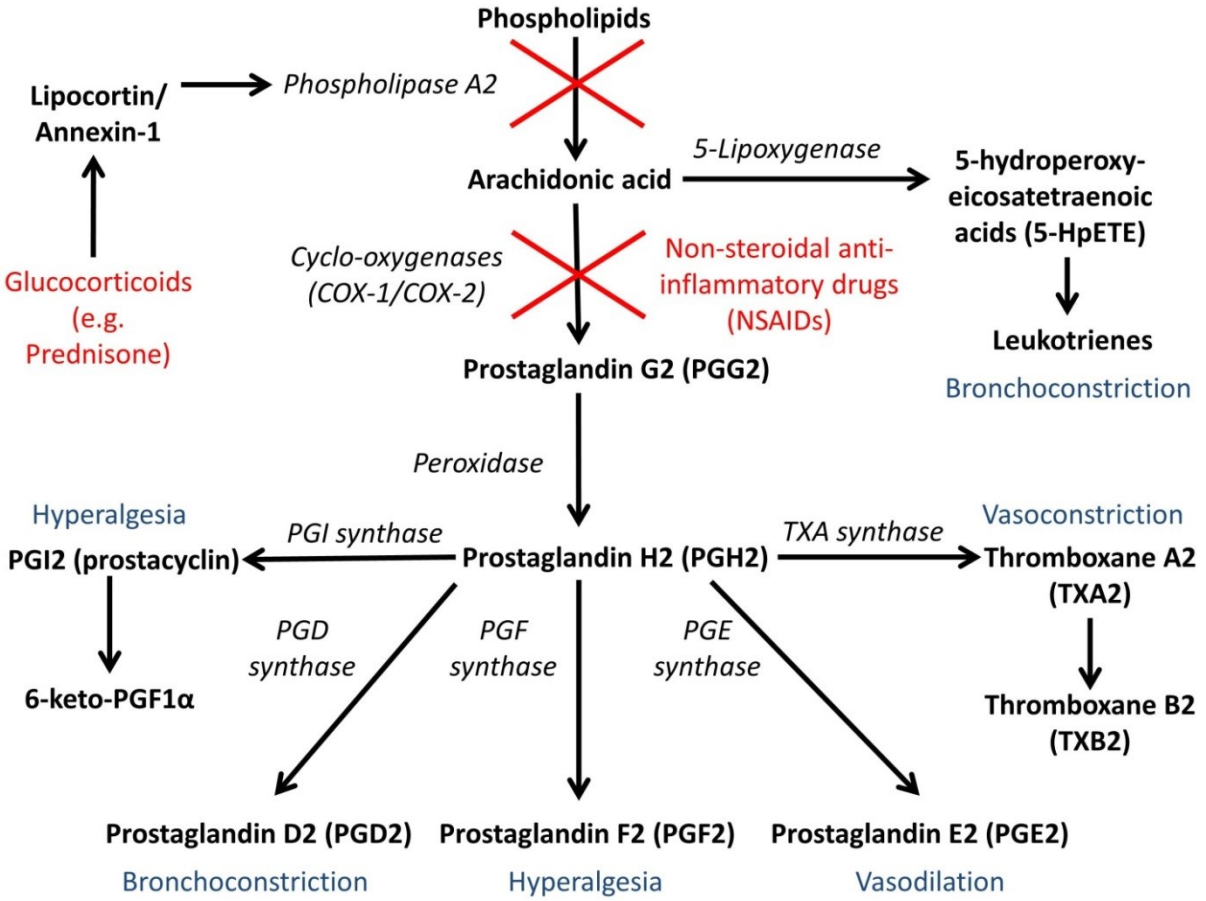

Figure 6.11 – Arachidonic acid pathway. *Free arachidonic acid is made from phospholipids via the action of the phospholipase A2. Arachidonic acid can then form leukotrienes via 5-lipoxygenase or it can be converted to prostaglandins via the action of cyclo-oxygenases. Both leukotrienes and prostaglandins have an important function as inflammatory mediators. Non-steroidal anti-inflammatory drugs (NSAIDs) block the synthesis of prostaglandin G_2. Glucocorticoids (e.g. prednisone) can increase the synthesis of the lipocortin (annexin-1) protein resulting in the inhibition of Phospholipase A2, thereby reducing levels of free arachidonic acid.*

Levodopa, d-penicillamine, 6-thioguanine, captopril, enalapril and tetracycline were all found to be false positives in the ChIn assay due to their ability to chelate copper. Particularly, d-penicillamine is a well-known copper chelator and its copper chelating ability is exploited therapeutically in the treatment of Wilson's disease, a genetic disease where excess copper builds up in tissues (Delangle and Mintz, 2012).

6.5.2 Current limitations and future perspectives of the zebrafish anti-inflammatory screen

In total out of the 28 reference drugs tested, the anti-inflammatory activity of 20 drugs was found to be the same between zebrafish larvae and humans/rodents showing good agreement (**Table 6.3**). Many of the drugs displaying anti-inflammatory activity in humans/rodents but not in zebrafish larvae are those drugs that only produce an anti-inflammatory response in certain conditions, e.g. in cases of microbial infection and disease. This highlights a limitation of the zebrafish larval anti-inflammatory screening set-up in that such conditions are not incorporated into the set-up and that only leukocyte migration is being recorded and no other endpoints of inflammation. Another limitation is that some drugs (e.g. prednisone) may not be able to penetrate into the zebrafish larva due to the short exposure time or unfavourable physiochemical properties therefore producing a negative result. As mentioned in previous chapters, a bioanalysis step would be useful to check that these drugs are indeed taken up into zebrafish larvae and whether equilibrium concentrations are reached. Using longer exposure times or creating a time series of different concentrations could help to determine whether the concentrations used are sufficient. However, for high throughput screening purposes using more than two different

concentrations and several exposure times would not be feasible, so a compromise would need to be reached.

Table 6.3 – Comparison between documented anti-inflammatory effects of 28 reference drugs reported in humans/rodents to those observed in zebrafish larvae.

Drugs	Reported anti-inflammatory effects in humans/rodents	Anti-inflammatory effects in zebrafish larvae
Malathion	X	√
Liothyronine	X	X
Amiloride	√	X
Glipizide	X	X
Terfenadine	√	√
Fenofibrate	√	X
Meclizine	√	√
L-thyroxine	X	X
D-penicillamine	X	X
Carbamazepine	X	X
Tetracycline	√	X
Prednisone	√	X
Folate	√	X
Chlorzoxazone	X	√
Enalapril	X	X
Metformin	√	√
Bendroflumethiazide	X	X
Flupenthixol	X	X
Thiamazole	√	√
Sulindac	√	√
Metoclopramide	X	X
Chlorprothixene	X	X
6-thioguanine	X	X
Hydrochlorothiazide	X	X
Amantadine	X	X
Levodopa	X	X
Captopril	X	X
Erythromycin	√	X

*Key: **red** = no effect observed, **green** = effect observed*

To determine the specificity of the anti-inflammatory responses observed concentration ranges at or close to lethality would need to be tested for both the toxic and non-toxic drugs. However, when doing this it would need to be taken into consideration that a specific mode of action leading to high toxicity may overlap with an unspecific anti-inflammatory effect. This could occur for example with a drug which causes hepatitis at a specific concentration. As hepatitis is associated with inflammatory cells migrating to the liver, a positive response may be observed in the ChIn assay as less inflammatory cells will be observed occupying neuromasts.

Future studies could be improved by testing more positive controls including anti-inflammatory drugs from different classes, increasing the exposure time, as well as adjusting the concentration ranges used for each compound as not all compounds will be active at the same concentrations. Furthermore, it would be useful to include follow up studies for hits to determine their exact mechanism of anti-inflammatory action if it is not already known. This could involve performing studies on zebrafish embryo mutants with defective zCOX.

Taken together these results demonstrate that the zebrafish larval anti-inflammatory set-up consisting of a manual tail-fin wounding assay, ChIn assay and SYTOX® blue staining has the potential to be implemented into pre-clinical drug testing routines and could aid in the identification of new anti-inflammatories. It can be envisaged that the ChIn assay could be combined together with other high throughput zebrafish screens to generate a multi-assay pipeline where both therapeutic and toxic properties of drugs could be investigated.

6.5.3 Anti-oxidant properties of selected reference drugs

A HyPer assay was performed in zebrafish larvae in order to determine whether the positive hits obtained from the zebrafish larval anti-inflammatory screening set-up also displayed anti-oxidant activity. The results obtained showed that malathion and the positive control d-penicillamine displayed anti-oxidant activity, whereas meclizine and chlorzoxazone did not.

Malathion was found to display marked anti-oxidant activity, despite being known to be a causative agent of oxidative stress (Ruckmani et al., 2011). However, in one study it was reported that when rats were exposed to sub-chronic sub-lethal doses of malathion there was an increase in the activity of super oxide dismutase and catalase in the blood and liver (Akhgari et al., 2003). This raises the possibility that in zebrafish larvae exposed to low levels of malathion there could be an over-stimulation of the anti-oxidant defence system in the absence of any overt toxic effects. Therefore, once tail-fin wounding is performed hydrogen peroxide is converted much more rapidly to water and oxygen. An alternative mechanism for malathion's anti-oxidant effects could be inhibition of NOXes or Duox. NOXes are the major source for generating hydrogen peroxide (see **Figure 6.12**) (Niethammer et al., 2009). There are five different types of NOXes in zebrafish, which all generate superoxide radicals which can be converted to hydrogen peroxide by superoxide dismutase (Niethammer et al., 2009). Zebrafish possess one isoform of Duox which can generate hydrogen peroxide directly (see **Figure 6.12**) (Niethammer et al., 2009). Whether or not the inhibition of NOXes or Duox is responsible for the anti-oxidant effects of malathion would require further investigation on a molecular level.

D-penicillamine is a known anti-oxidant and as expected displayed strong anti-oxidant effects in the HyPer assay. The anti-oxidant effects of d-penicillamine are due to its metal chelating abilities, as it can chelate pro-oxidant heavy metals like copper, thus reducing free radical generation (Soroka et al., 1992). D-penicillamine acts by directly scavenging hydrogen peroxide reducing it to water and in turn becoming oxidised itself in the process (Ledson et al., 1992). Additionally, the thiol moiety of d-penicillamine can also interact with aldehydes to form thiazolidines (Phelps et al., 1996).

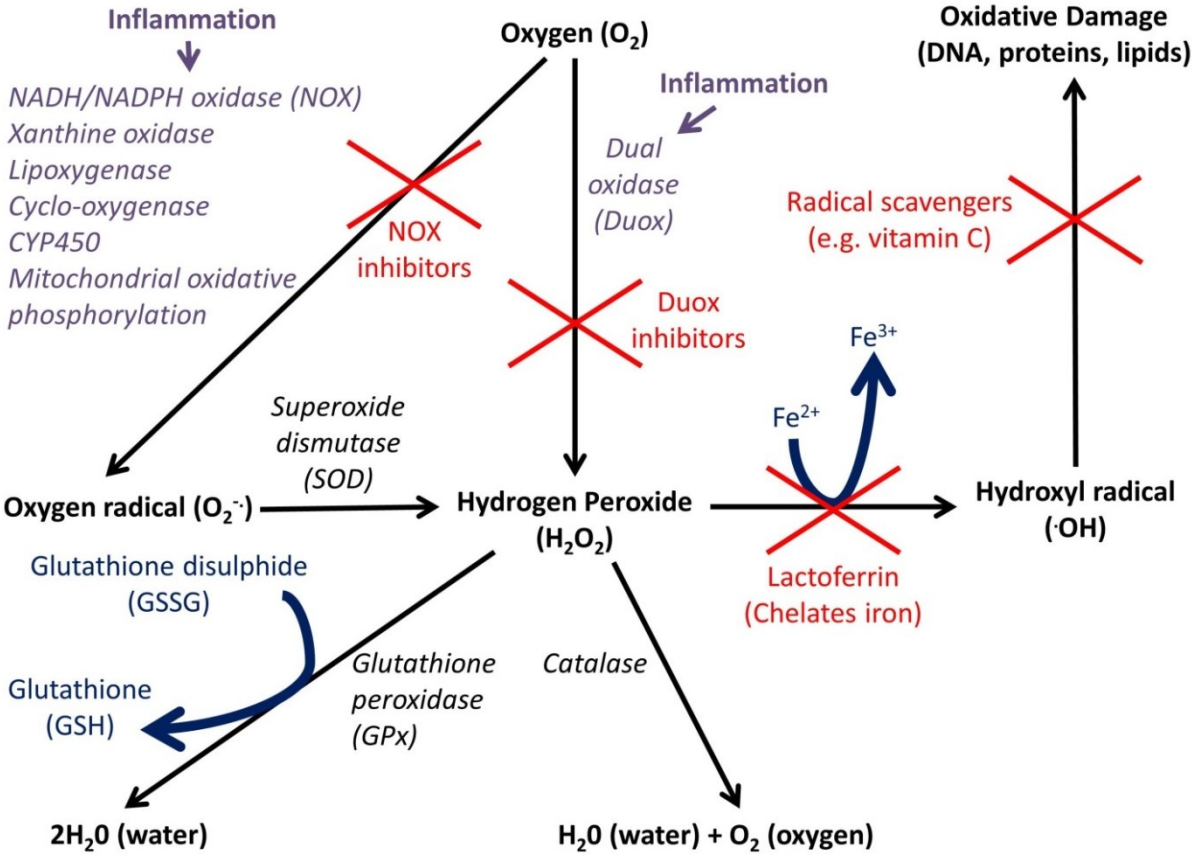

Figure 6.12 – Free radical generation and anti-oxidant defence mechanisms. *Inflammation due to manual wounding or drug exposure can lead to superoxide radical generation. The oxygen radical can form hydrogen peroxide by the actions of the superoxide dismutase enzyme. The hydrogen peroxide can then either be converted to harmless waste products (water and oxygen) by the actions of glutathione peroxidase and catalase or it can undergo a reaction with Fe^{2+} ions (Fenton's reaction) to form hydroxyl radicals and Fe^{3+} ions. These hydroxyl radicals are unstable and can lead to oxidative damage of DNA, proteins and lipids.*

6.5.4 Current limitations and future perspectives of the zebrafish HyPer screen

The HyPer assay highlights the usefulness of the zebrafish larva in identifying compounds with anti-oxidant effects. The study carried out however could be improved in the future by testing a larger number of drugs, including several positive controls and also by incorporating follow up studies, such as Duox/NOX inhibition studies to fully understand the anti-oxidant mechanisms. As mentioned previously, for the zebrafish larval anti-inflammatory set-up bioanalysis studies would also be useful to confirm drug uptake in zebrafish larvae. For this assay to be potentially implemented into pre-clinical testing routines the throughput would also need to be increased by automating the image analysis and increasing the numbers of zebrafish larvae that can be tested at one time.

6.6 Conclusion

A high throughput automated imaging assay for the evaluation of the anti-inflammatory effects of the 28 reference drugs in zebrafish larvae was found to produce interesting and surprising results. Through the completion of confirmatory tests in conjunction with the automated assay three compounds previously not reported as being anti-inflammatory agents (malathion, meclizine and chlorzoxazone) were uncovered as having anti-inflammatory properties. Furthermore, malathion was also uncovered as a potential anti-oxidant agent. As mentioned previously, further studies would need to be performed to confirm these initial findings and to determine the modes of action of these compounds in attenuating parts of the inflammatory response. Overall, the studies performed in this chapter show that the zebrafish larva presents a suitable model for therapeutic drug

screening and that particularly in the field of immunology it could advance the discovery of new anti-inflammatory and anti-oxidant compounds.

Chapter Seven: GENERAL DISCUSSION AND PERSPECTIVES

7.1 Overview

In this thesis, firstly a zebrafish embryo and larval ECG screening tool was developed to specifically address drug-induced cardiotoxicity, which represents one of the major reasons why drugs fail during development. Secondly, the biological activity of a novel group of compounds was assessed using the zebrafish embryo in order to determine whether differences in chemical structure influenced biological activity. Thirdly, a reference drug set was biologically characterised using the zebrafish embryo in order to create a predictive model which could be used to predict the toxicity of similar structured compounds. Finally, a reference drug set was assayed for anti-inflammatory activity using a high throughput zebrafish larval assay to determine potential anti-inflammatory effects of these drugs and to assess the suitability of the zebrafish larva as a model for therapeutic drug screens.

7.2 The implementation of the zebrafish embryo as a pre-clinical model in drug development

Currently, there is increased pressure on pharmaceutical companies to develop drugs that are effective, commercially valuable and safe (Roberts et al., 2014). In order to meet these requirements, drugs that present with toxicity or low efficacy need to be eliminated early on in the drug development process. Potential drug candidates are first identified through *in vitro* tests before safety and efficacy studies are performed *in vitro* and *in vivo*. *In vivo* testing is primarily conducted in rodents but depending on the drug indication and probable metabolic pathway of the drug, larger mammals such as dogs or primates may be needed. *In*

vivo testing also involves using a large number of animals, which is expensive and time-consuming. The zebrafish embryo however may present a quicker, more effective and inexpensive *in vivo* model for drug screening. Therefore, the main aim of this thesis was to evaluate the utility of the zebrafish embryo in pre-clinical drug testing regimes. Particularly, the idea of introducing the zebrafish embryo as the first step in candidate drug selection, as well as an intermediary step in pre-clinical testing, i.e. after initial *in vitro* drug candidate selection and before the commencement of *in vivo* testing was investigated.

To address this main aim, a reference set of 28 chemically diverse marketed compounds was biologically characterised using the zebrafish embryo in order to create a predictive model that could be used to predict the toxicity of similar structured compounds (see **Chapter 5**). A two tier toxicology screen was performed with an initial dose-range finding study followed by a morphological effect screen. Out of the 28 compounds tested, 9 were found to have minimal or no effects on zebrafish embryos, whereas the remaining 19 were found to produce pronounced morphological effects.

When comparing the zebrafish embryo logLC50 values to the logLD50 values of the adult rat and mouse the correlation between them was found to be weak. Some compounds were found to be more toxic or less toxic in zebrafish embryos than in rodents and vice versa, which has also been documented in other studies (Ali et al., 2014)(Ali et al., 2011). As discussed in **Chapter 5**, these differences may have been due to several reasons, but the main reason was probably the difference in exposure routes. Additionally, toxicity endpoints such as LC50/LD50 may not be the best endpoints to compare toxicity between different

species, as this endpoint only gives an indication of lethality without providing any further information on mechanisms. Also, the rodent foetus and human foetus may be more suitable comparisons for comparing zebrafish embryo toxicity. However, the problem persists that data on rodent foetus toxicity and human foetus toxicity is scarce, which means it is difficult to compare these to zebrafish embryo toxicity. Despite the drawbacks mentioned the QSAR model that was generated from the zebrafish embryo data showed good overall predictivity of toxicity. From the model it could be clearly seen that there was a strong association between increased toxicity (low LC50 values and high morphological feature severity scores) and a high logP value which describes the lipophilicity of a compound. This relationship has also been documented in other zebrafish studies (Weimin et al., 2001)(Chen et al., 2012) as well as in other organisms (Wayne Schultz et al., 1991)(Newsome et al., 1991)(Landis et al., 1993). For the majority of the drugs tested baseline toxicity (narcosis) was found to be the main mechanism of toxicity and only with a few drugs specific mechanisms of toxicity were observed.

The zebrafish studies used to create the model however could have been improved by determining additional toxicity endpoints or morphology scores. Furthermore, incorporating biological data from other zebrafish embryo assays into the model could increase its versatility, meaning that it could be used for other indications and not only toxicity determination in the future.

Overall, it can be envisioned that this prediction tool could be implemented after initial *in vitro* screens during drug development to predict toxicity of candidate drugs. This could

prevent drugs reaching the market which present with ADRs and significant toxicity, thus saving time, money and the number of animals tested, as well as preventing human fatalities and morbidity due to drug-induced toxicities. However, the model also has the potential to be applied in environmental toxicology for predicting fish aquatic toxicity for example to pharmaceuticals, agrochemicals and synergistic compound mixtures released into the environment.

7.3 Using the zebrafish embryo as a model to detect cardiotoxicity

As mentioned previously, drug toxicities remain a real problem of drug attrition, particularly in the case of cardiotoxicity which together with hepatotoxicity accounts for the most number of drug withdrawals during the drug development process (Roberts et al., 2014). Currently, there are no gold standard *in vivo* or *in vitro* models to screen for cardiotoxicity. Therefore, in **Chapter 3** of this thesis I aimed to develop a cardiotoxicity screening tool using the zebrafish embryo as a model organism. The aim was to develop an assay which had the potential to be implemented in pre-clinical testing routines as a screening tool. The cardiotoxicity screening tool that was developed was a zebrafish embryo and larval electrocardiogram (ECG) measurement set-up. ECG measurements were performed on zebrafish larvae treated with known QT prolonging drugs in humans in order to determine whether QT prolongation could be recapitulated using zebrafish larvae.

QT prolongation is a major cause of drug failure during drug development and can also have serious implications on patient health if it is not detected during pre-clinical testing (Yap and Camm, 2000). Currently, there is no gold standard animal model for detecting drug-induced

cardiotoxicity. Interestingly, all tested drugs known to cause QT prolongation in humans were found to induce QT prolongation in zebrafish larvae, which has not been documented before. These findings were extremely exciting, as zebrafish embryos are not regulated until 5 dpf and have the capacity to be tested in high numbers and at a reasonable throughput meaning that the zebrafish larva could potentially become a gold standard model for cardiotoxicity testing. Additionally, secondary conditions of cardiotoxicity, such as arrhythmia and AV block were also detectable and clearly observable using the ECG set-up, thus demonstrating the versatility of the ECG set-up in detecting many forms of cardiotoxicity.

To our surprise, verapamil which is not known to induce QT prolongation in humans except in rare cases of overdose was also found to cause QT prolongation in zebrafish larvae. The increased sensitivity of zERG to block compared to hERG may have been responsible for this effect (Langheinrich et al., 2003). This shows that for some drugs results may need to be interpreted with caution, as effects may be over-exaggerated in the zebrafish larva.

The measurement of zebrafish embryo/larval ECGs presents an exciting tool for detecting drug-induced cardiotoxicity, particularly QT prolongation. However, testing of further drugs known to be cardiotoxic in humans (e.g. QRS prolonging agents), as well as further development of the set-up to increase throughput would be required before it can be implemented into routine testing during drug development. It would also be of interest to see whether zebrafish mutants which present with short QT syndrome (e.g. zebrafish reggae mutants) (Hassel et al., 2008) can be rescued after treatment with QT prolonging drugs. This

would further validate the set-up and presents an additional area that could be explored. The main limitations of this set-up such as no automated analysis software, low throughput and uncertainty regarding drug uptake would need to be addressed in the future. Particularly, drug uptake presents an important factor, as for pre-clinical testing it would be important to know the exact dose that is inducing QT prolongation in the zebrafish larvae. To address this, bioanalysis may need to be incorporated as an additional step or alternatively drugs could be injected directly in the blood stream and toxicokinetic models developed which would be feasible but would make the process much more time consuming. However, in either case, a step would be needed to determine the internal concentrations of compounds.

If the above limitations are addressed, it is possible for the zebrafish embryo and larval ECG screening tool to be successfully implemented into routine pre-clinical testing in the future where it could potentially reduce drug failures by identifying those compounds causing cardiotoxicity early on in the drug development process. Additionally, the ECG screening tool could also be used to identify new therapies for diseases caused by electrophysiological abnormalities in the heart including those where a genetic component is involved, thus presenting an opportunity to perform chemical genetic screens.

7.4 The zebrafish larva as a model for therapeutic drug screening

In **Chapter 6**, the anti-inflammatory properties of the 28 reference drugs were explored in zebrafish larvae using an automated chemically induced inflammation assay (ChIn). Using the ChIn assay and associated confirmatory tests four drugs were found to show true anti-

inflammatory activity. Of these four drugs only one was a known anti-inflammatory, namely sulindac. Meclizine, chlorzoxazone and malathion represented drugs not previously documented to have anti-inflammatory properties. Furthermore, malathion was also found to show anti-oxidant activity. These findings potentially uncovered novel uses for drugs that were marketed for other indications. Further work, particularly on a cellular or molecular level may help to unravel how these compounds initiate their anti-inflammatory effects. Experiments could be performed to look at effects on calcium signalling, as calcium signalling is important for orchestrating an inflammatory response (Razzell et al., 2013). Additionally, experiments could be performed to determine changes in the expression of anti-inflammatory genes after drug exposure. For malathion, studies could be performed on Duox to determine whether this oxidase is inhibited by malathion and whether this is responsible for the observed anti-oxidant effects.

Overall, in this chapter the utility of the zebrafish larva for therapeutic drug screening and its possible implementation in initial drug candidate selection processes was demonstrated. The zebrafish larva provides additional advantages over current *in vitro* methods for drug candidate selection and it can be envisaged that further validation of the zebrafish ChIn assay in particular may lead to its routine implementation into drug candidate selection processes in the near future.

7.5 The zebrafish embryo as a screening tool to assess the biological activity of novel compounds

In **Chapter 4**, novel compounds previously not explored for biological activity were tested in zebrafish embryos. After treatment of zebrafish embryos with these compounds a variety of morphological effects were observed. Particularly, azetidine **2a** and Y-lactams **3a**, **3h** and **3f** presented with interesting phenotypes. Azetidine **2a** and Y-lactam **3a** presented with a specific type of hemorrhage, namely ventricular brain hemorrhage. Both compounds were found to show structural similarities which could possibly explain the likenesses seen in the effects they produced. It would be interesting in the future to test the separate isomers of Y-lactam **3a** to see whether one or both of them can recapitulate the ventricular brain hemorrhage phenotype. Additionally, studies on a molecular level to determine the mechanism responsible for ventricular brain hemorrhage formation would be invaluable. Such studies could focus on the *βPix* gene, as knockdown of both splice variants of this gene in zebrafish embryos has been shown to produce the same brain hemorrhage phenotype (Liu et al., 2007).

With compounds **3f** and **3h** it was postulated that their hepatotoxic effects were mediated by their side groups, as the furan and nitroxy groups have been extensively documented in the literature to cause liver toxicity in humans and other animals (Cordelli et al., 2010)(Tyl et al., 1987). To verify that this is really the case bioanalysis studies would need to be performed to determine which reactive intermediates are produced and if these are the same as those produced in humans and other animals. It would also be interesting to test these two compounds for potential anti-inflammatory activity in the future, as many drugs

known to cause hepatotoxicity are also anti-inflammatories (O'Brien, 1992), such as in the case of the NSAIDs.

The results obtained from testing these novel azetidines and Y-lactams showed that small changes in chemical structure produced diverse biological effects. It was seen that certain functional groups were associated with increased toxicity whereas others were not. These results could aid in the synthesis of new compounds which have more favourable properties. Eventually, using such a feedback loop between chemical synthesis and biological activity assessment may lead to the discovery of novel compounds that could be used for disease modelling or as therapeutics.

7.6 Overall conclusion

With the vast number of technologies and techniques available, such as automated zebrafish embryo sorting robots, automated imaging devices, liquid handling devices and various genetic techniques there is the possibility of performing the initial candidate drug selection process and pre-clinical testing fast and efficiently using only the zebrafish embryo. It can be envisaged that a high throughput automated screen such as the zebrafish ChIn assay described in this thesis could be used as the first step in such a pipeline where a compound library is screened for candidate drugs which attenuate a particular phenotype, in this case inflammation. Alternatively, targeted screens could also be performed by screening compound libraries against molecular targets, such as specific genes that induce a disease phenotype. After the initial drug candidate selection has been performed a QSAR model like the one described in this thesis could then be introduced to filter out those drugs predicted

to have a high toxicity in humans. After this filtering step the remaining candidate drugs could then be tested for general toxicity in high throughput zebrafish embryo assays where mortality and morphological effects are automatically quantified. Following on from this a bioanalysis step could be introduced in order to determine the ADME properties of the compounds, as well as potential metabolites formed. The candidate drugs remaining after this step could then be assessed for specific organ toxicities using specialized zebrafish embryo screening tools. These could include the ECG screening tool described in this thesis, which could be used to determine cardiotoxicity. Other tools that could be used include fluorescence-based screening tools where organs of interest (e.g. liver) are fluorescently labelled and changes in size or shape after compound exposure are used as endpoints. Using such a rigorous approach the candidate drugs that remain could be optimised and then tested in mammalian models before going into human clinical trials. Implementing such a method routinely in drug development could save time, resources and money, as well as reduce the number of animals that are tested.

Although, many questions still remain regarding drug uptake and metabolism in zebrafish embryos, particularly pharmacokinetics and internal drug concentrations, these are slowly being addressed. All in all, the zebrafish embryo presents a versatile vertebrate model that can be used to assess the toxicity and therapeutic effects of compounds *in vivo*.

Chapter Eight: APPENDIX

Supplementary Table 8.1 - Modelling parameters used to create log concentration mortality plots for selection of Y-lactams.

Y-lactam compounds	Modelling parameters					
	logLC50	HillSlope	F	Bottom	Top	Span
3a	1.45	1.07	= 50.01	-0.01	100.00	100.00
3b	1.74	2.08	= 50.00	-0.01	100.20	100.20
3c	0.91	11.20	= 50.00	0.00	100.00	100.00
3d	~ 2.15	~ 5.55	= 50.00	0.69	100.00	99.31
3e	2.15	~ 5.56	= 50.00	0.71	100.00	99.98
3f	1.26	3.97	= 50.00	5.56	100.10	94.50
3g	1.07	10.78	= 50.00	0.00	100.00	100.00
3h	3.20	10.61	= 50.00	0.00	13.89	13.89
3i	2.69	9.88	= 50.00	0.07	100.00	100.00

Supplementary Table 8.2 - Modelling parameters used to create log concentration response plots for selection of Y-lactams.

Y-lactam compounds	Modelling parameters					
	logEC50	HillSlope	F	Bottom	Top	Span
3a	1.18	3.71	= 50.00	1.85	100.00	98.19
3b	1.50	31.77	= 50.00	-11.99	100.00	112.00
3c	0.50	33.47	= 50.00	-59.78	100.00	159.80
3d	1.81	34.88	= 50.00	16.67	100.00	83.33
3e	~ 1.25	~ 5.36	= 50.00	0.93	100.00	99.08
3f	1.26	3.97	= 50.00	5.56	100.10	94.50
3g	1.50	37.03	= 50.00	-59.48	100.00	159.50
3h	1.80	34.82	= 50.00	4.20	100.00	95.80
3i	1.76	18.14	= 50.00	16.67	100.00	83.33

Chapter Nine: REFERENCES

Abdel-Azeem, A.Z., Abdel-Hafez, A.A., El-Karamany, G.S., et al. (2009) Chlorzoxazone esters of some non-steroidal anti-inflammatory (NSAI) carboxylic acids as mutual prodrugs: Design, synthesis, pharmacological investigations and docking studies. **Bioorganic & Medicinal Chemistry**, 17 (10): 3665–3670

Ahumada, G.G. (1987) **Cardiovascular pathophysiology**. Oxford University Press

Akhgari, M., Abdollahi, M., Kebryaeezadeh, A., et al. (2003) Biochemical evidence for free radical-induced lipid peroxidation as a mechanism for subchronic toxicity of malathion in blood and liver of rats. **Human & experimental toxicology**, 22 (4): 205–211

Alday, A., Alonso, H., Gallego, M., et al. (2014) Ionic channels underlying the ventricular action potential in zebrafish embryo. **Pharmacological Research**, 84: 26–31

Aldeco, M., Arslan, B.K. and Edmondson, D.E. (2011) Catalytic and inhibitor binding properties of zebrafish monoamine oxidase (zMAO): Comparisons with human MAO A and MAO B. **Comparative Biochemistry and Physiology Part B: Biochemistry and Molecular Biology**, 159 (2): 78–83

Alderton, W., Berghmans, S., Butler, P., et al. (2010) Accumulation and metabolism of drugs and CYP probe substrates in zebrafish larvae. **Xenobiotica**, 40 (8): 547–557

D' Alençon, C.A., Peña, O.A., Wittmann, C., et al. (2010) A high-throughput chemically induced inflammation assay in zebrafish. **BMC Biology**, 8 (1): 151

Ali, S., Aalders, J. and Richardson, M.K. (2014) Teratological Effects of a Panel of Sixty Water-Soluble Toxicants on Zebrafish Development. **Zebrafish**, 11 (2): 129–141

Ali, S., Mil, H.G.J. van and Richardson, M.K. (2011) Large-Scale Assessment of the Zebrafish Embryo as a Possible Predictive Model in Toxicity Testing. **PLoS ONE**, 6 (6): e21076

Alturfan, A.A., Zengin, E., Dariyerli, N., et al. (2007) Investigation of zinc and copper levels in methimazole-induced hypothyroidism: relation with the oxidant-antioxidant status. **Folia biologica**, 53 (5): 183–188

Amali, A.A., Rekha, R.D., Lin, C.J.-F., et al. (2006) Thioacetamide induced liver damage in zebrafish embryo as a disease model for steatohepatitis. **Journal of biomedical science**, 13 (2): 225–232

Amin, A.S., Herfst, L.J., Delisle, B.P., et al. (2008) Fever-induced QTc prolongation and ventricular arrhythmias in individuals with type 2 congenital long QT syndrome. **The Journal of Clinical Investigation**, 118 (7): 2552–2561

Andrews, C.W., Bennett, L. and Yu, L.X. (2000) Predicting Human Oral Bioavailability of a Compound: Development of a Novel Quantitative Structure-Bioavailability Relationship. **Pharmaceutical Research**, 17 (6): 639–644

Anyukhovsky, E.P. (2011) Early prediction of proarrhythmic cardiotoxicity in the drug development process. **Cardiovascular Research**, 91 (1): 7–8

Arnaout, R., Ferrer, T., Huisken, J., et al. (2007) Zebrafish model for human long QT syndrome. **Proceedings of the National Academy of Sciences**, 104 (27): 11316–11321

Aronov, A.M. (2005) Predictive in silico modeling for hERG channel blockers. **Drug Discovery Today**, 10 (2): 149–155

Aronowski, J. and Hall, C.E. (2005) New Horizons for Primary Intracerebral Hemorrhage Treatment: Experience From Preclinical Studies. **Neurological Research**, 27 (3): 268–279

Arrenberg, A.B., Stainier, D.Y.R., Baier, H., et al. (2010) Optogenetic control of cardiac function. **Science (New York, N.Y.)**, 330 (6006): 971–974

Artman, M., Benson, D.W., Srivastava, D., et al. (2008) **Cardiovascular Development and Congenital Malformations: Molecular & Genetic Mechanisms**. John Wiley & Sons

Barnes, B.J. and Hollands, J.M. (2010) Drug-induced arrhythmias. **Critical care medicine**, 38 (6 Suppl): S188–197

Barrionuevo, W.R. and Burggren, W.W. (1999) O2 consumption and heart rate in developing zebrafish (Danio rerio): influence of temperature and ambient O2. **American Journal of Physiology - Regulatory, Integrative and Comparative Physiology**, 276 (2): R505–R513

Barros, T.P., Alderton, W.K., Reynolds, H.M., et al. (2008) Zebrafish: an emerging technology for in vivo pharmacological assessment to identify potential safety liabilities in early drug discovery. **British journal of pharmacology**, 154 (7): 1400–1413

Behra, M., Cousin, X., Bertrand, C., et al. (2002) Acetylcholinesterase is required for neuronal and muscular development in the zebrafish embryo. **Nature Neuroscience**, 5 (2): 111–118

Belanger, S.E., Balon, E.K. and Rawlings, J.M. (2010) Saltatory ontogeny of fishes and sensitive early life stages for ecotoxicology tests. **Aquatic Toxicology**, 97 (2): 88–95

Belanger, S.E., Rawlings, J.M. and Carr, G.J. (2013) Use of fish embryo toxicity tests for the prediction of acute fish toxicity to chemicals. **Environmental Toxicology and Chemistry**, 32 (8): 1768–1783

Belousov, V.V., Fradkov, A.F., Lukyanov, K.A., et al. (2006) Genetically encoded fluorescent indicator for intracellular hydrogen peroxide. **Nature methods**, 3 (4): 281–286

Benatar, A. and Decraene, T. (2001) Comparison of formulae for heart rate correction of QT interval in exercise ECGs from healthy children. **Heart**, 86 (2): 199–202

Berghmans, S., Butler, P., Goldsmith, P., et al. (2008) Zebrafish based assays for the assessment of cardiac, visual and gut function--potential safety screens for early drug discovery. **Journal of Pharmacological and Toxicological Methods**, 58 (1): 59–68

Bhatia, A., Makkar, M. and Sohal, N. (1996) Effect of subchronic and sublethal doses of malathion on some haematological and immunological parameters. **International Journal of Environmental Studies**, 51 (1): 59–66

Billstein, S.A. (1994) How the pharmaceutical industry brings an antibiotic drug to market in the United States. **Antimicrobial Agents and Chemotherapy**, 38 (12): 2679–2682

Binder, V. and Zon, L.I. (n.d.) High throughput in vivo phenotyping: The zebrafish as tool for drug discovery for hematopoietic stem cells and cancer. **Drug Discovery Today: Disease Models** [online]. Available from: http://www.sciencedirect.com/science/article/pii/S174067571200014X [Accessed 31 January 2013]

Bolton, J.L., Trush, M.A., Penning, T.M., et al. (2000) Role of Quinones in Toxicology†. **Chemical Research in Toxicology**, 13 (3): 135–160

Bort, R., Ponsoda, X., Jover, R., et al. (1999) Diclofenac Toxicity to Hepatocytes: A Role for Drug Metabolism in Cell Toxicity. **Journal of Pharmacology and Experimental Therapeutics**, 288 (1): 65–72

Bowman, T.V. and Zon, L.I. (2010) Swimming into the Future of Drug Discovery: In Vivo Chemical Screens in Zebrafish. **ACS Chemical Biology**, 5 (2): 159–161

Braunbeck, T., Görge, G., Storch, V., et al. (1990) Hepatic steatosis in zebra fish (Brachydanio rerio) induced by long-term exposure to γ-hexachlorocyclohexane. **Ecotoxicology and Environmental Safety**, 19 (3): 355–374

Brana, I. and Tabernero, J. (2010) Cardiotoxicity. **Annals of Oncology**, 21 (suppl 7): vii173–vii179

Bresolin, T., de Freitas Rebelo, M. and Celso Dias Bainy, A. (2005) Expression of PXR, CYP3A and MDR1 genes in liver of zebrafish. **Comparative biochemistry and physiology. Toxicology & pharmacology: CBP**, 140 (3-4): 403–407

Briggs, J.P. (2002) The zebrafish: a new model organism for integrative physiology. **American Journal of Physiology - Regulatory, Integrative and Comparative Physiology**, 282 (1): R3–R9

Brines, L., Such-Miquel, L., Gallego, D., et al. (2012) Modifications of mechanoelectric feedback induced by 2,3-butanedione monoxime and Blebbistatin in Langendorff-perfused rabbit hearts. **Acta Physiologica**, 206 (1): 29–41

Brinkmann, U. and Eichelbaum, M. (2001) Polymorphisms in the ABC drug transporter gene MDR1. **The Pharmacogenomics Journal**, 1 (1): 59–64

Brown, S.B., Tucker, C.S., Ford, C., et al. (2007) Class III antiarrhythmic methanesulfonanilides inhibit leukocyte recruitment in zebrafish. **Journal of Leukocyte Biology**, 82 (1): 79–84

Buchner, D.A., Su, F., Yamaoka, J.S., et al. (2007) pak2a mutations cause cerebral hemorrhage in redhead zebrafish. **Proceedings of the National Academy of Sciences of the United States of America**, 104 (35): 13996–14001

Burns, C.G., Milan, D.J., Grande, E.J., et al. (2005) High-throughput assay for small molecules that modulate zebrafish embryonic heart rate. **Nature Chemical Biology**, 1 (5): 263–264

Busquet, F., Strecker, R., Rawlings, J.M., et al. (2014) OECD validation study to assess intra- and inter-laboratory reproducibility of the zebrafish embryo toxicity test for acute aquatic toxicity testing. **Regulatory Toxicology and Pharmacology**, 69 (3): 496–511

Buss, R.R., Bourque, C.W. and Drapeau, P. (2003) Membrane Properties Related to the Firing Behavior of Zebrafish Motoneurons. **Journal of Neurophysiology**, 89 (2): 657–664

Bylesjö, M., Rantalainen, M., Cloarec, O., et al. (2006) OPLS discriminant analysis: combining the strengths of PLS-DA and SIMCA classification. **Journal of Chemometrics**, 20 (8-10): 341–351

Cao, Y.-J., Dreixler, J.C., Roizen, J.D., et al. (2001) Modulation of Recombinant Small-Conductance Ca2+-Activated K+ Channels by the Muscle Relaxant Chlorzoxazone and Structurally Related Compounds. **Journal of Pharmacology and Experimental Therapeutics**, 296 (3): 683–689

Carlsson, L., Abrahamsson, C., Andersson, B., et al. (1993) Proarrhythmic effects of the class III agent almokalant: importance of infusion rate, QT dispersion, and early afterdepolarisations. **Cardiovascular Research**, 27 (12): 2186–2193

Chan, P.K., Lin, C.C. and Cheng, S.H. (2009) Noninvasive technique for measurement of heartbeat regularity in zebrafish (Danio rerio) embryos. **BMC Biotechnology**, 9 (1): 11

Chaudhari, G.H., Chennubhotla, K.S., Chatti, K., et al. (2013) Optimization of the adult zebrafish ECG method for assessment of drug-induced QTc prolongation. **Journal of Pharmacological and Toxicological Methods**, 67 (2): 115–120

Cheng, H.C., Incardona, J. and McCullough, B. (2006) Isolated perfused and paced guinea pig heart to test for drug-induced changes of the QT interval. **Journal of pharmacological and toxicological methods**, 54 (3): 278–287

Chen, Y.-H., Yang, Z.-S., Wen, C.-C., et al. (2012) Evaluation of the structure-activity relationship of flavonoids as antioxidants and toxicants of zebrafish larvae. **Food chemistry**, 134 (2): 717–724

Chézalviel-Guilbert, F., Davy, J.-M., Poirier, J.-M., et al. (1995) Mexiletine antagonizes effects of sotalol on QT interval duration and its proarrhythmic effects in a canine model of torsade de pointes. **Journal of the American College of Cardiology**, 26 (3): 787–792

Chi, N.C., Shaw, R.M., Jungblut, B., et al. (2008) Genetic and Physiologic Dissection of the Vertebrate Cardiac Conduction System. **PLoS Biol**, 6 (5): e109

Choi, J. and Tontonoz, P. (2013) Metabolism: Drug discovery goes for a swim. **Nature Chemical Biology**, 9 (2): 68–69

Clarke, J.M., Hamer, J., Shelton, J.R., et al. (1976) The rhythm of the normal human heart. **Lancet**, 1 (7984): 508–512

Cobo, A.M., Yu, F., Zhao, Y., et al. (2013) Implantable micro-Electrode Array for Long-term ECG Recording in Zebrafish. **FASEB Journal**, 27 (CaltechAUTHORS:20130711-105746475): Art. No. 706.9

Cohen, C., Welzl, H. and Bättig, K. (1991) Effects of nicotine, caffeine, and their combination on locomotor activity in rats. **Pharmacology, biochemistry, and behavior**, 40 (1): 121–123

Colquhoun, D., Dreyer, F. and Sheridan, R.E. (1979) The actions of tubocurarine at the frog neuromuscular junction. **The Journal of Physiology**, 293 (1): 247–284

Cordelli, E., Leopardi, P., Villani, P., et al. (2010) Toxic and genotoxic effects of oral administration of furan in mouse liver. **Mutagenesis**, 25 (3): 305–314

Coutinho, A.E. and Chapman, K.E. (2011) The anti-inflammatory and immunosuppressive effects of glucocorticoids, recent developments and mechanistic insights. **Molecular and Cellular Endocrinology**, 335 (1): 2–13

Crawford, A.D., Liekens, S., Kamuhabwa, A.R., et al. (2011) Zebrafish Bioassay-Guided Natural Product Discovery: Isolation of Angiogenesis Inhibitors from East African Medicinal Plants. **PLoS ONE**, 6 (2): e14694

Cronin, M.T.D. (2004) **Predicting Chemical Toxicity and Fate**. CRC Press. (00102)

Cryer, B. and Feldman, M. (1998) Cyclooxygenase-1 and Cyclooxygenase-2 Selectivity of Widely Used Nonsteroidal Anti-Inflammatory Drugs. **The American Journal of Medicine**, 104 (5): 413–421

Dean, M. and Annilo, T. (2005) Evolution of the ATP-binding cassette (ABC) transporter superfamily in vertebrates. **Annual Review of Genomics and Human Genetics**, 6: 123–142

Delangle, P. and Mintz, E. (2012) Chelation therapy in Wilson's disease: from D-penicillamine to the design of selective bioinspired intracellular Cu(I) chelators. **Dalton Transactions**, 41 (21): 6359–6370

Denvir, M.A., Tucker, C.S. and Mullins, J.J. (2008) Systolic and diastolic ventricular function in zebrafish embryos: Influence of norepenephrine, MS-222 and temperature. **BMC Biotechnology**, 8 (1): 21

Dhein, S., Perlitz, F. and Mohr, F.-W. (2008) An in vitro model for assessment of drug-induced torsade de pointes arrhythmia. **Naunyn-Schmiedeberg's Archives of Pharmacology**, 378 (6): 631–644

Diekmann, H. and Hill, A. (2013) ADMETox in zebrafish. **Drug Discovery Today: Disease Models**, 10 (1): e31–e35

Ding, F., Guo, J., Song, W., et al. (2011) Comparative quantitative structure–activity relationship (QSAR) study on acute toxicity of triazole fungicides to zebrafish. **Chemistry and Ecology**, 27 (4): 359–368

Dong, W., Yang, Z., Yang, F., et al. (2012) Suppression of Rap1 Impairs Cardiac Myofibrils and Conduction System in Zebrafish. **PLoS ONE**, 7 (11): e50960

Donovan, A., Brownlie, A., Dorschner, M.O., et al. (2002) The zebrafish mutant gene chardonnay (cdy) encodes divalent metal transporter 1 (DMT1). **Blood**, 100 (13): 4655–4659

Dorne, J.L.C.M., Walton, K. and Renwick, A.G. (2003) Human variability in CYP3A4 metabolism and CYP3A4-related uncertainty factors for risk assessment. **Food and Chemical Toxicology**, 41 (2): 201–224

Driessen, M., Kienhuis, A.S., Pennings, J.L.A., et al. (2013) Exploring the zebrafish embryo as an alternative model for the evaluation of liver toxicity by histopathology and expression profiling. **Archives of Toxicology**, 87 (5): 807–823

Driessen, M., Kienhuis, A.S., Vitins, A.P., et al. (2014) Gene expression markers in the zebrafish embryo reflect a hepatotoxic response in animal models and humans. **Toxicology Letters**, 230 (1): 48–56

DrugBank (ed.) (2013a) Chlorprothixene (DB01239). **DrugBank** [online]. Available from: http://www.drugbank.ca/drugs/DB01239 [Accessed 4 January 2014]

DrugBank (ed.) (2013b) Haloperidol (DB00502). **DrugBank** [online]. Available from: http://www.drugbank.ca/drugs/DB00502 [Accessed 5 January 2014]

DrugBank (ed.) (2013c) Nicotine (DB00184). **DrugBank** [online]. Available from: http://www.drugbank.ca/drugs/DB00184 [Accessed 28 February 2014]

DrugBank (ed.) (2013d) Pimozide (DB01100). **DrugBank** [online]. Available from: http://www.drugbank.ca/drugs/DB01100 [Accessed 9 January 2014]

DrugBank (ed.) (2013e) Prednisone (DB00635). **DrugBank** [online]. Available from: http://www.drugbank.ca/drugs/DB00635 [Accessed 29 January 2014]

DrugBank (ed.) (2013f) Verapamil. **DrugBank** [online]. Available from: http://www.drugbank.ca/drugs/DB00661 [Accessed 22 June 2014]

Duan, J., Ma, J., Zhang, P., et al. (2007) Verapamil blocks HERG channel by the helix residue Y652 and F656 in the S6 transmembrane domain1. **Acta Pharmacologica Sinica**, 28 (7): 959–967

Dübon, P., Farwick, A. and Helmchen, G. (2009) Enantioselective Syntheses of 2-Substituted Pyrrolidines from Allylamines by Domino Hydroformylation-Condensation: Short Syntheses of (S)-Nicotine and the Alkaloid 225C. **Synlett**, 2009 (09): 1413–1416

Dummula, K., Vinukonda, G., Chu, P., et al. (2011) Bone Morphogenetic Protein Inhibition Promotes Neurological Recovery after Intraventricular Hemorrhage. **The Journal of Neuroscience**, 31 (34): 12068–12082

Dvorakova, D. and Zapletal, O. (2001) Toxicity of methylxanthines - intoxications with chocolate in dogs and cats. **Veterinarstvi** [online], v. 51(8) p. 378-379. Available from: http://agris.fao.org/agris-search/search/display.do?f=2001/CZ/CZ01005.xml;CZ2001001138 [Accessed 23 April 2013]

Dykens, J.A. and Will, Y. (2007) The significance of mitochondrial toxicity testing in drug development. **Drug Discovery Today**, 12 (17–18): 777–785

Eda, R., Townley, R.G. and Hopp, R.J. (1994) Effect of terfenadine on human eosinophil and neutrophil chemotactic response and generation of superoxide. **Annals of allergy**, 73 (2): 154–160

Edwards, I.R. and Aronson, J.K. (2000) Adverse drug reactions: definitions, diagnosis, and management. **The Lancet**, 356 (9237): 1255–1259

Ehrman, T.M., Barlow, D.J. and Hylands, P.J. (2010) In silico search for multi-target anti-inflammatories in Chinese herbs and formulas. **Bioorganic & Medicinal Chemistry**, 18 (6): 2204–2218

Ekwall, B., Barile, F.A., Castano, A., et al. (1998) MEIC evaluation of acute systemic toxicity: Part VI. The prediction of human toxicity by rodent LD50 values and results from 61 in vitro methods. **ATLA. Alternatives to laboratory animals**, 26: 617–658

Ellett, F., Pase, L., Hayman, J.W., et al. (2011) mpeg1 promoter transgenes direct macrophage-lineage expression in zebrafish. **Blood**, 117 (4): e49–e56

Elmore, S.A., Ryan, A.M., Wood, C.E., et al. (2014) FutureTox II: Contemporary Concepts in Toxicology: "Pathways to Prediction: In Vitro and In Silico Models for Predictive Toxicology." **Toxicologic Pathology**, p. 0192623314537135

Elsalini, O.A. and Rohr, K.B. (2003) Phenylthiourea disrupts thyroid function in developing zebrafish. **Development genes and evolution**, 212 (12): 593–598

Enyeart, J.J., Price, W.A., Hoffman, D.A., et al. (1983) Profound hyperglycemia and metabolic acidosis after verapamil overdose. **Journal of the American College of Cardiology**, 2 (6): 1228–1231

Epstein, S.E. and Rosing, D.R. (1981) Verapamil: its potential for causing serious complications in patients with hypertrophic cardiomyopathy. **Circulation**, 64 (3): 437–441

Feula, A., Male, L. and Fossey, J.S. (2010) Diastereoselective Preparation of Azetidines and Pyrrolidines. **Organic Letters**, 12 (21): 5044–5047

Field, H.A., Ober, E.A., Roeser, T., et al. (2003) Formation of the digestive system in zebrafish. I. liver morphogenesis. **Developmental Biology**, 253 (2): 279–290

Fink, M., Callol-Massot, C., Chu, A., et al. (2009) A new method for detection and quantification of heartbeat parameters in Drosophila, zebrafish, and embryonic mouse hearts. **BioTechniques**, 46 (2): 101–113

Fischer, W.J. and Dietrich, D.R. (2000) Pathological and Biochemical Characterization of Microcystin-Induced Hepatopancreas and Kidney Damage in Carp (Cyprinus carpio). **Toxicology and Applied Pharmacology**, 164 (1): 73–81

Fleming, A., Sato, M. and Goldsmith, P. (2005) High-Throughput In Vivo Screening for Bone Anabolic Compounds with Zebrafish. **Journal of Biomolecular Screening**, 10 (8): 823–831

Forouhar, A.S., Hove, J.R., Calvert, C., et al. (2004) "Electrocardiographic Characterization of Embryonic Zebrafish." In **26th Annual International Conference of the IEEE Engineering in Medicine and Biology Society, 2004. IEMBS '04**. **1 September 2004**. IEEE. pp. 3615– 3617

Fossa, A.A., DePasquale, M.J., Raunig, D.L., et al. (2002) The Relationship of Clinical QT Prolongation to Outcome in the Conscious Dog Using a Beat-to-Beat QT-RR Interval Assessment. **Journal of Pharmacology and Experimental Therapeutics**, 302 (2): 828–833

Fransson-Steen, R., Goldsworthy, T.L., Kedderis, G.L., et al. (1997) Furan-induced liver cell proliferation and apoptosis in female B6C3F1 mice. **Toxicology**, 118 (2-3): 195–204

Fujii, K., Foster, C.D., Brading, A.F., et al. (1990) Potassium channel blockers and the effects of cromakalim on the smooth muscle of the guinea-pig bladder. **British Journal of Pharmacology**, 99 (4): 779–785

Gates, L.A., Lu, D. and Peterson, L.A. (2012) Trapping of cis-2-Butene-1,4-dial to Measure Furan Metabolism in Human Liver Microsomes by Cytochrome P450 Enzymes. **Drug Metabolism and Disposition**, 40 (3): 596–601

George, S., Xia, T., Rallo, R., et al. (2011) Use of a High-Throughput Screening Approach Coupled with In Vivo Zebrafish Embryo Screening To Develop Hazard Ranking for Engineered Nanomaterials. **ACS Nano**, 5 (3): 1805–1817

Gerace, E., Salomone, A., Pellegrino, S., et al. (2012) Evidence of Haldol (haloperidol) long-term intoxication. **Forensic Science International**, 215 (1–3): 121–123

Gerlai, R. (2010) High-Throughput Behavioral Screens: the First Step towards Finding Genes Involved in Vertebrate Brain Function Using Zebrafish. **Molecules**, 15 (4): 2609–2622

Ghysen, A. and Dambly-Chaudière, C. (2004) Development of the zebrafish lateral line. **Current Opinion in Neurobiology**, 14 (1): 67–73

Giardina, E.G., Bigger, J.T., Glassman, A.H., et al. (1979) The electrocardiographic and antiarrhythmic effects of imipramine hydrochloride at therapeutic plasma concentrations. **Circulation**, 60 (5): 1045–1052

Gillette, J.R., Mitchell, J.R. and Brodie, B.B. (1974) Biochemical Mechanisms of Drug Toxicity. **Annual Review of Pharmacology**, 14 (1): 271–288

Gillis, T.E. and Tibbits, G.F. (2002) Beating the cold: the functional evolution of troponin C in teleost fish. **Comparative Biochemistry and Physiology Part A: Molecular & Integrative Physiology**, 132 (4): 763–772

Glickman, N.S. and Yelon, D. (2002) Cardiac development in zebrafish: coordination of form and function. **Seminars in Cell & Developmental Biology**, 13 (6): 507–513

Gohil, V.M., Offner, N., Walker, J.A., et al. (2011) Meclizine is neuroprotective in models of Huntington's disease. **Human Molecular Genetics**, 20 (2): 294–300

Golan, D.E., Tashjian, A.H. and Armstrong, E.J. (2011) **Principios de farmacología clínica: bases fisiopatológicas del tratamiento farmacológico**. Lippincott Williams & Wilkins

Goldenberg, I., Zareba, W. and Moss, A.J. (2008) Long QT Syndrome. **Current Problems in Cardiology**, 33 (11): 629–694

Goldsmith, J.R. and Jobin, C. (2012) Think Small: Zebrafish as a Model System of Human Pathology. **BioMed Research International** [online], 2012. Available from: http://www.hindawi.com/journals/bmri/2012/817341/abs/ [Accessed 6 June 2013]

Goldsmith, P. (2004a) Zebrafish as a pharmacological tool: the how, why and when. **Current opinion in pharmacology**, 4 (5): 504–512

Goldstone, J.V., McArthur, A.G., Kubota, A., et al. (2010) Identification and developmental expression of the full complement of Cytochrome P450 genes in Zebrafish. **BMC Genomics**, 11 (1): 643

Gore, A.V., Lampugnani, M.G., Dye, L., et al. (2008) Combinatorial interaction between CCM pathway genes precipitates hemorrhagic stroke. **Disease Models & Mechanisms**, 1 (4-5): 275–281

Gould, J.C., Leonard, L.S., Maness, S.C., et al. (1998) Bisphenol A interacts with the estrogen receptor α in a distinct manner from estradiol. **Molecular and Cellular Endocrinology**, 142 (1–2): 203–214

Gupta, A., Lawrence, A.T., Krishnan, K., et al. (2007) Current concepts in the mechanisms and management of drug-induced QT prolongation and torsade de pointes. **American Heart Journal**, 153 (6): 891–899

Guilleminault, C., Connolly, S.J. and Winkle, R.A. (1983) Cardiac arrhythmia and conduction disturbances during sleep in 400 patients with sleep apnea syndrome. **The American Journal of Cardiology**, 52 (5): 490–494

Hagedorn, M., Kleinhans, F.W., Artemov, D., et al. (1998) Characterization of a Major Permeability Barrier in the Zebrafish Embryo. **Biology of Reproduction**, 59 (5): 1240–1250

Hall, C., Flores, M., Storm, T., et al. (2007) The zebrafish lysozyme C promoter drives myeloid-specific expression in transgenic fish. **BMC Developmental Biology**, 7 (1): 42

Halliwell, B. and Chirico, S. (1993) Lipid peroxidation: its mechanism, measurement, and significance. **The American Journal of Clinical Nutrition**, 57 (5): 715S–724S

Hanlon, D. and Shuman, S. (1975) Copper ion binding and enzyme inhibitory properties of the antithyroid drug methimazole. **Cellular and Molecular Life Sciences**, 31 (9): 1005–1006

Hansch, C., Hoekman, D., Leo, A., et al. (1995) The expanding role of quantitative structure-activity relationships (QSAR) in toxicology. **Toxicology Letters**, 79 (1–3): 45–53

Harmer, A., Valentin, J.-P. and Pollard, C. (2011) On the relationship between block of the cardiac Na+ channel and drug-induced prolongation of the QRS complex. **British Journal of Pharmacology**, 164 (2): 260–273

Harrah, M.D., Way, W.L. and Katzung, B.G. (1970) The interaction of d-tubocurarine with antiarrhythmic drugs. **Anesthesiology**, 33 (4): 406–410

Hassel, D., Scholz, E.P., Trano, N., et al. (2008) Deficient zebrafish ether-à-go-go-related gene channel gating causes short-QT syndrome in zebrafish reggae mutants. **Circulation**, 117 (7): 866–875

Haverkamp, W., Breithardt, G., Camm, A.J., et al. (2000) The potential for QT prolongation and pro-arrhythmia by non-anti-arrhythmic drugs: Clinical and regulatory implications Report on a Policy Conference of the European Society of Cardiology. **Cardiovascular Research**, 47 (2): 219–233

Hayashi, S. and Hashimoto, S. (1999) Anti-inflammatory actions of new antihistamines. **Clinical & Experimental Allergy**, 29 (12): 1593–1596

Hayes, A.W. (2001) **Principles and Methods of Toxicology**. CRC Press

Hecker, L., Khait, L., Sessions, S.K., et al. (2008) Functional evaluation of isolated zebrafish hearts. **Zebrafish**, 5 (4): 319–322

Hegarty, T.W. (1973) Temperature Coefficient (Q10), Seed Germination and Other Biological Processes. **Nature**, 243 (5405): 305–306

He, J.-H., Guo, S.-Y., Zhu, F., et al. (2013) A zebrafish phenotypic assay for assessing drug-induced hepatotoxicity. **Journal of Pharmacological and Toxicological Methods**, 67 (1): 25–32

Henn, K. and Braunbeck, T. (2011) Dechorionation as a tool to improve the fish embryo toxicity test (FET) with the zebrafish (Danio rerio). **Comparative Biochemistry and Physiology Part C: Toxicology & Pharmacology**, 153 (1): 91–98

He, Q., Liu, K., Wang, S., et al. (2012) Toxicity induced by emodin on zebrafish embryos. **Drug and chemical toxicology**, 35 (2): 149–154

Herbomel, P., Thisse, B. and Thisse, C. (1999) Ontogeny and behaviour of early macrophages in the zebrafish embryo. **Development**, 126 (17): 3735–3745

Herbomel, P., Thisse, B. and Thisse, C. (2001) Zebrafish Early Macrophages Colonize Cephalic Mesenchyme and Developing Brain, Retina, and Epidermis through a M-CSF Receptor-Dependent Invasive Process. **Developmental Biology**, 238 (2): 274–288

Hermsen, S.A.B., van den Brandhof, E.-J., van der Ven, L.T.M., et al. (2011) Relative embryotoxicity of two classes of chemicals in a modified zebrafish embryotoxicity test and comparison with their in vivo potencies. **Toxicology in vitro: an international journal published in association with BIBRA**, 25 (3): 745–753

He, T., Clifford, G. and Tarassenko, L. (2006) Application of independent component analysis in removing artefacts from the electrocardiogram. **Neural Computing & Applications**, 15 (2): 105–116

Hill, A.J., Teraoka, H., Heideman, W., et al. (2005) Zebrafish as a Model Vertebrate for Investigating Chemical Toxicity. **Toxicological Sciences**, 86 (1): 6–19

Hoffmann, P. and Warner, B. (2006) Are hERG channel inhibition and QT interval prolongation all there is in drug-induced torsadogenesis? A review of emerging trends. **Journal of Pharmacological and Toxicological Methods**, 53 (2): 87–105

Hondeghem, L.M., Lu, H.R., Rossem, K. van, et al. (2003) Detection of Proarrhythmia in the Female Rabbit Heart: **Journal of Cardiovascular Electrophysiology**, 14 (3): 287–294

Hong, E. and Brewster, R. (2006) N-cadherin is required for the polarized cell behaviors that drive neurulation in the zebrafish. **Development**, 133 (19): 3895–3905

Horne-Badovinac, S., Rebagliati, M. and Stainier, D.Y.R. (2003) A Cellular Framework for Gut-Looping Morphogenesis in Zebrafish. **Science**, 302 (5645): 662–665

Huang, F.-P., Xi, G., Keep, R.F., et al. (2002) Brain edema after experimental intracerebral hemorrhage: role of hemoglobin degradation products. **Journal of Neurosurgery**, 96 (2): 287–293

Huang, Y., Harrison, M.R., Osorio, A., et al. (2013) Igf Signaling is Required for Cardiomyocyte Proliferation during Zebrafish Heart Development and Regeneration. **PLoS ONE**, 8 (6): e67266

Hughes, J.D., Blagg, J., Price, D.A., et al. (2008) Physiochemical drug properties associated with in vivo toxicological outcomes. **Bioorganic & Medicinal Chemistry Letters**, 18 (17): 4872–4875

Hukkanen, J., Jacob, P. and Benowitz, N.L. (2005) Metabolism and Disposition Kinetics of Nicotine. **Pharmacological Reviews**, 57 (1): 79–115

Hu, N., Sedmera, D., Yost, H.J., et al. (2000) Structure and function of the developing zebrafish heart. **The Anatomical record**, 260 (2): 148–157

ICH Expert Working Group Topic Leaders:, Bode, G. and Olejniczak, K. (2002) ICH Topic: The draft ICH S7B step 2: Note for guidance on safety pharmacology studies for human pharmaceuticals. **Fundamental & Clinical Pharmacology**, 16 (2): 105–118

Ioannides, C. (1996) **Cytochromes: Metabolic and Toxicological Aspects**. CRC Press. (00118)

Ishaq, O., Negri, J., Bray, M.-A., et al. (2013) "Automated quantification of Zebrafish tail deformation for high-throughput drug screening." In **2013 IEEE 10th International Symposium on Biomedical Imaging (ISBI)**. **April 2013**. pp. 902–905

Isoda, K., Young, J.L., Zirlik, A., et al. (2006) Metformin Inhibits Proinflammatory Responses and Nuclear Factor-κB in Human Vascular Wall Cells. **Arteriosclerosis, Thrombosis, and Vascular Biology**, 26 (3): 611–617

Jacob, E., Drexel, M., Schwerte, T., et al. (2002) Influence of hypoxia and of hypoxemia on the development of cardiac activity in zebrafish larvae. **American Journal of Physiology - Regulatory, Integrative and Comparative Physiology**, 283 (4): R911–R917

Jaeschke, H. (2007) Troglitazone Hepatotoxicity: Are We Getting Closer to Understanding Idiosyncratic Liver Injury? **Toxicological Sciences**, 97 (1): 1–3

Jou, C.J., Spitzer, K.W. and Tristani-Firouzi, M. (2010) Blebbistatin Effectively Uncouples the Excitation-Contraction Process in Zebrafish Embryonic Heart. **Cellular Physiology and Biochemistry**, 25 (4-5): 419–424

Julkunen, R.J.K., Tannenbaum, L., Baraona, E., et al. (1985) First pass metabolism of ethanol: An important determinant of blood levels after alcohol consumption. **Alcohol**, 2 (3): 437–441

Jung, D.-W., Williams, D., Khersonsky, S.M., et al. (2005) Identification of the F1F0 mitochondrial ATPase as a target for modulating skin pigmentation by screening a tagged triazine library in zebrafish. **Molecular bioSystems**, 1 (1): 85–92

Jw, H. (1999) Nitrobenzene potential human cancer risk based on animal studies. **Toxicology and industrial health**, 15 (5): 458–463

Källén, B.A.J., Otterblad Olausson, P. and Danielsson, B.R. (2005) Is erythromycin therapy teratogenic in humans? **Reproductive Toxicology**, 20 (2): 209–214

Kamlet, M.J., Doherty, R.M., Abraham, M.H., et al. (1987) Solubility properties in polymers and biological media. 8. An analysis of the factors that influence toxicities of organic nonelectrolytes to the golden orfe fish (Leuciscus idus melanotus). **Environmental Science & Technology**, 21 (2): 149–155

Kammann, U., Vobach, M. and Wosniok, W. (2006) Toxic effects of brominated indoles and phenols on zebrafish embryos. **Archives of Environmental Contamination and Toxicology**, 51 (1): 97–102

Kaplowitz, N. (2004) Drug-Induced Liver Injury. **Clinical Infectious Diseases**, 38 (Supplement 2): S44–S48

Kari, G., Rodeck, U. and Dicker, A.P. (2007) Zebrafish: An Emerging Model System for Human Disease and Drug Discovery. **Clinical Pharmacology & Therapeutics**, 82 (1): 70–80

Katchman, A.N., Koerner, J., Tosaka, T., et al. (2006) Comparative Evaluation of HERG Currents and QT Intervals following Challenge with Suspected Torsadogenic and Nontorsadogenic Drugs. **Journal of Pharmacology and Experimental Therapeutics**, 316 (3): 1098–1106

Katritzky, A.R., Mehta, S., He, H.-Y., et al. (2000) Preparation of 1,5-Disubstituted Pyrrolidin-2-ones. **The Journal of Organic Chemistry**, 65 (14): 4364–4369

Kazan, S., Güra, A., Uçar, T., et al. (2005) Hydrocephalus after intraventricular hemorrhage in preterm and low–birth weight infants: analysis of associated risk factors for ventriculoperitoneal shunting. **Surgical Neurology**, 64: S77–S81

Kehrer, J.P. and Biswal, S.S. (2000) The Molecular Effects of Acrolein. **Toxicological Sciences**, 57 (1): 6–15

Khan, J.N., Prasad, N. and Glancy, J.M. (2010) QTc prolongation during therapeutic hypothermia: are we giving it the attention it deserves? **Europace**, 12 (2): 266–270

Kim, D.-H., Sun, Y., Yun, S., et al. (2004) "Mechanical property characterization of the zebrafish embryo chorion." In **26th Annual International Conference of the IEEE Engineering in Medicine and Biology Society, 2004. IEMBS '04**. **September 2004**. pp. 5061–5064

Kimmel, C.B., Ballard, W.W., Kimmel, S.R., et al. (1995) Stages of embryonic development of the zebrafish. **Developmental Dynamics**, 203 (3): 253–310

King Heiden, T.C., Dengler, E., Kao, W.J., et al. (2007) Developmental toxicity of low generation PAMAM dendrimers in zebrafish. **Toxicology and Applied Pharmacology**, 225 (1): 70–79

Kirchmaier, B.C., Poon, K.L., Schwerte, T., et al. (2012) The Popeye domain containing 2 (popdc2) gene in zebrafish is required for heart and skeletal muscle development. **Developmental Biology**, 363 (2): 438–450

Klee, E.W., Ebbert, J.O., Schneider, H., et al. (2011) Zebrafish for the Study of the Biological Effects of Nicotine. **Nicotine & Tobacco Research**, 13 (5): 301–312

Knight, T.R., Fariss, M.W., Farhood, A., et al. (2003) Role of Lipid Peroxidation as a Mechanism of Liver Injury after Acetaminophen Overdose in Mice. **Toxicological Sciences**, 76 (1): 229–236

Koen, Y.M., Williams, T.D. and Hanzlik, R.P. (2000) Identification of Three Protein Targets for Reactive Metabolites of Bromobenzene in Rat Liver Cytosol. **Chemical Research in Toxicology**, 13 (12): 1326–1335

Könemann, H. (1981) Quantitative structure-activity relationships in fish toxicity studies. Part 1: relationship for 50 industrial pollutants. **Toxicology**, 19 (3): 209–221

Kolega, J. (2004) Phototoxicity and photoinactivation of blebbistatin in UV and visible light. **Biochemical and biophysical research communications**, 320 (3): 1020–1025

Komosinska-Vassev, K., Olczyk, K., Kucharz, E.J., et al. (2000) Free radical activity and antioxidant defense mechanisms in patients with hyperthyroidism due to Graves' disease during therapy. **Clinica Chimica Acta**, 300 (1–2): 107–117

Kraft, J., Bauer, S., Keilhoff, G., et al. (1998) Biological effects of the dihydroorotate dehydrogenase inhibitor polyporic acid, a toxic constituent of the mushroom Hapalopilus rutilans, in rats and humans. **Archives of Toxicology**, 72 (11): 711–721

Krstić, D.Z., Čolović, M., Bavcon kralj, M., et al. (2008) Inhibition of AChE by malathion and some structurally similar compounds. **Journal of Enzyme Inhibition and Medicinal Chemistry**, 23 (4): 562–573

Lagorce, J.F., Moulard, T., Rousseau, A., et al. (1997) Anti-Inflammatory Action of Methimazole. **Pharmacology**, 55 (4): 173–178

Lam, S.H., Ung, C.Y., Hlaing, M.M., et al. (2013) Molecular insights into 4-nitrophenol-induced hepatotoxicity in zebrafish: Transcriptomic, histological and targeted gene expression analyses. **Biochimica et Biophysica Acta (BBA) - General Subjects**, 1830 (10): 4778–4789

Landis, W.G., Hughes, J.S. and Lewis, M.A. (1993) **Environmental Toxicology and Risk Assessment**. ASTM International. (00009)

Langheinrich, U. (2003) Zebrafish: a new model on the pharmaceutical catwalk. **BioEssays: news and reviews in molecular, cellular and developmental biology**, 25 (9): 904–912

Langheinrich, U., Vacun, G. and Wagner, T. (2003) Zebrafish embryos express an orthologue of HERG and are sensitive toward a range of QT-prolonging drugs inducing severe arrhythmia. **Toxicology and Applied Pharmacology**, 193 (3): 370–382

Lau, S.S. and Zannoni, V.G. (1981) Bromobenzene Metabolism in the Rabbit Specific Forms of Cytochrome P-450 Involved in 2,3- and 3,4-Epoxidation. **Molecular Pharmacology**, 20 (1): 234–235

Leclercq, I., Horsmans, Y., Desager, J.-P., et al. (1998) Reduction in hepatic cytochrome P-450 is correlated to the degree of liver fat content in animal models of steatosis in the absence of inflammation. **Journal of Hepatology**, 28 (3): 410–416

Ledson, M.J., Bucknall, R.C. and Edwards, S.W. (1992) Inhibition of neutrophil oxidant secretion by D-penicillamine: scavenging of H2O2 and HOCl. **Annals of the Rheumatic Diseases**, 51 (3): 321–325

Leong, I.U.S., Skinner, J.R., Shelling, A.N., et al. (2010) Zebrafish as a model for long QT syndrome: the evidence and the means of manipulating zebrafish gene expression. **Acta Physiologica**, 199 (3): 257–276

Lessigiarska, I., Worth, A.P., Netzeva, T.I., et al. (2006) Quantitative structure–activity–activity and quantitative structure–activity investigations of human and rodent toxicity. **Chemosphere**, 65 (10): 1878–1887

Letamendia, A., Quevedo, C., Ibarbia, I., et al. (2012) Development and Validation of an Automated High-Throughput System for Zebrafish In Vivo Screenings. **PLoS ONE**, 7 (5): e36690

Levin, E.D., Bencan, Z. and Cerutti, D.T. (2007) Anxiolytic effects of nicotine in zebrafish. **Physiology & behavior**, 90 (1): 54–58

Li, A.P. (2001) Screening for human ADME/Tox drug properties in drug discovery. **Drug Discovery Today**, 6 (7): 357–366

Lieschke, G.J. (2001) Zebrafish—an emerging genetic model for the study of cytokines and hematopoiesis in the era of functional genomics. **International Journal of Hematology**, 73 (1): 23–31

Lieschke, G.J. and Currie, P.D. (2007) Animal models of human disease: zebrafish swim into view. **Nature reviews. Genetics**, 8 (5): 353–367

Lieschke, G.J., Oates, A.C., Crowhurst, M.O., et al. (2001) Morphologic and functional characterization of granulocytes and macrophages in embryonic and adult zebrafish. **Blood**, 98 (10): 3087–3096

Lin, K.-Y., Chang, W.-T., Lai, Y.-C., et al. (2014) Toward Functional Screening of Cardioactive and Cardiotoxic Drugs with Zebrafish in Vivo Using Pseudodynamic Three-Dimensional Imaging. **Analytical Chemistry**, 86 (4): 2213–2220

Lin, S., Zhao, Y., Ji, Z., et al. (2013) Zebrafish High-Throughput Screening to Study the Impact of Dissolvable Metal Oxide Nanoparticles on the Hatching Enzyme, ZHE1. **Small**, 9 (9-10): 1776–1785

Liu, J., Fraser, S.D., Faloon, P.W., et al. (2007) A betaPix Pak2a signaling pathway regulates cerebral vascular stability in zebrafish. **Proceedings of the National Academy of Sciences of the United States of America**, 104 (35): 13990–13995

Logan, D.W., Burn, S.F. and Jackson, I.J. (2006) Regulation of pigmentation in zebrafish melanophores. **Pigment Cell Research**, 19 (3): 206–213

Logie, L., Harthill, J., Patel, K., et al. (2012) Cellular Responses to the Metal-Binding Properties of Metformin. **Diabetes**, 61 (6): 1423–1433

Lou, Q., Li, W. and Efimov, I.R. (2012) The role of dynamic instability and wavelength in arrhythmia maintenance as revealed by panoramic imaging with blebbistatin vs. 2,3-butanedione monoxime. **American Journal of Physiology - Heart and Circulatory Physiology**, 302 (1): H262–H269

Loynes, C.A., Martin, J.S., Robertson, A., et al. (2010) Pivotal Advance: Pharmacological manipulation of inflammation resolution during spontaneously resolving tissue neutrophilia in the zebrafish. **Journal of Leukocyte Biology**, 87 (2): 203–212

MacRae, C.A. (2013) Recent advances in in vivo screening for antiarrhythmic drugs. **Expert Opinion on Drug Discovery**, pp. 1–11

MacRae, C.A. and Peterson, R.T. (2003) Zebrafish-Based Small Molecule Discovery. **Chemistry & Biology**, 10 (10): 901–908

Mandrell, D., Truong, L., Jephson, C., et al. (2012) Automated Zebrafish Chorion Removal and Single Embryo Placement Optimizing Throughput of Zebrafish Developmental Toxicity Screens. **Journal of Laboratory Automation**, 17 (1): 66–74

Maricondi-Massari, M., Kalinin, A.L., Glass, M.L., et al. (1998) The effects of temperature on oxygen uptake, gill ventilation and ecg waveforms in the nile tilapia, Oreochromis niloticus. **Journal of Thermal Biology**, 23 (5): 283–290

Martin, R.L., McDermott, J.S., Salmen, H.J., et al. (2004) The utility of hERG and repolarization assays in evaluating delayed cardiac repolarization: influence of multi-channel block. **Journal of cardiovascular pharmacology**, 43 (3): 369–379

Masferrer, J.L. and Needleman, P. (2000) Anti-inflammatories for cardiovascular disease. **Proceedings of the National Academy of Sciences**, 97 (23): 12400–12401

Mathias, J.R., Dodd, M.E., Walters, K.B., et al. (2009) Characterization of zebrafish larval inflammatory macrophages. **Developmental & Comparative Immunology**, 33 (11): 1212–1217

Mathias, J.R., Perrin, B.J., Liu, T.-X., et al. (2006) Resolution of inflammation by retrograde chemotaxis of neutrophils in transgenic zebrafish. **Journal of Leukocyte Biology**, 80 (6): 1281–1288

Mattera, G.G., Vanoli, E., M, F.L., et al. (2012) **Detecting Drug-induced QT Interval Prolongation In Healthy Dogs: A Practical Approach**. [online]. Available from: http://www.webmedcentral.com/article_view/3615 [Accessed 3 April 2013]

Mayr, L.M. and Bojanic, D. (2009) Novel trends in high-throughput screening. **Current Opinion in Pharmacology**, 9 (5): 580–588

McGrath, P. (2012) **Zebrafish: Methods for Assessing Drug Safety and Toxicity**. John Wiley & Sons. (00005)

Meeker, N.D. and Trede, N.S. (2008) Immunology and zebrafish: Spawning new models of human disease. **Developmental & Comparative Immunology**, 32 (7): 745–757

Milan, D.J., Jones, I.L., Ellinor, P.T., et al. (2006) In vivo recording of adult zebrafish electrocardiogram and assessment of drug-induced QT prolongation. **American journal of physiology. Heart and circulatory physiology**, 291 (1): H269–273

Milan, D.J. and MacRae, C.A. (2005) Animal models for arrhythmias. **Cardiovascular Research**, 67 (3): 426–437

Milan, D.J., Peterson, T.A., Ruskin, J.N., et al. (2003) Drugs That Induce Repolarization Abnormalities Cause Bradycardia in Zebrafish. **Circulation**, 107 (10): 1355–1358

Minois, N., Carmona-Gutierrez, D. and Madeo, F. (2011) Polyamines in aging and disease. **Aging (Albany NY)**, 3 (8): 716–732

Mirkovic, T. and Rombough, P. (1998) The effect of body mass and temperature on the heart rate, stroke volume, and cardiac output of larvae of the rainbow trout, Oncorhynchus mykiss. **Physiological zoology**, 71 (2): 191–197

Mizgirev, I.V. and Revskoy, S. (2010) A new zebrafish model for experimental leukemia therapy. **Cancer Biology & Therapy**, 9 (11): 895–902

Murphey, R.D., Stern, H.M., Straub, C.T., et al. (2006) A Chemical Genetic Screen for Cell Cycle Inhibitors in Zebrafish Embryos. **Chemical Biology & Drug Design**, 68 (4): 213–219

Nath, N., Khan, M., Paintlia, M.K., et al. (2009) Metformin Attenuated the Autoimmune Disease of the Central Nervous System in Animal Models of Multiple Sclerosis. **The Journal of Immunology**, 182 (12): 8005–8014

Nelson, T.J. and Boor, P.J. (1982) Allylamine cardiotoxicity—IV: Metabolism to acrolein by cardiovascular tissues. **Biochemical Pharmacology**, 31 (4): 509–514

Nendza, M. (1998) **Structure—Activity Relationships in Environmental Sciences**. Springer. (00062)

Nendza, M. and Wenzel, A. (2006) Discriminating Toxicant Classes by Mode of Action - 1. (Eco)toxicity Profiles. **Environmental Science and Pollution Research**, 13 (3): 192–203

Nerbonne, J.M. and Kass, R.S. (2005) Molecular Physiology of Cardiac Repolarization. **Physiological Reviews**, 85 (4): 1205–1253

Newsome, L.D., Johnson, D.E., Lipnick, R.L., et al. (1991) A QSAR study of the toxicity of amines to the fathead minnow. **Science of The Total Environment**, 109–110: 537–551

Nguyen, C.T., Lu, Q., Wang, Y., et al. (2008) Zebrafish as a model for cardiovascular development and disease. **Drug Discovery Today: Disease Models**, 5 (3): 135–140

Nguyen, M., Poudel, M.K., Stewart, A.M., et al. (2013) Skin too thin? The developing utility of zebrafish skin (neuro)pharmacology for CNS drug discovery research. **Brain Research Bulletin**, 98: 145–154

Niemeijer, M.N., Berg, M.E. van den, Eijgelsheim, M., et al. (2014) Short-term QT variability markers for the prediction of ventricular arrhythmias and sudden cardiac death: a systematic review. **Heart**, pp. heartjnl–2014–305671

Niethammer, P., Grabher, C., Look, A.T., et al. (2009) A tissue-scale gradient of hydrogen peroxide mediates rapid wound detection in zebrafish. **Nature**, 459 (7249): 996–999

Ni-Komatsu, L. and Orlow, S.J. (2007) Identification of novel pigmentation modulators by chemical genetic screening. **The Journal of investigative dermatology**, 127 (7): 1585–1592

Nitrobenzene [MAK Value Documentation, 2003] (2002). In **The MAK-Collection for Occupational Health and Safety** [online]. Wiley-VCH Verlag GmbH & Co. KGaA. Available from: http://onlinelibrary.wiley.com/doi/10.1002/3527600418.mb9895e0019/abstract [Accessed 4 December 2013]

Nomiyama, H., Hieshima, K., Osada, N., et al. (2008) Extensive expansion and diversification of the chemokine gene family in zebrafish: Identification of a novel chemokine subfamily CX. **BMC Genomics**, 9: 222

O'Brien, J.M., Rockwood, R.P. and Suh, K.I. (1999) Haloperidol-Induced Torsade De Pointes. **Annals of Pharmacotherapy**, 33 (10): 1046–1050

O'Brien, W.M. (1992) "Hepatitis due to non-steroidal anti-inflammatory drugs (NSAIDs)." In Rainsford, K.D. and Velo, G.P. (eds.) **Side-Effects of Anti-Inflammatory Drugs 3**. Inflammation and Drug Therapy Series 5 [online]. Springer Netherlands. pp. 211–222. Available from: http://link.springer.com/chapter/10.1007/978-94-011-2982-4_26 [Accessed 2 September 2014]

Odenthal, J., Rossnagel, K., Haffter, P., et al. (1996) Mutations affecting xanthophore pigmentation in the zebrafish, Danio rerio. **Development**, 123 (1): 391–398

OECD (2013) **Test No. 236: Fish Embryo Acute Toxicity (FET) Test** [online]. Paris: Organisation for Economic Co-operation and Development. (00000). Available from: http://www.oecd-ilibrary.org/content/book/9789264203709-en [Accessed 21 July 2014]

Olivari, F.A., Hernández, P.P. and Allende, M.L. (2008) Acute copper exposure induces oxidative stress and cell death in lateral line hair cells of zebrafish larvae. **Brain Research**, 1244: 1–12

Oliveira, R., McDonough, S., Ladewig, J.C.L., et al. (2013) Effects of oxytetracycline and amoxicillin on development and biomarkers activities of zebrafish (Danio rerio). **Environmental toxicology and pharmacology**, 36 (3): 903–912

Olsen, N.J. (2004) Drug-induced autoimmunity. **Best Practice & Research Clinical Rheumatology**, 18 (5): 677–688

Olson, H., Betton, G., Robinson, D., et al. (2000) Concordance of the toxicity of pharmaceuticals in humans and in animals. **Regulatory toxicology and pharmacology: RTP**, 32 (1): 56–67

Olson, R.D. and Mushlin, P.S. (1990) Doxorubicin cardiotoxicity: analysis of prevailing hypotheses. **The FASEB Journal**, 4 (13): 3076–3086

Orme, I.M. (2011) Development of new vaccines and drugs for TB: limitations and potential strategic errors. **Future Microbiology**, 6 (2): 161–177

Ostapowicz, G. and Lee, W.M. (2000) Acute hepatic failure: A Western perspective. **Journal of Gastroenterology and Hepatology**, 15 (5): 480–488

Padilla, S., Corum, D., Padnos, B., et al. (2012) Zebrafish developmental screening of the ToxCast^{TM} Phase I chemical library. **Reproductive Toxicology**, 33 (2): 174–187

Pa, J., Cj, N., Kh, S., et al. (1968) Pimozide, a chemically novel, highly potent and orally long-acting neuroleptic drug. I. The comparative pharmacology of pimozide, haloperidol, and chlorpromazine. **Arzneimittel-Forschung**, 18 (3): 261–279

Panzica-Kelly, J.M., Zhang, C.X., Danberry, T.L., et al. (2010) Morphological score assignment guidelines for the dechorionated zebrafish teratogenicity assay. **Birth defects research. Part B, Developmental and reproductive toxicology**, 89 (5): 382–395

Pardo-Martin, C., Chang, T.-Y., Koo, B.K., et al. (2010) High-throughput in vivo vertebrate screening. **Nature Methods**, 7 (8): 634–636

Parker, B. and Connaughton, V.P. (2007) Effects of Nicotine on Growth And Development in Larval Zebrafish. **Zebrafish**, 4 (1): 59–68

Park, M.J., Lee, K.-R., Shin, D.-S., et al. (2013) Predicted drug-induced bradycardia related cardio toxicity using a zebrafish in vivo model is highly correlated with results from in vitro tests. **Toxicology Letters**, 216 (1): 9–15

Parng, C., Seng, W.L., Semino, C., et al. (2002) Zebrafish: A Preclinical Model for Drug Screening. **ASSAY and Drug Development Technologies**, 1 (1): 41–48

Pase, L., Nowell, C.J. and Lieschke, G.J. (2012) "Chapter eight - In Vivo Real-Time Visualization of Leukocytes and Intracellular Hydrogen Peroxide Levels During a Zebrafish Acute Inflammation Assay." In P. Michael Conn (ed.) **Methods in Enzymology** [online]. Academic Press. pp. 135–156. Available from: http://www.sciencedirect.com/science/article/pii/B9780123918567000329 [Accessed 30 April 2013]

Patel, D.V. and Gordon, E.M. (1996) Applications of small-molecule combinatorial chemistry to drug discovery. **Drug Discovery Today**, 1 (4): 134–144

Peal, D.S., Mills, R.W., Lynch, S.N., et al. (2011) Novel Chemical Suppressors of Long QT Syndrome Identified by an In Vivo Functional Screen. **Circulation**, 123 (1): 23–30

Peal, D.S., Peterson, R.T. and Milan, D. (2010) Small Molecule Screening in Zebrafish. **Journal of Cardiovascular Translational Research**, 3 (5): 454–460

Petersen, G.I. and Kristensen, P. (1998) Bioaccumulation of lipophilic substances in fish early life stages. **Environmental Toxicology and Chemistry**, 17 (7): 1385–1395

Peterson, L.A., Phillips, M.B., Lu, D., et al. (2011) Polyamines Are Traps for Reactive Intermediates in Furan Metabolism. **Chemical Research in Toxicology**, 24 (11): 1924–1936

Peterson, R.T., Link, B.A., Dowling, J.E., et al. (2000) Small molecule developmental screens reveal the logic and timing of vertebrate development. **Proceedings of the National Academy of Sciences**, 97 (24): 12965–12969

Peterson, R.T., Shaw, S.Y., Peterson, T.A., et al. (2004) Chemical suppression of a genetic mutation in a zebrafish model of aortic coarctation. **Nature biotechnology**, 22 (5): 595–599

Pettit, S., des Etages, S.A., Mylecraine, L., et al. (2010) Current and Future Applications of Toxicogenomics: Results Summary of a Survey from the HESI Genomics State of Science Subcommittee. **Environmental Health Perspectives**, 118 (7): 992–997

Petzold, A.M., Balciunas, D., Sivasubbu, S., et al. (2009) Nicotine response genetics in the zebrafish. **Proceedings of the National Academy of Sciences**, 106 (44): 18662–18667

Phelps, D., Lakatos, L. and Watts, J. (1996) “D-Penicillamine for preventing retinopathy of prematurity in preterm infants.” In **Cochrane Database of Systematic Reviews** [online]. John Wiley & Sons, Ltd. Available from: http://onlinelibrary.wiley.com/doi/10.1002/14651858.CD001073/abstract [Accessed 1 February 2014]

Pinney, S.P., Koller, B.S., Franz, M.R., et al. (1995) Terfenadine increases the QT interval in isolated guinea pig heart. **Journal of cardiovascular pharmacology**, 25 (1): 30–34

Ramos, E.U., Vermeer, C., Vaes, W.H.J., et al. (1998) Acute toxicity of polar narcotics to three aquatic species (Daphnia magna, poecilia reticulata and Lymnaea stagnalis) and its relation to hydrophobicity. **Chemosphere**, 37 (4): 633–650

Razzell, W., Evans, I.R., Martin, P., et al. (2013) Calcium Flashes Orchestrate the Wound Inflammatory Response through DUOX Activation and Hydrogen Peroxide Release. **Current Biology**, 23 (5): 424–429

Redfern, M., Hughes, R. and Chaffin, D. (1993) High-pass filtering to remove electrocardiographic interference from torso EMG recordings. **Clinical Biomechanics**, 8 (1): 44–48

Redfern, W.S., Carlsson, L., Davis, A.S., et al. (2003) Relationships between preclinical cardiac electrophysiology, clinical QT interval prolongation and torsade de pointes for a broad range of drugs: evidence for a provisional safety margin in drug development. **Cardiovascular Research**, 58 (1): 32–45

Ren, S. (2002) Predicting three narcosis mechanisms of aquatic toxicity. **Toxicology Letters**, 133 (2–3): 127–139

Renshaw, S.A. and Ingham, P.W. (2010) Zebrafish models of the immune response: taking it on the ChIn. **BMC Biology**, 8 (1): 148

Reyes, B.A., Pendergast, J.S. and Yamazaki, S. (2008) Mammalian Peripheral Circadian Oscillators Are Temperature Compensated. **Journal of Biological Rhythms**, 23 (1): 95–98

Rickert, D.E., Bond, J.A., Long, R.M., et al. (1983) Metabolism and excretion of nitrobenzene by rats and mice. **Toxicology and Applied Pharmacology**, 67 (2): 206–214

Ripoll, C., Lederer, W.J. and Nichols, C.G. (1990) Modulation of ATP-sensitive K+ channel activity and contractile behavior in mammalian ventricle by the potassium channel openers cromakalim and RP49356. **Journal of Pharmacology and Experimental Therapeutics**, 255 (2): 429–435

Roberts, D.M.S., Magnusson, B.M., Burczynski, F.J., et al. (2002) Enterohepatic Circulation. **Clinical Pharmacokinetics**, 41 (10): 751–790

Roberts, R.A., Kavanagh, S.L., Mellor, H.R., et al. (2014) Reducing attrition in drug development: smart loading preclinical safety assessment. **Drug Discovery Today**, 19 (3): 341–347

Roberts, S.A. (2005) "DRUG METABOLISM | Overview." In Editors-in-Chief: Paul Worsfold, Alan Townshend and Colin Poole (eds.) **Encyclopedia of Analytical Science (Second Edition)** [online]. Oxford: Elsevier. pp. 293–305. Available from: http://www.sciencedirect.com/science/article/pii/B0123693977001084 [Accessed 17 April 2013]

Rombough, P. (2002) Gills are needed for ionoregulation before they are needed for O2 uptake in developing zebrafish, Danio rerio. **Journal of Experimental Biology**, 205 (12): 1787–1794

Rombough, P. and Drader, H. (2009) Hemoglobin enhances oxygen uptake in larval zebrafish (Danio rerio) but only under conditions of extreme hypoxia. **Journal of Experimental Biology**, 212 (6): 778–784

Rombough, P.J. (2007) Ontogenetic changes in the toxicity and efficacy of the anaesthetic MS222 (tricaine methanesulfonate) in zebrafish (Danio rerio) larvae. **Comparative Biochemistry and Physiology Part A: Molecular & Integrative Physiology**, 148 (2): 463–469

Rottbauer, W., Baker, K., Wo, Z.G., et al. (2001) Growth and function of the embryonic heart depend upon the cardiac-specific L-type calcium channel alpha1 subunit. **Developmental Cell**, 1 (2): 265–275

Ruckmani, A., Nayar, P.G., Konda, V.G.R., et al. (2011) Effects of Inhalational Exposure of Malathion on Blood Glucose and Antioxidants Level in Wistar Albino Rats. **Research Journal of Environmental Toxicology**, 5 (5): 309–315

Sabeh, M., Kekhia, H. and MacRae, C. (n.d.) Optical Mapping in the Developing Zebrafish Heart. **Pediatric Cardiology**, pp. 1–7

Sachidanandan, C., Yeh, J.-R.J., Peterson, Q.P., et al. (2008) Identification of a Novel Retinoid by Small Molecule Screening with Zebrafish Embryos. **PLoS ONE**, 3 (4): e1947

Sadeghi-Bazargani, H., Banani, A. and Mohammadi, S. (2010) "Using SIMCA statistical software package to apply orthogonal projections to latent structures modeling." In **World Automation Congress (WAC), 2010**. **September 2010**. pp. 1–9

Sah, P. (1996) Ca2+-activated K+ currents in neurones: types, physiological roles and modulation. **Trends in Neurosciences**, 19 (4): 150–154

Salata, J.J., Jurkiewicz, N.K., Wallace, A.A., et al. (1995) Cardiac Electrophysiological Actions of the Histamine H1-Receptor Antagonists Astemizole and Terfenadine Compared With Chlorpheniramine and Pyrilamine. **Circulation Research**, 76 (1): 110–119

Schimmel, K.J.M., Richel, D.J., van den Brink, R.B.A., et al. (2004) Cardiotoxicity of cytotoxic drugs. **Cancer Treatment Reviews**, 30 (2): 181–191

Scholz, E.P., Niemer, N., Hassel, D., et al. (2009) Biophysical properties of zebrafish ether-à-go-go related gene potassium channels. **Biochemical and Biophysical Research Communications**, 381 (2): 159–164

Scholz, S., Fischer, S., Gündel, U., et al. (2008) The zebrafish embryo model in environmental risk assessment--applications beyond acute toxicity testing. **Environmental science and pollution research international**, 15 (5): 394–404

Scholz, S., Sela, E., Blaha, L., et al. (2013) A European perspective on alternatives to animal testing for environmental hazard identification and risk assessment. **Regulatory Toxicology and Pharmacology**, 67 (3): 506–530

Schulte, C. and Nagel, R. (n.d.) Testing acute toxicity in the embryo of zebrafish, Brachydanio rerio, as alternative to the acute fish test: preliminary results. **ATLA. Alternatives to laboratory animals**, 22 (1): 12–19

Schwartz, R.E., Helms, G.L., Bolessa, E.A., et al. (1994) Pramanicin, a novel antimicrobial agent from a fungal fermentation. **Tetrahedron**, 50 (6): 1675–1686

Schwerte, T. and Fritsche, R. (2003) Understanding cardiovascular physiology in zebrafish and Xenopus larvae: the use of microtechniques. **Comparative Biochemistry and Physiology Part A: Molecular & Integrative Physiology**, 135 (1): 131–145

Scornaienchi, M.L., Thornton, C., Willett, K.L., et al. (2010) Functional differences in the cytochrome P450 1 family enzymes from Zebrafish (Danio rerio) using heterologously expressed proteins. **Archives of Biochemistry and Biophysics**, 502 (1): 17–22

Sedmera, D., Reckova, M., deAlmeida, A., et al. (2003) Functional and morphological evidence for a ventricular conduction system in zebrafish and Xenopus hearts. **American journal of physiology. Heart and circulatory physiology**, 284 (4): H1152–1160

Selmi, S., El-Fazaa, S. and Gharbi, N. (2013) Oxidative stress and alteration of biochemical markers in liver and kidney by malathion in rat pups. **Toxicology and Industrial Health** [online]. Available from: http://tih.sagepub.com/content/early/2013/01/16/0748233713475507 [Accessed 19 February 2013]

Serbedzija, G.N., Flynn, E. and Willett, C.E. (1999) Zebrafish angiogenesis: A new model for drug screening. **Angiogenesis**, 3 (4): 353–359

Seth, A., Stemple, D.L. and Barroso, I. (2013) The emerging use of zebrafish to model metabolic disease. **Disease Models & Mechanisms**, 6 (5): 1080–1088

Shin, J.T. and Fishman, M.C. (2002) From Zebrafish to human: modular medical models. **Annual review of genomics and human genetics**, 3: 311–340

Silvette, H., Hoff, E.C., Larson, P.S., et al. (1962) The Actions of Nicotine on Central Nervous System Functions. **Pharmacological Reviews**, 14 (1): 137–173

Simões-Costa, M.S., Vasconcelos, M., Sampaio, A.C., et al. (2005) The evolutionary origin of cardiac chambers. **Developmental Biology**, 277 (1): 1–15

Simons, F.E.R. (2004) Advances in H1-Antihistamines. **New England Journal of Medicine**, 351 (21): 2203–2217

Sjöström, M., Kolman, A., Clemedson, C., et al. (2008) Estimation of human blood LC50 values for use in modeling of in vitro–in vivo data of the ACuteTox project. **Toxicology in Vitro**, 22 (5): 1405–1411

Sköld, C., Winiwarter, S., Wernevik, J., et al. (2006) Presentation of a Structurally Diverse and Commercially Available Drug Data Set for Correlation and Benchmarking Studies. **Journal of Medicinal Chemistry**, 49 (23): 6660–6671

Soldatow, V.Y., LeCluyse, E.L., Griffith, L.G., et al. (2013) In vitro models for liver toxicity testing. **Toxicology research**, 2 (1): 23–39

Somogyi, A., Albrecht, M., Kliems, G., et al. (1981) Pharmacokinetics, bioavailability and ECG response of verapamil in patients with liver cirrhosis. **British Journal of Clinical Pharmacology**, 12 (1): 51–60

Soroka, N.F., Kostiuk, V.A. and Potapovich, A.I. (1992) [The mechanism of the antioxidant action of D-penicillamine]. **Eksperimental'naia i klinicheskaia farmakologiia**, 55 (3): 42–43

Spitsbergen, J.M. and Kent, M.L. (2003) The State of the Art of the Zebrafish Model for Toxicology and Toxicologic Pathology Research—Advantages and Current Limitations. **Toxicologic Pathology**, 31 (1 suppl): 62–87

Spring, D.R., Krishnan, S., Blackwell, H.E., et al. (2002) Diversity-Oriented Synthesis of Biaryl-Containing Medium Rings Using a One Bead/One Stock Solution Platform. **Journal of the American Chemical Society**, 124 (7): 1354–1363

Stainier, D.Y., Fouquet, B., Chen, J.N., et al. (1996) Mutations affecting the formation and function of the cardiovascular system in the zebrafish embryo. **Development (Cambridge, England)**, 123: 285–292

Strähle, U., Scholz, S., Geisler, R., et al. (2012) Zebrafish embryos as an alternative to animal experiments--a commentary on the definition of the onset of protected life stages in animal welfare regulations. **Reproductive Toxicology (Elmsford, N.Y.)**, 33 (2): 128–132

Strmac, M. and Braunbeck, T. (1999) Effects of triphenyltin acetate on survival, hatching success, and liver ultrastructure of early life stages of zebrafish (Danio rerio). **Ecotoxicology and environmental safety**, 44 (1): 25–39

Su, L.M., Liu, X., Wang, Y., et al. (2014) The discrimination of excess toxicity from baseline effect: Effect of bioconcentration. **Science of The Total Environment**, 484: 137–145

Sun, P., Zhang, Y., Yu, F., et al. (2009) Micro-Electrocardiograms to Study Post-Ventricular Amputation of Zebrafish Heart. **Annals of Biomedical Engineering**, 37 (5): 890–901

Taglialatela, M., Pannaccione, A., Castaldo, P., et al. (1998) Molecular Basis for the Lack of HERG K+ Channel Block-Related Cardiotoxicity by the H1 Receptor Blocker Cetirizine Compared with Other Second-Generation Antihistamines. **Molecular Pharmacology**, 54 (1): 113–121

Taneda, Y., Konno, S., Makino, S., et al. (2010) Epigenetic control of cardiomyocyte production in response to a stress during the medaka heart development. **Developmental Biology**, 340 (1): 30–40

Tao, T. and Peng, J. (2009) Liver development in zebrafish (Danio rerio). **Journal of Genetics and Genomics**, 36 (6): 325–334

Taylor, K.L., Grant, N.J., Temperley, N.D., et al. (2010) Small molecule screening in zebrafish: an in vivo approach to identifying new chemical tools and drug leads. **Cell Communication and Signaling**, 8 (1): 11

Terada, H. (1990) Uncouplers of oxidative phosphorylation. **Environmental Health Perspectives**, 87: 213–218

Tessadori, F., van Weerd, J.H., Burkhard, S.B., et al. (2012) Identification and Functional Characterization of Cardiac Pacemaker Cells in Zebrafish. **PLoS ONE**, 7 (10): e47644

Testai, L., Cecchetti, V., Sabatini, S., et al. (2010) Effects of KATP openers on the QT prolongation induced by HERG-blocking drugs in guinea-pigs. **Journal of Pharmacy and Pharmacology**, 62 (7): 924–930

Thakker, D.R., Yagi, H., Akagi, H., et al. (1977) Metabolism of benzo[a]pyrene VI. Stereoselective metabolism of benzo[a]pyrene and benzo[a]pyrene 7,8-dihydrodiol to diol epoxides. **Chemico-Biological Interactions**, 16 (3): 281–300

Thomas, L.T., Welsh, L., Galvez, F., et al. (2009) Acute nicotine exposure and modulation of a spinal motor circuit in embryonic zebrafish. **Toxicology and Applied Pharmacology**, 239 (1): 1–12

Thomas, S.H., Stone, C.K. and Koury, S.I. (1996) Cardiac dysrhythmias in severe verapamil overdose: characterization with a canine model. **European journal of emergency medicine: official journal of the European Society for Emergency Medicine**, 3 (1): 9–13

Tong, D.A., Bartels, K.A. and Honeyager, K.S. (2002) "Adaptive reduction of motion artifact in the electrocardiogram." In **Engineering in Medicine and Biology, 2002. 24th Annual Conference and the Annual Fall Meeting of the Biomedical Engineering Society EMBS/BMES Conference, 2002. Proceedings of the Second Joint**. **2002**. pp. 1403–1404 vol.2

Tong, S., Bezerianos, A., Paul, J., et al. (2001) Removal of ECG interference from the EEG recordings in small animals using independent component analysis. **Journal of Neuroscience Methods**, 108 (1): 11–17

Tournebize, R., Doan, B.-T., Dillies, M.-A., et al. (2006) Magnetic resonance imaging of Klebsiella pneumoniae-induced pneumonia in mice. **Cellular Microbiology**, 8 (1): 33–43

Tran, T.C., Sneed, B., Haider, J., et al. (2007) Automated, Quantitative Screening Assay for Antiangiogenic Compounds Using Transgenic Zebrafish. **Cancer Research**, 67 (23): 11386–11392

Truong, L., Harper, S.L. and Tanguay, R.L. (2011) "Evaluation of Embryotoxicity Using the Zebrafish Model." In Gautier, J.-C. (ed.) **Drug Safety Evaluation**. Methods in Molecular Biology 691 [online]. Humana Press. pp. 271–279. Available from: http://link.springer.com/protocol/10.1007/978-1-60761-849-2_16 [Accessed 5 September 2014]

Tsai, C.-T., Wu, C.-K., Chiang, F.-T., et al. (2011) In-vitro recording of adult zebrafish heart electrocardiogram — A platform for pharmacological testing. **Clinica Chimica Acta**, 412 (21–22): 1963–1967

Tsutsui, H., Higashijima, S.-I., Miyawaki, A., et al. (2010) Visualizing Voltage Dynamics in Zebrafish Heart. **The Journal of Physiology**, 588 (12): 2017–2021

Tyl, R.W., France, K.A., Fisher, L.C., et al. (1987) Development toxicity evaluation of inhaled nitrobenzene in CD rats. **Fundamental and applied toxicology: official journal of the Society of Toxicology**, 8 (4): 482–492

Ujváry, I. (1999) "Nicotine and Other Insecticidal Alkaloids." In Yamamoto, I. and Casida, J.E. (eds.) **Nicotinoid Insecticides and the Nicotinic Acetylcholine Receptor** [online]. Springer Japan. pp. 29–69. Available from: http://link.springer.com/chapter/10.1007/978-4-431-67933-2_2 [Accessed 4 February 2014]

Usui, T., Sugiyama, A., Ishida, Y., et al. (1998) Simultaneous assessment of the hemodynamic, cardiomechanical, and electrophysiological effects of terfenadine on the in vivo canine model. **Heart and Vessels**, 13 (2): 49–57

Veneman, W.J., Stockhammer, O.W., Boer, L. de, et al. (2013) A zebrafish high throughput screening system used for Staphylococcus epidermidis infection marker discovery. **BMC Genomics**, 14 (1): 255

Verhaar, H.J.M., Urrestarazu Ramos, E. and Hermens, J.L.M. (1996) Classifying environmental pollutants. 2: Separation of class 1 (baseline toxicity) and class 2 ('polar narcosis') type compounds based on chemical descriptors. **Journal of Chemometrics**, 10 (2): 149–162

Vliegenthart, A.D.B., Tucker, C.S., Del Pozo, J., et al. (2014) Zebrafish as model organisms for studying drug induced liver injury. **British Journal of Clinical Pharmacology**, p. n/a–n/a

Wagner, G.S. (2008) **Marriott's Practical Electrocardiography: Galen S. Wagner**. Lippincott Williams & Wilkins

Wang, Y., Riederer, S.J. and Ehman, R.L. (1995) Respiratory Motion of the Heart: Kinematics and the Implications for the Spatial Resolution in Coronary Imaging. **Magnetic Resonance in Medicine**, 33 (5): 713–719

Wayne Schultz, T., Wilke, T.S., Bryant, S.E., et al. (1991) QSARs for selected aliphatic and aromatic amines. **Science of The Total Environment**, 109–110: 581–587

Webster, R., Allan, G., Anto-Awuakye, K., et al. (2001) Pharmacokinetic/pharmacodynamic assessment of the effects of E4031, cisapride, terfenadine and terodiline on monophasic action potential duration in dog. **Xenobiotica**, 31 (8-9): 633–650

Weigt, S., Huebler, N., Strecker, R., et al. (2011) Zebrafish (Danio rerio) embryos as a model for testing proteratogens. **Toxicology**, 281 (1–3): 25–36

Weimin, L., Daqiang, Y., Shiyin, L., et al. (2001) Acute Toxicity of Chloroanilines to Zebra Fish and 3D-QSAR Analysis. **Research of Environmental Sciences**, 15 (2): 6–7,11

Welsh, L., Tanguay, R.L. and Svoboda, K.R. (2009) Uncoupling nicotine mediated motoneuron axonal pathfinding errors and muscle degeneration in zebrafish. **Toxicology and Applied Pharmacology**, 237 (1): 29–40

Wen, D., Liu, A., Chen, F., et al. (2012) Validation of visualized transgenic zebrafish as a high throughput model to assay bradycardia related cardio toxicity risk candidates. **Journal of Applied Toxicology**, 32 (10): 834–842

Wheeler, G.N. and Brändli, A.W. (2009) Simple vertebrate models for chemical genetics and drug discovery screens: Lessons from zebrafish and Xenopus. **Developmental Dynamics**, 238 (6): 1287–1308

W, H., M, H., X, C., et al. (1993) [Torsade de pointes]. **Zeitschrift fur Kardiologie**, 82 (12): 763–774

Williams, J.. and Holder, N. (2000) Cell turnover in neuromasts of zebrafish larvae. **Hearing Research**, 143 (1–2): 171–181

WIRTSCHAFTER, Z.T. and WOLPAW, R. (1944) A CASE OF NITROBENZENE POISONING*. **Annals of Internal Medicine**, 21 (1): 135–141

Wittmann, C., Chockley, P., Singh, S.K., et al. (2012) Hydrogen Peroxide in Inflammation: Messenger, Guide, and Assassin. **Advances in Hematology** [online], 2012. Available from: http://www.hindawi.com/journals/ah/2012/541471/abs/ [Accessed 29 April 2013]

Wood, M. (1986) Plasma Drug Binding Implications for Anesthesiologists. **Anesthesia & Analgesia**, 65 (7): 786–804

Woods, I.G. and Talbot, W.S. (2005) The you Gene Encodes an EGF-CUB Protein Essential for Hedgehog Signaling in Zebrafish. **PLoS Biol**, 3 (3): e66

Woosley RL, Chen Y, Freiman JP, et al. (1993) MEchanism of the cardiotoxic actions of terfenadine. **JAMA**, 269 (12): 1532–1536

Xu, D., Nishimura, T., Nishimura, S., et al. (2014) Fialuridine Induces Acute Liver Failure in Chimeric TK-NOG Mice: A Model for Detecting Hepatic Drug Toxicity Prior to Human Testing. **PLoS Med**, 11 (4): e1001628

Yamamoto, I. and Casida, J.E. (1999) **Nicotinoid Insecticides and the Nicotinic Acetylcholine Receptor**. Springer. (00086)

Yamanaka, S. (2009) A Fresh Look at iPS Cells. **Cell**, 137 (1): 13–17

Yang, L., Kemadjou, J.R., Zinsmeister, C., et al. (2007) Transcriptional profiling reveals barcode-like toxicogenomic responses in the zebrafish embryo. **Genome Biology**, 8 (10): R227

Yap, Y.G. and Camm, J. (2000) Risk of torsades de pointes with non-cardiac drugs. **BMJ : British Medical Journal**, 320 (7243): 1158–1159

Yoong, S., O'Connell, B., Soanes, A., et al. (2007) Characterization of the zebrafish matrix metalloproteinase 9 gene and its developmental expression pattern. **Gene Expression Patterns**, 7 (1–2): 39–46

Yoo, S.K., Starnes, T.W., Deng, Q., et al. (2011) Lyn is a redox sensor that mediates leukocyte wound attraction in vivo. **Nature**, 480 (7375): 109–112

Yoshida, F. and Topliss, J.G. (2000) QSAR Model for Drug Human Oral Bioavailability1. **Journal of Medicinal Chemistry**, 43 (13): 2575–2585

Yoshida, M., Hirano, R. and Shima, T. (2009) Photocardiography: a novel method for monitoring cardiac activity in fish. **Zoological Science**, 26 (5): 356–361

Yu, F., Huang, J., Adlerz, K., et al. (2010) Evolving Cardiac Conduction Phenotypes in Developing Zebrafish Larvae: Implications to Drug Sensitivity. **Zebrafish**, 7 (4): 325–331

Yu, F., Zhao, Y., Gu, J., et al. (2012) Flexible microelectrode arrays to interface epicardial electrical signals with intracardial calcium transients in zebrafish hearts. **Biomedical Microdevices**, 14 (2): 357–366

Zareba, W. (2007) Drug induced QT prolongation. **Cardiology journal**, 14 (6): 523–533

Zeltser, D., Justo, D., Halkin, A., et al. (2004) Drug-induced atrioventricular block: prognosis after discontinuation of the culprit drug. **Journal of the American College of Cardiology**, 44 (1): 105–108

Zhang, X., Li, C. and Gong, Z. (2014) Development of a Convenient In Vivo Hepatotoxin Assay Using a Transgenic Zebrafish Line with Liver-Specific DsRed Expression. **PLoS ONE**, 9 (3): e91874

Zhang, X., Qin, W., He, J., et al. (2013) Discrimination of excess toxicity from narcotic effect: Comparison of toxicity of class-based organic chemicals to Daphnia magna and Tetrahymena pyriformis. **Chemosphere**, 93 (2): 397–407

Zhao, Y., Yu, F., Cao, H., et al. (2013) "A wearable percutaneous implant for long term zebrafish epicardial ECG recording." In **2013 Transducers Eurosensors XXVII: The 17th International Conference on Solid-State Sensors, Actuators and Microsystems (TRANSDUCERS EUROSENSORS XXVII)**. **2013**. pp. 756–759

Zhu, J.-J., Xu, Y.-Q., He, J.-H., et al. (2013) Human cardiotoxic drugs delivered by soaking and microinjection induce cardiovascular toxicity in zebrafish. **Journal of Applied Toxicology**, p. n/a–n/a

Zitting, A., Szumańska, G., Nickels, J., et al. (1982) Acute toxic effects of trinitrotoluene on rat brain, liver and kidney: role of radical production. **Archives of Toxicology**, 51 (1): 53–64

Zon, L.I. and Peterson, R.T. (2005) In vivo drug discovery in the zebrafish. **Nature Reviews Drug Discovery**, 4 (1): 35–44

Zou, J., Li, W.-Q., Li, Q., et al. (2011) Two Functional MicroRNA-126s Repress a Novel Target Gene p21-Activated Kinase 1 to Regulate Vascular Integrity in Zebrafish. **Circulation Research**, 108 (2): 201–209

Chapter Ten: PUBLICATIONS

1. **Dhillon SS**, Dóró É, Magyary I, Egginton S, Sík A, et al. (2013) Optimisation of Embryonic and Larval ECG Measurement in Zebrafish for Quantifying the Effect of QT Prolonging Drugs. PLoS ONE 8(4): e60552. doi:10.1371/journal.pone.0060552

2. Feula A, **Dhillon SS**, Byravan R, Sangha M, Ebanks R, et al. (2013) Synthesis of azetidines and pyrrolidines via iodocyclisation of homoallyl amines and exploration of activity in a zebrafish embryo assay. Org. Biomol. Chem., doi: 10.1039/C3OB41007B